HAEMOXYGENASE IN TUMOURS AND ITS ROLE IN VASCULAR TARGETING WITH COMBRETASTATIN A4 PHOSPHATE

by

Amel Feriel Khelifi

A thesis submitted to the University of London for the degree of

Doctor of Philosophy

Department of Oncology, University College London
Tumour Microcirculation Group, Gray Cancer Institute

2003

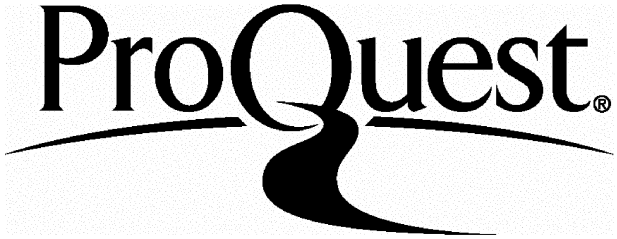

ABSTRACT

The present thesis describes *in vitro* and *in vivo* investigations into the role of haemoxygenase (HO) in tumours and in vascular targeting by the novel tubulin binding agent combretastatin A4-phosphate (CA-4-P). HO catalyses the degradation of haem, producing the biologically active molecules iron, bilirubin and carbon monoxide. HO-1, one of the three isozymes of HO, is induced in response to stress and in pathological conditions including cancer, inflammation and vascular injury and plays an important role in cytoprotection. CA-4-P binds to tubulin causing disruption of microtubule function leading to destabilisation of the cell cytoskeleton. *In vivo*, CA-4-P causes vascular collapse and haemorrhagic necrosis in various tumour models.

HO-1 protein levels were found to be high in rodent and xenografted tumour models. Further investigations demonstrated only a minor role played by the HO system in sustaining tumour growth and in the maintenance of tumour blood flow in the rat P22 tumour model.

In vivo, administration of CA-4-P at a clinically relevant dose caused induction of HO-1 in a sub-group of treated P22 rat tumours, as analysed by immunohistochemistry. HO-1 positive staining was localised in perinecrotic areas and tumour-associated macrophages were the predominant cell type expressing the protein. *In vitro*, CA-4-P exposure had greater anti-proliferative effects in P22 tumour cells than HUVECs, and the latter showed faster recovery of a distinct tubulin cytoskeleton than the former. Furthermore, CA-4-P caused a much more pronounced HO-1 induction in P22 tumour cells than in HUVECs. The antioxidant N-acetyl-L-cysteine (NAC) completely blocked CA-4-P-mediated HO-1 induction in tumour cells suggesting that CA-4-P is causing an imbalance in the redox state of cells possibly via glutathione depletion.

Finally, combination therapy with the HO inhibitor tin protoporphyrin IX (SnPP) and CA-4-P tended to improve the efficacy of CA-4-P alone in the P22 rat and CaNT mouse tumour models. This combination requires further investigation.

DECLARATION

I confirm that the research described in this thesis is my own work. I received some technical assistance for the in vivo experiments reported in Figures 6.5 to 6.12 because of the development of severe animal allergy during the course of this project. This necessitated stopping direct contact with experimental animals in January 2002.

ACKNOWLEDGEMENTS

I am very grateful to Gill Tozer for excellent supervision, and for her great help and support throughout the project. I would also like to thank Peter Hoskin, my UCL supervisor, for his advice and encouragement.

Completion of the work described in this thesis would not have been possible without the contribution and assistance of many people. I would like to greatly thank Vivien Prise who taught me, with great patience, about the various aspects of the *in vivo* work and who carried out some of the experiments on rats described in Chapter 6. I am also very grateful to Sally Hill and Gemma Lewis for their help and for conducting the experiments on mice reported in Chapter 6. Thank you to Ian Wilson for his assistance with the *in vivo* work and to Frances Daley for introducing me to the immunohistochemistry. I am extremely grateful to Chryso Kanthou for her great and valuable help with all aspects of the *in vitro* work and also for her continuous assistance and encouragement throughout. Thank you to Claudia Coralli for being there with always the right and wise advice and to Jo Tupper for listening and sharing the ups and downs. Finally, I would like to thank all of the Tumour Microcirculation Group for making it such a welcoming and friendly place.

I am indebted to several people at Northwick Park Institute for Medical Research. I would like to thank Roberto Motterlini for giving me the opportunity to learn about the HO assay in his laboratory and for stimulating and helpful discussions. Thank you to Roberta Foresti and James Clark for valuable teaching and practical assistance while there.

I am grateful to Cancer Research UK for funding this work and for financial support.

Finally, I would like to thank my parents and my brothers around the world for their ever-lasting support and encouragement. This work is dedicated to you.

TABLE OF CONTENTS

CHAPTER 5 EFFECTS OF COMBRETASTATIN A4-PHOSPHATE ON THE HAEMOXYGENASE SYSTEM: IN VITRO AND IN VIVO ANALYSIS

CHAPTER 6 EFFECTS OF MODIFYING HAEMOXYGENASE ACTIVITY ON TUMOUR GROWTH AND TREATMENT OUTCOME WITH COMBRETASTATIN A4-PHOSPHATE

LIST OF FIGURES

CHAPTER 1

CHAPTER 2

CHAPTER 3

CHAPTER 4

CHAPTER 5

CHAPTER 6

LIST OF TABLES

CHAPTER 1

CHAPTER 2

CHAPTER 5

CHAPTER 6

ABBREVIATIONS

AP-1	activator protein-1
AP	alkaline phosphatase
APAAP	alkaline phosphatase anti-alkaline phosphatase
Ang-1	angiopoeitin-1
Ang-2	angiopoeitin-2
bFGF	basic fibroblast growth factor
BSA	bovine serum albumin
CO	carbon monoxide
CA-4-P	combretastatin A4-phosphate
CuPP	copper protoporphyrin IX
cAMP	cyclic adenosine monophosphate
cGMP	cyclic guanosine monophosphate
DMXAA	dimethylxanthenone acetic acid
DTT	dithiothreitol
DMEM	Dulbecco's modified Eagle's medium
ECGS	endothelial cell growth supplement
ECL	enhanced chemiluminescence
FAA	flavone acetic acid
FDA	Food and Drug Administration
G6P	glucose-6-phosphate
G6PD	glucose-6-phosphate dehydrogenase
GDP	guanosine diphosphate
GTP	guanosine triphosphate
HO	haemoxygenase
H&E	haematoxylin and eosin
HPLC	high performance liquid chromatography
HRP	horseradish peroxidase
HUVECs	human umbilical vein endothelial cells
Hif-1	hypoxia inducible factor-1
iNOS	inducible nitric oxide synthase

IL	interleukin
IFN	interferon
ip	intraperitoneal
IAP	iodo-antipyrine
LPS	lipopolysaccharide
MHC II	major histocompatibility complex II
MMP	matrix metalloproteinase
MABP	mean arterial blood pressure
MAPKs	mitogen activated protein kinases
NAC	N-acetyl-L-cysteine
NADPH	nicotinamide adenine dinucleotide phosphate
NO	nitric oxide
NOS	nitric oxide synthase
NF-κB	nuclear factor-κB
PBS	phosphate-buffered saline
PBS-T	phosphate-buffered saline-tween
PDGF	platelet derived growth factor
PKA	protein kinase-A
PKC	protein kinase-C
PKG	protein kinase-G
RECA-1	rat endothelial cell antigen-1
SCID	severely compromised immuno-deficient
SDS-PAGE	sodium dodecylsulfate-polyacrylamide gel electrophoresis
sGC	soluble guanylate cyclase
TBS	tris-buffered saline
TSP	thrombospondin
SnPP	tin protoporphyrin IX
TIMPs	tissue inhibitors of metalloproteinases
TNF-α	tumour necrosis factor-alpha
VCAM-1	vascular cell adhesion molecule-1
VEGF	vascular endothelial growth factor
ZnPP	zinc protoporphyrin IX

CHAPTER 1

GENERAL INTRODUCTION

1.1 Angiogenesis and the Tumour Vasculature

1.1.1 Introduction

Tumours are populations of host-derived cells that have lost the ability to regulate growth and therefore are able to proliferate aberrantly. In the development of malignant tumours, normal cells accumulate a number of genetic mutations, which favour proliferation (activation of oncogenes) or remove control on growth (inactivation of tumour suppressor genes), leading to transformation into a malignant cell (Hanahan and Weinberg, 2000).

As for normal cells, malignant cells require an adequate supply of oxygen and nutrients and an effective means to remove waste products in order to meet metabolic demand and to sustain their survival. These requirements can be fulfilled by vascularisation. It is well known that in most cancers, solid tumour growth consists of an avascular followed by a vascular phase. During the avascular phase, the blood supply is not yet established and therefore tumour growth is restricted and dependent on simple diffusion of nutrients, oxygen and waste products through the surrounding tissue. During this phase, a tumour only grows slowly until equilibrium between the rate of cell proliferation at the periphery and the rate of cell death at the centre of the tumour is reached (Holmgren *et al.*, 1995). Early experiments carried out by Folkman and colleagues showed that absence of vascularisation limits the growth of solid tumours and established that in order for a tumour to grow beyond 1-2 mm in diameter, new blood vessel formation or angiogenesis is required (Folkman, 1971). Avascular tumours may remain dormant for many years until the process of angiogenesis is initiated (Holmgren *et al.*, 1995), which allows for malignant progression from a small localised tumour to an enlarging growing tumour able to metastasise (Folkman, 1971; Liotta *et al.*, 1974).

Several methods of tumour vascularisation have been suggested. As described above, tumour-induced neovascularisation can initiate in an avascular tumour, which grows until its centre region becomes hypoxic leading to the up-regulation of a variety of angiogenic factors (Figure 1.1A). However, It has also been proposed that tumour cells can initially

home in and grow as vascular tumours by co-opting existing host blood vessels. This causes the vessels to regress, thereby driving the tumour into an avascular hypoxic phase, which can be overcome by the induction of angiogenic factors (Yancopoulos *et al.*, 2000; Figure 1.1B). Alternatively, endothelial cell precursors circulating in the blood or derived from the bone marrow have been suggested to home into tumours and participate in the formation of tumour derived blood vessels by a process known as vasculogenesis (Lyden *et al.*, 2001; Figure 1.1C).

1.1.2 Angiogenesis

The adult vasculature is initially created in the embryo by vasculogenesis. This process involves differentiation of endothelial cell precursors named angioblasts into endothelial cells, which proliferate and assemble into a primitive network of blood vessels known as the primary capillary plexus (Risau, 1997). Remodelling into a more complex network then occurs by branching and sprouting of new vessels from pre-existing ones in the process of angiogenesis (Carmeliet, 2000). This involves the enlargement of venules, which form sprouts or become divided by pillars of periendothelial cells (intussusception) or by transendothelial cell bridges, which then split into individual capillaries (Carmeliet, 2000) (see Figure 1.2). The process of angiogenic sprouting has been extensively studied and is thought to be often initiated by vasodilatation mainly involving nitric oxide (NO) (Ziche and Morbidelli, 2000). An increase in vascular permeability mainly mediated by vascular endothelial growth factor (VEGF) allows extravasation of plasma proteins, which form a scaffold for migrating and proliferating endothelial cells that assemble into cords and subsequently acquire a lumen (Carmeliet, 2000). Angiogenesis is completed by a process known as vascular maturation, whereby pericytes are recruited to stabilise the new vessels by inhibiting endothelial cell proliferation and migration, and by stimulating the production of extracellular matrix (Carmeliet, 2000). Furthermore, large vessels may become covered with smooth muscle cells providing them with elasticity and vasomotor properties (Carmeliet, 2000).

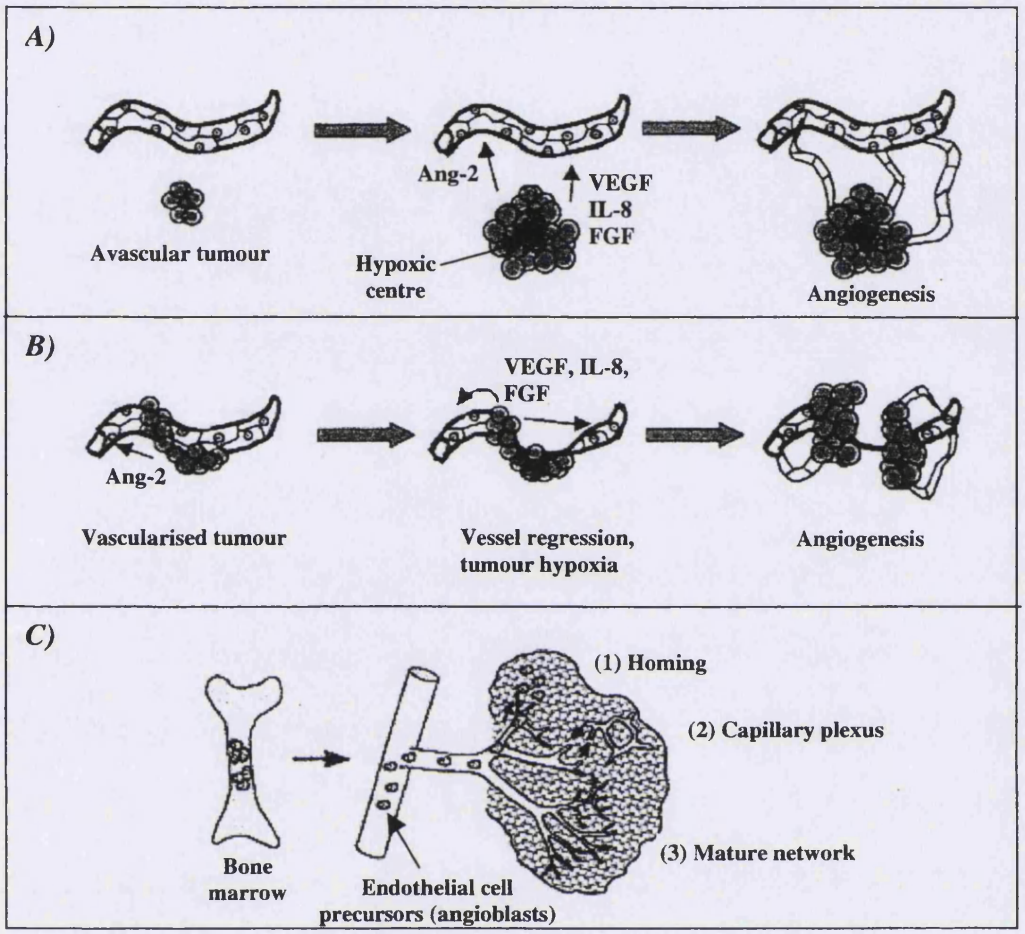

Figure 1.1 Mechanisms of tumour vascular growth. *A)* An initially avascular tumour can grow until its centre region becomes hypoxic leading to the up-regulation of a variety of angiogenic factors. *B)* Tumour cells can initially home in and grow as a vascular tumour by co-opting existing host blood vessels, this causes them to regress, thereby driving the tumour into an avascular hypoxic phase, which can be overcome by the induction of angiogenic factors. *C)* Endothelial cell precursors (angioblasts) circulating in the blood or derived from the bone marrow can home into tumours and participate in the formation of tumour derived blood vessels by the process of vasculogenesis. Adapted from Carmeliet, 2000 and Papetti and Herman, 2002.

In normal adults, the endothelial cells assembled into vessels are quiescent and angiogenesis is a tightly regulated process, which only occurs during the female menstrual cycle and physiological repair processes such as wound healing. The angiogenic process is complex, involving a cascade of events and a variety of cells, and is regulated by a number of pro- and anti-angiogenic factors (Papetti and Herman, 2002) (see Table 1.1).

For new blood vessels to form, pericytes need first to be removed from the branching vessels and the endothelial cell basement membrane and extracellular matrix degraded by proteases such as matrix metalloproteinases. A number of factors are also released that mediate endothelial cell migration and proliferation. These cells then assemble into tube-like structures, which are stabilised by the recruitment of pericytes and smooth muscle cells and the reconstitution of a basement membrane for blood flow to be established in the new vessel (Papetti and Herman, 2002).

Pathological angiogenesis occurs in various disease states such as diabetic retinopathy, rheumatoid arthritis and during growth and metastatic spread of tumours (Carmeliet and Jain, 2000).

1.1.3 Tumour-Induced Angiogenesis

As mentioned earlier, the continuous growth and expansion of malignant tumours is critically dependent on the establishment of a vascular network assuring nutritive blood flow (Folkman, 1990). Early experiments examining the mechanisms of tumour neovascularisation revealed that when a chamber containing tumour cells bounded by a porous membrane, which did not allow cells to exit, was implanted subcutaneously, a vasoproliferative reaction developed around the implant (Cavallo *et al.*, 1972; Cavallo *et al.*, 1973). These experiments therefore suggested that factors released from the tumour cells themselves were responsible for starting the angiogenic process. Various signals are thought to trigger this "angiogenic switch" including metabolic stress associated with hypoxia, low extracellular pH and hypoglycaemia, and mechanical stress induced by rapidly proliferating cells (Carmeliet and Jain, 2000). Furthermore, genetic mutations involving activation of oncogenes and inactivation of tumour suppressor genes are also thought to participate in the initiation of tumour angiogenesis (Hanahan and Weinberg, 2000).

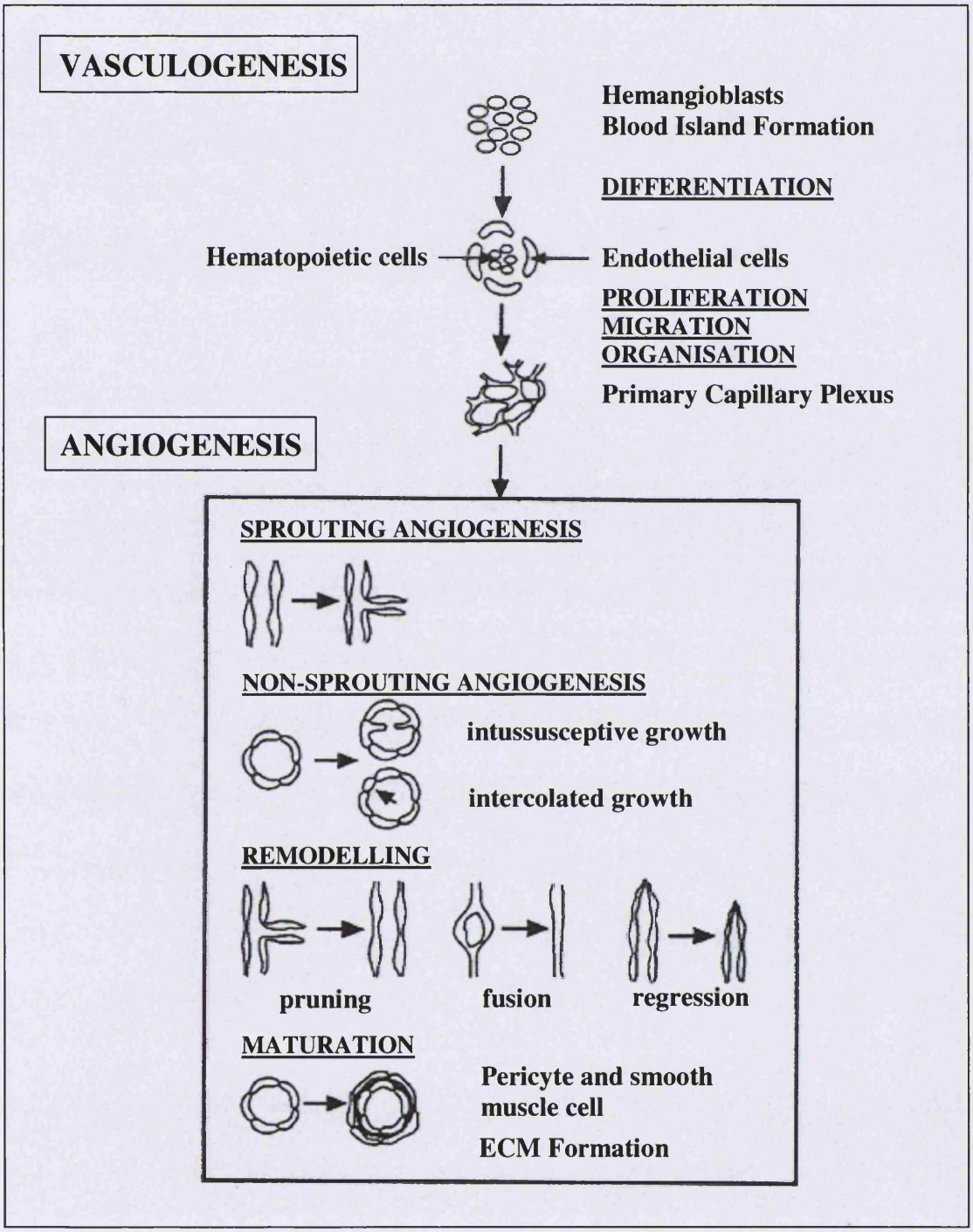

Figure 1.2 Schematic illustration of the processes of vasculogenesis and angiogenesis in the developing embryo. Adapted from Saaristo *et al.*, 2000.

All of these conditions promote angiogenesis by favouring the balance towards the production of pro-angiogenic factors. These are now known to be released not only from the tumour cells themselves, but also from immune cells infiltrating the tumour such as macrophages and mast cells, which are also thought to participate in the initiation of angiogenesis (Bingle *et al.*, 2002; Ribatti *et al.*, 2001). Furthermore, there is also evidence that pro-angiogenic factors can also be mobilised from the extracellular matrix as a result of protease activity (Vlodavsky *et al.*, 1990).

A number of factors, which participate in physiological angiogenesis have been shown to be also involved in tumour-induced angiogenesis. Table 1.1 lists some of the pro-angiogenic factors identified to date. The ones most well characterised in tumour angiogenesis are further described below.

Vascular endothelial growth factor (VEGF) is a potent and critical regulator of angiogenesis that has been shown to be highly up-regulated in most human cancers (Toi *et al.*, 2001). Administration of anti-VEGF antibodies to tumour-bearing animals significantly reduces tumour vessel density and suppresses tumour cell growth (Kim *et al.*, 1993). VEGF is involved in promoting vascular endothelial cell proliferation and increasing vascular permeability (Brown *et al.*, 1997). Furthermore, it is also thought not only to be pro-angiogenic but also to act as a survival factor for endothelial cells, especially in the immature blood vessels frequently found in tumours. Indeed, with the use of a tetracycline-regulated VEGF expression system in xenografted C6 glioma cells, it was demonstrated that shutting off VEGF production leads to the detachment of endothelial cells specifically from the walls of immature vessels and their subsequent death by apoptosis (Benjamin and Keshet, 1997). This would provide a mechanistic explanation for the fact that VEGF deprivation might lead not only to inhibition of further angiogenesis but also to regression of newly formed tumour blood vessels (Benjamin *et al.*, 1999). This phenomenon may therefore explain why anti-angiogenic therapies can sometimes produce tumour regression as well stasis. However important is the role mediated by VEGF in tumour-induced angiogenesis, other factors have been shown to be also essential in this process, acting in concert to promote blood vessel growth in tumours (Papetti and Herman, 2002).

Basic fibroblast growth factor (bFGF) has been reported to co-operate with VEGF to promote angiogenesis (Goto *et al.*, 1993; Asahara *et al.*, 1995), to increase its production in tumour cells (Deroanne *et al.*, 1997), and to augment VEGF receptor expression in endothelial cells enhancing their proliferation and migration (Mandriota and Pepper, 1997).

One of the most important partners of VEGF are thought to be the *angiopoeitin* family of growth factors. Angiopoetin-1 (Ang-1) and angiopoetin-2 (Ang-2) are the most well studied members (Yancopoulos *et al.*, 2000). Ang-1, by binding to its receptor Tie-2 on endothelial cells, is thought to play a role in vessel stabilisation by strengthening interactions between endothelial cells and their surrounding support cells and matrix (Yancopoulos *et al.*, 2000). Ang-2 is an antagonist of Ang-1 that also binds to the Tie-2 receptor and has been strongly implicated in tumour angiogenesis. Ang-2 mRNA expression has been identified as an early marker of tumour angiogenesis and was shown to be expressed in tumour associated endothelial cells and not in normal vessels (Zagzag *et al.*, 1999). Ang-2 produced by the host vessels is thought to play an important role in promoting their destabilisation and regression during the early stages of tumour growth around existing host vessels, resulting in the tumour becoming avascular and hypoxic. This condition induces VEGF production by the tumour cells promoting the onset of angiogenesis allowing for tumour survival and further growth (Yancopoulos *et al.*, 2000).

Interleukin-8 (IL-8) is another factor found to be up regulated in human tumours (Yuan *et al.*, 2000). It is thought to be involved in angiogenesis because of its ability to induce the production of the matrix metalloproteinase-2 (MMP-2), which is involved in the break-down of the basement membrane and remodelling of the extracellular matrix, two important steps in angiogenesis enabling cell invasion and migration (Luca *et al.*, 1997).

Although the above-described pro-angiogenic factors are important for the induction of tumour neovascularisation, the overall angiogenic phenotype of a tumour is critically dependent on the balance between pro-angiogenic and anti-angiogenic factors. For instance, Oshika and colleagues have shown that the expression of the angiogenic inhibitor thrombospondin-2 (described below in 1.2.2) correlated with decreased vascularity in non-small cell lung cancer and this feature was associated with significantly better prognosis (Oshika *et al.*, 1998). A number of endogenous inhibitors of

angiogenesis have been characterised and a list is provided in Table 1.1. The best studied of these factors are discussed below in section 1.2.2, along with their potential use in anti-angiogenic therapies.

Some Naturally Occurring Activators of Angiogenesis
Proteins
• Acidic fibroblast growth factor
• Angiogenin
• Basic fibroblast growth factor (bFGF)
• Epidermal growth factor
• Granulocyte colony-stimulating factor
• Hepatocyte growth factor
• Interleukin 8 (IL-8)
• Placental growth factor
• Platelet-derived endothelial growth factor
• Transforming growth factor alpha
• Vascular endothelial growth factor (VEGF)
Small Molecules
• Adenosine
• Nicotinamide
• Prostaglandins E1 and E2
Angiogenesis Inhibitors
Proteins
• Angiostatin
• Endostatin
• Interferons
• Platelet factor 4
• Prolactin 16 kDa fragment
• Thrombospondins
• TIMP-1 (tissue inhibitor of metalloproteinase-1)
• TIMP-2 (tissue inhibitor of metalloproteinase-2)
• TIMP-3 (tissue inhibitor of metalloproteinase-3)

Table 1.1 List of pro-angiogenic and anti-angiogenic factors. Adapted from the National Cancer Institute web site (www.nci.nih.gov).

1.1.4 Characteristics of the Tumour Vasculature

The established tumour vasculature displays numerous abnormalities. Unlike normal vasculature, the tumour-associated vasculature lacks a specified hierarchy (Konerding *et al.*, 1998). Tumour blood vessels show structural abnormalities in that many of them display an "immature" morphology because of lack of a surrounding basement membrane (Kakolyris *et al.*, 1999), functional pericytes and smooth muscle cells (Eberhard *et al.*, 2000), which contribute to vessel maturity, stabilisation and vasoactive control. This lack

of mural cells and excess endothelial cell proliferation, due to an increased production of pro-angiogenic factors, contribute to the formation of dilated, tortuous and saccular tumour blood vessels with an uneven diameter, excessive branching patterns and arterio-venous shunts. Tumour blood vessels are also hyper-permeable and leaky due to an incomplete or absent basement membrane, possess widened inter-endothelial junctions and are characterised by the presence of fenestrae (transendothelial circular openings of 400-800Å between the lumen and interstitium across the endothelial cell) and transcellular holes (Hashizume *et al.*, 2000). Furthermore, there is controversial evidence that the luminal lining of tumour blood vessels may not only be made up of endothelial cells but also tumour cells, which may form part of the vessel resulting in so called "mosaic blood vessels" (Chang *et al.*, 2000). All these structural abnormalities of blood vessels result in a temporally and spatially heterogeneous blood supply within the tumour (Tozer *et al.*, 1990). The variable tumour blood flow results in areas of hypoxia (Vaupel *et al.*, 1992) and intracellular acidosis (Kallinowski *et al.*, 1989), and the leakiness of the tumour blood vessels contributes to interstitial hypertension causing compression of blood vessels and further impairment of blood flow (Boucher *et al.*, 1990).

1.2 Targeting the Tumour Vasculature for Cancer Therapy

1.2.1 Introduction

The chaotic tumour microcirculation and the spatial and temporal heterogeneity in tumour blood supply have been implicated in the failure of several conventional chemotherapy and radiotherapy regimens (Molls and Vaupel, 1998). This problem has stimulated the search for new means for cancer treatment. Because of the critical dependence of tumours on a blood supply, tumour vascular targeting strategies have been developed as a potential promising new approach. Furthermore, this strategy also aims at selective targeting of the tumour vasculature by exploiting the differences between normal tissue and tumour vasculature. There are several potential advantages with such a strategy (Chaplin *et al.*, 1998). First, the targeted endothelial cells are next to the bloodstream thereby reducing delivery problems. Second, a large bystander effect should be observed because damage to a single vessel should kill a large number of tumour cells. Third, endothelial cells are thought to be genetically stable and therefore less likely to develop resistance to the

treatment (Boehm *et al.*, 1997). Finally, this strategy would theoretically be applicable to all solid tumours because it does not depend on the nature of the tumour cells themselves.

The following sections describe two vascular targeting strategies namely anti-angiogenic and anti-vascular therapies.

1.2.2 Anti-Angiogenic Therapy

Anti-angiogenic therapy interferes with the formation of new blood vessels in tumours. This strategy is based on the absolute requirement for tumour neovascularisation in order to sustain growth and invasion (Folkman, 1971). Several anti-angiogenic strategies have been developed against the various steps involved in the process of angiogenesis.

A number of endogenous anti-angiogenic factors have been discovered (Table 1.1). The best characterised are the thrombospondins (TSP), endostatin and angiostatin. TSP-1 and TSP-2 have been shown to be potent endogenous inhibitors of neovascularisation and tumour growth (Streit *et al.*, 1999a; Streit *et al.*, 1999b). The expression of TSP-1 was shown to be regulated by the tumour suppressor gene *p53* with mutations in *p53* resulting in the loss of TSP-1 production and a switch to the angiogenic phenotype (Dameron *et al.*, 1994; Grossfeld *et al.*, 1997). Angiostatin and endostatin are two endogenous angiogenic inhibitors generated from the proteolytic cleavage of plasminogen and collagen type XVIII, respectively (O'Reilly *et al.*, 1994; Folkman, 1995). Angiostatin inhibits endothelial cell proliferation and migration *in vitro* (Cao *et al.*, 1996) and potently suppresses neovascularisation and growth of a number of tumours and their metastases (Cao *et al.*, 1999). Endostatin specifically suppresses endothelial cell proliferation *in vitro* and potently suppresses angiogenesis and induces tumour regression and dormancy (O'Reilly *et al.*, 1997). Endostatin is currently being evaluated in Phase I clinical trials (Eder *et al.*, 2002).

Synthetic inhibitors of endothelial cell proliferation and migration have also been developed. TNP-470 (AGM-1470) is a synthetic compound derived from the antibiotic fumagillin, which has been shown to be an effective anti-tumour agent in a variety of animal models (reviewed in Liekens *et al.*, 2001). This compound is now in Phase II/III clinical trials for a variety of solid tumours.

A number of cytokines such as interferons (IFN) and interleukins (IL) have also been shown to have anti-angiogenic properties. IFN-α has been reported to inhibit angiogenesis *in vivo* possibly through down-regulation of bFGF and MMP-9 production (Ozawa *et al.*, 2001). IFN-α is approved by the Food and Drug Administration (FDA) for the treatment of certain types of cancers such as melanoma and Kaposi's sarcoma. IL-4 has been shown to mediate anti-tumour effects (Puri and Siegel, 1993), which are thought to be partly due to its ability to inhibit endothelial cell migration *in vitro* and to suppress angiogenesis *in vivo* (Volpert *et al.*, 1998).

Matrix metalloproteinases (MMPs) have been recognised as important players in the angiogenic process being involved in the breakdown and remodelling of the extracellular matrix allowing for endothelial cell migration (Vihinen and Kähäri, 2002). A number of endogenous MMP inhibitors (TIMPs) have been characterised and found to inhibit MMP activity resulting in suppression of angiogenesis, tumour growth, invasion and metastasis in experimental tumour models (Gomez *et al.*, 1997). Synthetic TIMPs have now been developed for clinical testing and include Marimastat, COL-3 and BMS-275291, with Marimastat being in phase III for small cell lung cancers (National Cancer Institute Web Site as updated in June 2002). Neovastat is an endogenous inhibitor of MMPs also in phase III for renal and non-small cell lung cancers, however multiple mechanisms of action including blocking of VEGF activity have also been defined for this agent (National Cancer Institute Web Site as updated in June 2002).

Integrins are essential cell adhesion receptors involved in cell-extracellular matrix and cell-cell interactions. A number of studies have demonstrated the importance of the αVβ3 and αVβ5 integrins in angiogenesis (reviewed in Eliceiri and Cheresh, 1999). The αVβ3 integrin is expressed on proliferating endothelium and monoclonal antibodies against it have been demonstrated to promote tumour regression by inducing endothelial cell apoptosis in experimental tumour models (Brooks *et al.*, 1994). Currently, the αVβ3 antibody Vitaxin II (Medi-522) is being tested in phase I/II clinical trials (National Cancer Institute Web Site as updated in June 2002).

Growth factor inhibitors have also been shown to be effective at blocking angiogenesis. Inhibitors of VEGF activity using anti-VEGF antibodies, soluble VEGF receptors or

dominant negative mutants of the VEGF receptor, Flk-1, were shown to decrease vessel density and reduce tumour growth in experimental models (reviewed in Liekens *et al.*, 2001). An anti-VEGF antibody is now in clinical trials for various types of advanced cancers (National Cancer Institute Web Site as updated in June 2002). Furthermore, a soluble inhibitor of the Tie-2 receptor, which is strongly implicated in tumour angiogenesis, has been shown to be effective in blocking angiogenesis causing a reduction in tumour growth (Lin *et al.*, 1997). A number of compounds, which interfere with growth factor receptor signalling, have also been developed. SU5416, currently being evaluated in phase I clinical trials, is a selective inhibitor of the VEGF receptor Flk-1 activity, and has been shown to inhibit angiogenesis and tumour growth in experimental models (Fong *et al.*, 1999). SU6668, also currently being evaluated in Phase I trials against advanced tumours, is a broad spectrum inhibitor of VEGF, bFGF and platelet-derived growth factor (PDGF) receptors activity, which has been reported to decrease tumour vascularisation and induce endothelial and tumour cell apoptosis (Shaheen *et al.*, 1999).

1.2.3 Anti-Vascular Therapy

In contrast to anti-angiogenic therapy which aims at suppressing the growth of new blood vessels, anti-vascular therapy aims at targeting the established tumour vasculature causing a direct shut down in tumour blood flow leading to secondary tumour cell death. The potential therapeutic benefits of interfering with tumour blood flow were demonstrated by clamping off the feeding vessel of a tumour, which resulted in tumour growth delay, and after prolonged occlusions, to cures (Denekamp *et al.*, 1983). Subsequently, various other strategies for targeting the tumour vasculature were investigated (Denekamp, 1990).

1.2.3.1 Hyperthermia

Hyperthermia has been shown to affect the tumour microcirculation producing vascular damage and secondary tumour cell death (Reinhold and Endrich, 1986). The relative selectivity of the tumour vasculature to hyperthermia-induced vascular collapse probably relates to the particular tumour microenvironment characterised by hypoxia and low extracellular pH. Indeed, the thermal sensitivity of cells *in vitro* was found to be increased in nutrient-deprived and hypoxic cells and when the pH of the medium was lowered (reviewed in Denekamp, 1990). Furthermore, proliferating endothelial cells have been

shown to have an increased susceptibility to thermal stress (Fajardo *et al.*, 1985). Hyperthermia has been shown to induce erythrocyte aggregation and leukocyte adhesion with oedema and thrombosis development (Eddy, 1980). However, the response of human tumours to hyperthermia has been less dramatic than the effects obtained in experimental tumour models. The technique is also limited to superficial tumours and requires invasive methods.

1.2.3.2 Photodynamic Therapy

Photodynamic therapy involves the systemic administration of a photosensitiser and its local activation by light. The photo-excited sensitiser generates highly reactive oxygen species, which cause damage to both the tumour cells and associated vessels resulting in blood flow stasis and haemorrhagic necrosis. Photodynamic therapy has been reported to cause tumour destruction partly by damaging the associated endothelial cells within the vasculature, leading to the initiation of a cascade of events involving platelet aggregation, the release of vasoactive molecules, leukocyte adhesion and an increase in vascular permeability (reviewed in Krammer, 2001).

1.2.3.3 Cytokines

A number of cytokines have been shown to mediate anti-vascular effects in addition to their known anti-angiogenic activity, and this is thought to contribute to their overall anti-tumour actions. Inetrleukin-12 (IL-12) has been shown to mediate tumour necrosis in mouse models consistent with an anti-vascular action (Yao *et al.*, 2000). More recently, its anti-vascular activity was shown to be dependent on tumour blood vessel maturity related to the extent of pericyte coverage, with a high percentage of pericyte covered blood vessels showing resistance to IL-12 (Lee *et al.*, 2002a). Furthermore, interferon α/β injected intratumourally or peritumourally were also shown to induce rapid and pronounced vascular endothelial cell damage resulting in tumour coagulative necrosis in subcutaneous experimental tumours in mice (Dvorak and Gresser, 1989). However, the most well documented and widely accepted anti-vascular effects mediated by a cytokine have been attributed to the anti-tumour effects of tumour necrosis factor (TNF)-α. TNF-α was originally identified as an endotoxin-induced factor that was able to induce haemorrhagic necrosis of tumours in mice (Carswell *et al.*, 1975). It was later reported to have anti-vascular actions by direct cytotoxicity to tumour-associated vascular

endothelium (Watanabe *et al.*, 1988). Vascular congestion due to thrombus formation, fibrin deposition, platelet aggregation and marked endothelial cell damage are common histological features following TNF-α administration *in vivo* (Shimomura *et al.*, 1988; Proietti *et al.*, 1988). *In vitro*, TNF-α induced endothelial cell apoptosis (Robaye *et al.*, 1991), and was shown in combination with interferon γ to reduce activation of the integrin αVβ3 leading to decreased αVβ3-dependent endothelial cell adhesion and survival (Ruegg *et al.*, 1998). The latter has been suggested as a possible explanation for the selective tumour anti-vascular effects of TNF-α, since the αVβ3 integrin is selectively expressed on angiogenic blood vessels (Lejeune, 2002). Despite the promising pre-clinical anti-tumour effects of TNF-α, its systemic use in the clinic with advanced cancers showed only rare responses and its administration was also limited by a very low maximum tolerated dose and serious systemic toxicity (Lejeune *et al.*, 1998). Today, TNF-α has found applications when administered regionally in advanced melanomas and soft-tissue sarcomas of the limbs, where high dose TNF-α in combination with chemotherapy, and with or without interferon-γ, proved to be a highly efficient regimen (Lejeune *et al.*, 1998).

1.2.3.4 Antibody-based Therapy

This strategy aims to specifically target antigens on the surface of endothelial cells of tumours by means of selective antibodies in order to deliver an effector molecule (Thorpe and Burrows, 1995). Proof of principle was demonstrated by Huang and colleagues using a murine tumour model transfected with the interferon-γ gene, which when secreted by tumour cells caused local vascular expression of major histocompatibility complex (MHC) class II antigen, that is normally absent from rodent blood vessels. Using antibodies recognising MHC II and conjugated to a truncated form of tissue factor, a major inducer of the coagulation cascade, they demonstrated thrombosis of tumour vasculature and dramatic tumour regression (Huang *et al.*, 1997). This approach was then tested using naturally occurring markers on tumour vasculature. Tissue factor-conjugated antibodies against vascular cell adhesion molecule-1 (VCAM-1), present on vascular endothelial cells in a number of human tumours and a few normal tissues, also caused thrombosis in tumour blood vessels and retardation in growth of human Hodgkin's tumour xenografts (Ran *et al.*, 1998). Other studies have also demonstrated the benefits of

antibody-based therapies, whereby immunotoxin-conjugated antibodies against endoglin, a proliferation-associated antigen on tumour endothelial cells, were shown to induce long lasting and complete regression of human tumour xenografts (Matsuno *et al.*, 1999). In search for new targets, Tsunoda and colleagues produced an antibody, that specifically binds to tumour vascular endothelium in various tumour types, by immunising animals with plasma membrane vesicles from isolated tumour-derived endothelial cells (Tsunoda *et al.*, 1999). Conjugation of the antibody to an anti-tumour agent, and systemic administration of the immuno-conjugate resulted in its accumulation in the tumour tissue and enhanced anti-tumour effects without increased toxicity (Makimoto *et al.*, 1999).

The potential of antibody-based anti-vascular cancer therapy lies in the discovery of specific target markers expressed only on tumour-associated vascular endothelial cells. Peptide libraries expressed on the surface of engineered bacteriophage have offered a new tool for identifying new markers, by selecting phage particles which specifically home to tumour vasculature and recognise specific protein targets (Ruoslahti, 2000). To date promising candidate markers to which antibodies could be targeted include prostate specific membrane antigen, the $\alpha v\beta 3$ integrin and E-selectin, which are highly expressed on the endothelium of several tumour types (Thorpe and Ran, 2000). Recently, Arap *et al.* reported for the first time *in vivo* screening of a systemically administered peptide library in a human patient revealing that the circulating peptides home into specific tissues (Arap *et al.*, 2002). The data generated from this large scale screening is extremely valuable for the potential construction of a molecular map of the human vasculature, which would eventually allow for the development of targeted therapies in cancer and other diseases with the aim of increasing treatment effectiveness and minimising unwanted side effects (Arap *et al.*, 2002).

1.2.3.5 Gene-based Therapy

This strategy aims to target therapeutic genes to tumour-associated vascular endothelial cells to either kill them directly or sensitise them to radiation or chemotherapeutic agents (Fan *et al.*, 1995; Chaplin and Dougherty, 1999). In theory, this strategy would allow for a more selective targeting of tumour blood vessels than conventional therapies allowing for relative sparing of the normal vasculature. Delivery of therapeutic genes to the vasculature should be less of a problem than delivery to tumour cells since the targeted

endothelial cells are in direct contact with the blood. Finally, even the low transfection efficiency rates that are currently achievable *in vivo* may cause enough vascular damage to significantly affect tumour growth. Despite these theoretical advantages, the main problem with this approach remains in finding both safe and effective ways of specifically delivering the wanted genes to tumour-associated endothelial cells *in vivo*. Retroviral and adenoviral vectors can be genetically engineered to alter their target cell specificity. This could be achieved by incorporating tumour-endothelial cell specific peptides into the viral envelope, which would allow for specific homing of the viruses into tumour blood vessels for introduction and expression of the therapeutic gene (Chaplin and Dougherty, 1999). A further level of selectivity could be achieved by inclusion within the vectors used of regulatory elements that will restrict gene expression in the intended target cell only. Examples of such regulatory gene expression include placing the therapeutic gene under the control of promoters, which normally drive genes in activated endothelial cells during angiogenesis, or regulatory elements that will drive gene expression only under hypoxic conditions or in response to external stimuli such as radiation for instance (Chaplin and Dougherty, 1999).

1.2.3.6 Drug-based Therapy

This approach is based on the use of low molecular weight compounds. Two main classes of compounds have been found to possess anti-vascular properties:

1.2.3.6.1 Flavonoid Derivatives

Flavone acetic acid (FAA) was shown to inhibit tumour growth and cause regression of tumours in mice (Plowman *et al.*, 1986). It was later demonstrated that the anti-tumour effects of FAA were due to a reduction in tumour blood flow leading to haemorrhagic necrosis (Hill *et al.*, 1989; Bibby *et al.*, 1989; Zwi *et al.*, 1989; Mahadevan *et al.*, 1990). Furthermore, induction in the synthesis of cytokines such as TNF-α and IFN-α, and vasoactive mediators such as serotonin (5-HT) and NO were also demonstrated to account for the anti-vascular and anti-tumour effects of FAA (Baguley, 2001). However, despite promising effects in experimental tumour models, FAA was inactive in the clinic when tested in phase I/II clinical trials as a single agent (Kerr *et al.*, 1989), or in combination with the cytokine IL-2 (Holmund *et al.*, 1995).

Dimethylxanthenone-acetic acid (DMXAA) is an improved analogue of FAA, which has completed phase I clinical trials in the UK and New Zealand. The mechanism of action of this compound is still unclear but, as for FAA, involves the production of the vasoactive mediators 5-HT and NO, as well as the intra-tumoural production of TNF-α (Baguley, 2001). The fact that DMXAA was shown to be equally potent at increasing the production of TNF-α from both mouse and human macrophage cells, as opposed to FAA which induced TNF-α in mouse cells only, could explain the inactivity of FAA in the clinic (Ching *et al.*, 1994). More recently, DMXAA was also shown to induce rapid vascular endothelial cell apoptosis in some murine and human tumours independently from TNF-α production (Ching *et al.*, 2002) suggesting another possible mechanism for the anti-vascular effects of this drug.

1.2.3.6.2 Tubulin-Binding Agents

The anti-vascular properties of tubulin-binding agents were recognised many years ago with colchicine and podophyllotoxin causing haemorrhagic necrosis in tumours (reviewed in Tozer *et al.*, 2002). However, the severe systemic toxicity of these compounds, seen at doses required to produce anti-vascular effects, prevented any further clinical evaluation. More recently, the vinca alkaloids such as vincristine and vinblastine have been shown to cause dramatic and prolonged reduction in tumour blood flow accompanied by haemorrhagic necrosis in tumour models, but also at close to their maximum tolerated doses (Baguley *et al.*, 1991; Hill *et al.*, 1993). These compounds have a well-established cytotoxicity and are potent anticancer drugs used in the clinic. The combretastatins are also microtubule binding agents that have demonstrated anti-vascular effects (reviewed in Tozer *et al.*, 2002). They have shown potential promise with extensive pre-clinical development of combretastatin A4-phosphate (CA-4-P) and its entry into Phase I clinical trials in the UK and the USA in late 1998, which have now been completed. A detailed review on CA-4-P is given in section 1.4.

1.3 Tubulin-Binding Agents and the Cell Cytoskeleton

1.3.1 Cell Cytoskeleton

In this section, structure and function of the cell cytoskeleton are described in order to understand how tubulin-binding agents such as CA-4-P interact with their cellular targets to mediate their effects. The cytoskeleton is a complex network of protein filaments

extending throughout the cytoplasm of eukaryotic cells. It is responsible for the control of cell shape, motility and division as well as the spatial organisation of the organelles and their movement within the cytoplasm. The cytoskeleton is made up of three main types of protein filaments: actin filaments, intermediate filaments and microtubules (Figure 1.3). These filaments interact with various proteins to regulate their assembly and interactions with one another, and also connect with other cellular components such as the plasma membrane.

Actin filaments are arranged in tight helical structures resulting from the polymerisation of globular actin monomers (Figure 1.3A). In most animal cells, actin filaments and their associated proteins are organised into a dense network just beneath the plasma membrane forming the cell cortex. This network is responsible for giving mechanical strength to the surface of the cell allowing it to change shape and move. Intermediate filaments are tough rope-like structures made up of cell-type specific fibrous polypeptides. These dimerise into coiled-coil structures which then associate with one another to form a protofilament. The final intermediate filament is thought to be made up of 8 such protofilaments (Figure 1.3B). In most animal cells, intermediate filaments are arranged around the nucleus and extend out to the cell periphery and are thought to play a structural and tension-bearing role. Microtubules are hollow tubes made up of 13 protofilaments, which result from the polymerisation of α- and β-tubulin heterodimers (Figure 1.3C). They usually radiate outward throughout the cytoplasm from a position close to the nucleus.

1.3.2 Microtubule Dynamics and Function

Microtubules are very labile structures in a dynamic state. This dynamic instability results in continual and rapid turnover of most microtubules, which have half-lives within the cells of only ~10 minutes. Tubulin molecules, on the other hand, have an average half-life of more than 20 hours and will therefore participate in the formation and dismantling of many microtubules during that lifetime. The tubulin subunits in a microtubule are arranged in a specific orientation giving the microtubule an inherent polarity, with a fast growing end (plus end) and a slow growing end (minus end). Each monomer of tubulin binds a guanine nucleotide. In the tubulin heterodimer, α-tubulin is oriented towards the minus end and is always bound to non-exchangeable GTP, whereas β-tubulin is oriented towards the plus end and exchanges GTP and GDP (Figure 1.4). A β-tubulin bound to

GTP is competent for assembly, and hydrolysis following polymerisation results in a microtubule containing GDP-tubulin (Figure 1.5). A growing microtubule may have a GTP cap at the plus end, which protects it from depolymerisation (Figure 1.5). Loss of the GTP cap causes rapid depolymerisation. In almost all animal cells, microtubules nucleate from one major microtubule organising centre known as the centrosome, which is located to one side of the nucleus. The minus ends of the microtubules are located within the centrosome and thus protected from depolymerisation, whereas the plus ends are free and subject to depolymerisation unless capped by a structure in a particular region of the cell preventing their depolymerisation and causing their stabilisation (Figure 1.6).

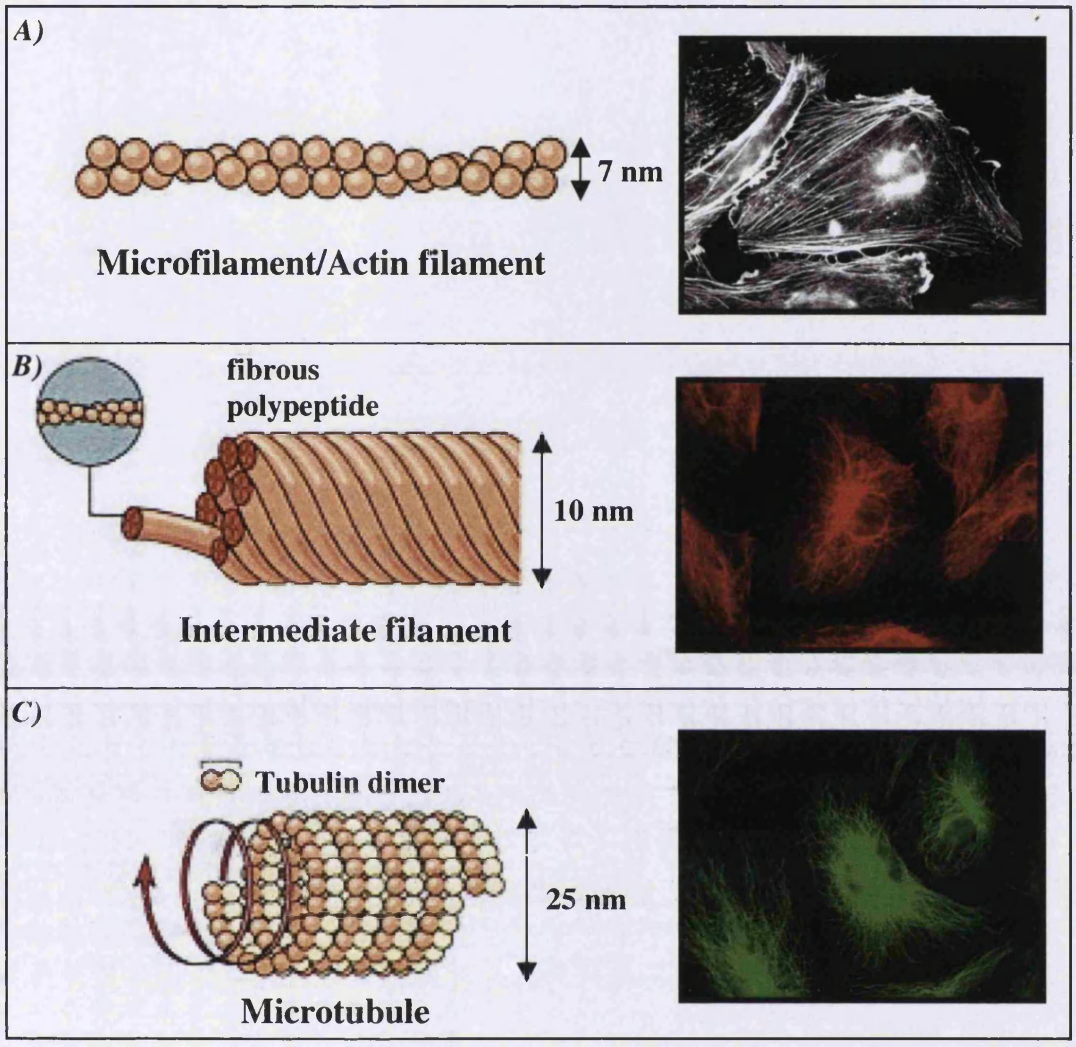

Figure 1.3 Structure of the three main filaments constituting the cell cytoskeleton. ***A)*** Actin filaments are arranged in tight helical structures of about 7-8 nm in diameter. The image on the right shows actin distribution in Human Umbilical Vein Endothelial Cells (HUVECs) stained by immunofluorescence using phalloidin. ***B)*** Intermediate filaments are tough rope-like structures of about 10 nm in diameter. The image on the right shows the distribution of intermediate filaments in HUVECs stained by immunofluorescence using an anti-vimentin antibody. ***C)*** Microtubules are hollow tubes of about 25 nm in diameter. The image on the right shows the distribution of microtubules in HUVECs stained by immunofluorescence using an anti-β-tubulin antibody. The immunofluorescence images were kindly provided by Dr Chryso Kanthou (Gray Cancer Institute).

The processes described above are characteristic events occurring in cells undergoing microtubule reorganisation in order to perform various functions such as movement or division. However, in quiescent and completely differentiated cells that no longer divide,

the microtubule network is in a more stable and mature state. This is achieved by post-translational modification of the tubulin subunits such as acetylation and detyrosination and also by interaction of microtubules with specific microtubule-associated proteins. The latter allow links to be established between microtubules and other cellular components such as the actin and intermediate filaments, as well as specific organelle membranes. Furthermore, specific microtubule-associated proteins are also involved in the movement of organelles along microtubules.

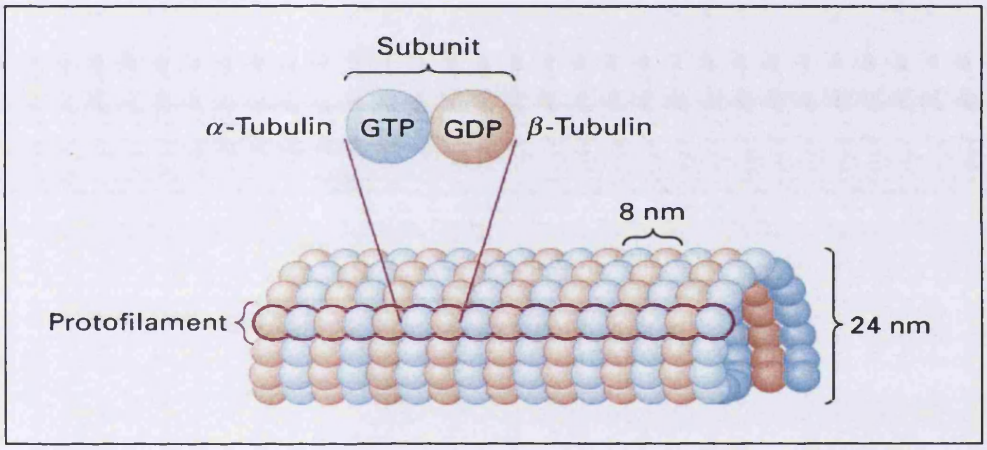

Figure 1.4 Microtubule structure. Each microtubule contains 13 protofilaments made up of α and β heterodimers. α-tubulin is bound to non-exchangeable GTP, whereas β-tubulin exchanges GTP and GDP.

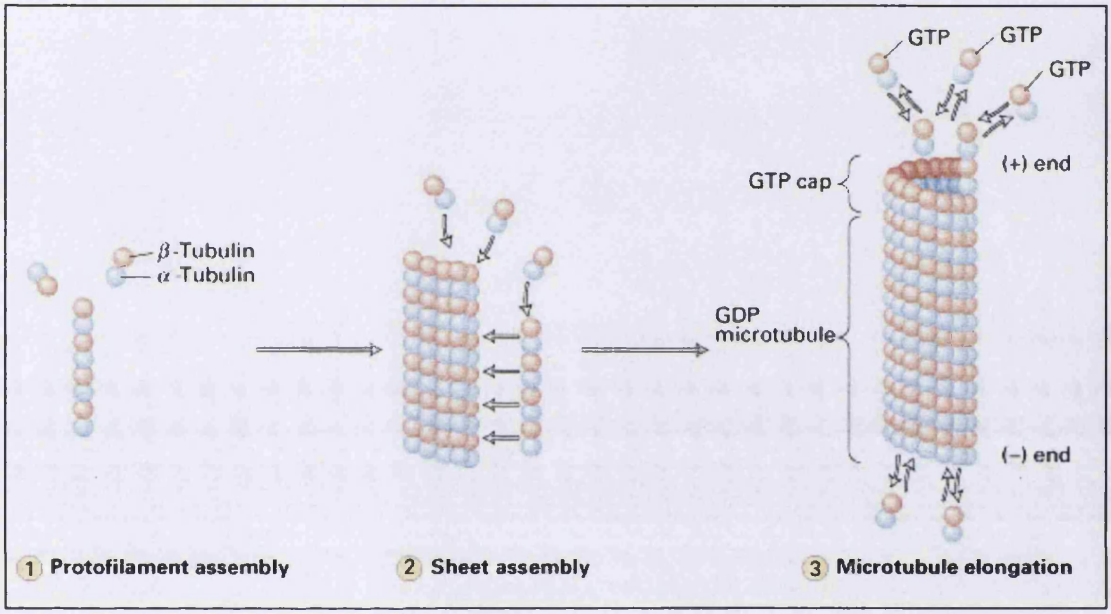

Figure 1.5 Microtubule assembly. The subunits made up of α and β heterodimers associate linearly to form protofilaments with the β-tubulin oriented towards the fast growing plus end (1). The protofilaments in turn associate laterally (2) and form the hollow cylindrical wall of the microtubule (3). A β-tubulin bound to GTP is competent for assembly, and hydrolysis following polymerisation results in a microtubule containing GDP-tubulin. A growing microtubule may have a GTP cap at the plus end, which protects it from depolymerisation (3). Loss of the GTP cap causes rapid depolymerisation.

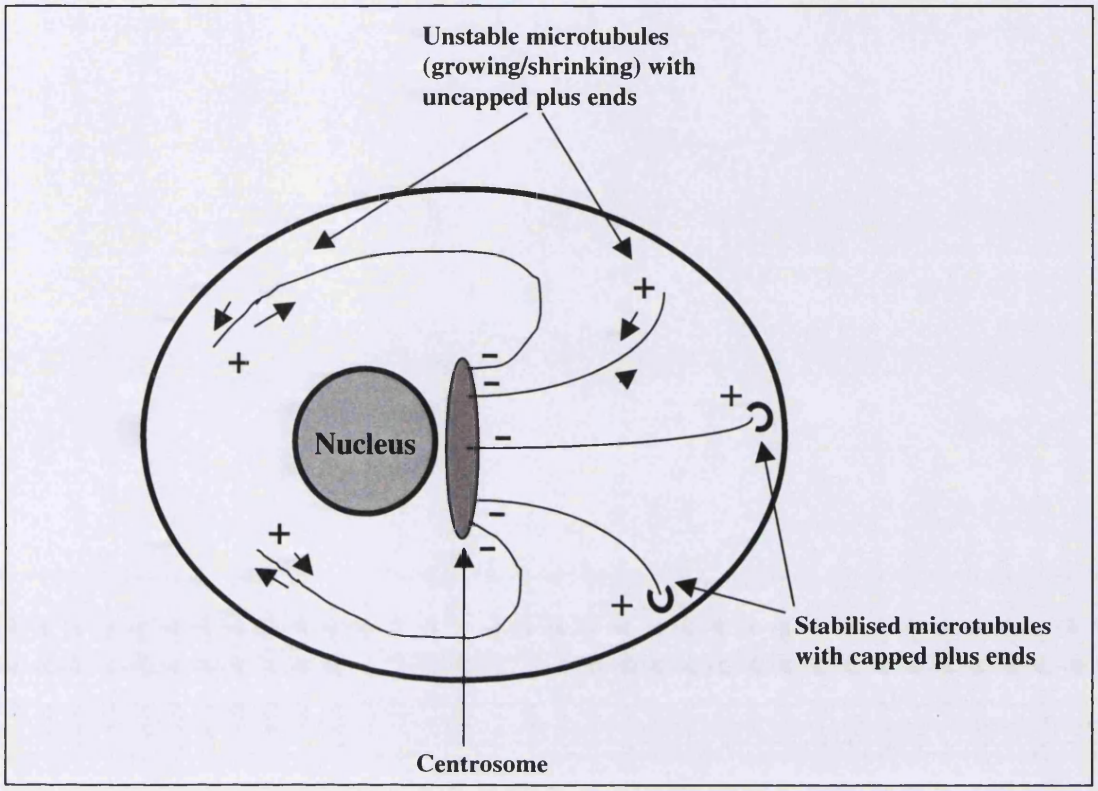

Figure 1.6 Dynamic instability of microtubule structures. Microtubules grow from one major microtubule organising centre called the centrosome, which is located to one side of the nucleus. The minus ends of the microtubules are located within the centrosome and thus protected from depolymerisation, whereas the plus ends are free and subject to depolymerisation unless capped by a structure in a particular region of the cell preventing their depolymerisation and causing their stabilisation. Adapted from Alberts, 1989.

1.3.3 Tubulin-Drug Interactions and Activation of Cell Signalling

Three main classes of tubulin-binding agents have been characterised, according to their binding sites on the protein, and include agents that interact with the colchicine site, the vinca domain or the taxol-binding site (Downing, 2000). In the following sections, the mechanism of action of the prototype compounds for each class, namely colchicine, the vinca alkaloids and taxol are described.

The dynamic instability of microtubules is fundamental for the rapid rearrangement of these structures in response to mitogenic signals. Thus, the formation of the mitotic spindle is the most sensitive process to drug-induced changes in microtubule dynamics.

This causes the treated cells to accumulate in the G2/M phase of the cell cycle, with progression to apoptosis in most cases (Jordan and Wilson, 1998). Studies with microtubule disrupting agents have also demonstrated accumulating evidence for an important role of the microtubule cytoskeleton in the control of gene expression (Gundersen and Cook, 1999).

1.3.3.1 Drug Interactions

Colchicine was originally isolated from the autumn crocus *Colchicum autumnale* and was extensively used in studies on mitosis. Colchicine mainly interacts with β-tubulin on the heterodimers, leading to inhibition of microtubule polymerisation (Margolis and Wilson, 1977). Colchicine is only used at low doses for the treatment of acute gout attacks because of serious side effects.

The *vinca alkaloids* were isolated from the plant *Catharanthus roseus* and include the chemically related vinblastine and vincristine and the novel semisynthetic derivative vinorelbine (Fahy, 2001). These compounds bind to tubulin heterodimers on a site thought to be located on the β-subunit and close to but distinct from the colchicine-binding site preventing further polymerisation of microtubules (Sackett, 1995). However, at high concentrations they were reported to be able to bind to tubulin on microtubules, although with an apparent lower affinity, causing microtubule depolymerisation (Jordan *et al.*, 1986; Jordan, 2002). In addition, they were shown to induce self-association of tubulin into non-microtubule polymers to form spirals and paracrystalline aggregates (Erickson, 1975; Na and Timasheff, 1982; Jordan, 2002). The vinca alkaloids are widely used in the clinic as anti-tumour agents for the treatment of leukaemias, lymphomas, and some solid tumours (e.g. breast and lung cancer). Vinorelbine is used to treat advanced breast and non-small cell lung cancers (British National Formulary, September 2002). Neurological toxicity is the major side effect of treatment with all the vinca alkaloids and is the limiting side effect of vincristine (British National Formulary, September 2002). Myelosuppression is the dose limiting toxicity of vinblastine and vinorelbine (British National Formulary, September 2002).

Finally, the *taxanes* were originally isolated from the bark of the Western yew tree *Taxus brevifolia*, and include Taxol (paclitaxel) and its semi-synthetic analogue Taxotere

(docetaxel). The taxanes preferentially bind to microtubules, rather than tubulin dimers, at sites distinct from the binding sites of the vinca alkaloids and colchicine (Sackett and Fojo, 1997). Taxanes bind to the β-tubulin of microtubules, and tubulin crystal structure has demonstrated one Taxol site per tubulin heterodimer affecting the interaction between protofilaments (Nogales *et al.*, 1995). Taxane binding causes stabilisation of microtubules by suppressing dynamic changes, growing and shortening, leading to mitotic arrest (Jordan *et al.*, 1993). Paclitaxel in combination with carboplatin or cisplatin is the treatment of choice for ovarian cancer (British National Formulary, September 2002). Paclitaxel is also used in the secondary treatment of metastatic breast cancer (British National Formulary, September 2002). The main side effects of paclitaxel include severe hypersensitivity reactions, myelosuppression, and peripheral neuropathy. Docetaxel is used in the treatment of advanced or metastatic breast cancer and in non-small cell lung cancer (British National Formulary, September 2002). Its side effects are similar to paclitaxel but also include fluid retention (British National Formulary, September 2002).

Some drugs have been shown to interact with microtubules on sites other than those mentioned above. *Estramustine* was originally designed as an alkylating agent being a combination of a nitrogen mustard and oestradiol, but it was then shown to mediate its effects not through DNA targets, failing to cause the formation of alkylating intermediates, but rather by interference with microtubules (Tew *et al.*, 1992). However, the target of this drug on microtubules is still unclear. Controversial findings have been reported with regard to whether estramustine directly interacts with tubulin to cause depolymerisation of microtubules (Dahllof *et al.*, 1993), or binds to microtubule-associated proteins to prevent microtubule stabilisation leading to their depolymerisation (Stearns and Tew, 1988). Estramustine is predominantly used for the treatment of prostate cancer (British National Formulary, September 2002).

1.3.3.2 Microtubule Disruption and Cell Signalling Pathways

Drugs that interfere with microtubules either to stabilise or destabilise them have been shown to have specific effects on diverse cellular processes involving signal transduction such as cell proliferation, gene expression, receptor signalling and apoptosis (Gundersen and Cook, 1999). It is thought that these agents bind specifically to tubulin/microtubules and have few other direct cellular targets, thereby strongly implicating a role for

microtubules in the control of these cellular processes (Gundersen and Cook, 1999). A number of studies have demonstrated a prominent involvement of the microtubule cytoskeleton in the activation of certain genes. Marczin and colleagues reported that an intact microtubule cytoskeleton is essential for the induction of inducible NOS (iNOS), whereby disruption of microtubules by colchicine or nocodazole decreased basal levels of iNOS and prevented the induction of this enzyme in response to inflammatory mediators in vascular smooth muscle cells (Marczin *et al.*, 1993; Marczin *et al.*, 1996). These studies also showed a differential regulation of the constitutive and inducible pathways of NO synthesis in response to microtubule disruption, in that unlike iNOS, constitutive NOS was not under cytoskeletal control since the same treatment did not affect constitutive synthesis of NO in endothelial cells (Marczin *et al.*, 1996). From these studies, it is still not clear at which level of the protein synthesis process microtubules play a critical role, although there is evidence that microtubule disruption could affect the stability of mRNA by interfering with the translation process (Walker and Whitfield, 1985).

Drug-induced disassembly of the microtubule cytoskeleton has also been shown to induce gene expression and it has been proposed that a possible way by which the cytoskeleton could affect this process would be by modulating the activity of transcription factors found in the cytoplasm. Indeed, a number of studies have provided evidence that a variety of agents and conditions that depolymerise microtubules are able to activate the transcription factor nuclear factor-κB (NFκB) and induce NFκB-dependent gene expression (Rosette and Karin, 1995; Das and White, 1997). In unstimulated cells, NFκB is found in the cytoplasm as a complex with its inhibitor IκB. In response to signals which lead to phosphorylation of IκB, NFκB is released and translocates into the nucleus where it recognises specific binding sites on the DNA and controls the expression of various genes. There is evidence that various microtubule disrupting agents induce phosphorylation of IκB via activation of protein kinase C (PKC), thereby leading to activation of NFκB (Das and White, 1997). Furthermore, there is also evidence that microtubule disruption could lead to the activation of another transcription factor named activator protein-1 (AP-1) and induction of AP-1-dependent gene expression. This was demonstrated to occur via activation of members of the mitogen activated protein kinases (MAPKs), rather than through the PKC activation pathway (Irigoyen *et al.*, 1997). MAPKs are serine/threonine protein kinases that occupy a central role in the signalling

cascades regulating cellular processes such as cell growth, differentiation and apoptosis. Once activated, MAPKs can phosphorylate many transcription factors and ultimately lead to changes in gene expression. The JNK and p38 enzymes are generally thought to be activated by various stress-related stimuli, including heat shock, inflammatory cytokines, oxidative stress and proapoptotic agents, while the ERK pathways generally mediate cellular processes related to proliferation and differentiation (Schaeffer and Weber, 1999).

In summary, it appears that drug-induced microtubule disruption can indeed result in changes in gene expression occurring via the activation of kinases and transcription factors ultimately leading to modulation of the expression of those genes whose expression is under the control of those particular activated transcription factors.

1.4 Combretastatin A4-Phosphate

1.4.1 In Vivo and In Vitro Effects of Combretastatin A4-Phosphate

Combretastatin A4-phosphate (CA-4-P) belongs to the family of combretastatins, which are compounds that have been isolated from the South African tree *Combretum caffrum* (Pettit *et al.*, 1987). The active drug CA-4 is structurally similar to the tubulin binding agent colchicine (Figure 1.7). It has been shown to bind to tubulin at the colchicine-binding site causing disruption of microtubule function leading to destabilisation of the cell cytoskeleton (Pettit *et al.*, 1989; Woods *et al.*, 1995). CA-4-P pro-drug (Figure 1.7) is a more soluble derivative, which is cleaved *in vivo* to the active form CA-4 by endogenous non-specific phosphatases.

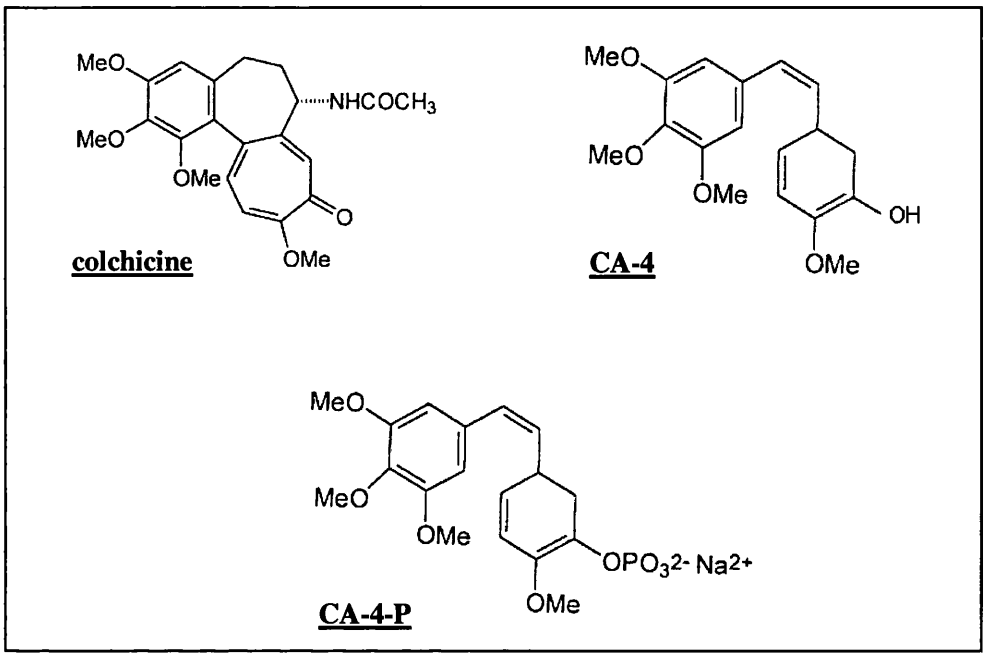

Figure 1.7 Structures of colchicine, CA-4 and CA-4-P.

In vivo, CA-4-P has been shown to cause vascular collapse in a range of transplanted and spontaneous murine tumours as well as xenografted human tumours and vascularised metastases at relatively non-toxic doses (Dark *et al.*, 1997; Horsman *et al.*, 1998; Chaplin *et al.*, 1999a; Tozer *et al.*, 1999; Malcontenti-Wilson *et al.*, 2001). Its selectivity for decreasing blood flow in the tumour as compared to a range of normal tissues was demonstrated in a rat tumour model (Tozer *et al.*, 1999). Histological studies have shown extensive haemorrhagic necrosis resulting from vascular damage with only a small rim of viable tumour remaining in the periphery (Dark *et al.*, 1997, Li *et al.*, 1998). It is thought that this surviving population of cells could be eradicated using conventional radiation or chemotherapeutic agents (see section 1.4.2).

To further elucidate the mechanism of action of CA-4-P, a number of *in vitro* studies have been carried out. These have demonstrated that exposure of both endothelial and tumour cells to CA-4-P can lead to profound long-term antiproliferative/cytotoxic effects (Dark *et al.*, 1997; Nabha *et al.*, 2000; Boehle *et al.*, 2000; Boehle *et al.*, 2001). There is evidence that endothelial cells may be particularly sensitive to CA-4-P with regard to both the extent of microtubule depolymerisation and cytotoxicity (Dark *et al.*, 1997; Boehle *et al.*,

2000). At present the mechanisms leading to cytotoxicity are still unclear and both apoptosis-dependent and independent pathways of cell death have been identified (Iyer *et al.*, 1998; Boehle *et al.*, 2000; Nabha *et al.*, 2000). More recently, the signalling pathways activated following exposure to CA-4-P have been examined in endothelial cells, and phosphorylation and activation of the stress-induced kinase p38 was reported, suggesting potential down-stream activation of transciption factors leading to modulation in the expression of target genes (Kanthou and Tozer, 2002).

Although the cytotoxic effects reported in *in vitro* studies are likely to play a role *in vivo*, they cannot explain the rapid blood flow shut down that occurs in tumours after a single dose of CA-4-P (Tozer *et al.*, 2001; Tozer *et al.*, 2002). CA-4-P causes a rapid increase in permeability of an endothelial cell monolayer to high molecular weight dextrans (Kanthou and Tozer, 2002) and an increase in vascular permeability of tumour blood vessels *in vivo*, within minutes of drug exposure (Tozer *et al.*, 2001). This increase in vascular permeability is a likely trigger for vascular shut down via development of tissue oedema, followed by an increase in blood viscosity and/or an increase in interstitial fluid pressure. These effects are probably enhanced by direct effects on tumour vascular resistance arising from changes in endothelial cell shape. These effects have been reported for endothelial cells *in vitro,* where they have been shown to contract and round up within minutes of exposure to CA-4-P (Galbraith *et al.*, 2001; Kanthou and Tozer, 2002). These vascular effects of CA-4-P *in vivo* closely resemble that of an acute inflammatory-type of reaction (Tozer *et al.*, 2001).

The effects mediated by CA-4-P have also been examined at later times, at which a significant recruitment of neutrophils into tumours is observed (Parkins *et al.*, 2000), suggesting their involvement in the late phase events, namely tumour cell kill via the production of oxygen free radicals. Furthermore, it has been suggested that endogenous NO production plays a protective role against CA-4-P vascular damage. Studies have shown that administration of CA-4-P in the presence of the NOS inhibitor, L-NAME, potentiates the effects mediated by CA-4-P alone in the tumour with much less significant effects in normal tissues (Tozer *et al.*, 1999; Parkins *et al.*, 2000). This protective effect of NO has been suggested to be partially mediated by an anti-neutrophil action of NO

characterised by limiting neutrophil infiltration into the tumour tissue (Parkins *et al.*, 2000).

These complex events suggest the potential involvement of several other factors/pathways, which could contribute in enhancing or diminishing the final outcome seen following CA-4-P administration. In this regard, investigating the role of potential protective enzymes such as haemoxygenase-1 (see section 1.5), during this injury/inflammatory-type of reaction could open new avenues for improving the therapeutic potential of CA-4-P.

1.4.2 Combination Therapy Strategies with Combretastatin A4-Phosphate

Recent pharmacokinetic data obtained for CA-4-P demonstrated that the plasma exposure achieved with 10 mg/kg in the rat is similar to that achievable in the clinic after the maximum tolerated dose of 65 mg/m^2 (Prise *et al.*, 2002). This dose proves to be significantly lower than that used in most of the animal work published on CA-4-P. Recent studies using this 10 mg/kg clinically relevant dose of CA-4-P have shown that the initial acute decrease in blood flow achieved with this dose was similar to the much higher dose of 100 mg/kg, but recovery was much quicker with the lower dose and as a result the development of tumour necrosis was less extensive (Tozer *et al.*, 1999; Prise *et al.*, 2002). These studies also confirmed previous observations of viable cells remaining at the tumour periphery following treatment with CA-4-P (Dark *et al.*, 1997; Li *et al.*, 1998). This viable rim of tumour cells serves to re-populate the tumour and, probably accounts for the relative ineffectiveness of CA-4-P as a single anti-tumour agent (Chaplin *et al.*, 1999a). The fact that this spared tumour rim is often well vascularised and therefore probably well oxygenated constitutes the rationale for combining CA-4-P with conventional cancer therapies (reviewed in Tozer *et al.*, 2002).

In this regard, several studies have demonstrated that CA-4-P can selectively enhance the radiation response of tumours with no detrimental effects to the normal surrounding tissue (Chaplin *et al.*, 1999a; Murata *et al.*, 2001a). Murata and colleagues have shown that in some tumour models the outcome of treatment was dependent on the sequence in which CA-4-P and radiation were given (Murata *et al.*, 2001a). The authors suggest that in these particular tumour types CA-4-P treatment may increase tumour hypoxia if given before

radiation, thereby rendering this new hypoxic tumour cell population resistant to subsequent radiation damage. In tumours where such an effect could occur the time of CA-4-P administration becomes a very important factor to take into account when choosing a particular scheduling regimen. However, in other tumour types where such a careful scheduling was shown not to be so important, it was suggested that CA-4-P may be enhancing radiation-induced damage by elimination of the radio-resistant hypoxic cell population (Murata *et al.*, 2001a; Li *et al.*, 1998). These findings have obvious therapeutic implications and emphasise the importance of a careful scheduling strategy for particular tumour types.

The anti-tumour effects of CA-4-P were also found to be enhanced by hyperthermia (Horsman *et al.*, 2000; Eikesdal *et al.*, 2001). In addition, when mild hyperthermia was added to a CA-4-P combined to radiation regimen, a further increased therapeutic benefit was observed, although this also led to an increase in normal tissue damage (Murata *et al.*, 2001b).

CA-4-P was also tested in combination with conventional chemotherapeutic agents. Horsman and colleagues have shown that administration of cisplatin 1h following CA-4-P had only an additive effect, although with this treatment regimen the dose of cisplatin could be reduced by 25% resulting in less systemic toxicity (Horsman *et al.*, 2000). Better results were obtained in a previous study, where cisplatin was given 15 minutes prior to CA-4-P (Chaplin *et al.*, 1999a). Improved anti-tumour effects of CA-4-P were also observed when combined with doxorubicin (Nelkin *et al.*, 2001) and 5-fluorouracil (Grosios *et al.*, 2000). However, no significant lengthening in the tumour growth delay induced by CA-4-P alone was obtained in combination with the anti-angiogenic agent TNP-470 (Landuyt *et al.*, 2001). In this study TNP-470 was given after CA-4-P, an inadequate scheduling regimen possibly due to the extensive blood flow shut down mediated by CA-4-P stopping TNP-470 from reaching its target. This further demonstrates the complications encountered when having to choose an appropriate scheduling regimen in order to maximise the effectiveness of combination strategies.

Impressive results were obtained recently with CA-4-P combined with radioimmunotherapy (Pedley *et al.*, 2001). In radioimmunotherapy, radionuclides are specifically targeted to the tumour by tagging them to antibodies, which will selectively

accumulate in the tumour. The rationale for this combination strategy relates to the fact that these tagged antibodies tend to accumulate in the outer well-perfused regions of the tumour and not in the centre. Whereas, CA-4-P treatment usually spares the outer rim of the tumour being most effective at killing the cells in the centre. The effectiveness of this combination was shown in colorectal xenografts where 5 out of 6 mice were completely cured for over 9 months (Pedley *et al.*, 2001). Although very high doses of CA-4-P were used in these studies and are therefore unlikely to be clinically applicable, the results obtained reflect the importance of taking into consideration the heterogeneity of the tumour when designing combination regimens in order to obtain maximally effective results.

Finally, our laboratory has also found benefits in combining CA-4-P and bioreductive drugs, which are only metabolised to toxic products in hypoxic areas of the tumour. Agents such as tirapazamine and AQ4N have no anti-tumour effects on their own but are able to significantly enhance the growth delay mediated by CA-4-P alone in the CaNT mouse mammary carcinoma (Tozer *et al.*, 2002; unpublished data). These findings indicate that CA-4-P treatment may be inducing transient hypoxia in a sub-population of tumour cells, which are able to recover and participate in the re-population of the tumour. This also suggests that agents that would interfere with this recovery pathway may be useful in enhancing the therapeutic potential of CA-4-P.

1.5 The Haemoxygenase System

Haemoxygenase (HO) is an essential enzyme responsible for the catabolism of haem. It was initially thought to be only responsible for the degradation of haem but recently evidence has emerged for a more complex role of the HO pathway in the control of cellular homeostasis. The generation of mice deficient in functional HO-1 revealed a partial prenatal lethality among the HO-1 knockout animals with a lower than expecetd survival percentage of 20% (Poss and Tonegawa, 1997a). The surviving adult mice showed retarded growth and developed an anaemia due to low serum iron levels. However, in these mice an iron deposition was observed in both liver and kidneys that contributed to oxidative tissue injury and chronic inflammation (Poss and Tonegawa, 1997a). Furthermore, embryonic fibroblasts isolated from the HO-1 knockout animals showed increased sensitivity to oxidative challenge (Poss and Tonegawa, 1997b). The

first human case of HO-1 deficiency reported by Yachie *et al.* in a 6-year old boy showed very similar phenotypical characterstics to the mouse knockout involving growth retardation, anaemia, iron deposition and increased susceptibility to oxidative stimuli (Yachie *et al.*, 1999). More recently, the products resulting from the degradation of haem by HO, namely bilirubin and carbon monoxide have also been the focus of a number of studies which have demonstrated their important biological functions (see section 1.5.4). Recent evidence has also implicated the HO system in cell proliferation and angiogenesis thereby highlighting the potential importance of this enzyme in tumour progression. These points are discussed in detail in the following sections.

1.5.1 The Haem Degrading System

In 1968 Tenhunen *et al.* described a microsomal enzyme system in rat liver capable of degrading haem to the bile pigment bilirubin, named haemoxygenase (Tenhunen *et al.*, 1968). It was later confirmed that HO is the rate-limiting enzyme involved in the physiological degradation of haem to produce biliverdin, iron and carbon monoxide (CO) (Figure 1.8). The HO enzyme is exclusively localised in the endoplasmic reticulum in cells and is predominantly restricted to the smooth endoplasmic reticulum. HO has a hydrophobic region on the carboxyl C-terminus that is responsible for anchoring the enzyme to the membrane of the endoplasmic reticulum. On the other hand, the amino N-terminus of the protein has a hydrophilic sequence that remains cytoplasmic. The reaction catalysed by HO requires molecular oxygen and NADPH as well as the concerted action of NADPH-cytochrome P-450 reductase. The reducing agent NADPH is needed for the activation of oxygen and the reduction of ferric iron (Fe^{3+}) to ferrous iron (Fe^{2+}) or the maintenance of the iron in the latter state. The haem molecules of the b-type are preferentially cleaved at the α-meso carbon-bridge to produce biliverdin IXα. During this reaction CO and free iron are also released. In mammals, biliverdin is subsequently converted to the bile pigment bilirubin by the cytosolic enzyme biliverdin reductase. Bilirubin is conjugated with glucuronates (sugars) and excreted in the bile as a more water-soluble molecule (Figure 1.8).

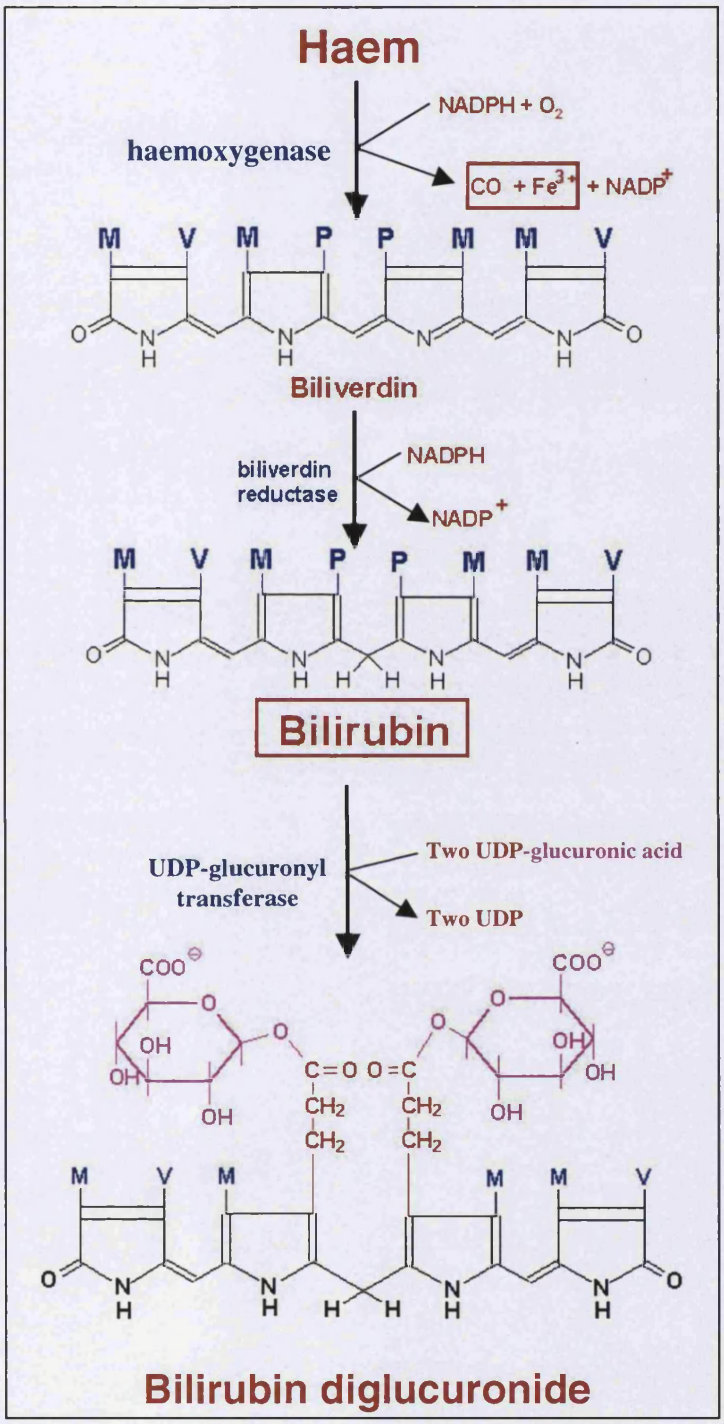

Figure 1.8 The haem degradation pathway. The oxidation of haem by HO produces the linear tetrapyrrol biliverdin, ferric iron (Fe^{3+}) and CO. In the next reaction biliverdin is reduced by biliverdin reductase producing bilirubin. In hepatocytes, uridine diphosphate (UDP)-glucuronyl transferase adds two glucuronic acid molecules to bilirubin producing a more water soluble bilirubin diglucuronide derivative. M: methyl ($-CH_3$); V: vinyl ($-CH=CH_2$); P: proprionic ($-CH_2-CH_2-COOH$).

1.5.2 The Haemoxygenase Isozymes

To date three isozymes of HO have been identified, HO-1, HO-2 and HO-3. These proteins have been shown to be the products of different genes (Cruse *et al.*, 1988; McCoubrey *et al.*, 1997) and to share few similarities with regard to tissue distribution, structure and biochemical regulation (McCoubrey and Maines, 1994; McCoubrey *et al.*, 1997). HO enzyme activity has been observed in all systemic organs analysed to date. However, the level of activity and the relative isozyme abundance vary between different tissues. In the rat, the HO activity has been reported to be highest in the spleen, testes, brain and liver in decreasing order, with the kidney, lung, heart and small intestine showing much lower values, again in decreasing order (Maines, 1988).

1.5.2.1 HO-1

HO-1 is a 32 kDa protein, which is also known as heat shock protein-32 (HSP-32). HO-1 is a single-copy gene and the protein is the product of a single mRNA transcript of ~1.8 kb (Yoshida *et al.*, 1974). HO-1 is inducible and has been shown to be present at very low levels, if at all, in most tissues under unstimulated conditions. The spleen is the only exception in that it shows high resting levels of HO-1, probably due to its role in erythrocyte recycling and the resulting need for haem degradation (Braggins *et al.*, 1986). HO-1 was shown to be significantly induced in a variety of tissues and cells in response to a variety of unrelated stimuli and pathological conditions (Morse and Choi, 2002). A common feature to these inducers and some of the listed conditions is their involvement in causing an imbalance in the redox state of the cell resulting in cellular and tissue injury (Otterbein and Choi, 2000). These findings have suggested that increased HO-1 protein levels under such stressed conditions could be a cellular defence mechanism which would protect the tissue from injury via the production of the biologically active molecules bilirubin and CO (Otterbein and Choi, 2000). Several *in vitro* and *in vivo* studies have demonstrated the protective effects of HO-1. The cytoprotective roles of HO-1 induction and the products of haem degradation by this enzyme are discussed in detail later in this Chapter (see sections 1.5.3 and 1.5.4).

1.5.2.2 HO-2

HO-2 is an approximately 36 kDa protein and a separate gene product from the other isozymes (Cruse *et al.*, 1988; McCoubrey *et al.*, 1997). HO-2 and HO-1 share less than

50% homology in both amino acid and nucleotide sequence (Rotenberg and Maines, 1990; Rotenberg and Maines, 1991). However, studies have shown that there is a 24 amino acid sequence which is highly conserved between the isozymes and which is thought to represent the haem binding/catalytic pocket (Maines, 1988; Rotenberg and Maines, 1991). Studies have shown that HO-2 is a single-copy gene although the protein is the product of two or more mRNA transcripts (McCoubrey and Maines, 1994; McCoubrey *et al.*, 1995). The HO-2 gene is constitutively expressed and uninducible, being refractory to the stimuli which cause induction of HO-1, thereby demonstrating different regulatory mechanisms for the two isozymes (Maines *et al.*, 1986; Trakshel *et al.*, 1986; Shibahara *et al.*, 1993). Up to date, HO-2 has been shown to be only responsive to adrenal glucocorticoids and this is due to the presence of a single functional glucocorticoid responsive element in the promoter region of the gene (Raju *et al.*, 1997). However, enhancement of HO-2 enzyme activity has been shown to be possible in response to phorbol esters via protein kinase C-mediated phosphorylation of the HO-2 protein (Doré *et al.*, 1999). HO-2 is catalytically active and shares with HO-1 similar substrate specificity and co-factor requirements (Maines *et al.*, 1986; Trakshel *et al.*, 1986). With regard to tissue distribution, HO-2 has been shown to be most abundant in the brain and testes, supporting a role for this enzyme in both the nervous and male reproductive systems (Maines, 2000; Liu *et al.*, 2000). However, HO-2 is present at lower levels in most tissues including the liver, kidney, spleen, as well as the cardiovascular system and the vasculature comprising the endothelial and smooth muscle cell lining of blood vessels (Maines, 1988; Maines, 1997).

The localisation of the HO isozymes to the vasculature is of particular interest in this project with regard to possible roles of the HO system in the regulation of vascular tone in tumours. Several studies have shown that HO-2 (and HO-1 under stressful conditions) is present in the endothelial and smooth muscle lining of blood vessels and that HO activity under unstimulated conditions contributes to the regulation of vascular tone via the generation of CO (Zhang *et al.*, 2001). In one study, HO-2 was shown to be immunolocalised to the endothelium of blood vessels, where endothelial cells of pulmonary and mesenteric arteries showed prominent positive staining (Zakhary *et al.*, 1996). Furthermore, HO-2 protein was also detected by western blotting in homogenates of arterioles, and endogenous HO enzyme activity in these resistance vessels was shown to contribute to the regulation of their diameter (Kozma *et al.*, 1999). The contribution of

the HO system to the regulation of vascular tone, via the generation of CO, is discussed further in section 1.5.4.3.1.

1.5.2.3 HO-3

HO-3 is a newly characterised 33 kDa protein. The HO-3 transcript can be found in a variety of organs including spleen, liver, thymus, prostate, heart, kidney, brain and testes and is the product of a single copy gene (McCoubrey *et al.*, 1997). The HO-3 amino acid structure shares 90% homology with the HO-2 protein. HO-3 seems to be only a poor catalyst of haem, however the presence of two haem regulatory motifs suggests its potential involvement in haem-sensing and/or binding (McCoubrey *et al.*, 1997).

1.5.3 Haemoxygenase-1 Induction and Its Role in Cytoprotection

1.5.3.1 HO-1 and Oxidative Stress

Tenhunen and colleagues demonstrated in 1970 that microsomal HO could be stimulated by hemin, a haem analogue (Tenhunen *et al.*, 1970). Since then, a considerable number of unrelated stimuli as well as pathological conditions, including cancer, have been shown to increase HO activity via the induction of HO-1 (Otterbein and Choi, 2000; Morse and Choi, 2002). However, one common feature to these various inducers and conditions is their ability to cause an imbalance in the redox state of cells, which is thought to lead to HO-1 induction. Indeed, early experiments in various mammalian cells in culture demonstrated that HO-1 induction is a general response to oxidative stress induced by various agents (Applegate *et al.*, 1991). These agents were either capable of generating active oxygen intermediates or alternatively interfered with intracellular glutathione levels (Applegate *et al.*, 1991). Early in 1990, Stocker proposed that HO-1 induction might provide cellular protection against oxidative stress (Stocker, 1990). Later, an important role for HO-1 in the protection of tissues and cells from oxidant injury was shown in HO-1 knockout mice *in vivo* and their derived cells *in vitro*, which appeared more susceptible to oxidative challenge than their wild type counterparts (Poss and Tonegawa, 1997a,b). There is now substantial evidence that induction of HO-1 is an adaptive and protective mechanism in various stress conditions (Otterbein and Choi, 2000; Morse and Choi, 2002). However, it is worth mentioning that despite most of the literature reporting the cytoprotective effects of HO-1 induction, a few studies have shown detrimental effects resulting from HO-1 over-expression. These reports implicate the accumulation of

reactive iron released during the degradation of haem by HO-1 and suggest that a beneficial threshold for HO-1 over-expression exists making exaggerated expression of HO-1 an unlikely cytoprotective mechanism (Suttner and Dennery, 1999; Lamb *et al.*, 1999).

1.5.3.2 HO-1 and Inflammation

Inflammatory lesions are stressful environments in which reactive oxygen species may also be participating in causing tissue damage (Cuzzocrea *et al.*, 2001). The expression of HO-1 has been shown to play an important modulatory role in models of inflammation and to mediate tissue protection in these conditions. Willis and colleagues demonstrated an important role for HO-1 during the resolution phase of the inflammatory response, with HO-1 inducers mediating significant anti-inflammatory effects, whereas HO inhibitors showed pro-inflammatory effects (Willis *et al.*, 1996; Willoughby *et al.*, 2000). More recently, the potent anti-inflammatory cytokine interleukin-10 (IL-10) was shown to induce the expression of HO-1 in mice, and co-treatment with the HO inhibitor zinc protoporphyrin IX (ZnPP) abolished IL-10-mediated protection in a model of septic shock (Lee and Chau, 2002). These findings suggest that the anti-inflammatory effects of IL-10 are mediated by HO-1.

1.5.3.3 HO-1 and Apoptosis

Apoptosis, or programmed cell death, is an active and tightly regulated process that occurs during normal development, but can also be induced in various disease states and in response to drugs. Furthermore, apoptosis has been shown to be a common response to oxidant-mediated cellular stress (Ueda *et al.*, 2002). The induction of HO-1 observed following oxidative stress has therefore prompted researchers to investigate the potential anti-apoptotic properties of HO-1 as a means for its cytoprotective abilities in various conditions. Indeed, there is now substantial *in vitro* and *in vivo* evidence in support of such a role for HO-1. Experiments investigating HO-1 as an anti-apoptotic molecule *in vitro*, have used hemin pre-treatment to show a substantial decrease in apoptosis mediated by potent oxidising agents such as peroxynitrite or anti-cancer drugs such as cisplatin (Foresti *et al.*, 1999; Shiraishi *et al.*, 2000). Furthermore, transgenic mice deficient in HO-1 were shown to develop more severe renal injury resulting from an increase in apoptotic cells following treatment with cisplatin as compared to their wild type

counterparts (Shiraishi *et al.*, 2000). Finally, *in vitro* and *in vivo* studies have demonstrated that HO-1 over-expression by gene transfer promotes cell survival during stress by an anti-apoptotic mechanism (Soares *et al.*, 1998; Otterbein *et al.*, 1999).

1.5.3.4 HO-1 and Cell Proliferation

Recently, over-expression of HO-1 has been shown in a number of studies to affect cell growth. Gene transfer of HO-1 into smooth muscle cells, renal and pulmonary epithelial cells leading to over-expression of HO-1 protein and activity has been shown to inhibit cell proliferation by causing cell cycle arrest (Zhang *et al.*, 2002; Inguaggiato *et al.*, 2001; Lee *et al.*, 1996). The anti-proliferation effects of HO-1 were reversed in the presence of HO inhibitors (Zhang *et al.*, 2002; Lee *et al.*, 1996). Furthermore, vascular smooth muscle cells lacking HO-1 displayed an enhanced proliferation rate compared to their HO-1 expressing counterparts (Duckers *et al.*, 2001). Studies examining the mechanism by which HO-1 may affect cell proliferation have demonstrated that HO-1 over-expression either by gene transfer or hemin treatment caused up-regulation of p21 (Inguaggiato *et al.*, 2001; Duckers *et al.*, 2001). p21, also known as WAF1, CIP1 or SDI1, is a cyclin-dependent kinase inhibitor acting as a down-stream target of p53 tumour suppressor gene and is involved in promoting cell cycle arrest in the G1 phase of the cell cycle. The mechanisms by which HO-1 over-expression activates p21 expression is currently unclear but these findings strongly suggest the ability of HO-1 to influence the cell cycle and its regulators.

1.5.3.5 Mechanisms of Haemoxygenase-1 Induction

Since stimulation of HO-1 expression by various stimuli and conditions is mainly regulated at the level of gene transcription, a number of studies have attempted to elucidate the signalling pathways and the specific molecular players involved in the induction of *ho-1* gene expression in response to various stimuli. The diversity of HO-1 inducers suggests the presence of various signals and multiple regulatory elements on the gene. Figure 1.9 summarises the signalling pathways and transcription factors which have been shown to play a role in the induction of HO-1 in response to various stimuli, and it also highlights the complexity of the regulatory machinery that may be involved in the regulation of *ho-1* gene transcription. Further complicating the issue is the findings that

the activated pathways in response to a specific stimulus are often cell-type specific resulting in discrepancies between studies.

1.5.4 Mechanisms of Cytoprotection by Haemoxygenase-1

1.5.4.1 Introduction

It is only recently that the mechanism by which HO-1 confers protection is beginning to be elucidated. At least part of the antioxidant function of HO-1 is thought to be related to its role in the degradation of free haem, a pro-oxidant molecule also involved in cellular damage (Ryter and Tyrrell, 2000). However, substantial evidence now also points at the important biological functions of the haem degradation products bilirubin and CO in mediating not only the anti-oxidant functions of HO-1 but also its recent attributed anti-inflammatory, anti-apoptotic and anti-proliferative roles.

1.5.4.2 Role of Biliverdin/Bilirubin in Cytoprotection against Oxidative Damage

Up until recently bilirubin, the end product of haem degradation, was considered to be a harmful and potentially cytotoxic lipid soluble waste product that requires elimination from the body. In humans, hyperbilirubinemia is common in neonates, a condition known as "neonatal jaundice" (Maines, 1990). In most cases this condition is only benign and subsides within a few days after birth. However in certain cases, high levels of bilirubin in the plasma have been associated with neurotoxicity and irreversible brain damage in neonates, a condition known as kernicterus (Maines, 1990; Gourley, 1997).

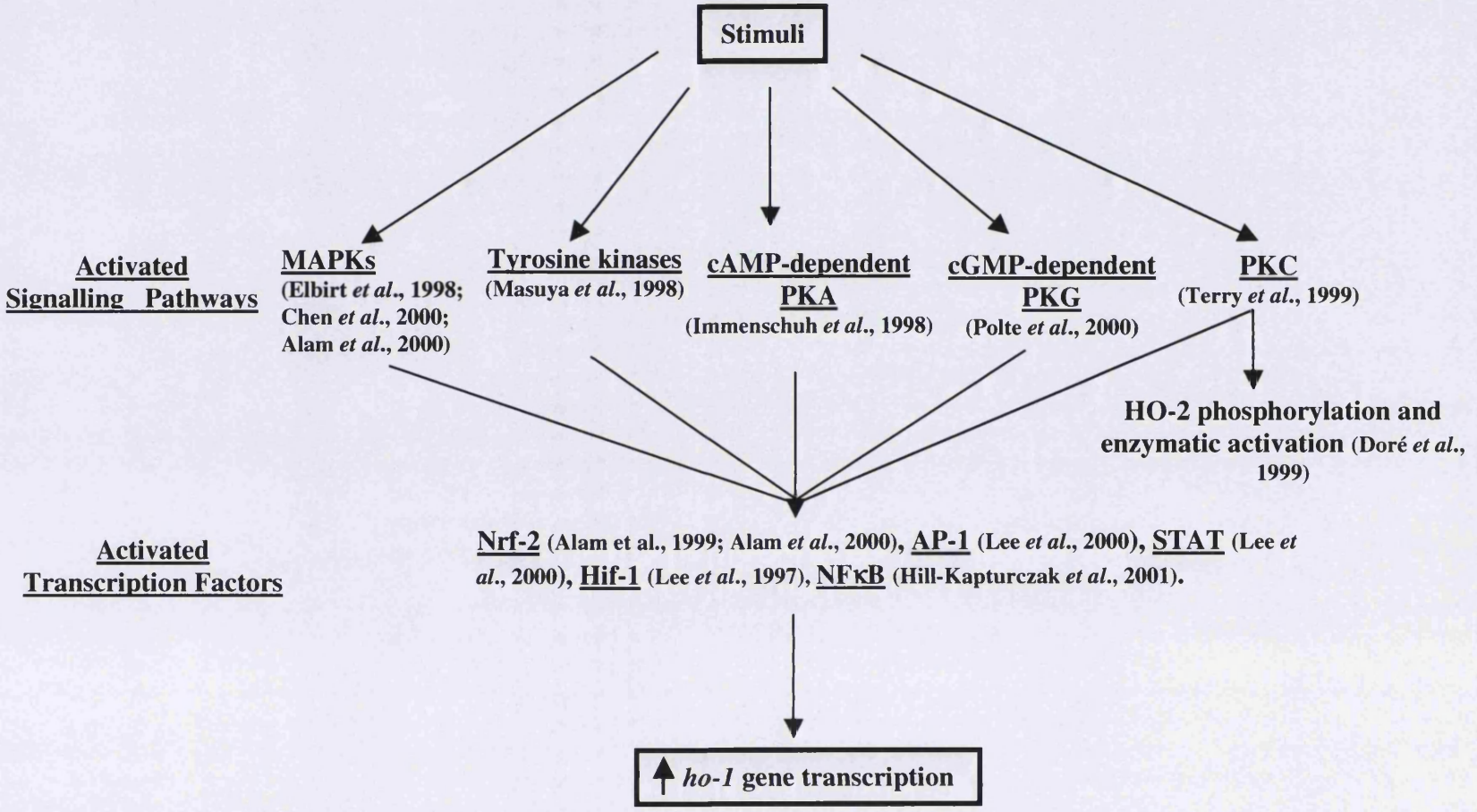

Figure 1.9 Molecular mechanisms shown to be involved in stimuli-induced *ho-1* gene expression. Mitogen activated protein kinases (MAPKs); Protein kinase A (PKA); Protein kinase G (PKG); Protein kinase C (PKC); NF-E2-Related Factor-2 (Nrf-2); Activator protein-1 (AP-1); Signal transducer and activator of transcription (STAT); Hypoxia inducible factor-1 (Hif-1); Nuclear factor-κB (NFκB).

However, more and more evidence is now emerging with regard to the potential important protective and antioxidant properties of bilirubin at low concentrations. The initial studies were conducted by Stocker and colleagues who examined the antioxidant activity of bilirubin in an *in vitro* system (Stocker *et al.*, 1987a). Bilirubin contains an extended system of conjugated double bonds as well as a reactive hydrogen atom which have been suggested to be important for the antioxidant properties of this molecule (Stocker *et al.*, 1987a). Stocker *et al.* assessed the effects of bilirubin on the rate of peroxyl radical-induced oxidation of linoleic acid, a polyunsaturated fatty acid essential to the human diet. Bilirubin, at micromolar concentrations, was shown to efficiently scavenge peroxyl radicals. Furthermore, the antioxidant activity of bilirubin was shown to increase as the experimental concentration of oxygen decreased from 20% to the more physiologically relevant concentration of 2%. In addition, when the experiments were carried out in a more biologically relevant system, whereby bilirubin was incorporated into liposomes, and under 2% oxygen, the antioxidant activity of bilirubin was as important as that mediated by α-tocopherol, one of the best antioxidants of lipid peroxidation (Stocker *et al.*, 1987a). Stocker and co-workers also examined the antioxidant effects of albumin-bound bilirubin and showed that the latter, at concentrations found in the plasma of healthy adults, is also very efficient at scavenging peroxyl radicals (Stocker *et al.*, 1987b).

Studies demonstrating overt beneficial antioxidant/protective effects of bilirubin treatment have been reported in cell culture experiments, isolated organ perfusions and *in vivo*. Both exogenous bilirubin complexed to human serum albumin and free bilirubin formed by activation of HO-2 was shown to protect neurones against oxidative stress injury mediated by hydrogen peroxide (Doré *et al.*, 1999). Furthermore, bovine vascular smooth muscle cells exposed to either exogenous bilirubin or hemin, which results in augmented bilirubin levels, showed a high resistance to injury induced by glucose oxidase, an oxidant generating system producing hydrogen peroxide (Clark *et al.*, 2000a). The role of bilirubin was further demonstrated in cardioprotection against ischaemia-reperfusion injury in an isolated heart preparation (Clark *et al.*, 2000b). Again both 24h hemin pre-treatment and exogenously applied bilirubin at low concentrations significantly restored myocardial function and minimised both infarct size and mitochondrial damage upon reperfusion following a 30-minute ischaemia in isolated heart preparations (Clark *et al.*, 2000b).

Bilirubin has also been implicated in mediating some anti-inflammatory processes via inhibiting the expression of adhesion molecules such as selectins involved in leukocyte-endothelial interactions during inflammatory reactions and tissue injury specifically resulting from oxidative changes (Hayashi *et al.*, 1999). Bilirubin was shown to suppress hydrogen peroxide-induced venular-leukocyte adhesion in the mesenteric microvasculature (Hayashi *et al.*, 1999). Furthermore, biliverdin injected *in vivo* was shown to be as effective as hemin in attenuating liopolysaccharide (LPS)-induced selectin expression in various tissues (Vachharajani *et al.*, 2000). This supports the possible role of biliverdin and/or bilirubin in modulating inflammatory responses by altering the expression of endothelial cell adhesion molecules, which are involved in the recruitment of leukocytes in inflamed tissues. More recently, HO-1 over-expression and bilirubin treatment were shown to modulate stimulus-induced mast cell activation (Takamiya *et al.*, 2002). Mast cells are activated during allergic reactions and are also thought to be involved in sensing tissue injury. Their activation results in the release of a number of inflammatory mediators thereby playing an important role in modulating the inflammatory process.

The antioxidant/protective effects of bilirubin can be mediated at nanomolar concentrations (Doré *et al.*, 1999; Clark *et al.*, 2000b). Recent evidence suggests that bilirubin is able to exert its protective effects at low concentrations thanks to an oxidation-reduction cycling mechanism which allows each molecule of bilirubin to be oxidised to biliverdin. The latter is then immediately reduced back to bilirubin by the action of biliverdin reductase, an enzyme that is abundant in tissues (Baranano and Snyder, 2001). Evidence for the occurrence of this redox cycling of bilirubin comes from experiments demonstrating increased susceptibility to oxidative stress in a cell line deficient in biliverdin reductase (Baranano and Snyder, 2001).

1.5.4.3 Role of Carbon Monoxide

There is now increasing evidence pointing to important biological functions of CO both as a neurotransmitter and a vasodilator, with actions very similar to NO. Furthermore, recent studies have demonstrated the anti-inflammatory, anti-apoptotic and growth modulatory functions of CO in addition to its known vasorelaxation properties. The production of this diatomic gas molecule *in vivo* is mainly via HO enzymatic activity although it is thought

that a small fraction could also result from non-enzymatic degradation such as oxidation of organic molecules, lipid peroxidation and from the activity of intestinal bacteria (Stevenson *et al.*, 2000).

1.5.4.3.1 Carbon Monoxide and Vasodilatation

As mentioned earlier, HO-2 was found to be expressed in the brain as well as the endothelial and smooth muscle layer of blood vessels. These findings support the idea that CO generated as a result of HO enzyme activity may play a role in neurotransmission and vasoregulation under both physiological and pathological conditions (Verma *et al.*, 1993; Dawson *et al.*, 1994; Durante and Schafer, 1998; Coceani, 2000; Zhang *et al.*, 2001). Of interest in this project is the potential importance of CO with regard to the regulation of vascular tone in tumours and the potential for exploiting this system as a tumour blood flow modifier. Research in this area has examined the roles of the NOS/NO system, the vasoconstrictor endothelin-1, and other various pharmacological and non-pharmacological means for modification of tumour blood flow (Chaplin *et al.*, 1998). In the following sections, evidence for CO-mediated vasoregulation in other systems than tumours as well as the mechanisms by which its actions are mediated will be reviewed.

In support for the potential generation of CO in the vasculature are immunohistochemical studies which have shown the expression of HO isoforms in both endothelial and smooth muscle cells (Zakhary *et al.*, 1996; Marks *et al.*, 1997). Furthermore, HO activity and HO isozyme proteins were detected in homogenates of various types of blood vessels including arteries and veins (Marks *et al.*, 1997; Kozma *et al.*, 1999). The generation of CO was also directly measured in vascular tissues (such as aorta, interlobular artery, gracilis muscle arteriole and middle cerebral artery) by gas chromatography-mass spectroscopy (Zhang *et al.*, 2001). Moreover, the addition of an HO inhibitor to *ex vivo* blood vessel incubations was shown to greatly reduce the amount of CO released, thereby suggesting that vascular HO is active and largely responsible for the production of CO (Zhang *et al.*, 2001). The role of CO in the regulation of vascular tone was further demonstrated in isolated blood vessel preparations where HO inhibition was shown to induce vasoconstriction, while hemin treatment suppressed phenylephrine-induced vasoconstriction (Wang *et al.*, 1997a; Kozma *et al.*, 1999). In addition, several studies have demonstrated that CO directly mediates vasoactive actions in various types of

vessels from various species. Indeed, exogenous CO induced vasodilatation in pre-contracted isolated vessels from rat thoracic aortas, femoral, carotid and coronary arteries of the dog, porcine coronary arteries and veins, pulmonary arteries and veins, arterioles isolated from the rat gracilis muscle and rat tail arteries (Lin and McGrath, 1988; Vedernikov *et al.*, 1989; Graser *et al.*, 1990; Wang *et al.*, 1997a; Naik and Walker, 2001). Finally, the importance of the HO/CO system was investigated in the liver microcirculation, where it has been shown to play a major role. Indeed, Suematsu *et al.* have demonstrated that administration of the HO inhibitor, ZnPP, suppresses CO production and promotes an increase in the perfusion pressure of an isolated rat liver (Suematsu *et al.*, 1994; Suematsu *et al.*, 1995). The latter effect was reversed by directly adding CO or the cyclic guanosine monophosphate (cGMP) analogue, 8-bromo-cGMP, confirming the importance of this pathway in the regulation of hepatic vascular tone (Suematsu *et al.*, 1994).

Several studies have examined the possible mechanisms by which CO mediates the vasoactive effects described above. It appears that the most common way by which CO induces vasorelaxation is similar to NO, and involves activation of the enzyme soluble guanylate cyclase (sGC) with the consequent generation of cGMP (Brune and Ullrich, 1987; Ramos *et al.*, 1989; Naik and Walker, 2001). Furthermore, inhibitors of sGC activity have been shown to either completely or partially inhibit CO-mediated vasorelaxation (Wang *et al.*, 1997a; Naik and Walker, 2001). The vasorelaxation brought about following the generation of cGMP is the result of a cascade of events. The activation of cGMP protein kinase by cGMP causes the phosphorylation of voltage gated Ca^{++} channels on the cell membrane and intracellular Ca^{++} transporters on the sarcoplasmic reticulum leading to a decrease in intracellular levels of Ca^{++}. Activation of K^+ channels follows, with the K^+ ions diffusing out of the cell causing membrane hyperpolarisation. This acts as a positive feedback mechanism leading to an enhancement of inhibition of Ca^{++} channels and a further reduction in intracellular Ca^{++}. The latter causes inactivation of myosin light chain kinase, a protein involved in the contractile events, thereby leading to vasorelaxation.

Although the above studies show convincing evidence for the involvement of the cGMP pathway in CO-mediated vasorelaxation, there is some uncertainty with regard to the

degree of affinity of CO for sGC *in vivo* and *ex vivo*. This is because, in *in vitro* experiments CO has been shown only to have a low affinity for purified preparation of sGC and therefore to possess a rather poor sGC-activating property as compared to NO (4 fold versus 100-200 fold, respectively) (Kharitonov *et al.*, 1995). However, *in vitro* studies examining this issue have demonstrated that sGC could be highly sensitised to CO by a molecule known as YC-1, thereby resulting in CO being capable of stimulating this enzyme to a degree similar to NO (Friebe *et al.*, 1996). The question of whether such a molecule exists *in vivo* to account for the CO-induced increase in cGMP mentioned above is still a subject of research.

The cGMP pathway is not the only mechanism by which CO can mediate its vasoactive effects. Studies by Wang *et al.* have shown that the CO-induced vasorelaxation was only partially blocked by a sGC inhibitor thereby suggesting the involvement of cGMP independent mechanisms (Wang *et al.*, 1997a). Indeed, by selectively blocking large conductance K^{+}_{Ca} channels using a toxin, Wang and co-workers demonstrated the inhibition of the cGMP-independent vasorelaxing effect of CO on isolated rat tail arteries (Wang *et al.*, 1997a). In subsequent experiments on smooth muscle cells isolated from rat tail arteries, CO was shown to mediate a direct modulatory action on these high conductance channels independently from cGMP. This led to membrane hyperpolarisation causing a decrease in intracellular Ca^{++} concentration and thereby vasorelaxation (Wang *et al.*, 1997a; Wang *et al.*, 1997b). Other mechanisms which have also been associated with CO-mediated vasorelaxation include inhibition of a cytochrome P-450-based reaction controlling the formation of the vasoconstrictor endothelin-1 (Morita and Kourembanas, 1995). More recently, CO was shown to be able to attenuate the sensitivity of vessels to vasoconstrictors such as phenylephrine and vasopressin (Kaide *et al.*, 2001). The type of mechanism(s) involved in CO-mediated vasorelaxation seem to differ greatly depending on the type of vessel used in a particular set of experiments. For example, while Wang *et al.* have shown that both cGMP and K^{+}_{Ca} channels are involved in CO-dependent vasorelaxation of isolated rat tail artery, Naik and Walker's studies on the pulmonary vasculature demonstrated involvement of only the cGMP pathway (Wang *et al.*, 1997a; Naik and Walker, 2001).

The importance of the HO/CO system has also been examined under stress conditions such as hypoxia, since HO-1 has been shown to be induced under such conditions (Motterlini *et al.*, 2000; Panchenko *et al.*, 2000). Indeed, CO seems to be a major contributor to the regulation of vascular tone in situations where HO-1 is induced as demonstrated in vessels overexpressing HO-1 (Caudill *et al.*, 1998; Sammut *et al.*, 1998). Furthermore, CO overproduced by HO-1 was also shown to play a more important role than NO in the reduction of vascular resistance in perfused rat liver (Wakabayashi *et al.*, 1999). These studies point to the potential importance of CO in the maintenance of vascular homeostasis under pathological conditions.

Finally, CO has been shown to be involved in other vascular regulatory processes in addition to its effects on vascular tone. CO was demonstrated to inhibit platelet aggregation and vascular smooth muscle cell proliferation by a cGMP-dependent mechanism (Brune and Ullrich, 1987; Morita and Kourembanas, 1995; Durante and Schafer, 1998).

Collectively, these studies demonstrate the emerging biological role of CO with important functions in the vasculature under physiological and pathological conditions characterised by over-expression of HO-1.

1.5.4.3.2 Carbon Monoxide and Inflammation

As mentioned earlier, evidence suggests an important role for CO in the regulation of the inflammatory response in a variety of disease models. A number of studies have now shown that the protective effects of HO-1 induction can be re-produced in cells or whole animals by exposure to low concentrations of exogenous CO. This was shown in a well characterised model of LPS-induced inflammation, where the effects of HO-1 over-expression were mimicked by CO at low concentrations and was shown to selectively inhibit the production of pro-inflammatory cytokines, such as TNF-α, while increased the expression of the anti-inflammatory cytokine IL-10 both *in vitro* and *in vivo* (Otterbein *et al.*, 2000). These anti-inflammatory effects of CO did not involve the sGC/cGMP pathway, which has been implicated in the vasoactive effects of CO (see section 1.5.4.3.1), or the NO system. Instead, the mechanism seems to involve the MAPK signalling pathway and in particular activation of the p38 kinase subfamily (Otterbein *et al.*, 2000). This mechanism is further supported in a recent study whereby CO was shown

to attenuate the phosphorylation of ERK1/2 but accentuated the phosphorylation of p38 MAPK in TNF-α-treated endothelial cells (Sethi *et al.*, 2002). Thus, these findings provide a mechanism by which HO-1/CO may play a role in modulating the inflammatory response through differential activation of the MAPK pathway. In a similar model of LPS-induced inflammation, Lee and colleagues have shown that HO-1 mediates the anti-inflammatory effects of IL-10 in mice with the HO inhibitor, ZnPP, attenuating the protective effects of IL-10 administration in this model (Lee and Chau, 2002). Furthermore, their *in vitro* studies demonstrated the involvement of CO in the anti-inflammatory effects of IL-10, with the CO scavenger haemoglobin shown to reverse the effects of IL-10 on LPS-induced TNF-α production. Taken together, these two studies suggest the presence of a positive feedback loop mechanism by which the anti-inflammatory effects mediated by CO may be amplified. Thus, HO-1 induction by a pro-inflammatory stimulus leads to CO generation, which in turn increases the expression of anti-inflammatory cytokines such as IL-10, possibly via modulation of the MAPK pathway (Otterbein *et al.*, 2000). In turn, IL-10 expression further induces the expression of HO-1 (Lee and Chau, 2002), which would lead to more CO production and a further increased expression of anti-inflammatory cytokines.

Collectively, these studies show compelling evidence for an important emerging anti-inflammatory role of low concentrations of CO.

1.5.4.3.3 Carbon Monoxide and Apoptosis

As mentioned in section 1.5.3.4, HO-1 was shown to be involved in the protection of cells against apoptosis. There is now evidence that the anti-apoptotic effects of HO-1 may be mediated via CO. Indeed, using murine fibroblasts, Petrache and colleagues demonstrated that overexpression of HO-1 prevents TNF-α-induced apoptosis and this inhibition was not observed in the presence of the HO inhibitor tin-protoporphyrin IX (SnPP) or in cells over-expressing antisense HO-1 (Petrache *et al.*, 2000). These authors reported that these anti-apoptotic effects of HO-1 could be reproduced by exogenous administration of low concentrations of CO and were dependent on activation of sGC and the generation of cGMP. The anti-apoptotic effects of CO were also demonstrated in endothelial cells, where exogenous CO exposure under inhibition of HO-1 activity by SnPP substitutes HO-1 in preventing endothelial cell apoptosis (Brouard *et al.*, 2000). In contrast to the study

by Petrache *et al.*, the mechanism by which HO-1/CO mediated the anti-apoptotic effects in endothelial cells was shown to be independent from the sGC/cGMP pathway but required activation of the p38 MAPK signal transduction pathway (Brouard *et al.*, 2000). The group of Brouard *et al.* has gone one step further in investigating the mechanism of action of CO in mediating its anti-apoptotic effects in endothelial cells and have demonstrated that inhibition of NF-κB activation suppresses the anti-apoptotic effect of CO (Brouard *et al.*, 2002). This function of CO was restored by expression of certain of NF-κB family members or NF-κB-dependent anti-apoptotic genes. NF-κB is a transcription factor involved in the induction of the expression of genes involved in physiological processes as well as in response to injury and stress. NF-κB activation has been implicated in the control of cell proliferation and apoptosis and in the response of cells to a number of stimuli including inflammatory cytokines and oxidative stress (Bowie and O'Neill, 2000).

Collectively, these studies point to the important role of CO as an anti-apoptotic molecule. The mechanism by which CO mediates its effect seem to be cell-type specific. In some cases it may involve activation of the sGC/cGMP pathway and in others activation of the p38 MAPK signal transduction pathways. More recent studies in endothelial cells suggest the requirement of activation of the transcription factor NF-κB and the expression of a subset of NF-κB-dependent anti-apoptotic genes for CO to suppress apoptosis (Soares *et al.*, 2002).

1.5.4.3.4 Carbon Monoxide and Cell Proliferation

CO has also been implicated in the anti-proliferative role mediated by HO-1. CO has been suggested to indirectly influence cell growth by regulating the release of growth factors, as demonstrated in a co-culture system where CO-derived from vascular smooth muscle cells was shown to decrease the endothelial cell synthesis of the mitogens endothelin-1 and platelet-derived growth factor (PDGF) (Morita and Kourembanas, 1995). However, more direct mechanisms in the anti-proliferative effects of CO have also been demonstrated. In this respect, Togane and colleagues reported that endogenous CO inhibits angiotensin-II-induced smooth muscle cell proliferation by sGC/cGMP-dependent and independent mechanisms (Togane *et al.*, 2000). In addition, the growth inhibitory role of CO was further demonstrated in serum-stimulated vascular smooth muscle cells,

whereby exogenous administration of CO blocked cell proliferation (Peyton *et al.*, 2002). The authors of this study suggested yet another mechanism of action of CO involving its interaction with various molecular components of the cell cycle machinery.

Note: HO-1-mediated haem degradation not only produces bilirubin and CO but also releases free iron (Figure 1.7). The major deleterious effects of iron are related to its ability to participate in chemical reactions generating reactive oxygen species (Fenton reaction), which in turn can cause cellular damage (Boldt, 1999). Studies have reported that HO-1 induction by hemin, for instance, is followed by an induction of ferritin, an intracellular protein involved in iron storage and detoxification (Balla *et al.*, 1992; Balla *et al.*, 1993; Gonzales *et al.*, 2002). These findings suggest the possible importance of ferritin and its role in iron sequestration as a potential contributor to the cytoprotective mechanisms mediated by HO-1. Further investigations need to be conducted in order to establish whether this concomitant ferritin induction is a generalised response occurring shortly following HO-1 induction.

1.5.5 Role of Haemoxygenase-1 in Cancer

1.5.5.1 Haemoxygenase-1 Expression in Tumours

In recent years, a number of studies have investigated the potential roles of HO expression/activity in tumours. In human brain tumour specimens, HO-1 mRNA was found to be expressed at higher levels than in normal brain tissue (Hara *et al.*, 1996). Furthermore, increased HO-1 immunoreactive staining was observed in benign prostatic hyperplasia and malignant prostate tissue (Maines and Abrahamsson, 1996). HO-1 over-expression was also detected in biopsy samples from human renal cell carcinomas as compared to normal renal tissue (Goodman *et al.*, 1997). With regard to animal tumour models, there is evidence for HO-1 expression from an experimental solid tumour model (AH136B hepatoma) in rats (Doi *et al.*, 1999). We also found high HO activity in subcutaneous transplants of the P22 rat carcinosarcoma, which was of the same order as that found in normal rat liver (Tozer *et al.*, 1998; also see results section of Chapter 3). *In vitro*, studies using tumour spheroids of the A431 squamous carcinoma cell line have shown that HO expression and activity is enhanced in this three dimensional tumour model as compared to monolayer cultures (Murphy *et al.*, 1993).

More recently, it has been suggested that HO-1 could be used as a predictive factor in cancer therapy. A recent clinicopathological and immunohistochemical study has examined the role of HO-1 in predicting the response to radiotherapy in human oesophageal squamous cell carcinomas (Yokoyama *et al.*, 2001). Although the study was carried out on only a small number of specimens (from 13 oesophageal squamous cell cancer patients), a strong correlation was found between the presence of HO-1 in cancer tissues and increased radiation response. Both the former and the latter were independent from tumour size, stage or histologic grade. It, however, remains unclear as to why tumours with high HO-1 expression are better responders to radiotherapy than tumours with a lower HO-1 expression. It is possible that tumours expressing HO-1 have higher levels of CO. Since CO has been shown to possess vasodilatory properties (see section 1.5.4.3.1) it is possible that these tumours are better oxygenated than tumours with lower HO activity and are therefore better responders to radiotherapy (Gray *et al.*, 1953).

Although from the above studies there seem to be a relationship between malignant behaviour and HO-1 over-expression, the significance of these findings is unclear. It has been suggested that this increase in HO-1 levels may be due to local factors released from the tumour cells, and to the specific tumour microenvironment characterised by hypoxia and oxidative stress, two well-known inducers of HO-1 (Goodman *et al.*, 1997). However more recently, evidence has emerged that HO-1 is involved in angiogenesis, an important process for tumour growth and invasion.

1.5.5.2 Role of Haemoxygenase-1 in Angiogenesis

Two recent clinical studies have linked HO-1 expression with angiogenesis in human gliomas and human vertical growth melanomas (Nishie *et al.*, 1999; Torisu-Itakura *et al.*, 2000). Expression of HO-1 mRNA was mainly associated with infiltrating macrophages and correlated with vascular density. More direct evidence showing a relationship between HO-1 expression and new blood vessel formation comes from *in vitro* studies investigating the effects of gene transfer of human HO-1 into endothelial cells (Deramaudt *et al.*, 1998). This report provides direct evidence that over-expression of the HO-1 gene in endothelial cells not only increased their proliferation rate, but also induced an increase in the formation of both branches and anastomosing capillary-like cords in an *in vitro* model of angiogenesis. At present the mechanism involving HO-1 in angiogenesis

remains unclear. However, studies have shown that the HO-1 gene is up-regulated in response to mediators such as TNF-α and interleukin 1-α, which have also been shown to up-regulate known angiogenic stimulating factors, such as VEGF (Terry *et al.*, 1998; Torisu *et al.*, 2000). Moreover, binding sites for several transcription factors (e.g. AP-1, AP-2 and NF-κB) on the VEGF gene promoter can also be found on the HO-1 gene promoter (Tischer *et al.*, 1991; Gille *et al.*, 1997; Lavrovsky *et al.*, 1994; Alam *et al.*, 1992). This suggests possible cross talk between these different proteins in promoting/mediating angiogenesis. Further evidence for a putative role of HO-1 in tumour progression relates to its possible involvement in promoting cell proliferation and tumour cell growth. In this regard, ZnPP, a HO inhibitor, was shown to significantly suppress tumour growth when injected intra-arterially to a solid tumour (Doi *et al.*, 1999). This is in contrast to the studies reported in section 1.5.3.5 whereby HO-1 over-expression resulted in cell growth arrest. It is likely that these effects of HO-1 on cell proliferation are cell-type and condition specific and perhaps dependent on the level of HO-1 expression achieved. Further support for a potential role of HO-1 in angiogenesis can be found in a recent study that demonstrated the presence of regulatory sequences for the transcription factors ETS-1, FLI-1 or ERG in the promoter region of the human HO-1 gene (Deramaudt *et al.*, 1999). These transcription factors belong to the Ets-family of proteins, which were shown to be widely expressed during development and cell proliferation. Moreover, the evidence for the role of this family of transcription factors in angiogenesis (Sato, 2001), further supports a possible involvement of HO-1 in mediating/promoting this phenomenon. More recently, HO activity has been reported to modulate the synthesis of a key pro-angiogenic player, VEGF, under both normoxic and hypoxic conditions (Dulak *et al.*, 2002). Hemin treatment was shown to enhance VEGF production, while SnPP was able to block this effect and the hypoxia-induced increase in VEGF synthesis. This study also demonstrated the important role of CO in mediating these effects, with exposure to low levels of CO (1%) resulting in a marked increase in VEGF synthesis. The fact that HO-1/CO is able to directly modulate the expression of key pro-angiogenic factors such as VEGF strongly implicates a potential role of this enzyme system in modulating the angiogenic process.

Collectively, these studies point to the potential importance of the HO system both in cancer progression and therapy and clearly further studies are warranted in order to fully elucidate the role of this enzyme system in cancer.

1.6 Aims of the Project

There is increasing evidence pointing at an important biological role of the HO system extending beyond its primary function in haem degradation. HO-1, the inducible form of the enzyme, has been shown to be over-expressed in a number of pathological conditions including cancer suggesting its potential role in tumours. The HO system, through CO generation, has been implicated in the control of vascular tone and in modulating the angiogenic process and pharmacological modification of these parameters in tumours has an important therapeutic potential. Furthermore, several studies have also demonstrated the cytoprotective roles mediated by HO-1 induction in various conditions including oxidative stress, inflammation and vascular injury, a function attributed to the biologically active haem degradation products bilirubin and CO. Based on the above findings, the present project aimed to:

- Examine the overall HO enzyme activity and HO isozyme protein levels in two rodent tumours and three human xenograft models (Chapter 3).
- Investigate the role of the HO/CO system in the maintenance of tumour blood flow (Chapter 4).
- Examine the importance of the HO system in endothelial and tumour cell proliferation *in vitro* and tumour growth *in vivo* (Chapters 4 and 6).
- Investigate the potential protective roles of HO-1 in tumours against the vascular injury mediated by the novel vascular targeting agent CA-4-P. The effects of CA-4-P on the HO system were examined *in vitro* and *in vivo* (Chapter 5), and the potential for HO inhibitors to improve the therapeutic efficacy of CA-4-P was also investigated *in vivo* (Chapter 6).

CHAPTER 2

MATERIALS AND METHODS

2.1 Introduction

This chapter describes the general materials and methods used throughout these studies. More specific methods and experimental protocols can be found in individual chapters. All animal procedures were carried out in accordance with the UK Home Office Animals (Scientific Procedures) Act 1986 and with the approval of the Ethical Review Committee of the Gray Cancer Institute (Project Licence number 70/4552).

2.2 Tumour Models

2.2.1 P22 Rat Carcinosarcoma Tumour

The P22 rat carcinosarcoma tumour was used for most of these studies due to the extensive background information available on this tumour model and its high resting overall HO enzyme activity (Tozer and Shaffi, 1993; Tozer *et al.*, 1998; Prise *et al.*, 2002; results in Chapter 3). The P22 tumour arose in male BD9 rats following irradiation of the spinal cord, and maintenance of the tumour line is performed by serial subcutaneous transplantation of tumour pieces up to the 10^{th} generation before returning to early generation frozen stocks (Tozer and Shaffi, 1993). Experiments were performed on tumours between the 5^{th} and 10^{th} generation. For each transplant a donor tumour-bearing rat was sacrificed by CO_2 asphyxiation (Schedule 1 procedure, Animal (Scientific Procedures) Act 1986) and the tumour was excised, cut into approximately 1 mm^3 pieces and kept on ice in a sterile Petri dish containing HBSS solution (Gibco BRL). Rats aged 8-9 weeks were anaesthetised using halothane (Merial Animal Health Ltd.) via an anaesthetic machine (Fluovac) with a suitable gas scavenging system. A small skin incision was made on the shaved left flank and the subcutaneous fat cleared using blunt forceps to produce a 2-3 cm-long channel. One tumour piece was then placed on the underside of the skin. The wound was closed using autoclips and sprayed with local anaesthetic xylocaine. At day 10 post-transplantation, the tumours were checked and the clips removed. The tumours were used for experimentation when their geometric mean diameter reached 11-14 mm, approximately 14 to 21 days after transplant.

2.2.2 CaNT Murine Mammary Carcinoma

The CaNT murine mammary adenocarcinoma is a spontaneous tumour, which arose at the Gray Cancer Institute (Northwood, UK) and has been maintained through many generations in the inbred strain of origin. Tumours were initiated in the rear dorsum of female CBA/Gy f TO mice by subcutaneous injection of 0.05 ml of a crude tumour cell suspension prepared by mechanical dissociation of an excised tumour from a donor animal. The transplantation was performed under metofane (C-vet Ltd.) anaesthesia using an "open–drop" method with suitable air extraction. Tumours were used for experimentation when their geometric mean diameter reached ~ 6 mm, approximately 3-4 weeks after implantation.

2.2.3 LoVo, HT-29 and SW-1222 Human Colon Xenograft Tumours

LoVo, HT29 and SW-1222 cell lines originate from human colorectal adenocarcinomas. The LoVo and HT-29 established human cell lines were purchased from the American Type Culture Collection (ATCC) and maintained in tissue culture. The SW-1222 cell line was kindly provided by Dr B. Pedley (Department of Oncology, Royal Free and University College Medical Sachool). Tumours were initiated in female Severely Compromised Immuno-Deficient (SCID) mice by subcutaneous injection of a tumour cell suspension (10^6 cells) into the rear dorsum under metofane anaesthesia. Tumours were used for experimentation when their geometric mean diameter reached ~ 6 mm, approximately 4-8 weeks after implantation for the LoVo, ~ 3 weeks for the HT-29 and ~ 2 weeks for the SW-1222.

2.3 Cell Culture

2.3.1 P22 Tumour Cells

P22 tumour cells were previously derived from rat P22 tumours. The established cell line was maintained in Dulbecco's Modified Eagle's Medium (DMEM; Life Technologies), supplemented with 10% foetal calf serum (Sigma), 100 U/ml penicillin (Sigma, UK), 100 μg/ml streptomycin (Sigma) and 2 mM glutamine (Life Technologies). Cells were incubated in a humidified incubator at 37 °C and 5% CO_2/air. Cells were regularly checked for mycoplasma contamination.

2.3.2 Human Umbilical Vein Endothelial Cells (HUVECs)

HUVECs from pooled donors were purchased frozen from TCS CellWorks (TCS CellWorks Ltd.). If not seeded on arrival, cells were transferred into the liquid nitrogen storage facility. Otherwise, cells were thawed in a 37 °C water bath then transferred into tubes containing warm media and centrifuged at 1000 rpm for 5 minutes. The pellet was resuspended in warm medium and transferred into 75 cm^2 flasks, which had been previously coated with 0.2% gelatin (Sigma). The primary cultures were maintained in Medium 199 with Earl's salt (M-199; Life Technologies) supplemented with 20% foetal calf serum, 100 U/ml penicillin, 100 μg/ml streptomycin, 2 mM glutamine, 10 mM Hepes buffer (Gibco BRL), 5 U/ml heparin (CP Pharmaceuticals Ltd.) and 10 mg/ml Endothelial Cell Growth Supplement (ECGS; First Link). Cells were used for experimentation between passages 1 and 4.

2.4 Preparation of Tissue Microsomal Fractions

2.4.1 Principle

HO is a microsomal enzyme found on the endoplasmic reticulum. Ultra-centrifugation (rotation at high speed) can be used to separate different cellular components according to their size. The tissue's cellular membranes need first to be broken up into fragments by homogenisation, after which they reseal immediately to form small closed vesicles. The various particles, including the microsomes, which are the vesicles derived from the endoplasmic reticulum, will retain most of their biochemical properties provided an appropriate homogenisation medium is used. Routinely, most tissues are homogenised in 0.25 M sucrose, buffered with an organic buffer such as Tris or Hepes at a pH between 7 and 8, thus providing an iso-osmotic homogenisation buffer, which allows preservation of structural and functional integrity. At low speed (1000 g for ~ 10 minutes), nuclei and unbroken cells form a pellet at the bottom of the centrifuge tube while at medium speed (20000 g for ~ 20 minutes) a pellet containing the mitochondria will form. Higher speeds and longer periods of centrifugation (80000 g for ~ 1h) allow for small vesicles and microsomes to sediment and form a pellet which can be re-suspended in buffer and used for biochemical analysis.

2.4.2 Buffers

Sucrose (0.25 M)-TrisHCl (0.05 M)

42.8 g sucrose (Sigma)

3.94 g Trizma-HCl (Sigma)

400 ml distilled water

1 tablet protease inhibitor/50 ml (Roche Diagnostics)

Adjust to pH 7.4 with NaOH (2 M) and make up volume to 500 ml with distilled water.

Phosphate buffered saline (100 mM)-Magnesium chloride (2 mM) (PBS-$MgCl_2$)

3.4 g potassium phosphate (KH_2PO_4; Sigma)

47.6 mg magnesium chloride ($MgCl_2$; Sigma)

150 ml distilled water

Adjust to pH 7.4 with NaOH (2 M) and make up volume to 250 ml with distilled water.

2.4.3 Protocol

Animals were sacrificed by cervical dislocation (Schedule 1 procedure, Animal (Scientific Procedures) Act 1986). Tissues were quickly excised and, where applicable, flushed with 0.9% ice-cold saline until blanched. The organs were rapidly frozen in –40°C isopentane (Sigma) and stored at –86°C for further processing. For microsomal extraction the tissues were weighed, minced and then homogenised in 4-5 volumes of sucrose Tris-HCl buffer, containing a cocktail of protease inhibitors. The tissue homogenates were then transferred into centrifuge tubes (Beckman Coulter Ltd.) and ultra-centrifuged at 27000 g for 10 minutes at 4°C. The remaining supernatant was transferred into clean tubes and re-centrifuged at 105000 g for 90 minutes at 4°C. The resulting pellet constituting the microsomal fraction was re-suspended in PBS-$MgCl_2$, and stored at –86°C for further analysis.

2.5 Haemoxygenase Activity Assay

The HO enzyme activity assay is a spectrophotometric assay of bilirubin production. Bilirubin, one of the end products of haem degradation by HO, is extracted in chloroform and the amount produced is determined by the absorbance of the solution at 464 and 530 nm. The reaction mixture is carried out in the presence of the unknown sample, an excess of the HO substrate, hemin, and the enzyme biliverdin reductase, which is responsible for

the conversion of biliverdin to bilirubin. The reaction also requires the presence of oxygen and the co-factor NADPH. The reducing agent NADPH is needed for the activation of oxygen and the reduction of ferric iron (Fe^{3+}) in the hemin molecule to ferrous iron (Fe^{2+}) or the maintenance of the iron in the latter state. The enzyme glucose-6-phosphate dehydrogenase and its substrate glucose-6-phosphate are also supplied in the reaction mixture as an NADPH generating system.

2.5.1 Buffers and Reagents

PBS (100 mM)-$MgCl_2$ (2 mM)

See section 2.4.2 above.

hemin (1 mM)

6.52 mg of hemin chloride (Sigma) was dissolved in 50 µl NaOH (2 M) and 950 µl distilled water and made up to 10 ml with PBS-$MgCl_2$.

Made fresh before assay.

glucose-6-phosphate (G6P; 20 mM)

6.1 mg G6P (Sigma)

1 ml PBS-$MgCl_2$

Aliquot and store at –86°C

glucose-6-phosphate dehydrogenase (G6PD; 50 U/ml)

50 U G6PD (Sigma)

1 ml PBS-$MgCl_2$

Aliquot and store at –86°C

β-nicotinamide adenine dinucleotide phosphate reduced tetrasodium salt (NADPH; 40 mM)

33.33 mg NADPH (Sigma)

1 ml PBS-$MgCl_2$

Aliquot, wrap in aluminium foil and store at –86°C

2.5.2 HO Activity Protocol

HO enzyme activity was measured in sonicated whole cell extracts and tissue microsomal fractions. The method has been published previously (Motterlini *et al.*, 1996).
The reaction was carried out in glass test tubes. The reagents were added in this sequence in a final volume of 1 ml:

300 µl PBS-$MgCl_2$ pH 7.4
Liver cytosol (3 mg total protein/ml) as a source of biliverdin reductase (see section 2.6)
25 µl hemin (25 µM final)
50 µl G6P (1 mM final)
15 µl G6PD (0.75 U/ml final)
Unknown sample (1-2 mg total protein)
25 µl NADPH (1 mM final)

Tubes were vortexed, covered with parafilm and wrapped in aluminium foil. They were then incubated at 37°C for 30 (tissue microsomes) or 60 minutes (whole cell extracts). The reaction was terminated by the addition of 1 ml of chloroform (Sigma). The tubes were then vortexed well and centrifuged at 2000 rpm for 5 minutes at room temperature. The absorption of the lower chloroform layer containing the bilirubin was measured at 464 and 530 nm using a Hewlett Packard model 8452A diode array spectrophotometer. The HO enzyme activity was expressed as pmol bilirubin produced/mg total protein/hour and was calculated as follows:

a) Bilirubin concentration in chloroform

$$[Bilirubin] = (OD464-OD530)/E \; \mathbf{mM}$$

$E = 40\ mM^{-1}cm^{-1}$ (extinction coefficient of bilirubin in chloroform)

b) 1 ml of choroform contains

$(OD464-OD530)/(40\times10^3)$ ***mmoles bilirubin*** formed in 1 tube*

*If the reaction is carried out for 30 minutes only then b) needs to be multiplied by 2 to get the amount of bilirubin formed in 60 minutes.

c) HO activity in **pmoles bilirubin formed/mg protein/hour**

$$(OD464\text{-}OD530)\times 10^6/(40\times \textit{protein content of the sample in mg})$$

The total protein content of samples was measured using a colourimetric assay according to the manufacturer's instructions (BIO-RAD protein kit) and bovine gamma globulin was used as a standard.

2.6 Preparation of Rat Liver Cytosol

Liver cytosol was prepared from fresh rat livers as a source of biliverdin reductase for the HO enzyme activity assay (section 2.5). Biliverdin reductase is a cytosolic enzyme responsible for the conversion of biliverdin to bilirubin.

2.6.1 Buffers and Reagents

KCl (1.15%; w/v)-Tris (20 mM)

2.87 g KCl (Sigma)

0.79 g Trizma-HCl (Sigma)

150 ml distilled water

Adjust to pH 7.4 with NaOH (2 M) and make up volume to 250 ml with distilled water

Biliverdin dihydrochloride (1 mM)

6.55 mg biliverdin (ICN Biomed) was dissolved in 50 µl NaOH (2 M) and 950 µl distilled water and made up to 10 ml with PBS-$MgCl_2$.

2.6.2 Protocol

The liver was excised and perfused with ice-cold 0.9% saline until blanched. It was then weighed, minced and homogenised in 2-3 volumes of ice-cold KCl-Tris buffer. The homogenate was transferred into centrifuge tubes (Beckman Coulter Ltd.) and centrifuged at 27000 g for 20 minutes at 4°C. The supernatant was collected and re-centrifuged at 105000 g for another 60 minutes at 4°C. The cytosol (supernatant) was removed and

aliquots were stored at –86°C. Biliverdin reductase activity in the liver cytosol was assessed by the following assay:

600 µl PBS-$MgCl_2$ pH 7.4
100 µl liver cytosol
25 µl biliverdin (25 µM final)
50 µl G6P (1 mM final)
15 µl G6PD (0.75 U/ml final)
25 µl NADPH (1 mM final)

Tubes were vortexed, covered with parafilm and wrapped in aluminium foil. They were then incubated at 37°C for 30 minutes. The reaction was terminated by the addition of 1 ml of chloroform (Sigma). The tubes were well vortexed and then centrifuged at 2000 rpm for 5 minutes at room temperature. The absorption of the lower chloroform layer containing the bilirubin was measured between 464 and 530 nm using a Hewlett Packard model 8452A diode array spectrophotometer. A typical absorbance of 0.3-0.4 at 464 nm was obtained and indicative of high biliverdin reductase activity. The total protein content of the liver cytosol was also determined as previously described. A volume containing a total amount of protein of 3 mg was added to the HO activity reaction described in 2.5 (typically between 90-120 µl).

2.7 Protein Electrophoresis and Western Blotting

2.7.1 Principle of Protein Electrophoresis

Electrophoresis is the process of moving charged particles in solution by applying an electrical field across the mixture. Molecules in an electrical field move with a speed dependent on their shape, size and charge making this a useful tool for separation of large molecules such as proteins. Polyacrylamide gels are cross-linked sponge-like structures used to separate most proteins by electrophoresis. The gel also acts as a size-selective sieve in the separation, whereby molecules smaller than the gel pore size will move freely through the gel, while molecules larger than the gel pore size will be blocked. Gels of different concentrations are characterised by different pore sizes and, as the concentration increases, the effective pore size of the gel decreases. Here SDS polyacrylamide gel eletrophoresis (SDS-PAGE) was utilised, a technique which allows the separation of

proteins on the basis of their molecular weight. Sodium dodecylsulfate (SDS) is an anionic detergent used to denature proteins by wrapping around the polypeptide backbone, thereby conferring to it a net negative charge in proportion to its length. Combined heat and dithiothreitol (DTT) treatments are also used to further denature proteins and break disulphide bonds.

2.7.2 Principle of Western Blotting

Western blotting consists of the transfer of proteins separated by SDS-PAGE from the gel onto a membrane by electrophoretic elution, followed by immunodetection of the immobilised proteins on the membrane. Different types of membrane materials can be used; nitrocellulose is the most generally applicable and works well with proteins. For a semi-dry transfer, the blotting paper and membrane are pre-soaked in transfer buffer and the transfer sandwich is then assembled as shown in Figure 2.1. Following transfer (see section 2.7.5), the membrane is incubated with a blocking solution to block all the non-specific binding sites. The immobilised proteins on the membrane are then probed with a primary antibody specific to the protein of interest followed by a secondary antibody specific for the general class of primary antibodies. A reporter enzyme, either peroxidase or alkaline phosphatase, is tagged to the secondary antibody and the immunoreactive bands are detected by either colour development or enhanced chemiluminescence (ECL) by applying the appropriate enzyme substrates (Figure 2.2 section 2.7.3).

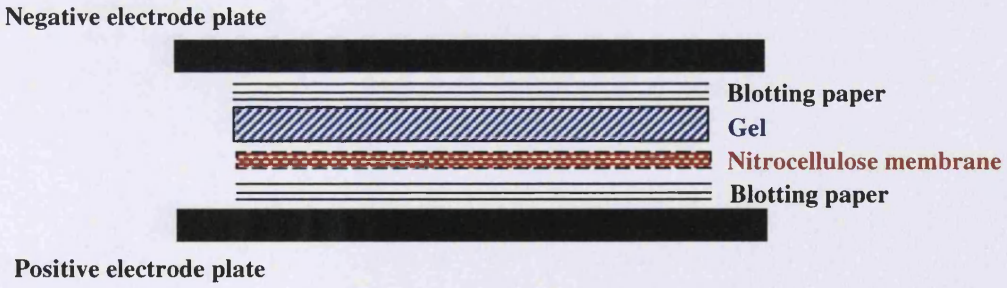

Figure 2.1 Schematic representation of the transfer sandwich. The assembled sandwich is used for the transfer of proteins from the gel onto the nitrocellulose membrane.

2.7.3 Principle of Enhanced Chemiluminescence (ECL) Detection

Luminescence is the emission of light resulting from the dissipation of energy from a substance in an excited state. In chemiluminescence, excitation of the substance is achieved through a chemical reaction and one of the most well characterised systems is the horseradish peroxidase (HRP)/hydrogen peroxide catalysed oxidation of luminol in alkaline conditions. The excitation state of luminol, which occurs immediately following its oxidation by HRP in the presence of hydrogen peroxide (H_2O_2), decays to ground by emitting light at a wavelength of 428 nm. This can be detected by a short exposure to blue-light sensitive autoradiography film. Strong enhancement of the light emission can be achieved by performing the oxidation of luminol by HRP in the presence of chemical enhancers such as phenols. This process is known as enhanced chemiluminescence (ECL) (Figure 2.2).

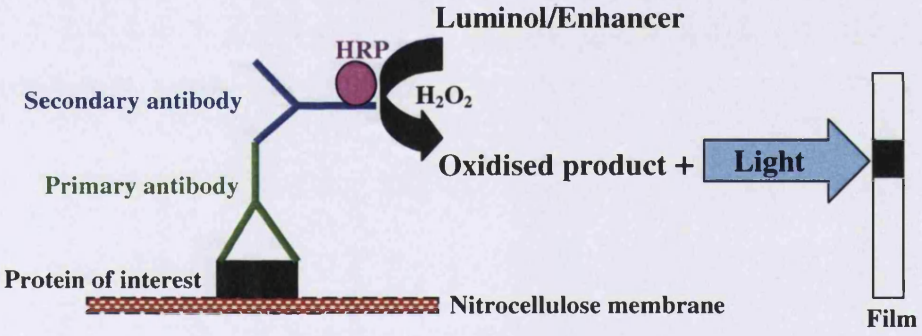

Figure 2.2 Schematic representation of the principles of western blotting using ECL as a detection method.

2.7.4 Buffers and Reagents

Sample buffer (2x; final volume of 10 ml)

1.25 ml Tris-HCl pH 6.8 (1 M stock and 125 mM final)

4 ml of 10% SDS solution (4% final; Gibco BRL)

2 ml glycerol (20% final; Sigma)

2.6 ml distilled water

150 µl bromophenol blue (tracking dye; 0.1% w/v)

154.2 mg DTT (100 mM final; Sigma)

Tris-HCl (1 M)

12 g Tris base (Sigma)

60 ml distilled water

Adjust to pH 6.8 with HCl and make up volume to 100 ml

Running buffer

Purchased from National Diagnostics as a 10x solution containing: Tris (0.25 M), glycine (1.92 M) and SDS (1%). Diluted 1/10 for working concentration.

Transfer buffer for semi-dry transfers

2.9 g glycine (39 mM) (Sigma).

5.8 g Tris Base (48 mM) (Sigma).

3.7 ml of 10% SDS solution (Gibco BRL)

200 ml methanol

Make up to 1 L with distilled water.

Phosphate buffered saline (PBS)

1 tablet/100 ml distilled water (Oxoid)

PBS-Tween (0.1%) (PBS-T)

1 L PBS

5 ml of a 20% Tween-20 solution (Sigma)

Membrane blocking solution

PBS

0.1% Tween-20

1% bovine serum albumin (BSA; Sigma)

10% dry-powdered milk (Waitrose)

Primary/secondary antibody solution

PBS

0.1% Tween-20

1% BSA

3% dry-powdered milk

Primary or secondary antibody

Coomassie blue stain

50% methanol (BDH)

10% acetic acid (BDH)

0.1% coomassie blue (BDH)

Destain solution

50% methanol

10% acetic acid

2.7.5 Protocol

Western blotting was performed on whole cell extracts or tissue microsomes. A total amount of protein of 40 μg (cells) or 100 μg (tissues) was re-suspended in sample buffer (2x) in a final volume of 30 μl and boiled at 95°C for 5 minutes. Rainbow™ coloured protein molecular weight markers (Amersham Life Science) were also prepared in the same way. Samples were analysed by SDS-PAGE using precast 12% polyacrylamide gels (Invitrogen) and run at a constant voltage of 125 V for ~ 2h. The proteins on the gel were then transferred onto a nitrocellulose membrane (Genetic Research Instrumentation) using a semi-dry blotting system (Nova Blot, Pharmacia Biotech). The transfer conditions were set at 0.8 mA/cm^2 membrane surface area for 60-90 minutes. The membrane was then washed in PBS-T and incubated in blocking solution for 2h. The primary antibody solution containing either the anti-HO-1 antibody (1:2000 dilution; Bioquote) or the anti-HO-2 antibody (1:5000 dilution; Bioquote) was applied to the membrane overnight at 4°C. The next day the membrane was washed 1x15 minutes and 4x5 minutes in PBS-T before the secondary antibody solution containing an HRP-conjugated goat anti-rabbit antibody (1:1000 dilution; Dako) was applied for 1h at room temperature. The membrane was then washed again 1x15 minutes and 4x5 minutes in PBS-T and the immunoreactive bands were detected using the ECL kit according to the manufacturer's instructions (Amersham Pharmacia). The immunoreactive bands were detected on x-ray film (Amersham Pharmacia). When a membrane had to be re-probed, it was first stripped with the Restore™ western blot stripping solution (Pierce) for 20 minutes, washed in PBS-T 3x10 minutes and incubated for 2h in blocking solution before the other primary antibody was applied. Subsequent steps were carried out as described above.

2.8 Measurement of Tissue Blood Flow Rate

2.8.1 Principle

Measurement of tissue blood flow rate was performed using the tissue uptake of the radiolabelled tracer iodoantipyrine (^{125}I-IAP). This technique is well established for measurement of blood flow rate in experimental tumours as well as normal tissues (Tozer and Shaffi, 1993; Tozer *et al.*, 1994). The method is based on the theory devised by Kety for the exchange of inert and readily diffusible tracers between blood and tissues (Kety, 1960a, b). The model described by Kety derives from the Fick principle and applies the theory of material conservation and accountability to the circulation. That is, within a time interval, the quantity of a substance in the blood brought into a tissue must be equal to the quantity accumulated in the tissue, converted or removed from the tissue. Upon this principle, Kety developed a model for quantification of local blood flow rate using an intravenous bolus of an inert, freely diffusible tracer (Kety, 1960a, b). The equation shown below is known as the "Kety equation" and was used to calculate tissue blood flow rate per unit mass of tissue using a constant infusion of the radiolabelled tracer iodoantipyrine (^{125}I-IAP) over a short time period (30 seconds):

$$C_{tiss}(T) = k_1 C_a(t) \otimes e^{-k_2(t)} \qquad (1)$$

Where:

$C_{tiss}(T)$: is the concentration of the tracer in the tissue at the end of the infusion.

$k_1 = F_V$ (volume tissue blood flow rate in ml of blood per g of whole tissue per minute ($ml.g^{-1}.min^{-1}$).

$C_a(t)$: is the concentration of the tracer in the arterial blood entering the tissue as a function of time.

$\otimes$: denotes the convolution integral.

$k_2 = k_1/\alpha\lambda$ where α is the fraction of tumour effectively perfused and λ is the tissue:blood partition coefficient for the tracer for each tissue of interest.

$k_2 = F_V/\alpha\lambda$ and $\alpha\lambda$ is the apparent volume of distribution (VD_{app}) of the tracer in the tissue relative to the blood.

Equation (1) can be solved for k_2 or k_1 knowing:

- $C_{tiss}(T)$ at T = 30 seconds, this is the concentration of the tracer ^{125}I-IAP in the tissue at end of the infusion time and can be obtained by excising the tissues of interest at the end of a 30 seconds' infusion and measuring tissue ^{125}I levels using a gamma counter.
- C_a from t = 0 to t = T = 30 seconds, this is the concentration of ^{125}I-IAP in arterial blood, which can be obtained by arterial sampling during the 30 second infusion time and measuring blood ^{125}I levels using a gamma counter.
- λ: is the Tissue:Blood partition coefficient for ^{125}I-IAP for each tissue of interest, which had been previously determined for each tissue (Tozer and Morris, 1990).
- α: is the perfused tumour fraction, which is equal to VD_{app}/λ and was assumed to be 1.

Calculation of tissue blood flow rate was carried out using an in-house computer program using the above parameters. As part of the calculation, the program corrects the blood curve for the delay and dispersion or smearing effect that occurs in the arterial plastic catheter. An example of the calculation is shown in Table 2.1 and a typical corrected blood curve is represented in Figure 2.3. Values for delay and dispersion in the plastic catheters of a specific length and diameter were previously obtained from measurements made *in vitro* (Tozer G.M., personal communication). Briefly, this involved delivering a pulse of "hot" blood to the catheter (square-wave input) and plotting counts/g blood versus time from the radioactivity of blood exiting the catheter (smeared output). The dispersion constant (*d*) was derived from mathematical deconvolution of the smeared output against the square-wave input. By varying the linear flow rate of blood through the catheter, *d* was calculated for a range of values, which covered the range of linear flow rates obtained for the *in vivo* experiments.

From the corrected blood curve, a theoretical tissue curve is then produced using equation (1) and a range of values for blood flow (an example is shown in Figure 2.4). A look-up table is produced relating $C_{tiss}(T)$ at 30 seconds over the range of blood flow rates. The experimental value for $C_{tiss}(T)$ is then fed into the table to obtain the corresponding blood flow rate k_1 (an example of the final blood flow calculation is shown in Table 2.2).

Table of Blood Count and Corrections for Delay and Dispersion

Notes		Cannula Information		Misc. Information	
1st Reference:	21	Length (cm):	30	Background count value	
2nd Reference:	control	Diameter (cm):	0.058	5.0	
No of data points:	31	Correction Factors for Delay and Dispersion			
Vol. dist.	1.01	Dispersion:	0.526	Delay (s):	2.353

Data Point	Weight of tube (g)	Weight of tube and blood (g)	Weight of blood (g)	Count (counts/min)	Time (second)	C_a (counts/g)	C_a corrected for dispersion and delay (counts/g)
1	3.4926	3.68202	0.18942	7	0.63	10.55855	
2	3.53737	3.58029	0.04292	10	1.74	116.49581	-9.6
3	3.54569	3.57653	0.03084	7	2.72	64.85084	-89.7
4	3.52816	3.56009	0.03193	5	3.73	0.00000	-44.8
5	3.49528	3.54182	0.04654	4	4.93	-21.48689	-534.4
6	3.49516	3.52676	0.0316	-3	6.04	-253.16456	327.8
7	3.47898	3.5264	0.04742	5	7.1	0.00000	6755.9
8	3.49797	3.52997	0.032	104	8.23	3093.75000	61228.7
9	3.54754	3.59461	0.04707	1343	9.29	28425.74888	96875.5
10	3.50418	3.53574	0.03156	1871	10.39	59125.47529	124567.4
11	3.4726	3.52058	0.04798	4260	11.5	88682.78449	123628.9
12	3.48976	3.52121	0.03145	3287	12.6	104356.12083	133165.8
13	3.495	3.54204	0.04704	5526	13.71	117368.19728	147009.7
14	3.51956	3.56668	0.04712	6188	14.87	131218.16638	152037.0
15	3.53041	3.56261	0.0322	4533	15.98	140621.11801	158657.2
16	3.51347	3.56173	0.04826	7179	17.07	148653.12889	160520.6
17	3.50545	3.53752	0.03207	4943	18.17	153975.67820	171129.0
18	3.48922	3.52109	0.03187	5171	19.35	162096.01506	171415.6
19	3.54246	3.59064	0.04818	8019	20.47	166334.57866	161035.0
20	3.4943	3.52682	0.03252	5338	21.55	163991.38991	177038.3
21	3.50352	3.53665	0.03313	5640	22.71	170087.53396	181183.7
22	3.52519	3.57295	0.04776	8376	23.87	175272.19430	175649.6
23	3.53299	3.57613	0.04314	7574	25.06	175452.01669	193202.3
24	3.50588	3.53729	0.03141	5773	26.2	183635.78478	176253.4
25	3.50205	3.55114	0.04909	8856	27.31	180301.48706	199589.1
26	3.5339	3.58189	0.04799	9061	28.37	188705.98041	188645.5
27	3.50626	3.53824	0.03198	6039	29.39	188680.42527	199412.2
28	3.5304	3.57882	0.04842	9369	30.46	193391.16068	202263.7
29	3.48827	3.53684	0.04857	9594	31.58	197426.39489	211677.0
30	3.5221	3.56964	0.04754	9703	32.72	203996.63441	201917.6

Table 2.1 Example of correction of the arterial blood ^{125}I-IAP concentration (C_a) for delay and dispersion.

Note: Tube 1 (data point 1) is used for testing that blood is free flowing before the start of timed collection. Therefore, data from this tube is excluded from the analysis.

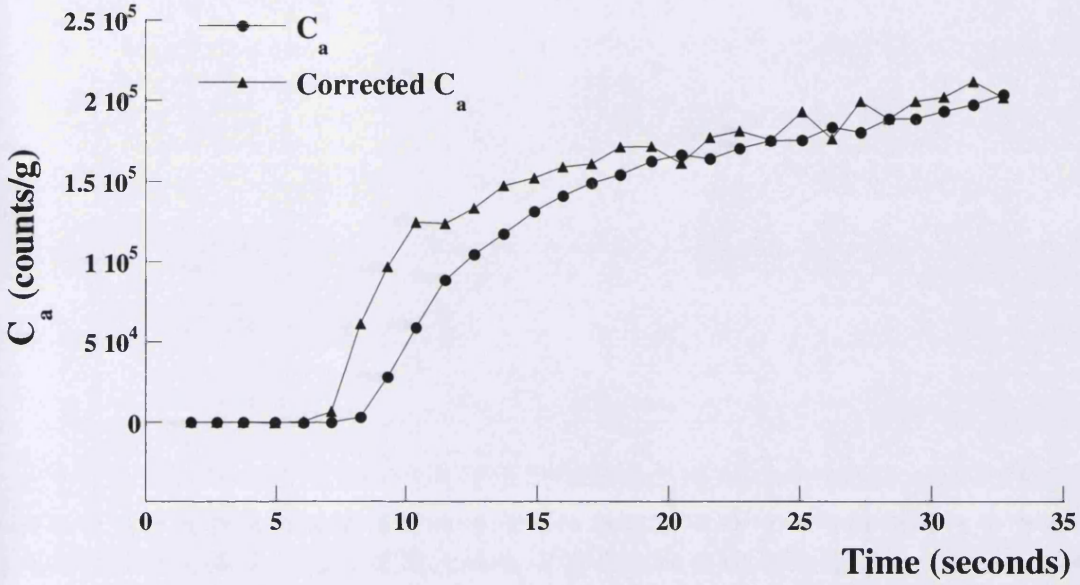

Figure 2.3 Blood curve showing the experimental values for the concentration of the tracer ^{125}I-IAP in arterial blood (C_a) and the corrected C_a for delay and dispersion. The data are from Table 2.1.

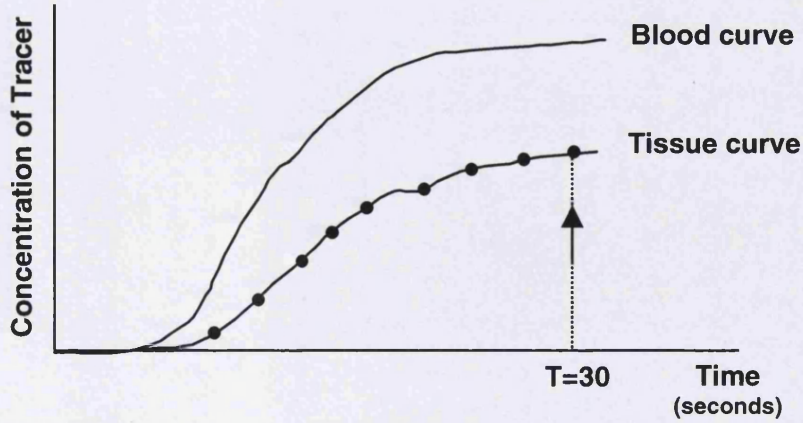

Figure 2.4 Theoretical tissue curve showing tissue levels of the tracer ^{125}I-IAP for a particular blood curve and blood flow value. This is repeated over a range of blood flow values for each blood curve and each animal.

Table of Volume Distribution, Tissue Count and Blood Flow					
First ref: 21 Second ref: Control					
	Volume Distribution (vd)	**Tissue Weight (g)**	**Count**	**C_{tiss} (counts/g)**	**Blood Flow ($ml.g^{-1}.min^{-1}$)**
Tumour	0.8	1.655	58566	35384	0.5927
Skin over tumour	0.73	2.148	29990	13959	0.2158
Skin	0.73	1.957	22528	11509	0.1761
Muscle	0.82	0.691	19823	28680	0.4658
Brain	0.8	1.184	81912	69178	1.3674
Heart	1.14	0.756	136271	180246	4.0214
Kidney	1.36	1.094	288898	264070	5.6929
Spleen	0.48	0.721	69039	95748	3.3385
Gut	1.01	0.760	56061	73758	1.3759

Table 2.2 Blood flow rate calculation in $ml.g^{-1}.min^{-1}$ for each tissue.

Drug administration, ^{125}I-IAP infusion and arterial blood sampling require cannulation of blood vessels. The following sections describe the surgical procedures for cannulation of rat tail veins and arteries as well as the detailed experimental protocol allowing collection of experimental data for the above parameters ($C_{tiss}(T)$ and $C_a(t)$) required for calculation of tissue blood flow rate.

2.8.2 Cannulation of Rat Tail Blood Vessels

2.8.2.1 Reagents and Materials

Anaesthetic mixture

1 part of fentanyl citrate (0.315 mg/ml) and fluanisone (10 mg/ml) ("Hypnorm", Janssen-Cilag Ltd.)

1 part of midazolam (5 mg/ml) (Phoenix Pharma Ltd.)

2 parts of injection water (B.Braun Medical Ltd.)

Given ip at a dose of 3.2 ml/kg

Heparinised saline

0.3 ml of 1000 U/ml heparin (CP Pharmaceuticals Ltd.)

10 ml injection saline (0.9 % w/v) (Steripak Ltd.)

Catheters

Polythene catheters of 0.58 mm internal diameter and 0.96 mm external diameter (SIMS Portex Ltd.) connected to 1 ml syringes filled with heparinised saline.

The artery catheter's length was set at 30 cm (this is important for the model used to calculate blood flow rate, see above).

2.8.2.2 Cannulation of the Artery

Anaesthesia was induced using halothane and maintained for ~ 45 minutes by injection of the Hypnorm/midazolam anaesthetic mixture. The anaesthetised rat was placed on a heating blanket and kept warm during the entire procedure. The animal's temperature was monitored using a rectal probe connected to a temperature monitor. The artery to be cannulated lies deep in the midline of the underside of the tail. The animal was placed on its back under a dissecting microscope. An incision was made on either side of the midline of the tail. Using forceps, the skin was cleared from the underlying connective tissue and cut at the distal end to form a flap. A slit into the thick connective tissue was made using a scalpel and the underlying artery was exposed. Sutures were placed under the artery at the distal and proximal ends and the distal suture was tied off securely. Using blunt forceps, a microvascular clamp was placed around the proximal end of the artery to occlude the vessel completely. A v-shaped cut was then made in the distal end of the vessel using spring scissors and a catheter containing heparinised saline was gently inserted into the lumen of the vessel. The clamp was removed and the cannula inserted further into the vessel for ~ 2 cm. The cannula was secured by tying up the proximal and distal sutures and taping up the wound. Approximately 0.2 ml heparinised saline was injected into the cannulated artery to ensure patency.

2.8.2.3 Cannulation of Veins

Two large veins lie laterally and superficially on each side of the tail. The anaesthetised animal was placed on its side and an incision made in the skin as for the artery. Using forceps, the skin was cleared from the underlying connective tissue and cut at the distal end to form a flap. The vein is clearly visible as the flap is lifted off the skin. The vessel was then carefully freed from the surrounding connective tissue and sutures were placed under the vessel at the distal and proximal ends with the distal suture tied off securely. The rest of the procedure is the same as for cannulation of the artery. The vein is more

friable than the artery and care was taken not to rupture it. The procedure was repeated for the second vein lying on the other side of the tail. At the end of the procedure gauze swab was wrapped around the wound and secured with tape.

2.8.3 Experimental Protocol for Quantifying Tissue Blood Flow Rate

2.8.3.1 Solutions and Reagents

^{125}I-IAP preparation

The required volume of ^{125}I-IAP (0.3 MBq ^{125}I/rat) (Institute of Cancer Research, Sutton) in methanol was removed from the stock vial and dispensed into a 5 ml-bottle. The methanol was evaporated using a gentle nitrogen flow and the ^{125}I-IAP was re-dissolved in injection saline (0.8 ml/rat). The ^{125}I-IAP solution was loaded onto a Monoject 2 ml syringe attached to a 23G needle and stored behind a lead shield until required.

heparin (1000 U/ml) (CP Pharmaceuticals Ltd.)

Injected just before blood flow measurement at 0.1 ml/rat via one of the tail vein catheters to ensure that blood will flow freely from the arterial catheter when collected.

Euthatal (Rhône Mérieux Ltd.)

Injected ~ 0.2 ml via one of the tail vein catheters for rapid killing of the animal at the end of the experiment.

2.8.3.2 Protocol

Following cannulation of the blood vessels, the tail artery catheter was connected to a Linseis L250E pressure transducer (CP Instruments) for measurements of mean arterial blood pressure and heart rate. One of the tail vein catheters was used to inject heparin and was later connected to the ^{125}I-IAP syringe held in an infusion pump set at a constant flow of 1.6 ml/minute according to the appropriate syringe diameter. The other tail vein catheter was connected to the syringe containing Euthatal. Shortly before blood flow measurement was due, the arterial catheter was clamped and disconnected from the pressure transducer and cut at the 30-cm mark (this is important for the model used to calculate blood flow). The catheter was then connected to a fraction collector set to collect free-flowing arterial blood samples at 1-second intervals into pre-weighed glass tubes. When ready, the arterial catheter was unclamped, the tracer infused over a 30-second period during which the arterial blood was collected. At 30 seconds, the animal

was killed by an injection of Euthatal and the tumour, overlying skin, skin from contralateral flank, gastrocnemius muscle, spleen, left kidney, small intestine, heart and brain were rapidly excised and placed into a glass jar containing moistened gauze. Tissues were blotted to remove excess blood and freed of connective tissue. The small intestine was cleared of food. Tissues were then weighed and placed into counting vials. The glass tubes containing blood were weighed and then both blood and tissue samples were counted for ^{125}I levels using a Wallac 1282 Compugamma Universal Gamma Counter.

Blood flow for each tissue was calculated in ml blood.g^{-1}.min^{-1} using the Kety equation (1) and tissue levels of ^{125}I, arterial levels of ^{125}I derived from arterial blood counts and the tissue:blood partition coefficient for IAP. All the calculations were performed using the in-house blood flow calculation computer programme as described above (section 2.8.1).

2.9 Immunohistochemistry

Staining of tissue sections by immunohistochemistry allows the detection of specific antigens on fixed frozen or paraffin embedded tissue material. This method permits histological localisation of specific antigens using antibodies, which have been raised against the protein of interest. The following sections describe how tissue sections are prepared and the various methods used for staining.

2.9.1 Tissue Preparation

Immunohistochemistry was performed on frozen or paraffin embedded material from rat P22 tumour and normal tissues. For the preparation of frozen material, the tumours and normal tissues were excised and quickly embedded in OCT tissue embedding medium (Sakura) and rapidly frozen in –40°C isopentane. The material was then stored in a –86°C freezer until processed. Frozen sections were cut at 5-10 μm thickness using a cryostat. After drying, the sections were fixed in –20°C acetone for 15 minutes at –20°C and stored in a –20°C freezer until immunohistochemistry was performed. For the preparation of the paraffin embedded material, excised tumours and normal tissues were fixed in 10% formalin solution (Sigma) and processed for paraffin wax embedding and cutting by the histology department (Gray Cancer Institute).

2.9.2 Staining Methods

There are several immunoenzymatic staining methods, which can be used to localise antigens. Two such techniques for light microscopy, which have been used in these studies, are the avidin-biotin and the soluble enzyme immune complex methods. The following sections describe the methodologies in general and more detailed experimental protocols can be found in Chapter 5.

2.9.2.1 Avidin-Biotin Method

This method utilises the high affinity of avidin or streptavidin for biotin. Avidin is a glycoprotein derived from egg white, which has a very high affinity for biotin, and streptavidin is similar in properties but has a lower affinity for biotin (biotin is a vitamin from the B complex found in egg yolk and liver). Avidin has four binding sites for biotin allowing for amplification of the signal and greater sensitivity in the technique. The avidin-biotin method used in these studies is an enzyme labelled avidin-biotin technique, which uses a biotinylated secondary antibody as a link antibody. Following incubation with the primary antibody, the tissue sections are exposed to the biotinylated secondary antibody followed by the avidin-biotin enzyme complex (Figure 2.5). Horseradish peroxidase and alkaline phosphatase are commonly used as enzyme labels and a variety of chromogenic substrates are available for detection of the antigens. Some tissues are rich in endogenous biotin or avidin resulting in non-specific background staining. This problem can be minimised by pre-incubation of tissue sections with avidin and biotin solutions in order to block the endogenous biotin and avidin binding activities.

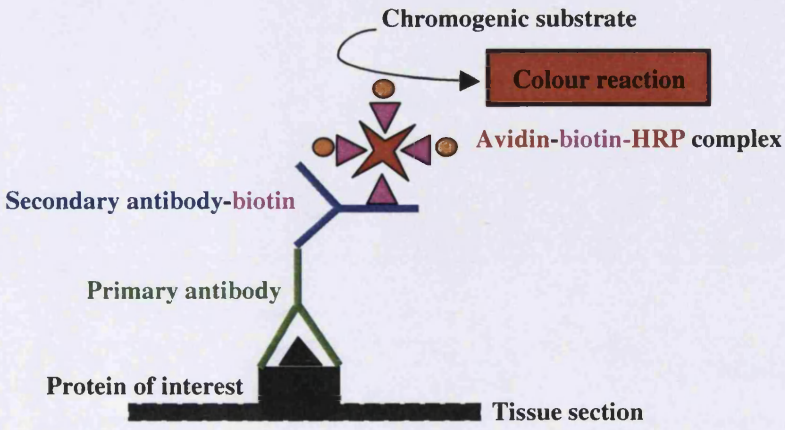

Figure 2.5 Schematic representation of the avidin-biotin method.

2.9.2.2 Soluble Enzyme Immune Complex Method

This method utilises a pre-formed soluble enzyme anti-enzyme immune complex consisting of an antigen, which in this case is the enzyme itself, and the antibody raised against the enzyme. In these studies an alkaline phosphatase anti-alkaline phosphatase complex (APAAP) was used. Following incubation with the primary antibody, the tissue sections are treated with a secondary antibody, which acts as a link antibody followed by the enzyme immune complex (Figure 2.6). The primary and secondary antibodies as well as the enzyme complex have to be from the same species. Detection of the protein of interest is then performed using an appropriate substrate for the alkaline phosphatase enzyme.

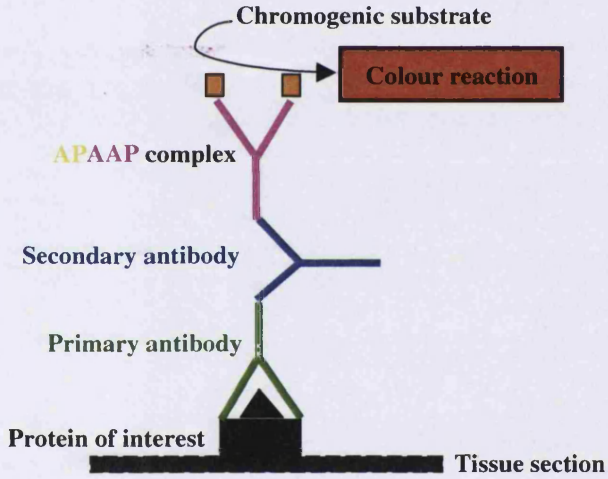

Figure 2.6 Schematic representation of the APAAP method.

2.10 Immunofluorescence

The immunofluorescence technique is based on the same principles as the immunohistochemistry described above only that it uses fluorescence as the detection tool. Immunofluorescence visualisation of the tubulin cytoskeleton was carried out on fixed cells, which had been seeded on microslides using an avidin/biotin method. Briefly, following incubations with the primary and biotinylated secondary antibodies, cells were exposed to fluorescein-labelled avidin and the protein of interest visualised using a fluorescence microscope (Figure 2.7).

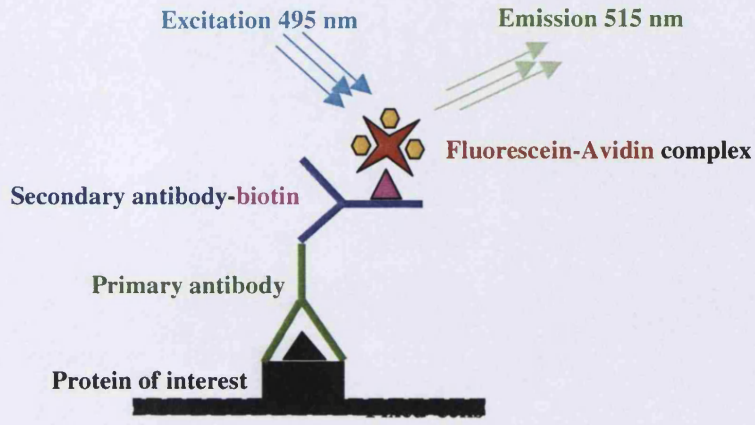

Figure 2.7 Schematic representation of the immunofluorescence staining procedure using an avidin-biotin method.

2.11 Immunofluorescence Double Labelling

Double labelling experiments allow for detection of two different antigens on the same tissue section. The use of two fluorochromes is the recommended method for double labelling antigens that may co-localise. To use two fluorochromes on the same specimen, each antigen must be recognised by only one of the labelled reagents. One way of achieving this distinction is by using two detection reagents that are species specific. Here for instance, a polyclonal rabbit antibody and a monoclonal mouse antibody specific for two different antigens were used (Figure 2.8). The polyclonal rabbit antibody was detected by the avidin-biotin method using a biotinylated anti-rabbit secondary antibody as a link antibody, and fluorescein-labelled avidin (Vector) as the fluorochrome. On the other hand, the monoclonal mouse antibody was detected with an anti-mouse secondary antibody tagged to another fluorochrome known as AlexaFluor 594 (Cambridge Bioscience) (Figure 2.8).

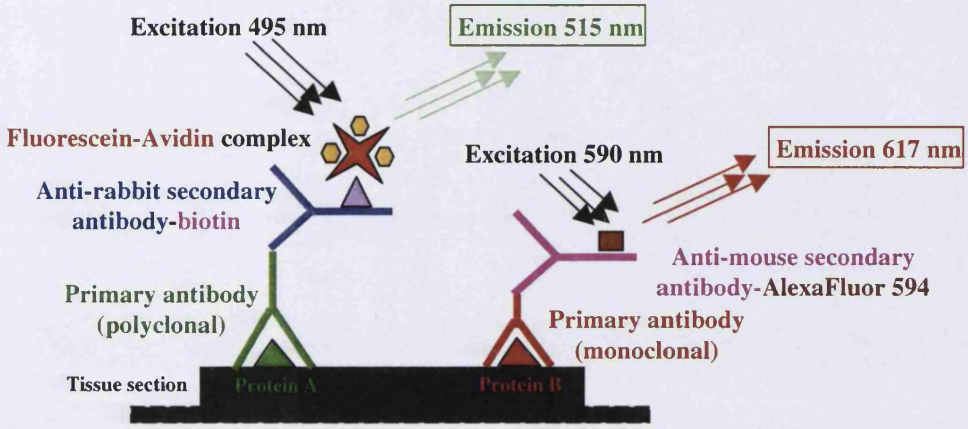

Figure 2.8 Schematic representation of the immunofluorescence double labelling using an avidin-biotin method and a labelled secondary antibody.

2.12 Statistics

Significance tests were carried out on the data groups using analysis of variance (ANOVA) followed by a comparison between the specific groups using the Student's *t*-test. The analyses were conducted using the JMP statistical package (SAS Institute Inc., USA). Values of $p<0.05$ were considered significant.

CHAPTER 3

HAEMOXYGENASE IN TUMOURS AND NORMAL TISSUES

3.1 Introduction

As described in section 1.5.5.1 of Chapter 1, HO enzyme activity and HO-1 expression has been detected in both animal tumour models and human tumour biopsies. For instance, HO-1 expression was measured in an experimental solid tumour model (AH136B hepatoma) in rats (Doi *et al.*, 1999). High HO activity was also measured in subcutaneous transplants of the P22 rat carcinosarcoma, which was of the same order as that found in normal rat liver (Tozer *et al.*, 1998 and results in this chapter). *In vitro*, studies using tumour spheroids of the human A431 squamous carcinoma cell line have shown that HO expression and activity is enhanced in this three dimensional tumour model as compared to monolayer cultures (Murphy *et al.*, 1993). In human tumours, HO-1 mRNA was found to be expressed at higher levels in human brain tumour specimens than normal brain tissue (Hara *et al.*, 1996). Furthermore, increased HO-1 immunoreactive staining was observed in benign prostatic hyperplasia and malignant prostate tissue (Maines and Abrahamsson, 1996). HO-1 over-expression was also detected in biopsy samples from human renal cell carcinomas as compared to normal renal tissue (Goodman *et al.*, 1997). In a more recent study, HO-1 positive staining was found to be present in ~ 50% of human oesophageal squamous cell carcinomas (Yokoyama *et al.*, 2001).

In this chapter, data will be presented on overall HO enzyme activity and HO-1/HO-2 protein levels in five tumour models. These are subcutaneous transplants of the rat P22 carcinosarcoma, the mouse CaNT mammary carcinoma and the LoVo, HT-29 and SW-1222 human colorectal adenocarcinoma xenografts.

3.2 Materials and Methods

Detailed methodology for tumour transplantation, microsome preparation, HO activity assay and western blotting protocols can be found in Chapter 2.

3.3 Results

3.3.1 Overall HO Enzyme Activity in Tumours and Rat Normal Tissues

HO enzyme activity was measured in microsome fractions extracted from rodent tumours (rat P22 and mouse CaNT) and human colorectal xenografts (HT-29, LoVo and SW-1222), and the results were compared to the levels of HO enzyme activity in microsome fractions extracted from a range of rat normal tissues. Figure 3.1 shows that HO enzyme activity could be detected in all the tumour types but that the level of activity varied. HO activity was highest in the rat P22 tumour with the mouse CaNT, and the xenografts HT-29, LoVo and SW-1222 showing lower activities in decreasing order (Figure 3.1). The level of HO activity in the P22 tumour was of the same order as that measured in the normal rat liver and brain (Figure 3.1). Amongst the rat normal tissues, the activity was highest in the spleen, testes, brain and liver in decreasing order, with the kidney, heart, skeletal muscle and small intestine showing much lower values, again in decreasing order (Figure 3.1). These patterns are in accordance with reported studies (Maines, 1988).

3.3.2 HO-1 and HO-2 Protein Levels in Tumours

HO-1 and HO-2 protein levels were measured in microsome fractions extracted from rodent tumours (rat P22 and mouse CaNT) and human colorectal xenografts (HT-29, LoVo and SW-1222), and the results were compared to the protein levels in microsome fractions extracted from rat spleen and brain. Figure 3.2 demonstrates that the HO-1 protein, the inducible form of HO, is present in all tumour types at relatively high levels. The HO-1 protein levels are even higher in the spleen but absent in brain microsomes (Figure 3.2). In the double band present in the SW-1222 samples and also the spleen, the lower molecular weight band is probably a degradation product due to protease activity.

Figure 3.3 shows that the HO-2 protein, the constitutive form of HO, is also present abundantly in all the tumour types analysed. The HO-2 levels in the tumours are comparable to levels in normal rat brain and spleen (Figure 3.3). In the P22 tumour samples, the smeared HO-2 bands may be due to either protein degradation as a result of protease activity or alternatively, to the presence of variants of the protein since it is known that the HO-2 protein is the product of two or more mRNA transcripts (McCourbey and Maines, 1994; McCourbey et al., 1995).

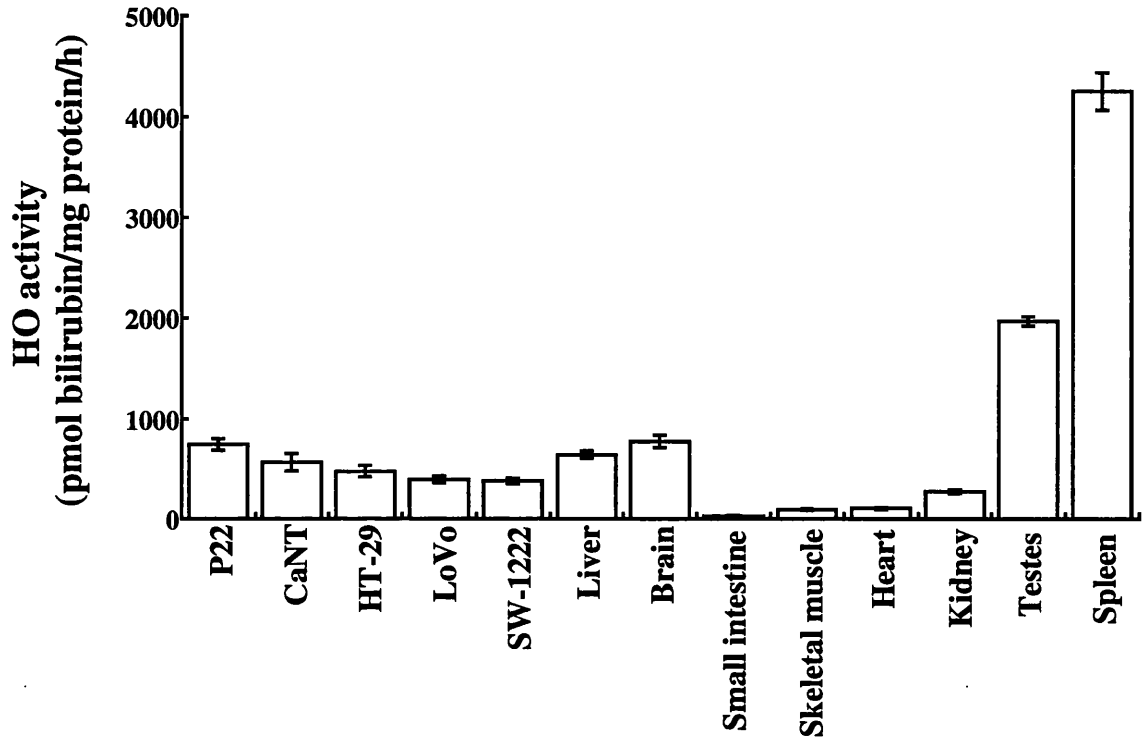

Figure 3.1 Comparison of overall HO enzyme activity in a range of tumour models and rat normal tissues. HO enzyme activity was measured in microsome fractions isolated from P22 rat carcinosarcomas, CaNT mouse mammary carcinomas, and HT-29, LoVo and SW-1222 human colon xenografts and also from a range of rat normal tissues. The data are means of 3-6 tumour-bearing animals per group. Error bars are ± 1 standard error of the mean. Note: For the P22, microsomes were from individual tumours, whereas a pool of 4 tumours was necessary for the other, smaller, tumours growing in mice. The rat normal tissues were from tumour-bearing animals.

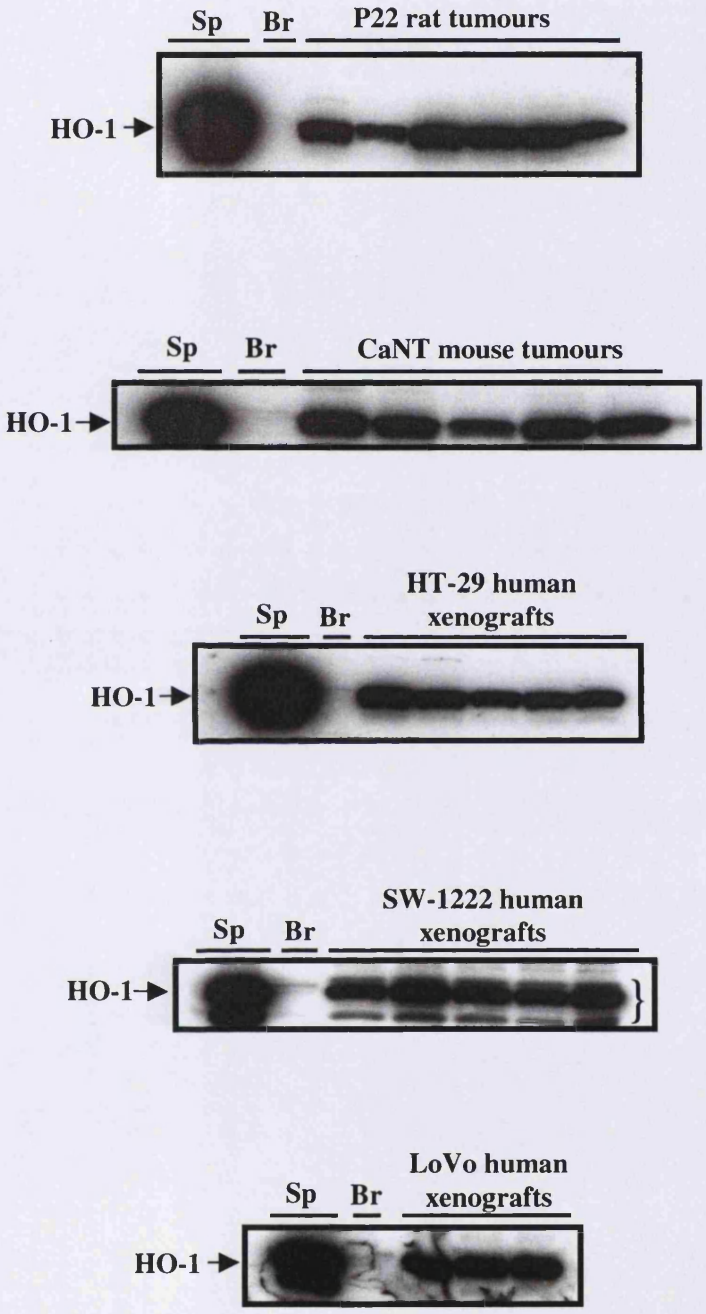

Figure 3.2 HO-1 protein levels in a range of tumour types. Western blots showing endogenous levels of HO-1 protein in the rat P22 rat carcinosarcoma, CaNT mouse carcinoma, HT-29, LoVo and SW-1222 human colon xenografts. The samples are the same as those used for HO enzyme activity analysis in Figure 3.1. *Note:* Bands for the P22 are of individual tumours, whereas bands for the other tumour types represent separate pools of 4 tumours. Sp: spleen, Br: brain.

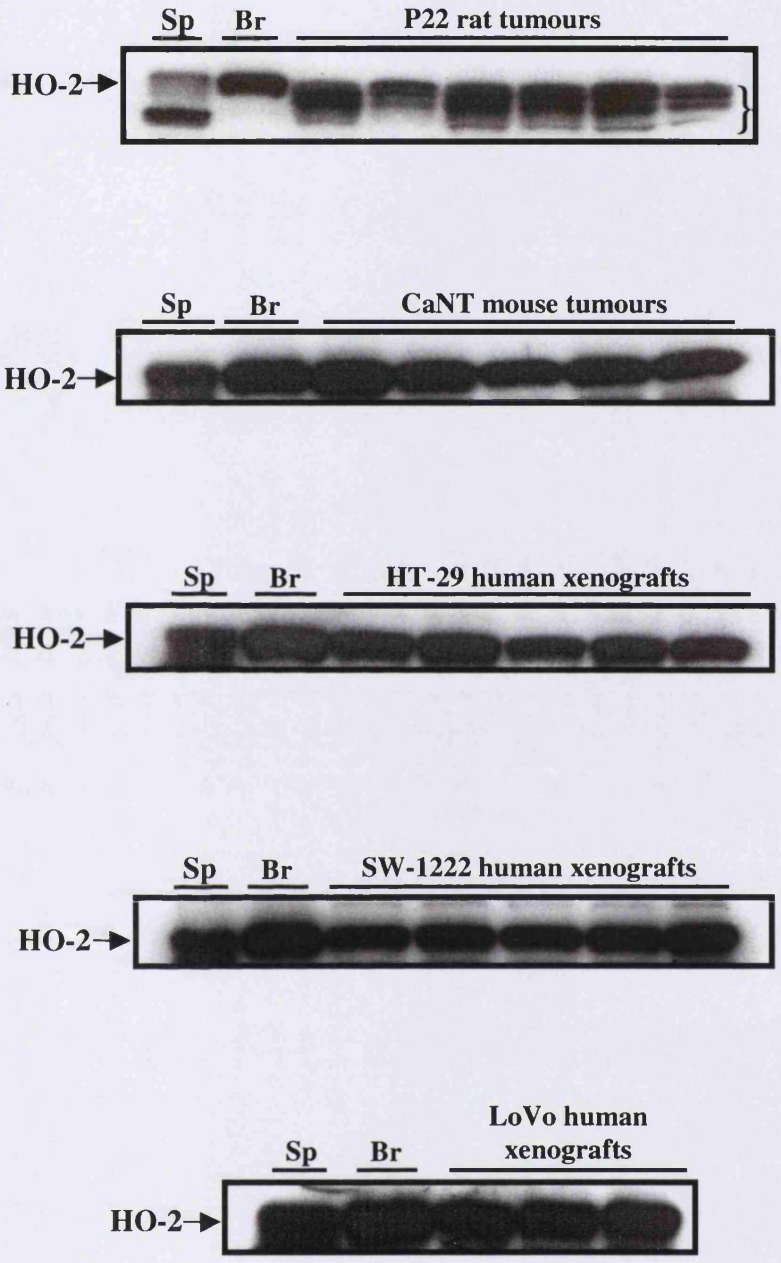

Figure 3.3 HO-2 protein levels in a range of tumour types. Western blots showing endogenous levels of HO-2 protein in the rat P22 rat carcinosarcoma, CaNT mouse carcinoma, HT-29, LoVo and SW-1222 human colon xenografts. The same blot as used for HO-1 probing was stripped and re-probed for HO-2. The samples are from the same as those used for HO enzyme activity analysis in Figure 3.1. *Note:* Bands for the P22 are of individual tumours, whereas bands for the other tumour types represent separate pools of 4 tumours. Sp: spleen, Br: brain.

3.4 Discussion

In vivo HO characterisation of a range of rodent and xenografted human tumours has shown a high resting level of HO enzyme activity which was comparable to normal rat liver and brain. Furthermore, western blotting has also shown that this activity is attributed to both the HO-1 and HO-2 isozymes, with the HO-1 protein level being highly expressed in these tumours. With regard to the cell types that could be the source of both HO-1 and HO-2 in these tumours, the contribution of not only the tumour cells themselves but also the immune cells infiltrating the tumour tissue and the endothelial and smooth muscle cells lining blood vessels has to be taken into consideration. Here, the enzyme activity and isozyme protein levels reflects the overall contribution of potentially various cell types since microsome fractions were obtained from whole homogenised tumours. Previous studies have shown by immunohistochemistry prominent expression of HO-1 in infiltrating macrophages rather than tumour cells in both experimental rat and human brain tumours (Deininger *et al.*, 2000; Nishie *et al.*, 1999). Furthermore, several studies have shown that HO-2 (and HO-1 under stressful conditions) is present in the endothelial and smooth muscle lining of blood vessels (Zhang *et al.*, 2001; Zakhary *et al.*, 1996), although there are no studies in the literature examining the localisation of HO-2 (or HO-1) to tumour blood vessels.

The current results give rise to two major questions. First, why does the tumour tissue contain high levels of HO-1 under unstimulated conditions, and second what could be the putative roles of this enzyme system in these tumours? HO-1 is known to be an inducible protein, except in the spleen where it is expressed at high levels under unstimulated conditions, probably due to a need for continuous haem degradation as a result of erythrocyte recycling which occurs in this organ. In tumours, high HO-1 levels may be due to local factors released from the tumour cells themselves or the tumour-associated immune cells such as macrophages and neutrophils. Moreover, the particular characteristics of the microenvironment in tumours may also contribute to high resting levels of HO-1. Hypoxia for example, which is frequently found in tumours, has been shown to induce HO-1 (Motterlini *et al.*, 2000; Panchenko *et al.*, 2000). Furthermore, as described in the General Introduction (Chapter 1), the vascular network of tumours is rather inefficient due to spatial and temporal heterogeneity in blood supply. Therefore, it

is possible that transient fluctuations in blood flow could cause the generation of oxygen free radicals due to ischaemia-reperfusion. Again the latter has been demonstrated to induce HO-1 in tumours (Doi *et al.*, 1999) and other systems (Maines *et al.*, 1993; Maulik *et al.*, 1996). NO could be another stimulus for HO-1 production in tumours. Previous *in vitro* studies have demonstrated the ability of NO donors to induce HO enzymatic activity (Motterlini *et al.*, 1996). Furthermore, Doi *et al.* have shown in an *in vivo* experimental solid tumour model (AH136B rat hepatoma) that HO-1 levels were modified by NOS inhibitors (Doi *et al.*, 1999). Previous studies assessing NO production in the P22, CaNT, LoVo and HT-29 tumours by nitrate and nitrite measurements have shown highest levels in the P22, with the CaNT, LoVo and HT-29 tumours showing lower levels in decreasing order (unpublished data, Gray Cancer Institute Annual Report, 2001). This order follows a similar pattern to the HO enzyme activity levels, as shown in Figure 3.1. It would be interesting to examine whether NO contributes to the high resting levels of HO-1 in these tumour models using NOS inhibitors.

Currently, the putative roles of HO-1 in tumours are still unclear. The products of haem degradation by HO-1, namely bilirubin and CO, may be important in cytoprotection against radical damage and maintenance of vascular homeostasis, respectively. More recently, HO-1 has been implicated in modulating the processes of angiogenesis and cell proliferation (see sections 1.5.3.5, 1.5.4.3.4, 1.5.5.2 of Chapter 1) suggesting its potential importance for tumour growth and expansion.

The levels of HO-2 protein were also high in all the tumour types examined as compared to the levels in normal rat brain (Figure 3.3), suggesting a potential important role of this enzyme system in tumours. HO-2 was shown to be present in the endothelial and smooth muscle lining of blood vessels and to play an important role in the regulation of vascular tone via the generation of CO (see sections 1.5.2.2 and 1.5.4.3.1 of Chapter 1). The potential for such a role in tumours needs to be investigated.

It should be noted that there seem to be some inconsistency between the HO enzyme activity and the western blotting results. For instance, the LoVo and SW-1222 tumours show as high HO-1 and HO-2 protein levels as the P22 but have lower overall HO enzyme activity than the P22 (Figures 3.1, 3.2 and 3.3). Western blotting is only a semi-quantitative method for assessing the level of expression of a protein, and comparison

between different blots is difficult because of possible differences in the antibody titre used and also differences in the time of film exposure. More accurate comparisons are possible between the intensity of bands on the same blot, which are normalised to the protein content of the sample. On the other hand, the HO enzyme activity gives an indication of the functional characteristics of an enzyme and its ability to catalyse a particular reaction. Therefore, the discrepancies highlighted above may be due to several factors such as the difficulty in comparing protein levels between blots, insensitivity of the HO assay or to the fact that not all the HO-1/HO-2 protein expressed *in vivo* are functional. In the LoVo and SW-1222 tumours, the latter possibility could explain the lower overall HO enzyme activity in these tumours compared to the P22 (Figure 3.1), despite similar HO-1 and HO-2 isozyme levels (Figures 3.2 and 3.3).

3.5 Summary

This study demonstrated that HO enzyme activity could be measured in various tumour models, where the levels are comparable to the activity measured in normal rat brain and liver. All the tumour types showed high resting levels of HO-1 and also HO-2 proteins, suggesting a potential important role of this enzyme system in tumours. The potential vascular and growth modulatory roles of HO are presented in Chapters 4 and 6, whereas the potential cytoprotective roles of HO-1 against CA-4-P-mediated tissue damage are presented in Chapter 5.

CHAPTER 4

ROLE OF HAEMOXYGENASE IN THE CONTROL OF TUMOUR BLOOD FLOW

4.1 Introduction

As described in the General Introduction, the continuous growth and expansion of solid tumours is critically dependent on the establishment of a vascular network providing nutritive blood flow, thereby, making the tumour vasculature an attractive target for cancer therapy (Folkman 1990; Chaplin *et al.*, 1998). Currently, there is still a need to understand the mechanisms, which regulate and maintain blood flow to tumours. In their resting state, many tumours are under the influence of a vasodilatory tone and there is substantial evidence that one of the prime mediators of this is NO (Tozer and Everett, 1997). Indeed, in experimental tumour models, inhibition of NOS activity has been shown to result in a significant reduction in blood flow (Tozer *et al.*, 1997) and chronic NOS inhibition has been shown to significantly slow tumour growth (Orucevic and Lala, 1996). In the present study, the role of the vasodilating molecule CO was investigated. Evidence for the important role of CO in vasoregulation in various systems can be found in Chapter 1 (see section 1.5.4.3.1). Of particular interest in this project is the potential importance of CO in the regulation of vascular tone in tumours and consequently, the possibilities for exploiting this system for modifying tumour blood flow.

The importance of the HO/CO system in the regulation and maintenance of tissue blood flow was investigated in the P22 rat tumour model. High resting levels of HO activity were detected in this tumour, which were comparable to normal rat liver (see Figure 3.1 in Chapter 3). This was also reflected by high resting levels of the HO isozymes, HO-1 and HO-2 (see Figures 3.2 and 3.3 in Chapter 3). These findings suggest that CO production resulting from HO activity could be an important contributor to maintenance of blood flow in this tumour. However, previous studies in our laboratory, using the HO inhibitor zinc-protoporphyrin IX (ZnPP) have failed to conclusively establish a role for HO in regulating tumour blood flow due to the lack of inhibition of tumour HO activity by ZnPP *in vivo* (Tozer *et al.*, 1998).

The aim of the present study was to further clarify the potential vascular role of endogenous HO in tumours using an effective inhibitor of HO in the P22 rat tumour model. Tin-protoporphyrin IX (SnPP) was chosen for these investigations as it was shown to inhibit HO in various organs including liver, spleen, kidney, and skin of the rat at doses of 20, 25 and 50 μmol/kg subcutaneously or 10 μmol/kg intravenously (Drummond and Kappas, 1981; Anderson *et al.*, 1984). Other investigators did however report a lack of inhibition of intestinal HO (Hintz *et al.*, 1988). These differential effects between organs are thought to be attributed to possible differential isozyme abundance or differential tissue distribution and disposition of the compound (Maines, 1988). SnPP is a synthetic metalloporphyrin which acts as a competitive substrate for haem in the HO reaction, but because it lacks the central iron atom it cannot bind molecular oxygen and therefore does not undergo oxidative degradation by the enzyme (Kappas and Drummond, 1986; Figure 4.1). It is also the only metalloporphyrin that has been used in humans, including newborn infants, to suppress serum bilirubin levels (Berglund *et al.*, 1988; Kappas *et al.*, 1988).

Initial experiments were conducted to verify the ability of SnPP to inhibit tumour HO activity before determining the effects of the compound on tumour blood flow rate. Copper-protoporphyrin IX (CuPP) was used as a negative control in these studies since it has been reported to have no inhibitory effects on HO activity *in vivo* (Drummond and Kappas, 1981) and to be only a poor inhibitor *in vitro* (Zakhary *et al.*, 1996) (Figure 4.1).

Studies were also conducted to investigate the effect of over-expression of HO-1 on tissue blood flow rate using hemin treatment. Hemin, also known as ferri-protoporphyrin IX chloride, is a haem analogue and a known inducer of HO-1 (Figure 4.2). Hemin is also a substrate for the HO enzyme and undergoes degradation to produce the biologically active molecules bilirubin and CO.

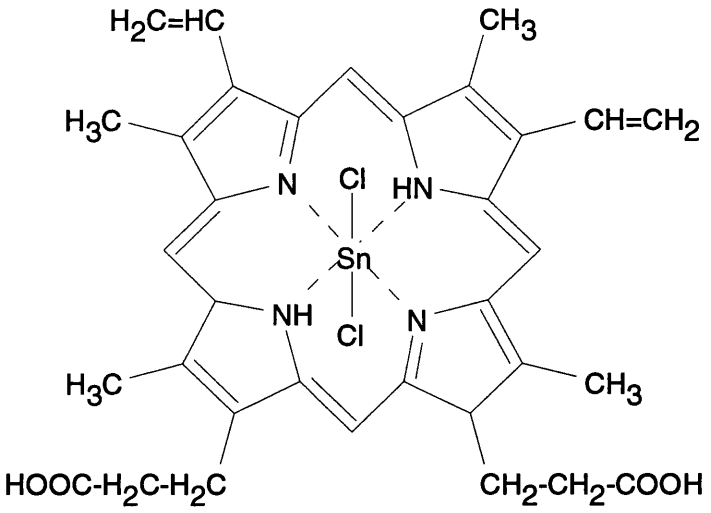

SnPP

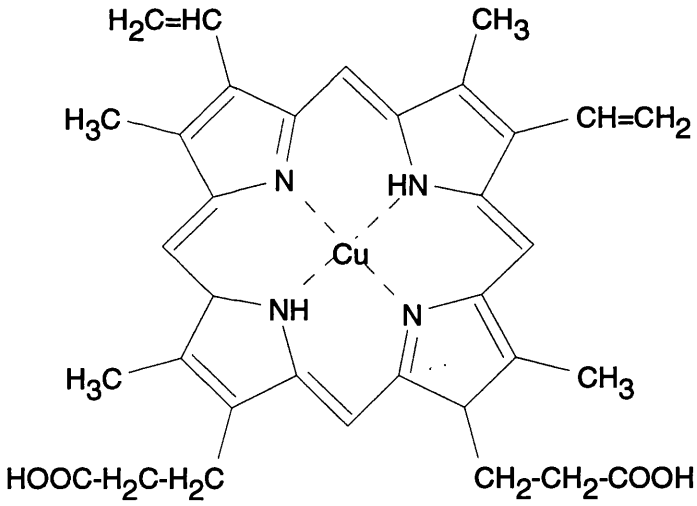

CuPP

Figure 4.1 Structures of tin-protoporphyrin IX dichloride (SnPP) and copper-protoporphyrin IX (CuPP).

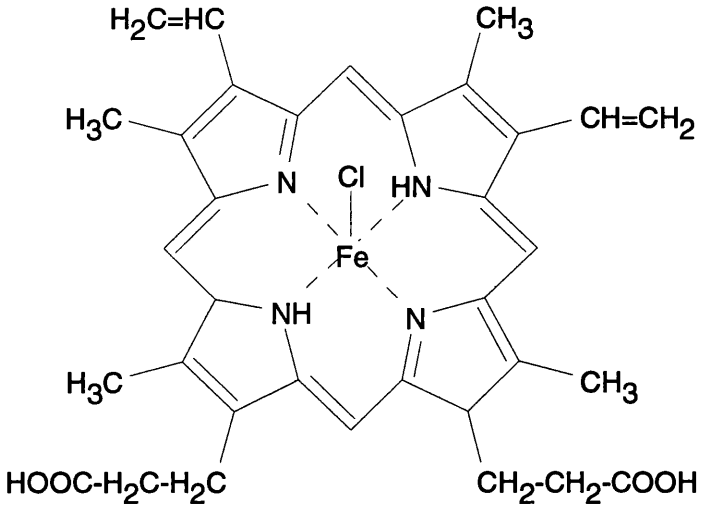

Hemin

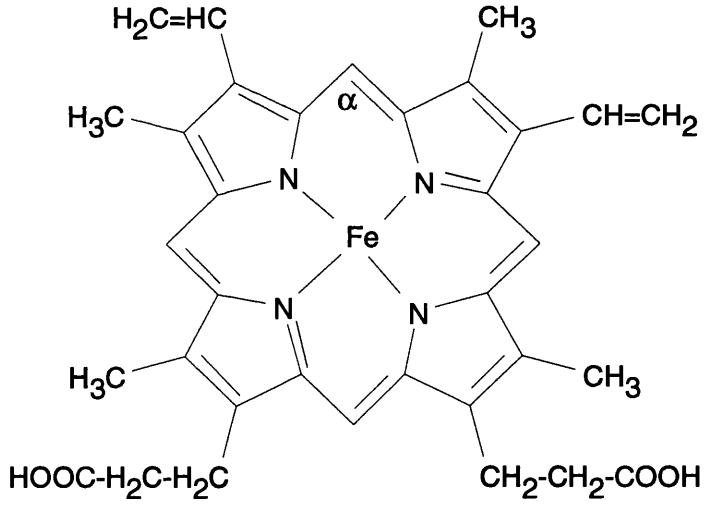

Haem

Figure 4.2 Structures of haem and its analogue hemin (ferri-protoporphyrin IX chloride).

4.2 Materials and Methods

4.2.1 Drug Preparation

sodium carbonate as drug vehicle (Na_2CO_3; 50 mM)

0.53 g Na_2CO_3 (Sigma)

100 ml distilled water

copper-protoporphyrin IX (CuPP; Affiniti Research Products)

Dissolved in Na_2CO_3 (50 mM); shield from light during preparation and injection into the animal.

Administered intraperitoneally (ip) at 3 ml/kg rat body weight

tin-protoporphyrin IX (SnPP; Affiniti Research Products)

Dissolved in Na_2CO_3 (50 mM); shield from light during preparation and injection into the animal.

Administered ip at 3 ml/kg rat body weight

hemin (Sigma)

Dissolved in Na_2CO_3 (50 mM)

Administered ip at 3 ml/kg rat body weight

4.2.2 Experimental Protocol

The present studies were carried out using the P22 rat tumour model (see section 2.2.1 of Chapter 2). Animals were selected when the subcutaneously transplanted tumours had reached a geometrical mean diameter of 11-12 mm.

In the first part of the study, the effects of hemin treatment on tumour and normal tissue blood flow rate were examined (see section 2.8 of Chapter 2). Initial experiments were conducted to confirm the ability of hemin, administered at a dose 10 mg/kg, to induce tumour HO enzyme activity and HO-1 protein levels at 6 and 24h post-treatment (see sections 2.4, 2.5 and 2.7 of Chapter 2). Preliminary studies showing an increase in overall HO enzyme activity using this dose of hemin had been previously carried out in our laboratory (unpublished data). For the blood flow experiments, hemin (10 mg/kg) was administered 24h prior to blood flow rate measurements based on the HO enzyme activity studies.

The second part of the study involved investigating the role of endogenous HO activity in the regulation of tissue blood flow rate using the HO inhibitor SnPP. Initial experiments were conducted in order to determine the extent and time-course of HO inhibition in response to SnPP and CuPP both given at a dose of 45 μmol/kg. The animals were sacrificed at 15, 30 and 60 minutes post-treatment and the tumour, liver and kidney were excised for analysis. Microsomes were prepared and analysed for HO enzyme activity as described in Chapter 2 (see sections 2.4 and 2.5). The effects of HO activity inhibition on tumour and normal tissue blood flow rate were then examined (see section 2.8 of Chapter 2). For these studies, either SnPP or CuPP were administered to tumour-bearing rats 15 minutes prior to blood flow rate measurement at a dose of 45 μmol/kg based on the HO enzyme activity inhibition studies.

4.2.3 Statistics

Statistical analysis was applied as described in Chapter 2 (see section 2.12).

4.3 Results

4.3.1 Hemin-Mediated Increase in HO Activity and HO-1 Protein Levels

In vivo administration of hemin induced an increase in HO activity and HO-1 protein levels in the P22 tumour (Figure 4.3). At a dose of 10 mg/kg, hemin administration increased HO activity by ~ 2 fold at 24h but had no effect on HO activity at 6h post-treatment (Figure 4.3A). These changes were reflected by an increase in the level of the HO-1 protein at 24h as shown by western blotting (Figure 4.3B).

A)

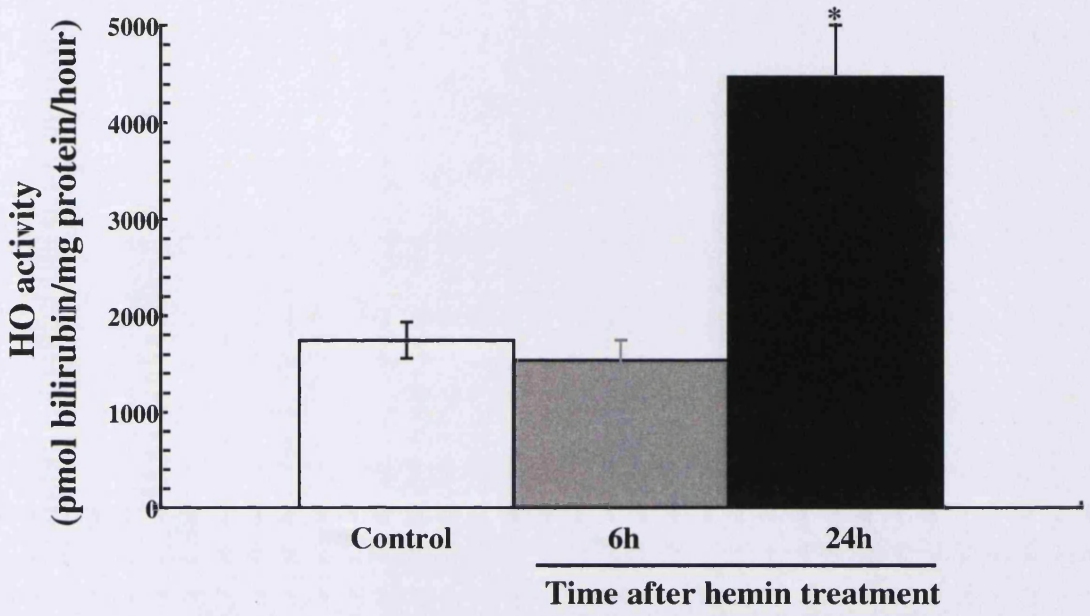

B)

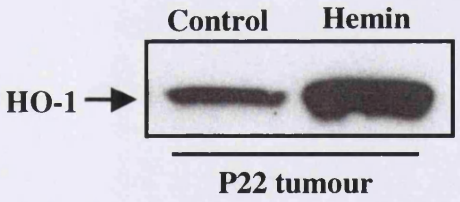

Figure 4.3 Effects of hemin on HO in the P22 tumour. *A)* Effects of hemin (10 mg/kg ip) on HO activity in microsome fractions from P22 tumours at 6 and 24h post-treatment. The graph data are means of 5-6 animals per group. Error bars are ± 1 standard error of the mean. * represents a significant difference from controls ($p<0.05$). *B)* Western blot showing hemin-mediated increase in HO-1 protein levels at 24h post-treatment.

4.3.2 HO-1 Induction and Tissue Blood Flow Rate

The results presented in Figure 4.4 show that administration of a single dose of hemin (10 mg/kg ip) 24h prior to blood flow rate measurement did not cause any changes in either tumour or normal tissue blood flow rate. This is despite the fact that this dosing and timing regimen effectively increased tumour HO activity and HO-1 protein levels (Figure 4.3). Furthermore, hemin administration did not affect either mean arterial blood pressure (MABP) or heart rate (Figure 4.5).

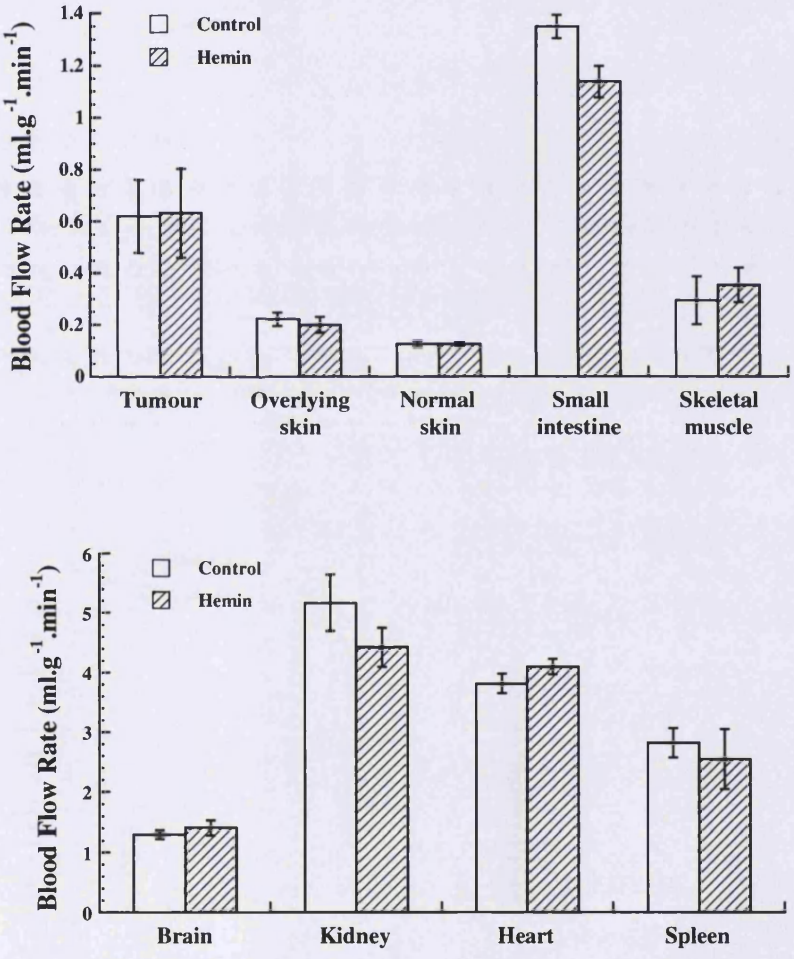

Figure 4.4 Effects of hemin on tissue blood flow rate. Effects of ip injection of hemin (10 mg/kg) on blood flow rate in the P22 tumour and a range of normal tissues 24h post-treatment. Values are the means of 3-5 animals per group. Error bars are means ± 1 standard error of the mean.

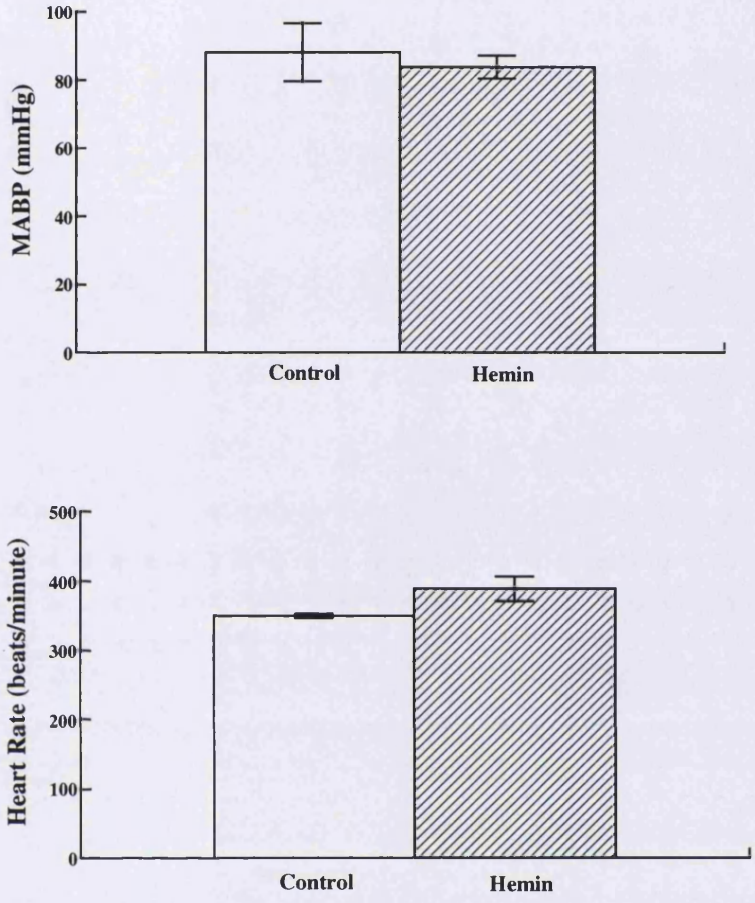

Figure 4.5 Effects of hemin on MABP and heart rate. Hemin (10 mg/kg) was administered 24h prior to MABP and heart rate measurements. Values are the means of 3-5 animals per group. Error bars are means ± 1 standard error of the mean for the same group of animals shown in Figure 4.4.

4.3.3 Various Dosing Regimen for Hemin

The negative results obtained above raised the question of whether the level of HO enzyme activity induction with 10 mg/kg hemin was enough to mediate changes in tissue blood flow rate. Therefore, experiments were conducted to investigate whether higher doses of hemin could further increase levels of HO activity. Here, the level of increase in overall HO activity in response to a 50 mg/kg i.p dose of hemin was examined. The results plotted in Figure 4.6 show that a 5 times higher dose of hemin (50 mg/kg) caused only a moderate increase in total HO activity. It was felt that this increase was not

sufficient to justify assessing the effects of this dose of hemin on tissue blood flow rate. A multiple dosing regimen with hemin was also examined, whereby hemin was administered at a dose of 26 mg/kg ip/dose given 24h apart. However, this double dosing with hemin resulted in rats developing diarrhoea and inflammation of the eyes thereby preventing further testing the effects of this dosing regimen on tissue blood flow rate.

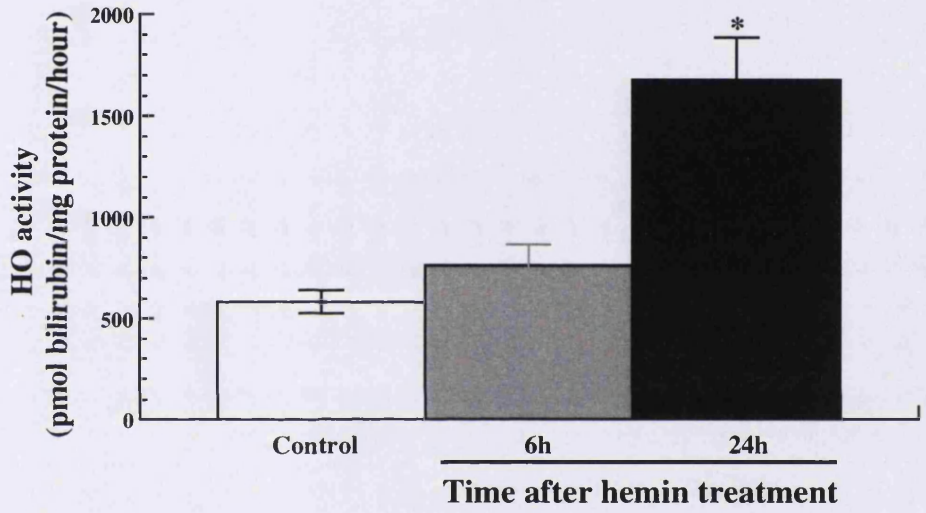

Figure 4.6 HO enzyme activity in response to hemin. Effects of hemin (50 mg/kg ip) on HO activity levels at 6 and 24h post-treatment. The data are means of 5 animals per group. Error bars are ± 1 standard error of the mean. * represents significant difference from controls ($p<0.05$).

Note: The large differences in the absolute values of HO enzyme activity in control tumours between Figures 4.3 and 4.6 are due to the fact that the HO enzyme activity assay was conducted in different laboratories. Investigations into the reasons for such discrepancies revealed that they were due to differences in the readings given by the spectrophotometric machines in the two laboratories.

4.3.4 SnPP-Mediated HO Inhibition

Administration of a single dose of SnPP (45 μmol/kg ip) caused HO enzyme activity to decrease to zero within the first 15 minutes of treatment. It remained inhibited for at least 1h post-treatment (Figure 4.7). On the other hand, the same dose of CuPP did not affect the HO enzyme activity at the same time points examined (Figure 4.7). The latter result is consistent with previously reported data for this tumour (Tozer *et al.*, 1998).

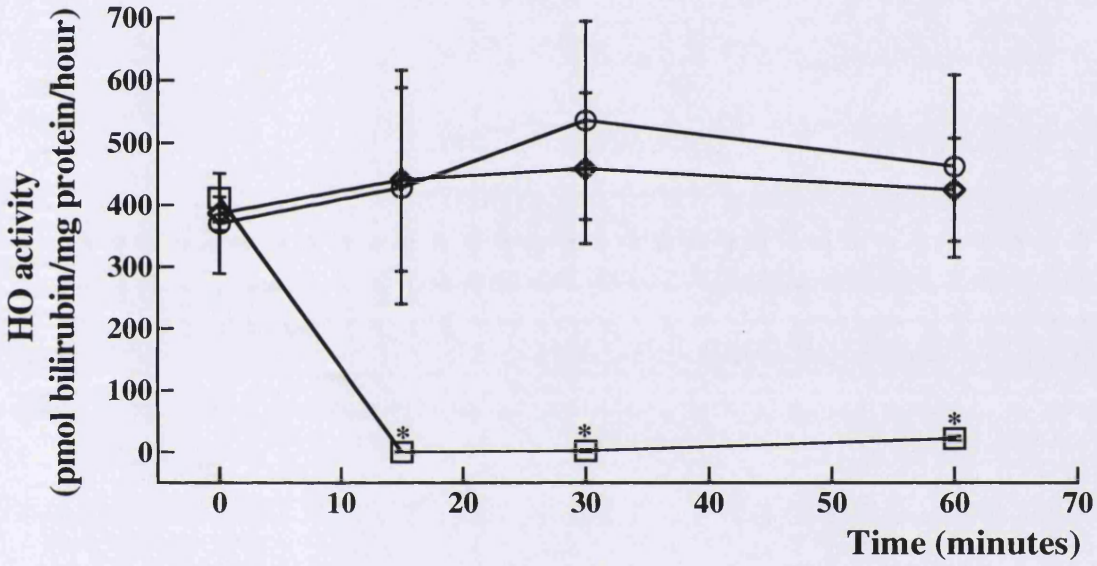

Figure 4.7 Effects of SnPP and CuPP on tumour HO enzyme activity. Tumour-bearing rats were administered SnPP or CuPP at 45 μmol/kg ip and the HO enzyme activity was measured in microsome fractions of P22 tumours at 15, 30 and 60 minutes post-treatment. The data are means of 2-3 animals per group. Error bars are means ± 1 standard error of the mean. * represents a significant difference from the respective controls ($p<0.05$). O: Control; ◇: CuPP; □: SnPP.

The effects of SnPP and CuPP were also examined in the liver and kidney where SnPP is known to inhibit HO enzyme activity (Drummond and Kappas, 1981; Anderson *et al.*, 1983). The results shown in Figure 4.8 demonstrate that SnPP is also effective at inhibiting HO activity in both the liver and kidney, thereby confirming previous findings. In the liver, the HO enzyme activity was inhibited by 88% at 15 minutes post-treatment and decreased further to 91% at 1h. In the kidney, the enzyme activity decreased to zero within the first 15 minutes and remained inhibited by 86% at 1h post-treatment. This is in

contrast to CuPP administration, which did not affect HO enzyme activity in either of these organs.

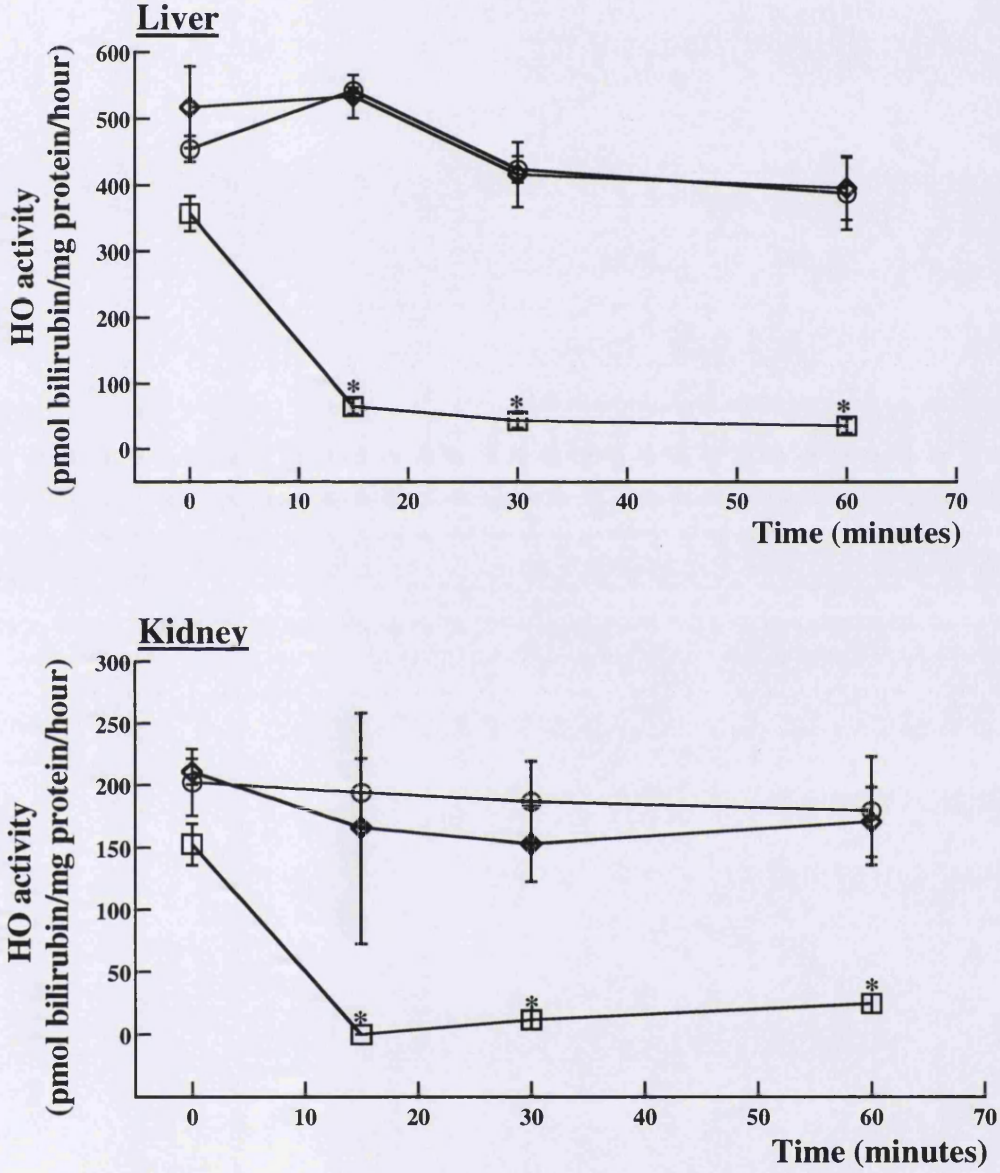

Figure 4.8 Effects of SnPP and CuPP on rat liver and kidney HO enzyme activity. Tumour-bearing rats were administered SnPP or CuPP at 45 μmol/kg ip and the HO enzyme activity was measured in tissue microsome fractions at 15, 30 and 60 minutes post-treatment. The data are means of 2-3 animals per group and are from the same group of animals shown in Figure 4.7. Error bars are means ± 1 standard error of the mean. * represents a significant difference from the respective controls ($p<0.05$). ○: Control; ◇: CuPP; □: SnPP.

4.3.5 HO Inhibition and Tissue Blood Flow Rate

The effects of SnPP and CuPP on tissue blood flow rate were strikingly different. The results presented in Figure 4.9 show that a single 45 μmol/kg dose of the selective HO inhibitor, SnPP, tended to reduce blood flow to several tissues including the tumour but none of the effects were significant with the number of animals used. On the other hand, the same dose of CuPP mediated a 45% decrease in tumour blood flow. Significant reductions in blood flow were also observed in skin and small intestine. In contrast to any other tissue, blood flow in skeletal muscle was almost doubled in the CuPP-treated group compared to control (Figure 4.9). Furthermore, while MABP and heart rate remained unaffected by SnPP, CuPP increased heart rate to around 125 % of control (Figure 4.10). The tendency for CuPP to decrease MABP did not reach statistical significance.

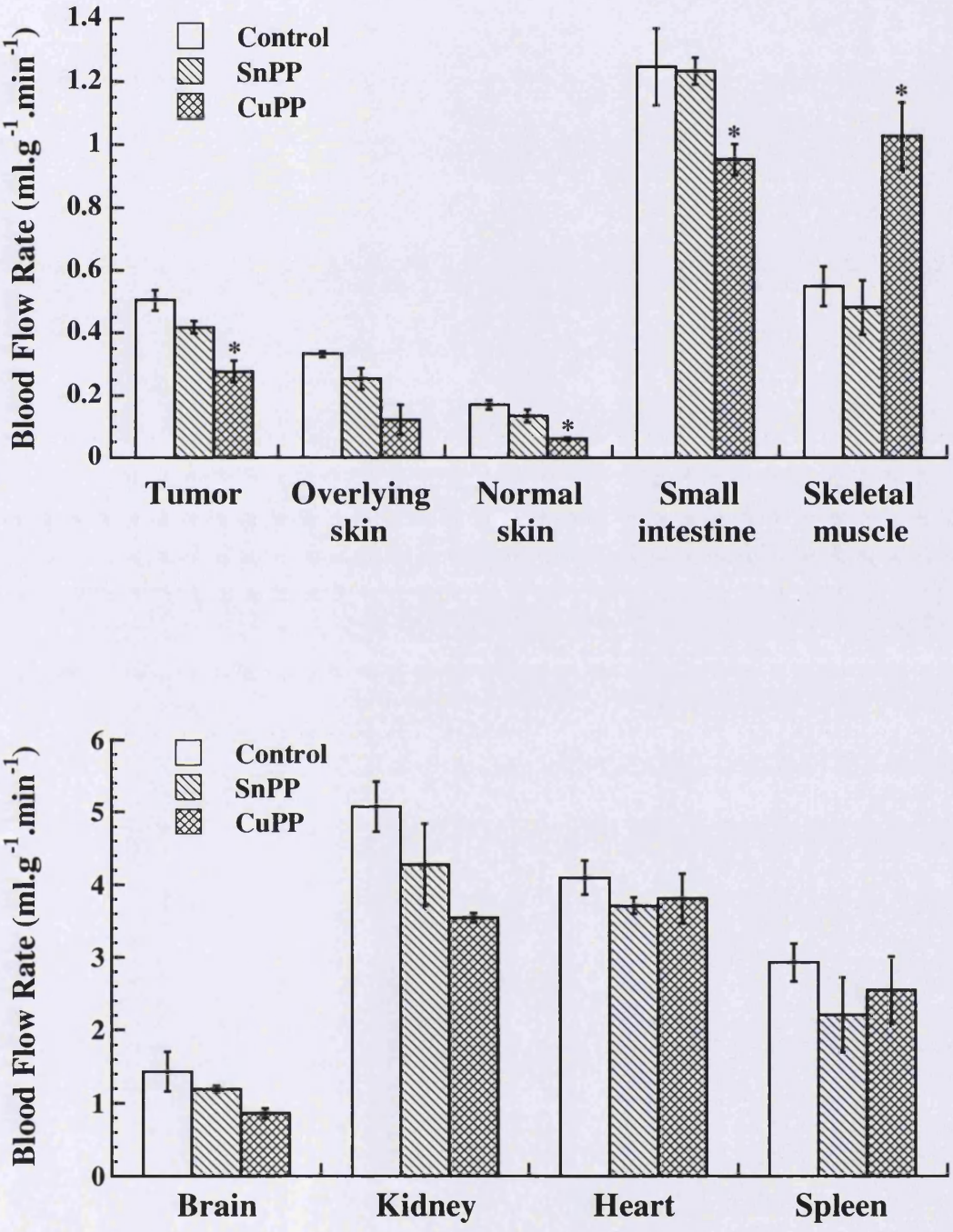

Figure 4.9 Effects of SnPP and CuPP on tissue blood flow rate. The compounds were injected at a dose of 45 μmol/kg ip 15 minutes prior to measurement of blood flow rate in the P22 tumour and a range of normal tissues. Values are the means of 4-5 animals per group. Error bars are means ± 1 standard error of the mean. * represents a significant difference from control ($p<0.05$).

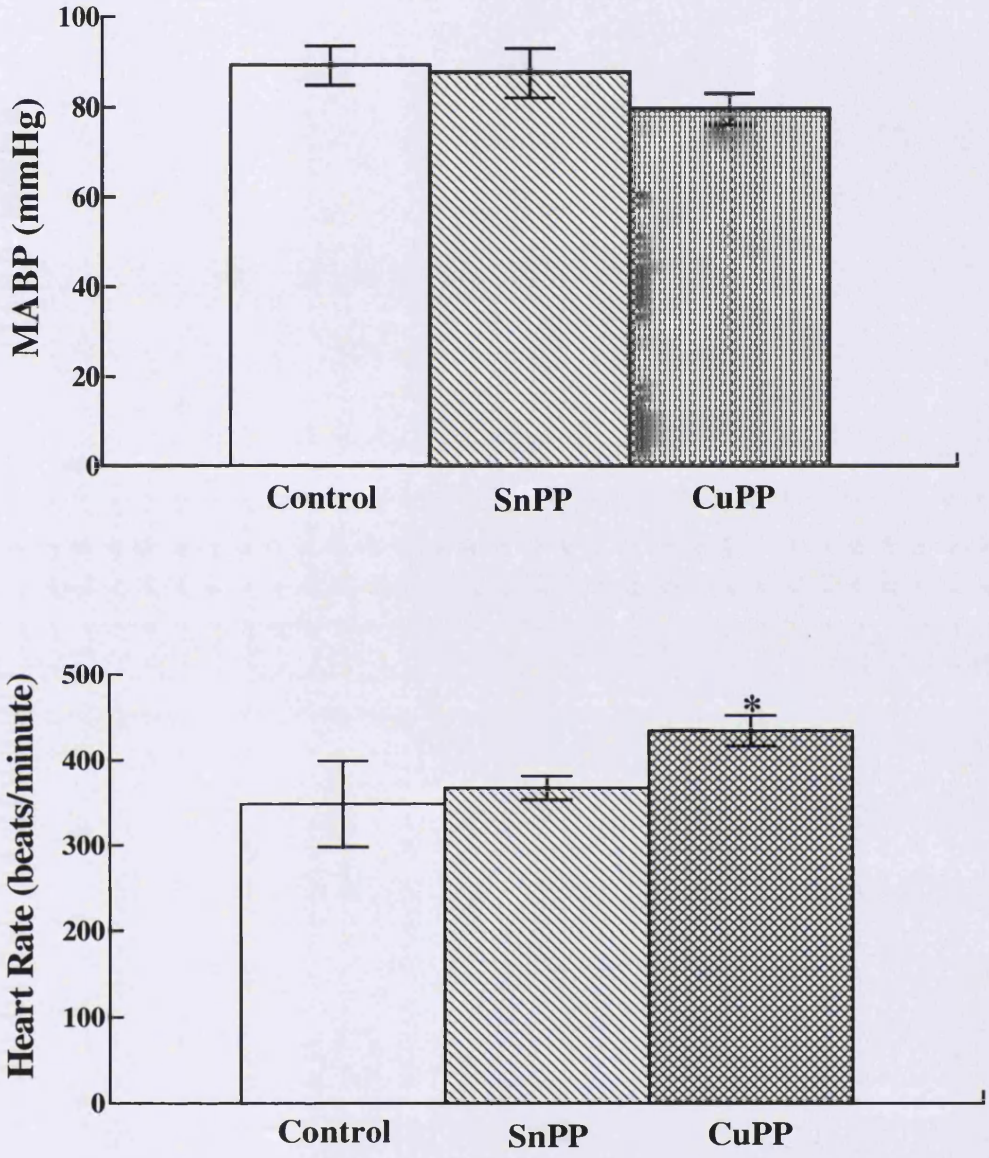

Figure 4.10 Effects of SnPP and CuPP on MABP and heart rate. The compounds were injected at a dose of 45 μmol/kg ip 15 minutes prior to mean arterial blood pressure (MABP) and heart rate measurements. Values are means ± 1 standard error of the mean for the same group of animals as shown in Figure 4.9. * represents a significant difference from the control ($p<0.05$).

4.4 Discussion

In the first part of this study hemin was used to examine the effects of HO-1 over-expression on the control of blood flow in the rat P22 tumour model. We found that a 10 mg/kg ip dose of hemin effectively increased tumour HO activity by ~ 2 fold and also induced HO-1 protein levels at 24h post-treatment. However, under these conditions, blood flow to the tumour and a range of normal tissues was unaffected. Additional studies using a 5 times higher dose of hemin only mediated a moderate further increase in HO activity compared to the initial dose of 10 mg/kg, suggesting a possible saturation in the induction of HO-1 expression in response to hemin. The ineffectiveness of hemin in mediating changes in tissue blood flow rate may be related to the fact that the up-regulation in the HO enzyme activity measured in response to hemin using the *in vitro* assay may not necessarily reflect an up-regulation of the products *in vivo* namely bilirubin and CO. This could be due to a possible *in vivo* shortage of substrate availability for the HO enzyme. Indeed, investigators have shown that in cells in culture exposed to hemin, the latter is consumed by HO in a relatively short period of time after being taken up and its availability becomes the limiting factor in the generation of bilirubin/CO despite HO-1 protein expression remaining elevated (Clark *et al.*, 2000a). Therefore, in our system it is possible that despite the fact that HO-1 protein expression is still high at 24h post-hemin treatment, the levels of the products generated are not elevated enough, due to a lack of substrate availability for HO, to mediate any changes in tissue blood flow rate. Therefore, in order to overcome this problem the effects of administration of 2 doses of hemin at 26 mg/kg ip given 24h apart were investigated. The idea was that the first dose would result in HO-1 induction and the second would provide the substrate for generation of the active products. Unfortunately, it was found that this dosing regimen with hemin was rather toxic to the animals resulting in diarrhoea and inflammation around the eyes preventing further investigating the effects of such a hemin-dosing regimen on tissue blood flow rate. The nature of this toxicity mediated by hemin is unclear. However, degradation of hemin by HO releases iron, which is known to participate in chemical reactions generating reactive oxygen species. It is possible that this situation led to a pro-oxidant and inflammatory-type of state, which was manifested as diarrhoea and the redness/inflammation observed around the eyes of the animals.

Several conclusions can be drawn from the first part of this study. Firstly, the absence of blood flow modifying effects of hemin could be due to inadequate amounts of CO generation, either because of an insufficient induction in HO enzyme activity by hemin or because of insufficient substrate availability for CO generation *in vivo*. One way to overcome this problem would be to directly expose rats to low concentrations of CO in order to assess its effects on P22 tumour blood flow rate. Previous studies in our laboratory have examined the effects of CO breathing, using laser Doppler flowmetry, in a mouse sarcoma tumour model and have unexpectedly found that this treatment decreased tumour blood flow. This may have been due to systemic vasodilatory effects mediated by CO resulting in a fall in the perfusion pressure to the tumour (Hill S.A., unpublished data). Secondly, it is possible that hemin administration and the resulting CO generation did not affect tumour blood flow because, under resting conditions, the tumour blood vessels are near to maximally dilated and consequently, vasodilating compounds are often ineffective (Peterson, 1991). Further studies, under conditions where tumour blood vessels are pre-constricted, would clarify whether CO is capable of playing a vasodilatory role in the tumour vasculature. Finally, it may be that the HO/CO system does not actually play a role in the control of tumour blood flow, hence the absence of any effects. This suggestion is further supported in the studies described below using the HO inhibitor SnPP.

In the second part of this study the role of endogenous HO activity in the control of tissue blood flow using the HO inhibitor SnPP was investigated. In this study, SnPP was used to examine the importance of the HO/CO system in the regulation and maintenance of blood flow to the P22 rat carcinosarcoma tumour. It was found that SnPP administration at a dose of 45 μmol/kg ip effectively inhibited tumour HO activity *in vivo*. These effects were observed at 1h following a single ip dose of SnPP and persisted for up to 24h (see Table 6.3 in Chapter 6). These results are consistent with a previous study with SnPP in the rat, which showed prolonged inhibitory effects with this compound on spleen, liver and kidney HO enzyme activity for up to 7 days following a single subcutaneous dose of the agent at 20 μmol/kg (Anderson *et al.*, 1983). The authors found that this prolonged enzyme inhibition correlated with tissue retention of SnPP suggesting that the compound may remain bound to the enzyme for prolonged periods of time. These results show that

SnPP is a very effective HO inhibitor in both tumour and normal tissue of the rat. However, it should be borne in mind that measurement of enzyme activity "*ex vivo*" might not represent the true *in vivo* situation. For example, in our case, SnPP may bind to non-enzymatic targets within the tissue *in vivo*, and then be released during preparation for the *ex vivo* assay, only then becoming available for complexing with free HO enzyme molecules in the *ex vivo* state (Anderson *et al.*, 1983). In this case, the *ex vivo* results would overestimate the real extent of HO enzyme activity inhibition *in vivo*. A more accurate way of determining the real time-course of SnPP-mediated HO activity inhibition would be by directly measuring bilirubin levels in blood samples or preferably tumour tissue. Bilirubin levels in plasma have been previously measured (Drummond and Kappas, 1981; Anderson *et al.*, 1983; Berglund *et al.*, 1988), although there are no reported studies of direct tissue measurements of bilirubin.

Withstanding the above caveat, the results showed that effective HO inhibition using SnPP had no significant effects on either tumour or normal tissue blood flow rate. Previous studies in our laboratory with the HO inhibitor, ZnPP, showed a significant reduction in tumour blood flow by ~ 30% (Tozer *et al.*, 1998). However, under these conditions, tumour HO activity was not inhibited by ZnPP, indicating that the blood flow responses were completely independent from HO activity (Tozer *et al.*, 1998). Indeed, the effects of ZnPP were very similar to CuPP in terms of both lack of effect on HO activity and blood flow response. This is in contrast to the effects of SnPP and CuPP, in the current study, where clear differences were demonstrated, thereby suggesting distinct mechanisms of action for the two agents. SnPP effectively inhibited HO activity but had no effect on tissue blood flow rate. On the other hand, CuPP as expected, had no effect on HO activity but significantly reduced blood flow in tumours and some of the normal tissues examined, whilst increasing blood flow to skeletal muscle. The blood flow effects of CuPP and ZnPP are clearly not the result of HO inhibition and the results for SnPP conclusively establish only a minor role played by the HO/CO system in the maintenance and regulation of blood flow in this tumour model under resting conditions. The blood flow modifying effects of CuPP and ZnPP are difficult to interpret but are likely to relate to various reported vascular effects of these agents, which are unrelated to HO. For instance, ZnPP (and SnPP) has been shown to inhibit sGC and NOS (Grundemar and Ny,

1997). Previous studies in our laboratory, have shown that ZnPP and CuPP had a different blood flow modifying profile in normal tissues from that of the NOS inhibitor L-NNA suggesting a mechanism of action somewhat different from NOS inhibition (Tozer *et al.*, 1998). Furthermore, ZnPP was also shown to abolish the increase in cAMP and cGMP evoked by vasoactive intestinal peptide and atrial natriuretic peptide thereby inhibiting relaxation mediated by these agents in rat aorta (Ny *et al.*, 1995). These studies demonstrate the non-selectivity of these agents in mediating their actions and the difficulty of choosing the most appropriate inhibitor for HO (Foresti and Motterlini, 1999). Furthermore, little is known about the isozyme specificity of these metalloporphyrins. There is some evidence that SnPP is far more inhibitory to HO-2-dependent activity as compared to ZnPP, with both compounds being equally inhibitory to HO-1 activity (Maines and Trekshel, 1992). This could explain the differential effects of SnPP and ZnPP on overall tumour HO activity in this tumour model which was shown to have high resting levels of both isozymes (see Figures 3.2 and 3.3 in Chapter 3).

The lack of blood flow effects of SnPP in the P22 tumour was quite surprising in view of the relatively high HO activity in this tumour (see results in Chapter 3) and the efficacy of SnPP-induced HO inhibition (Figure 4.7). Our laboratory has previously shown that NOS inhibition causes a large reduction in blood flow to the P22 tumour and this pathway may represent the major contributor to blood flow regulation and maintenance in this model (Tozer *et al.*, 1997).

In conclusion, this study has clearly demonstrated that the HO/CO system in the P22 tumour plays only a minor vasodilatory role. It is possible to speculate that the HO/CO system could have more important vascular roles in tumours where NO is not the major vasodilatory molecule. The current findings also highlight the important blood flow modifying effects mediated by CuPP. Elucidation of its mechanism of action would allow further understanding of the factors/pathways responsible for the regulation and maintenance of blood flow in tumours.

4.5 Summary

In this study, the role of HO in the maintenance of blood flow to tumours was assessed. The major findings are that, whilst, the metalloporphyrin SnPP effectively inhibited tumour HO activity, it mediated only a modest decrease in tumour blood flow. In contrast, CuPP had no effect on HO activity, yet it significantly decreased blood flow to the tumour. These findings clearly show that the alterations in blood flow mediated by CuPP are not the result of an inhibition in HO activity. Furthermore, this study also demonstrates the minor role played by the HO system in tumour blood flow maintenance. Further investigations into the potential therapeutic usefulness of these metalloporphyrins are reported in Chapter 6.

CHAPTER 5

EFFECTS OF COMBRETASTATIN A4-PHOSPHATE ON THE HAEMOXYGENASE SYSTEM: *IN VITRO* AND *IN VIVO* ANALYSIS

5.1 Introduction

As described in the General Introduction, CA-4-P is the lead compound of a group of tubulin binding agents which show promise as tumour vascular targeting agents. For the further development of this strategy, there is a clear need to understand both the mechanisms by which CA-4-P causes selective tumour vascular injury and the processes which lead from the initial blood flow shut down to tumour cell death. In this regard, the role of the HO system was investigated, based on increasing evidence for an important cytoprotective role of the HO system *in vitro* and *in vivo* (see Chapter 1).

The potential protective roles of HO-1 in vascular repair following vascular injury in normal tissues have been addressed and reviewed in a number of recent papers (Aizawa *et al.*, 1999; Togane *et al.*, 2000; Duckers *et al.*, 2001; Durante and Schafer, 1998; Schwartz, 2001). Durante and Schafer have reviewed the cytoprotective role of HO-1 induction during blood vessel injury (Durante and Schafer, 1998). In this review they suggest that, in pathological states where vascular injury has occurred by endothelial damage, HO-1 is induced in vascular smooth muscle cells because of their exposure to both inflammatory cytokines and fluid shear stress. The consequent release of CO would stimulate cGMP production leading to blood vessel relaxation and inhibition of both smooth muscle cell proliferation and platelet activation thereby promoting vascular homeostasis. Furthermore, the release of biliverdin/bilirubin would be important in scavenging free radicals generated as a result of tissue injury and inflammation. Indeed, HO-1 induction has been reported in arteries following vascular injury and has been suggested to protect the damaged vessels from pathological responses (Togane *et al.*, 2000; Duckers *et al.*, 2001). For instance, Togane and colleagues have demonstrated that HO-1 is induced in vascular smooth muscle cells following arterial balloon injury (Togane *et al.*, 2000). This induction led to inhibition of neointimal formation, an effect mediated by CO. These effects were shown to be modulated by HO inhibitors and inducers. In addition, Duckers

et al. have further demonstrated the potential protective role of HO-1 in vascular wound repair (Duckers *et al.*, 2001). These authors report the beneficial effects of the HO-1 pathway in moderating the severity of vascular injury by both stimulating vascular relaxation and reducing vascular smooth muscle cell growth and proliferation by a mechanism involving cGMP and independent from NO. Furthermore, vascular injury may also lead to HO-1 induction in the damaged endothelium, where this would act to promote endothelial cell survival and proliferation. Indeed, there is *in vitro* evidence demonstrating that HO-1 promotes the proliferation of endothelial cells (Deramaudt *et al.*, 1998) and protects them from apoptosis (Brouard *et al.*, 2000).

In an inflammatory context, HO-1 was also shown to play an important modulatory and cytoprotective role (see sections 1.5.3.3 and 1.5.4.3.2 of Chapter 1). Various inflammatory mediators were demonstrated to induce HO-1 (Terry *et al.*, 1998; Lee and Chau, 2002), which was shown to be particularly important during the resolution phase of the inflammatory response (Willis *et al.*, 1996; Willoughby *et al.*, 2000).

In the light of these findings, we hypothesised that the HO enzyme system could play a protective role during/following the vascular injury and inflammatory-type of reaction mediated by the tubulin binding agent CA-4-P *in vivo*. The aim of the present study was to investigate the effects of CA-4-P on the HO enzyme system *in vitro* and *in vivo*. The relevant data on the effects of CA-4-P on HO activity and isozyme protein levels in both the P22 tumour model and normal tissues *in vivo* as well as in endothelial and P22 tumour cells *in vitro* will be presented in this chapter.

5.2 Materials and Methods

5.2.1 Drug Solutions

CA-4-P for *in vitro* experiments (1 mM stock)

2.2 mg CA-4-P

5 ml Na_2CO_3

hemin for *in vitro* experiments (1 mM stock)

6.52 mg hemin (Sigma)

50 µl NaOH (2 M)

Make up to 10 ml with PBS-$MgCl_2$

N-acetyl-L-cysteine for *in vitro* experiments (NAC; 50 mM stock)

81.6 mg NAC (Sigma)

10 ml PBS

sodium carbonate (Na_2CO_3; 50 mM) as drug vehicle

Section 4.2.1 of Chapter 4

CA-4-P for *in vivo* experiments

Dissolved in Na_2CO_3 (50 mM)

Administered ip.

hemin for *in vivo* experiments

Dissolved in Na_2CO_3 (50 mM)

Administered ip.

5.2.2 In Vitro Experimental Protocol

P22 tumour cells were seeded at 10^4 cells/cm^2 and allowed to grow to confluence. In a first set of experiments, the inducibility of HO-1 in this cell line was established using hemin, a known inducer of HO-1. Cells were exposed to 50, 100 or 200 µM final concentrations of hemin in the medium for 2h. The hemin drug vehicle was also tested. The cells were then washed 3 times with warm medium and collected 4 or 22h later.

In a second set of experiments, we investigated the effects of CA-4-P on HO enzyme activity and isozyme protein levels. Confluent P22 tumour cell cultures were exposed to increasing concentrations of CA-4-P (10^{-4}, 10^{-2}, 1 and 10 µM final concentrations in the medium) for 1h. In all the experiments with CA-4-P, the cells were washed 3 times with warm media after the 1-h drug exposure and collected 5, 23, 29 or 47h later. Similar experiments were carried out using HUVECs. Cell viability in P22 tumour cells and

HUVECs was assessed following CA-4-P treatment using the trypan blue exclusion assay. The cell suspension was diluted in trypan blue at a dilution of 1:3 (trypan blue:cell suspension). Cells that did not take up the dye were counted as viable using a haemocytometer. Using immunofluorescence staining, the tubulin cytoskeleton of P22 tumour cells and HUVECs was visualised following exposure to CA-4-P (1 μM). For this purpose cells were plated on Lab-Tek chamber slides (Fisher Scientific) and sub-confluent cultures were used. At the end of the 1h-incubation period with CA-4-P, cells were washed 3 times, incubated with fresh medium and fixed at 5, 23, 29 or 47h post-treatment. They were then analysed by immunofluorescence using an anti-β-tubulin antibody as described below (section 5.2.4).

In a third set of experiments, the effects of N-acetyl-L-cysteine (NAC) in combination with CA-4-P on HO activity and isozyme protein levels were examined. P22 cells were pre-incubated with NAC for 1h at a final concentration of 1 mM in the media. This was followed by co-incubation with CA-4-P (1 μM) for 1h. Cells were then washed 3 times with warm medium and supplied with fresh medium containing NAC. Cells were collected 29 or 47h later. The medium was changed at 24h with fresh NAC added.

For HO enzyme activity and HO isozymes protein level determination cells were washed twice with ice-cold PBS containing a cocktail of protease inhibitors (Roche Diagnostics) and gently scraped with a cell scraper (Sigma). The cell suspension was centrifuged at 1000 rpm for 5 minutes at 4°C. The pellet was re-suspended in PBS-$MgCl_2$ and stored at –86°C for further analysis. Prior to HO activity assay and western blotting, the cell suspension was sonicated on ice for 2 cycles of 10 seconds using a Status ultrasonic homogeniser (Philip Harris Scientific) in order to break cell membranes.

5.2.3 In Vivo Experimental Protocol

The P22 carcinosarcoma was used in these studies (see section 2.2.1 of Chapter 2). The first set of experiments aimed at examining the effects of CA-4-P treatment on HO enzyme activity and HO-1 protein levels *in vivo*. After the subcutaneous transplanted tumours had reached the desired size of 11-12 mm in mean geometrical diameter, the animals were treated with either CA-4-P at a dose of 30 mg/kg or drug vehicle (Na_2CO_3).

The dose of CA-4-P was chosen as that which causes significant vascular damage in the P22 tumour with acceptable toxicity (see Chapter 6). The animals were sacrificed at 6, 24, 30, 48h, 4 or 7 days post-treatment and the tumour and a range of normal tissues were excised for analysis. Microsomes were prepared from all the excised tissues and analysed for HO enzyme activity and HO-1 protein levels as described in Chapter 2.

Tumour sections from control and CA-4-P-treated animals were also analysed by immunohistochemistry for HO-1 protein localisation and macrophage infiltration. Blood vessel distribution in control P22 tumours was also examined for co-localisation with HO-1. For these experiments, CA-4-P was administered at 10 or 30 mg/kg ip and the tumours excised 24 or 48h post-treatment. The samples were processed as described in Chapter 2 for preparation of frozen tissue material (section 2.9.1).

5.2.4 Tubulin Staining by Immunofluorescence

5.2.4.1 Buffers, Solutions and Reagents

PBS

See section 2.7.4 of Chapter 2

Blocking solution

PBS

1% BSA (Sigma)

5% horse serum (Vector)

Antibodies solution

PBS

1% BSA

5% horse serum

Primary or secondary antibody

Hepes (10 mM)-NaCl (0.15 M) pH 7.5

2.5 ml NaCl (3 M stock) (Sigma)

0.5 ml Hepes (1 M stock) (Gibco BRL)

47 ml distilled water

5.2.4.2 Protocol

Cells were seeded on Lab-Tek chamber slides (Fisher Scientific). Following the relevant treatments the medium was drained off and the cells were fixed with formaldehyde (3.7%; Sigma) for 20 minutes at room temperature and permeabilised with a PBS-Triton-X 0.1% solution for 5 minutes at room temperature. The cells were then washed several times with PBS and incubated with blocking solution for either 1h at room temperature or overnight at 4°C in order to block non-specific antibody binding sites. After washing, avidin and biotin solutions (Avidin/Biotin Blocking Kit; Vector) were applied sequentially for 15 minutes each. This was followed by incubation for 1h at room temperature with an anti-β-tubulin monoclonal primary antibody (Sigma) at a dilution of 1/500 in blocking solution, and then with a biotinylated anti-mouse/anti-rabbit secondary antibody (Vector) diluted at 1/100 in blocking solution for 1h at room temperature. All subsequent steps were performed in the dark and involved incubation with Fluorescein Avidin-D solution (Vector) diluted at 1/250 in Hepes-NaCl buffer, for 1h at room temperature. After washing with PBS, slides were mounted using Vectashield mounting medium for fluorescence (Vector) and the tubulin cytoskeleton was visualised using a Nikon Eclipse TE200 inverted microscope and a cooled CCD camera (Cohu, San Diego, CA). The images were then processed using Paint Shop Pro7 software (JascSoftware).

5.2.5 Immunohistochemistry

5.2.5.1 Solutions

Tris Buffered Saline (TBS)

250 ml Tris Buffer

2250 ml distilled water

20.25 g NaCl (Merck)

Adjust to pH 7.6

Tris Buffer

0.1 M Tris (12 g/L) (Merck)

0.1 M HCl (10 ml/L) (Merck)

Adjust to pH 7.4-7.6

5.2.5.2 HO-1 Staining

P22 rat tumours were transplanted and the excised tissues (control or CA-4-P-treated) prepared for staining as described in Chapter 2 (sections 2.2.1 and 2.9.1). Immunohistochemistry was performed on frozen material (for tissue preparation, see section 2.9.1 of Chapter 2) using the streptavidin-biotin ABC method (see section 2.9.2 of Chapter 2) and the following steps were undertaken during the procedure:

1. Sections were rinsed in TBS and the excess fluid drained off. They were then incubated with normal goat serum (Dako) diluted 1/5 in TBS for 1h.
2. The avidin block was then applied for 15 minutes (Vector).
3. Sections were washed with TBS and the Biotin block applied for 15 minutes (Vector).
4. Sections were washed again with TBS and incubated with the polyclonal anti-HO-1 antibody (Stressgen) diluted 1/500 in TBS for 1h at room temperature. One drop of protein block (Dako) was added per ml of diluted antibody to minimise any non-specific binding and background staining.
5. Sections were washed 3 times in TBS for 3 minutes.
6. Excess fluid was drained off and biotinylated goat anti-rabbit immunoglobulins were applied (Dako) diluted 1/400 in TBS for 1h at room temperature.
7. Sections were washed 3 times in TBS for 3 minutes.
8. Excess fluid was drained off and the StreptABComplex/HRP (Dako) was applied for 1h at room temperature.
9. Sections were washed 3 times in TBS for 3 minutes.
10. Excess fluid was drained off and the NovaRed substrate for peroxidases (Vector) was applied for ~ 1 minute.
11. Sections were rinsed with distilled water and washed well in running tap water.
12. The nuclei were counterstained with Gills number 1 hematoxylin.
13. Sections were washed well in running tap water and dehydrated in increasing concentrations of ethanol, cleared in xylene and mounted using a non-aqueous mounting media (DPX).
14. The results show the HO-1 expressing cells in red/brown and the nuclei in blue.

5.2.5.3 Blood Vessel Staining

A rat endothelial cell-specific antibody (RECA-1) (Serotec) was used as a vascular stain. The antibody recognises a *r*at *e*ndothelial *c*ell *a*ntigen expressed on the cell surface of all rat endothelial cells. Studies on RECA-1 have demonstrated that it is rat endothelial cell-specific showing no cross-reactivity with other cell types or endothelial cells in tissues of various species (Duijvestijn *et al.*, 1992). Immunohistochemistry was performed on frozen material (for tissue preparation, see section 2.9.1 of Chapter 2) using the APAAP method (see section 2.9.2 of Chapter 2) and the following steps were undertaken during the procedure:

1. Sections were rinsed in TBS and incubated with normal rabbit serum (Dako) diluted 1/5 in TBS for 1 hour at room temperature.
2. They were then washed in TBS again and the excess fluid drained off. They were then incubated with the monoclonal RECA-1 antibody (Serotec) diluted 1/100 in TBS for 1h at room temperature. One drop of protein block was added per ml of diluted antibody (Dako).
3. Sections were washed 3 times in TBS for 3 minutes.
4. The excess fluid was drained off and the sections were incubated with rabbit anti-mouse immunoglobulins (Dako) diluted 1/20 in TBS for 30 minutes.
5. Sections were washed 3 times in TBS for 3 minutes.
6. The excess fluid was drained off and the sections were incubated with the APAAP complex (Dako) diluted 1/100 in TBS for 30 minutes.
7. Sections were washed 3 times in TBS for 3 minutes.
8. The Vector Red substrate for alkaline phosphatase (AP) was applied (Vector) for ~15 minutes.
9. Sections were then washed well in running tap water.
10. The nuclei were counterstained with Gills number 1 Haematoxylin.
15. Sections were then washed well in running tap water and dehydrated in increasing concentrations of ethanol, cleared in xylene and mounted using a non-aqueous mounting media (DPX).
11. The results show blood vessels in red and the nuclei blue.

5.2.5.4 Macrophage Staining

In these studies, an antibody that specifically recognises rat macrophages (ED-1; Serotec) was used. ED-1 has been successfully used as a rat macrophage marker (Deininger *et al.*, 2000). The antibody recognises a 90-100 kDa glycoprotein expressed predominantly on the lysosmal membrane of myeloid cells. The antigen is expressed by the majority of tissue macrophages and weakly by peripheral blood granulocytes. Immunohistochemistry was performed on frozen sections (for tissue preparation, see section 2.9.1 of Chapter 2) using the APAAP method (see section 2.9.2 of Chapter 2), and the procedure was carried out as described in section 5.2.5.3 above using ED-1 as the primary antibody (diluted 1/100 in TBS).

5.2.5.5 Immunofluorescence Double Labelling

Double labelling using HO-1 and the macrophage marker ED-1 was performed on frozen tumour sections using immunofluorescence detection (see section 2.11 of Chapter 2). HO-1 was probed using FITC-labelled avidin, whereas ED-1 was probed using an Alexa Fluor 594-tagged secondary antibody. The steps undertaken during the procedure are described below:

1. Sections were rinsed in PBS and the excess fluid drained off. They were then incubated with normal goat serum (Dako) diluted 1/5 in PBS for 1h.
2. The avidin block was then applied for 15 minutes (Vector).
3. Sections were washed with PBS and the Biotin block applied for 15 minutes (Vector).
4. Sections were washed again with PBS and incubated with the anti-HO-1 antibody (Stressgen) diluted 1/500 in PBS for 1h at room temperature. Sections were washed 3 times in PBS for 3 minutes.
4. Excess fluid was drained off and a mixture of biotinylated goat anti-rabbit immunoglobulins (Dako) diluted 1/400 and ED-1 antibody diluted 1/100 was applied to the sections for 1h at room temperature.
5. Sections were washed 3 times in PBS for 3 minutes.

All the subsequent steps were performed in the dark.

6. A mixture of Alexa Fluor 594-tagged secondary anti-mouse immunoglobulins (Cambridge Bioscience) diluted 1/3000 and FITC-tagged avidin (Vector) diluted 1/250 in Hepes-NaCl buffer was applied to the sections for 1h at room temperature.

7. Sections were washed 3 times in PBS for 3 minutes and mounted using Vectashield Mounting Medium for Fluorescence (Vector). HO-1 (green) and ED-1 (red) protein distributions were visualised using a Nikon Eclipse TE200 inverted microscope and a cooled CCD camera (Cohu, San Diego, CA). The images were processed using Paint Shop Pro7 software (JascSoftware).

5.3 Results

5.3.1 HO Characterisation of P22 Tumour Cells

The inducibility of HO-1 in P22 tumour cells was initially investigated using hemin. Cells were incubated with various concentrations of hemin for 2h. They were then washed and incubated with fresh medium for 4 or 22h. Figure 5.1 shows a dose-dependent increase in HO-1 protein levels in response to hemin treatment. This confirms the ability of this cell line to induce HO-1 in response to stimulation with hemin. The HO-1 protein induction seemed more prominent at 6 compared to 24h post-hemin exposure suggesting that the effects of hemin start to subside by 24h.

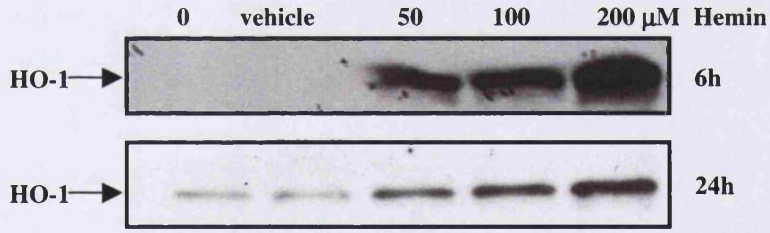

Figure 5.1 Effects of hemin treatment on HO-1 protein levels in P22 tumour cells. Western blot showing induction of HO-1 protein in response to 0, 50, 100 and 200 μM hemin in confluent P22 tumour cells at 6 and 24h post-treatment.

5.3.2 Effects of CA-4-P on the HO System in P22 Tumour Cells In Vitro

Confluent P22 tumour cells were exposed to increasing concentrations of CA-4-P for 1h. The drug was then washed away, the medium replaced and the cells were collected 5h later. Figure 5.2A shows that CA-4-P caused a dose-dependent decrease in HO enzyme activity at 6h post-treatment. The HO enzyme activity decreased by ~ 33 and 41% in

response to 1 and 10 μM CA-4-P, respectively. This decrease in HO enzyme activity was reflected by a decrease in HO-1 protein levels at 6h post-CA-4-P treatment as shown by western blotting (Figure 5.2B).

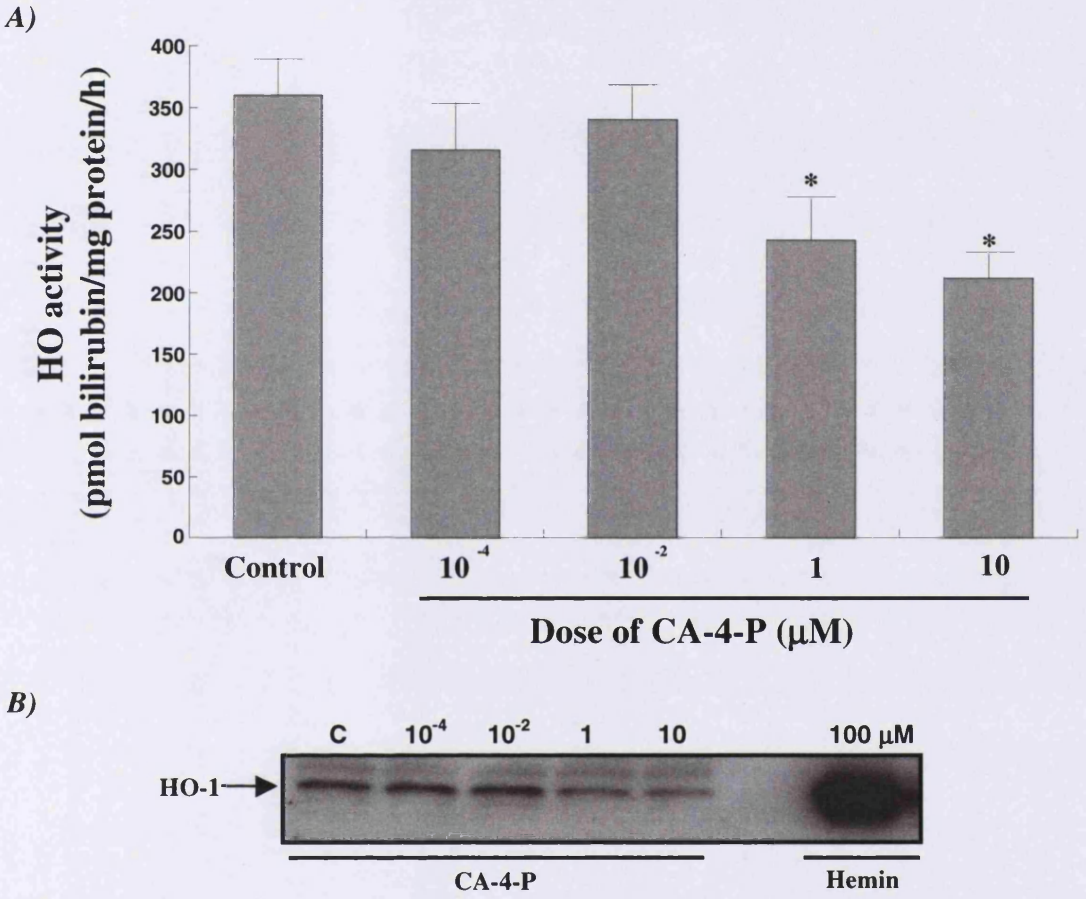

Figure 5.2 Effects of CA-4-P on HO enzyme activity and HO-1 protein levels at 6h. ***A)*** HO enzyme activity in confluent P22 tumour cells decreases dose-dependently in response to CA-4-P at 6h post-treatment. The data are of 3-4 independent experiments. * represents a significant difference from control ($p<0.05$). ***B)*** Representative western blot showing the dose-dependent decrease in HO-1 protein levels in confluent P22 tumour cells in response to CA-4-P at 6h post-treatment.

Further examination of the time-course of the effects mediated by CA-4-P on HO enzyme activity and HO-1 protein levels revealed that the HO enzyme activity and HO-1 protein levels return to the control levels at 24h but are induced at 30 and 48h following a 1h exposure to CA-4-P (1 μM). The HO activity significantly increased to 221 and 254% of

control at 30 and 48h post-treatment, respectively (Figure 5.3A). This increase in HO activity was reflected by an increase in HO-1 protein levels at these time points, as shown by western blotting in Figure 5.3B.

The effects of CA-4-P on P22 tumour cell proliferation/viability were examined by exposing cells to CA-4-P for 1h and then counting live cells at different time intervals using the trypan blue exclusion assay. Exposure to CA-4-P (1 μM) inhibited the proliferation of P22 tumour cells as compared to the untreated controls (Figure 5.4).

A)

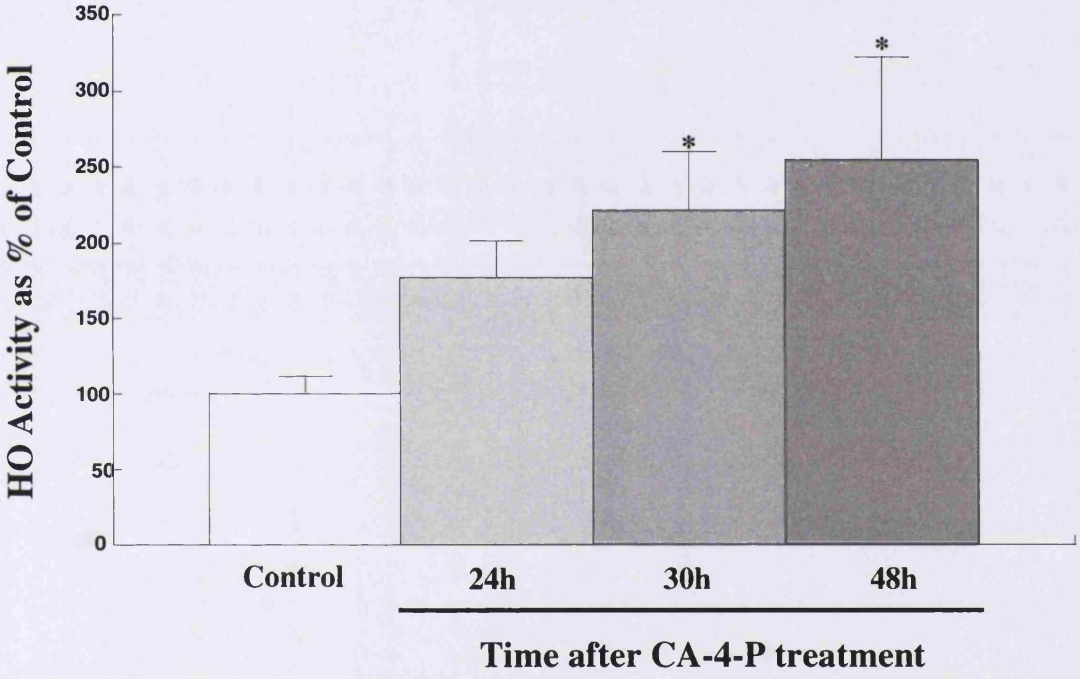

B)

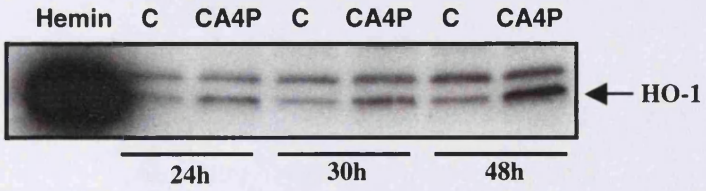

Figure 5.3 Time-course of the delayed effects of CA-4-P on the HO system. ***A)*** Effects of CA-4-P (1 μM) on HO enzyme activity in confluent P22 tumour cells at 24, 30 and 48h post-treatment. The data are of 4 independent experiments. * represents a significant difference from control ($p<0.05$). ***B)*** Representative western blot showing the effects of CA-4-P (1 μM) on HO-1 protein levels in confluent P22 tumour cells at 24, 30 and 48h post-treatment.

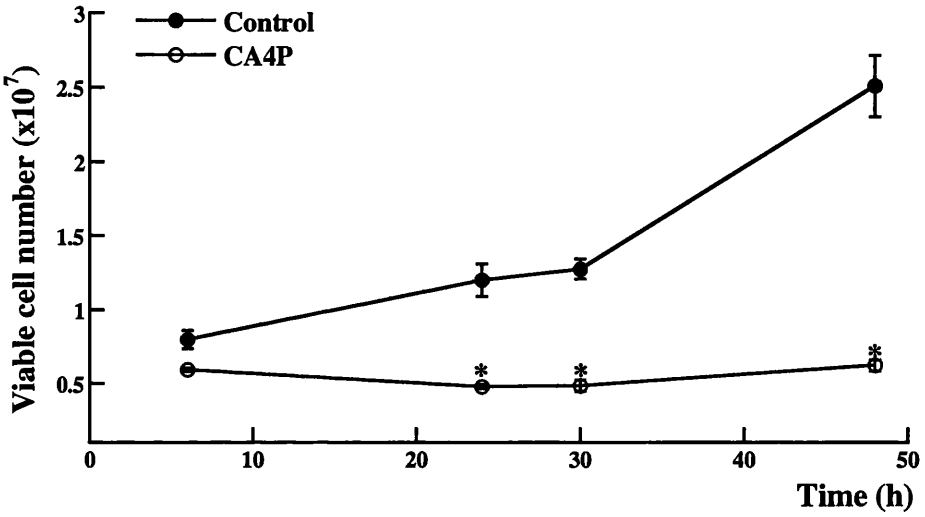

Figure 5.4 Viability of P22 tumour cells following CA-4-P treatment. Effects of 1h exposure to CA-4-P (1 μM) on cell viability at 6, 24, 30 and 48h post-treatment as compared to control untreated cells at the same time points. Each point is the mean of triplicate values. * represents a significant difference from the respective controls ($p<0.05$).

Examining the tubulin cytoskeleton by immunofluorescence following CA-4-P treatment revealed that the changes in HO enzyme activity and HO-1 protein levels followed a similar time-course to the changes in the cytoskeleton (Figure 5.5). At 6h post-CA-4-P (1 μM) exposure, P22 tumour cells assumed a rounded up morphology and lacked a distinct tubulin cytoskeleton, in contrast to control cells which were well spread and had distinct microtubules. At this time point, a decrease in HO activity and HO-1 protein levels was also measured (Figure 5.2). At 24h, only a small proportion of cells exhibited a normal morphology while most cells still had a disrupted tubulin cytoskeleton. At the later time points of 30 and 48h, cells recovered a complete tubulin cytoskeleton and assumed a normal morphology. This correlated with an increase in HO enzyme activity and HO-1 protein levels (comparing Figures 5.3 and 5.5).

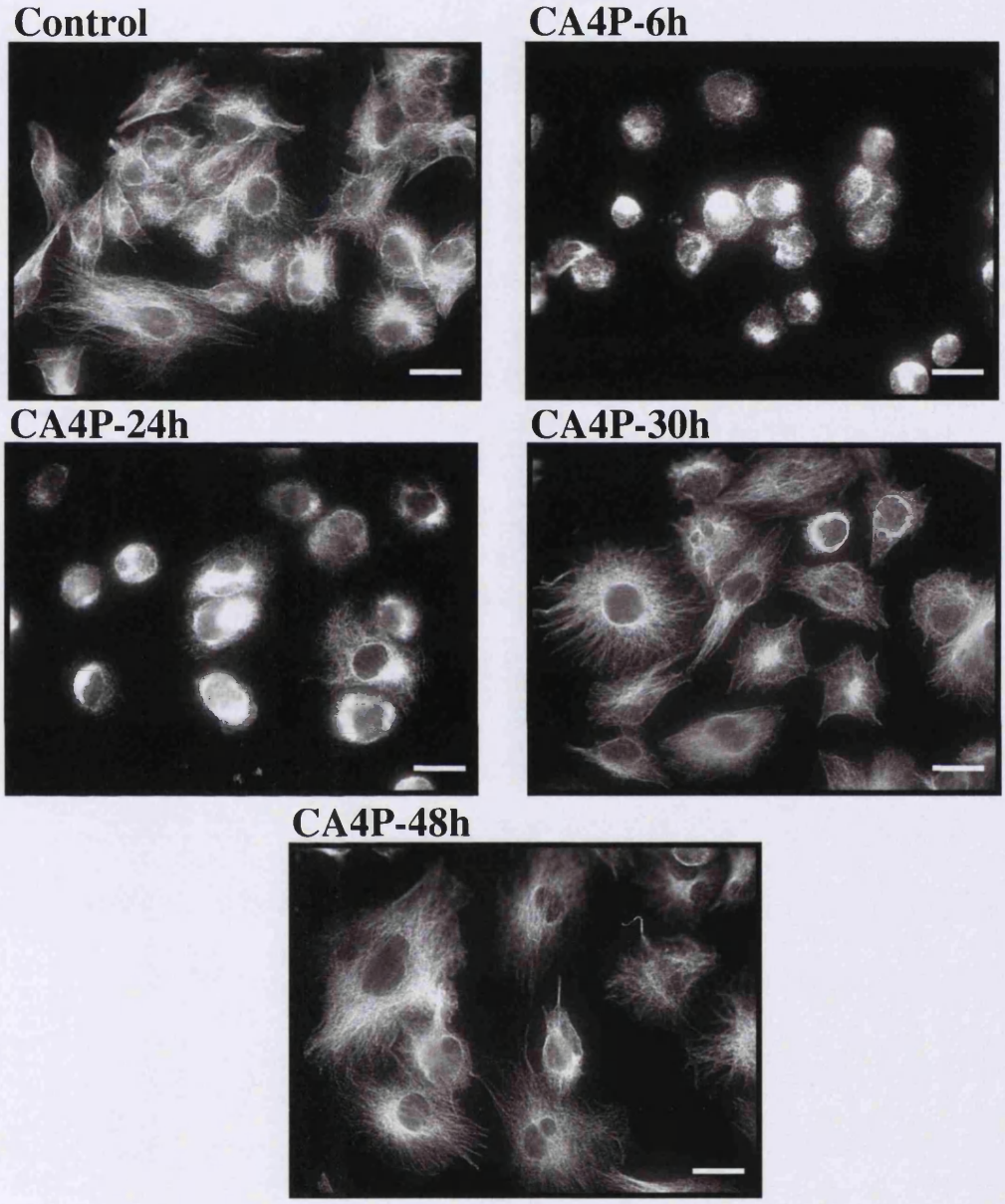

Figure 5.5 Effects of CA-4-P on the tubulin cytoskeleton in P22 tumour cells. Following exposure to CA-4-P (1 μM for 1h), cells were fixed at 6, 24, 30 and 48h post-treatment and analysed by immunofluorescence using an anti-β-tubulin antibody. The images are representative of typical results obtained from an experiment performed in quadruplicates. Scale bar = 30 μm.

5.3.3 Effects of the Anti-Oxidant NAC on CA-4-P-Mediated HO-1 Induction

Here the potential involvement of oxidative stress in the induction of HO-1 mediated by CA-4-P was examined using NAC as an anti-oxidant. In the continuous presence of NAC (1 mM) throughout the incubation period CA-4-P-mediated HO-1 induction was completely inhibited, whereas HO-2 protein levels remained unchanged by either CA-4-P alone or the combination NAC and CA-4-P as shown by western blotting analysis in Figures 5.6B, C. However, under the same experimental conditions, the increase in overall HO enzyme activity mediated by CA-4-P (1 μM for 1h) at 30 and 48h post-treatment was only partially blocked by NAC (Figure 5.6A).

A)

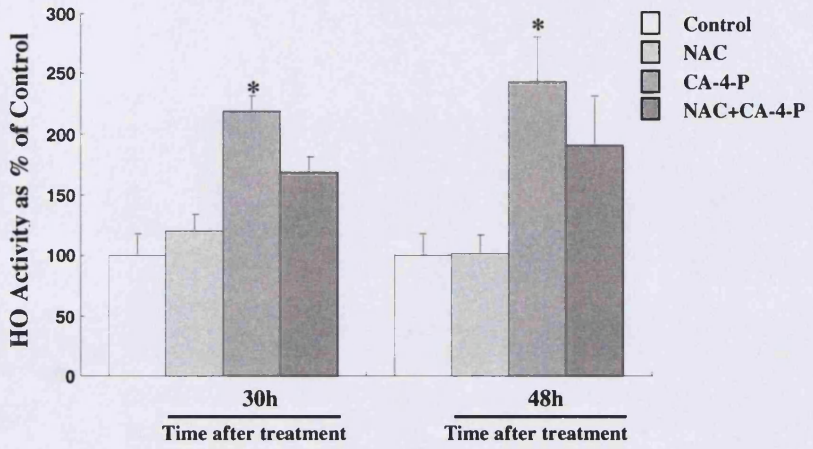

B)

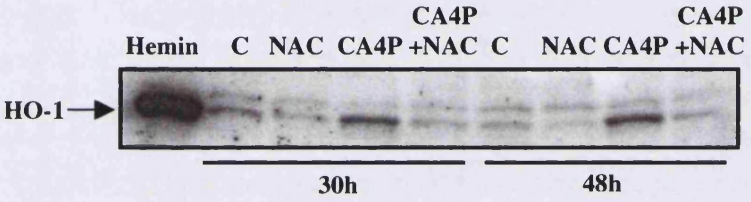

C)

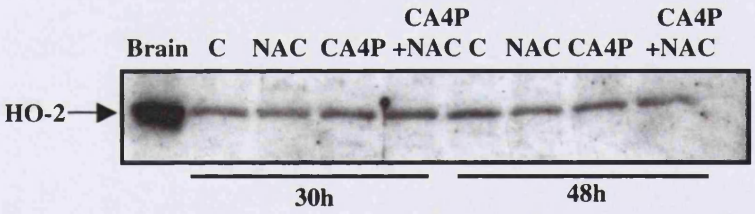

Figure 5.6 Effects of NAC on CA-4-P-mediated HO-1 induction in P22 tumour cells. ***A)*** NAC (1 mM) partially blocked the CA-4-P-mediated increase in HO activity. The data are means of 3 independent experiments. Error bars are ± 1 standard error of the mean. * represents a significant difference from control ($p<0.05$). ***B)*** Western blot showing the complete reversal of CA-4-P-mediated increase in HO-1 protein levels in response to NAC (1 mM). Hemin (100 μM)-treated cells were used as a positive control for HO-1. ***C)*** Western blot showing unchanged HO-2 protein levels following CA-4-P (1 μM) exposure alone or in combination with NAC. Microsomes extracted from brain tissue were used as a positive control for HO-2.

5.3.4 Effects of CA-4-P on the HO System in HUVECs

Similar experiments to those carried out on P22 tumour cells were repeated using HUVECs. In this cell type, we found that CA-4-P treatment did not affect HO-1 or HO-2 protein levels at 6h (Figure 5.7). This is in contrast to the P22 tumour cells, where CA-4-P mediated a *decrease* in overall HO activity and HO-1 protein levels (Figure 5.2).

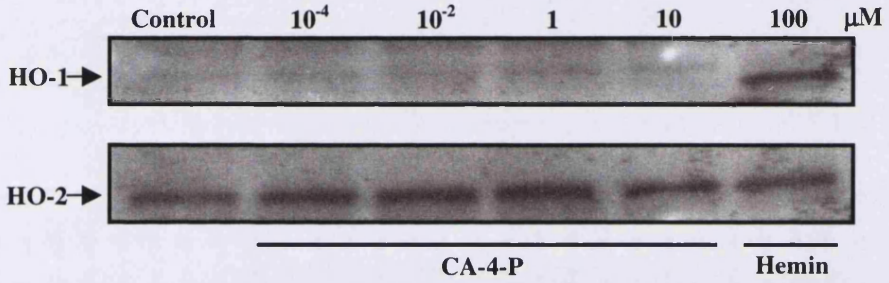

Figure 5.7 Effects of CA-4-P on HO-1 and HO-2 protein levels in HUVECs. Western blot showing unchanged protein levels of HO-1 and HO-2 in confluent HUVECs at 6h post-CA-4-P exposure. The blot is of a single experiment.

Examining the time-course of the effects mediated by CA-4-P on HO activity in HUVECs showed that the overall enzyme activity is not affected until 48h after exposure to CA-4-P (1 μM) (Figure 5.8). At this time point, the HO enzyme activity only increased modestly to ~ 144% of control. This is in contrast to the P22 tumour cells, where the increase in HO activity occurred earlier and was of greater magnitude with a ~ 221 and 254% increase above control at 30 and 48h post-CA-4-P treatment, respectively.

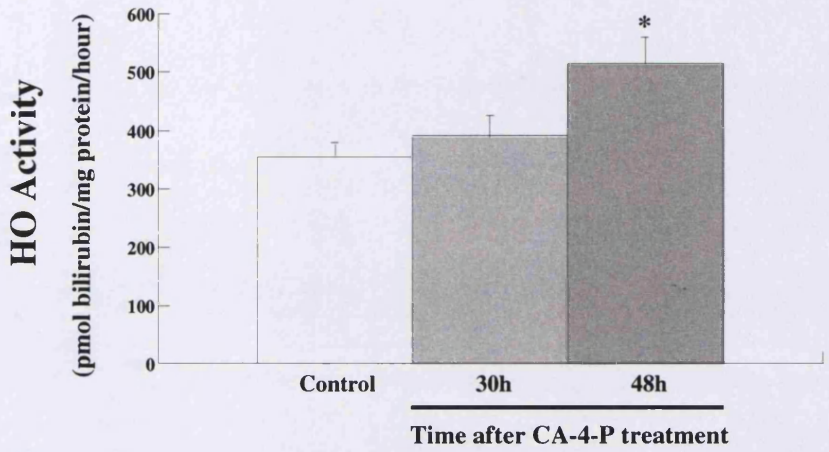

Figure 5.8 Time-course of the effects mediated by CA-4-P on HO activity in HUVECs. Effects of CA-4-P exposure (1 μM) on HO enzyme activity in confluent HUVECs at 30 and 48h post-treatment. The data are the results of 3 independent experiments. * represents a significant difference from control ($p<0.05$).

Viability/proliferation of HUVECs was examined using the trypan blue exclusion assay in cells treated for 1h with CA-4-P (1 μM) and then washed and incubated in fresh medium for 5, 23, 29 and 47h. Figure 5.9 shows that CA-4-P treatment did not significantly affect the viability/proliferation of HUVECs at 6, 24 and 30h. Only at 48h was a small but significant decrease in proliferation measured. This is in contrast to the effects of the same treatment on P22 tumour cells whereby a significant inhibition in cell proliferation was seen (Figure 5.4).

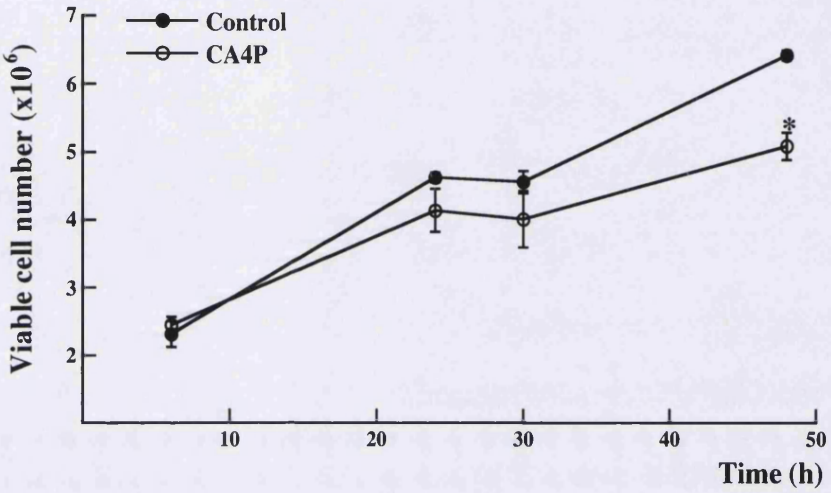

Figure 5.9 Viability of HUVECs following CA-4-P treatment. Effects of 1h exposure to CA-4-P (1μM) on cell viability at 6, 24, 30 and 48h post-treatment as compared to control untreated cells at the same time points. Each point is the mean of triplicate values. * represents a significant difference from the respective control ($p<0.05$).

Examining the HUVECs' tubulin cytoskeleton by immunofluorescence following CA-4-P treatment showed a normal cell morphology at 6 and 24h post-treatment (Figure 5.10). This is in contrast to P22 tumour cells, where the tubulin cytoskeleton was still severely disrupted at 24h (Figure 5.5). It should be noted that previous work from the Gray Cancer Institute Tumour Microcirculation Group has shown severe disruption of the tubulin cytoskeleton in HUVECs at very early times after CA-4-P exposure (1 μM for 30 minutes) (Galbraith *et al.*, 2001; Kanthou and Tozer, 2002). Taken together, the findings of the current study indicate that the initial level of CA-4-P-induced cytoskeletal damage is similar in P22 tumour cells and HUVECs but that recovery is much more rapid in the endothelial cells.

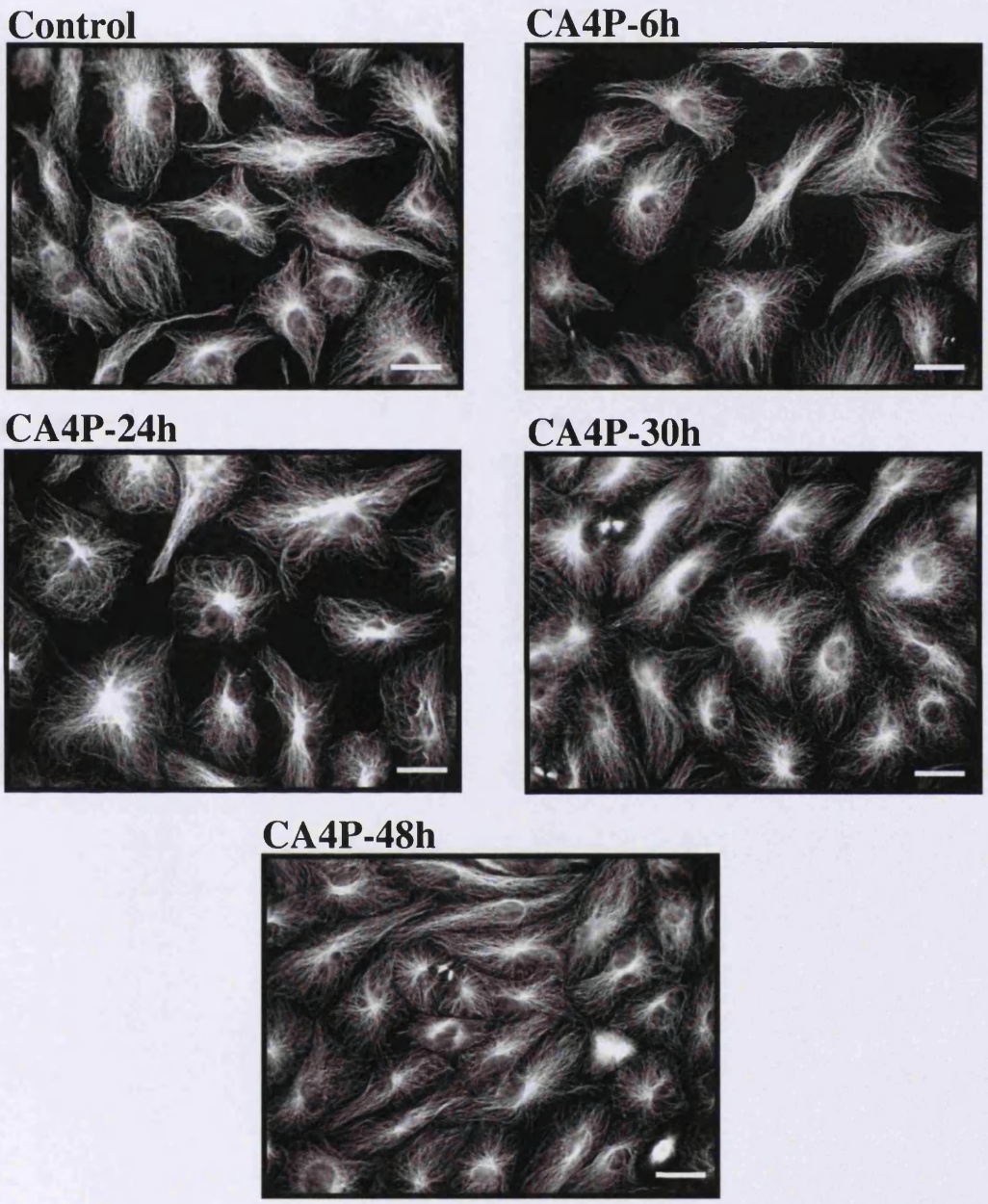

Figure 5.10 Effects of CA-4-P on the tubulin cytoskeleton in HUVECs. Following exposure to CA-4-P (1 μM for 1h), cells were fixed at 6, 24, 30 and 48h post-treatment and analysed by immunofluorescence using an anti-β-tubulin antibody. The images are representative of typical results obtained from an experiment performed in quadruplicates. Scale bar = 30 μm.

5.3.5 Effects of CA-4-P on the HO System In Vivo

The effects of CA-4-P administration on overall HO enzyme activity and HO-1 protein levels were examined in the rat P22 tumour model and a range of rat normal tissues. HO activity analysis of tumour microsomal fractions revealed a decrease in total HO activity at 24 and 30h post-CA-4-P treatment (decrease to ~ 53 and 22% of control, respectively), with the activity recovering at 48h, 4 and 7 days following a single dose of CA-4-P (30 mg/kg ip) (Figure 5.11A). For the normal tissues, no changes were seen in the brain, heart, testes, skeletal muscle, spleen or kidney (Figure 5.12) but an increase in HO activity was measured in the liver and small intestine (Figure 5.11A). For the liver, the HO activity was increased by ~ 54% at 24h following CA-4-P treatment. A peak increase of ~ 2 fold was measured at 30h post-treatment in this organ. In small intestine, the peak increase seemed to be at 24h with ~ 8 fold increase in HO activity. Changes in the HO enzyme activity in the tumour, liver and small intestine were reflected by changes in the level of HO-1 protein as shown by western blotting (Figure 5.11B). The western blot in Figure 5.11B only shows the 24h time point for the tumour and liver.

A)

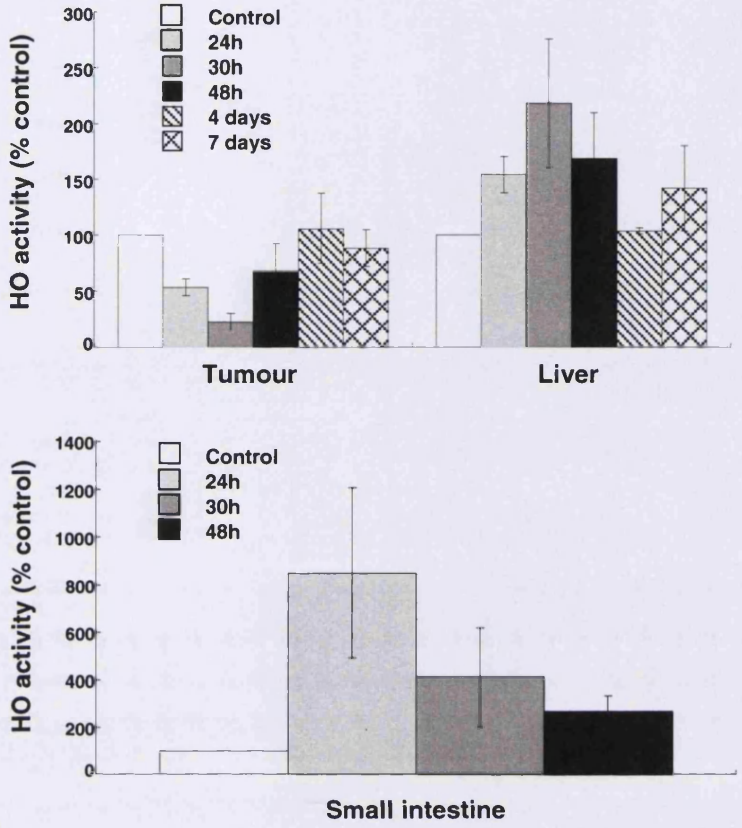

B)

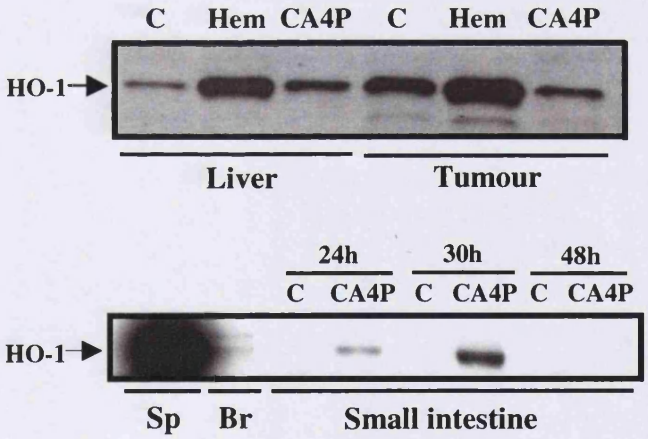

Figure 5.11 Effects of CA-4-P administration on the HO system in tumour, liver and small intestine. ***A)*** CA-4-P (30 mg/kg ip) mediated changes in HO activity in the P22 tumour, liver and small intestine. The data are means of 3-6 animals per group. Error bars are ± 1 standard error of the mean. ***B)*** Western blot showing the effects of CA-4-P (30 mg/kg ip) on HO-1 protein levels in the P22 tumour, liver and small intestine. The tumour and liver blot only shows the 24h time-point following CA-4-P. Hem: hemin (10 mg/kg)-treated animals at 24h post-treatment; C: control; Sp: spleen; Br: brain.

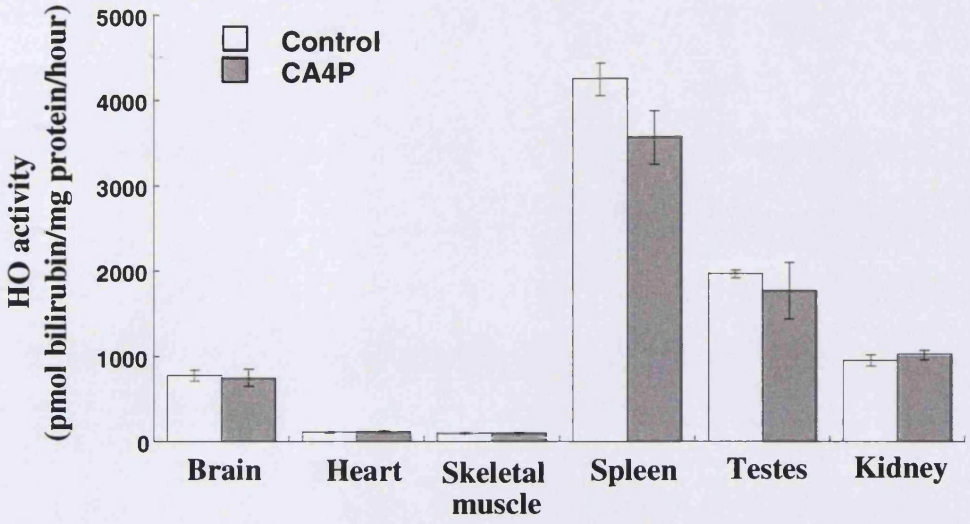

Figure 5.12 Effects of CA-4-P administration on HO activity in other normal tissues. CA-4-P (30 mg/kg ip) did not to affect total HO activity in brain, heart, skeletal muscle, spleen, testes or kidney at 24h post-treatment. The data are means of 3-6 animals per group. Error bars are ± 1 standard error of the mean.

5.3.6 HO-1 Immunohistochemical Analysis of Control P22 Tumours

Immunohistochemistry using an anti-HO-1 antibody was carried out in order to examine the distribution of HO-1 in control and hemin-treated rat P22 tumours. HO-1 positive staining was found to be absent in 3 out of 4 control tumours analysed (an example is shown in Figure 5.13). Necrosis was present in 1 out of the 4 control tumours and this tumour showed HO-1 positive staining localised to peri-necrotic areas (Figure 5.14). Furthermore, in Figure 5.15 an increase in the density of HO-1 positive staining is demonstrated in a tumour excised 24h following hemin treatment at 10 mg/kg ip. Although no further studies have been conducted to identify the nature of the HO-1 expressing cells in hemin-treated tumours, it is likely that a significant proportion will be tumour cells since the positive staining is homogeneously spread throughout the tumour section. Also, it was shown *in vitro* that P22 tumour cells are able to induce HO-1 in response to hemin exposure (Figure 5.1). This does not exclude the possibility that a proportion of HO-1 positive cells could be contributed by tumour-associated immune cells.

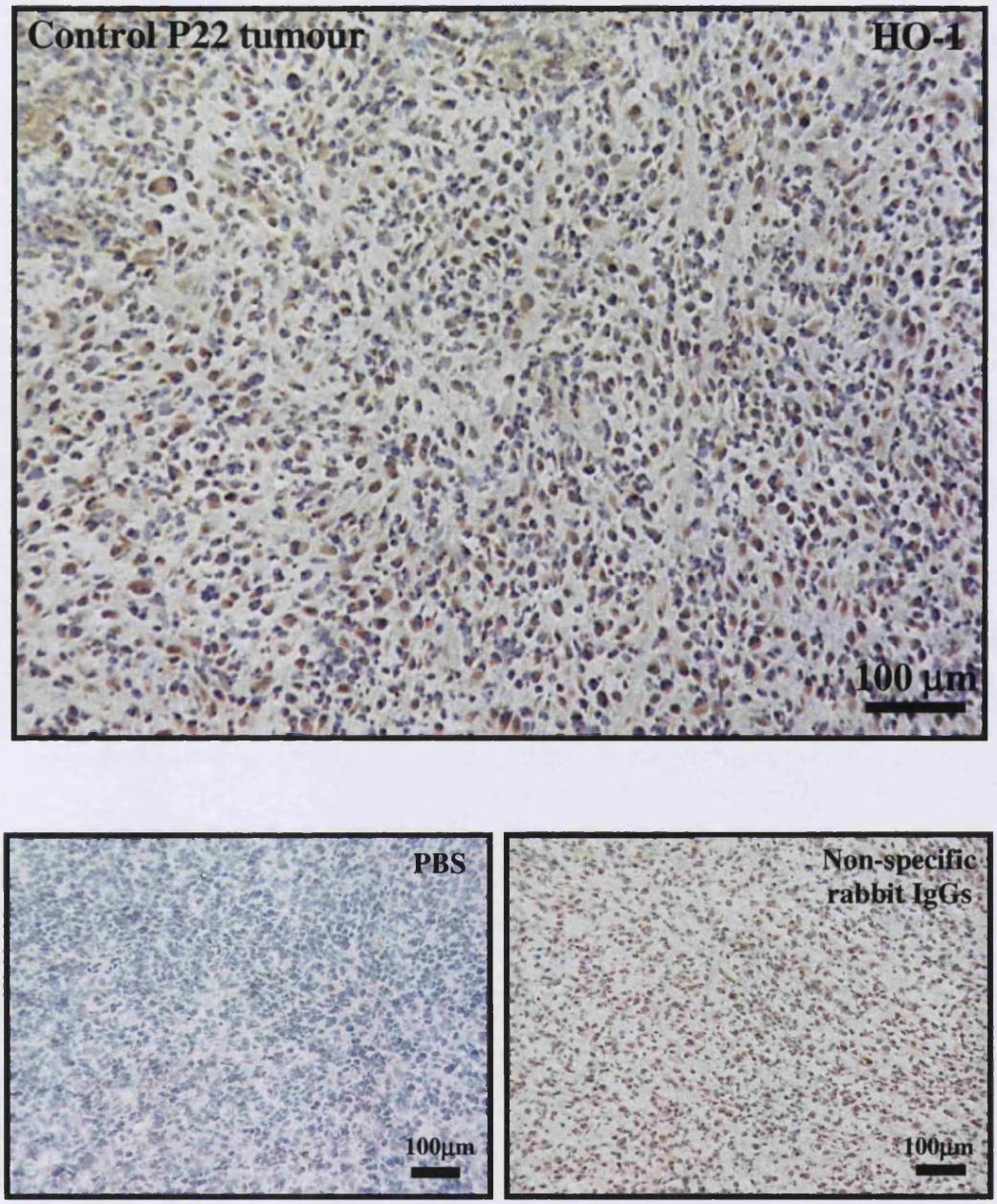

Figure 5.13 Control P22 tumour stained for HO-1. Top image shows a control P22 tumour staining negative for HO-1. Bottom images are negative controls where the primary antibody was substituted with either buffer (PBS) or non-specific rabbit immunoglobulins.

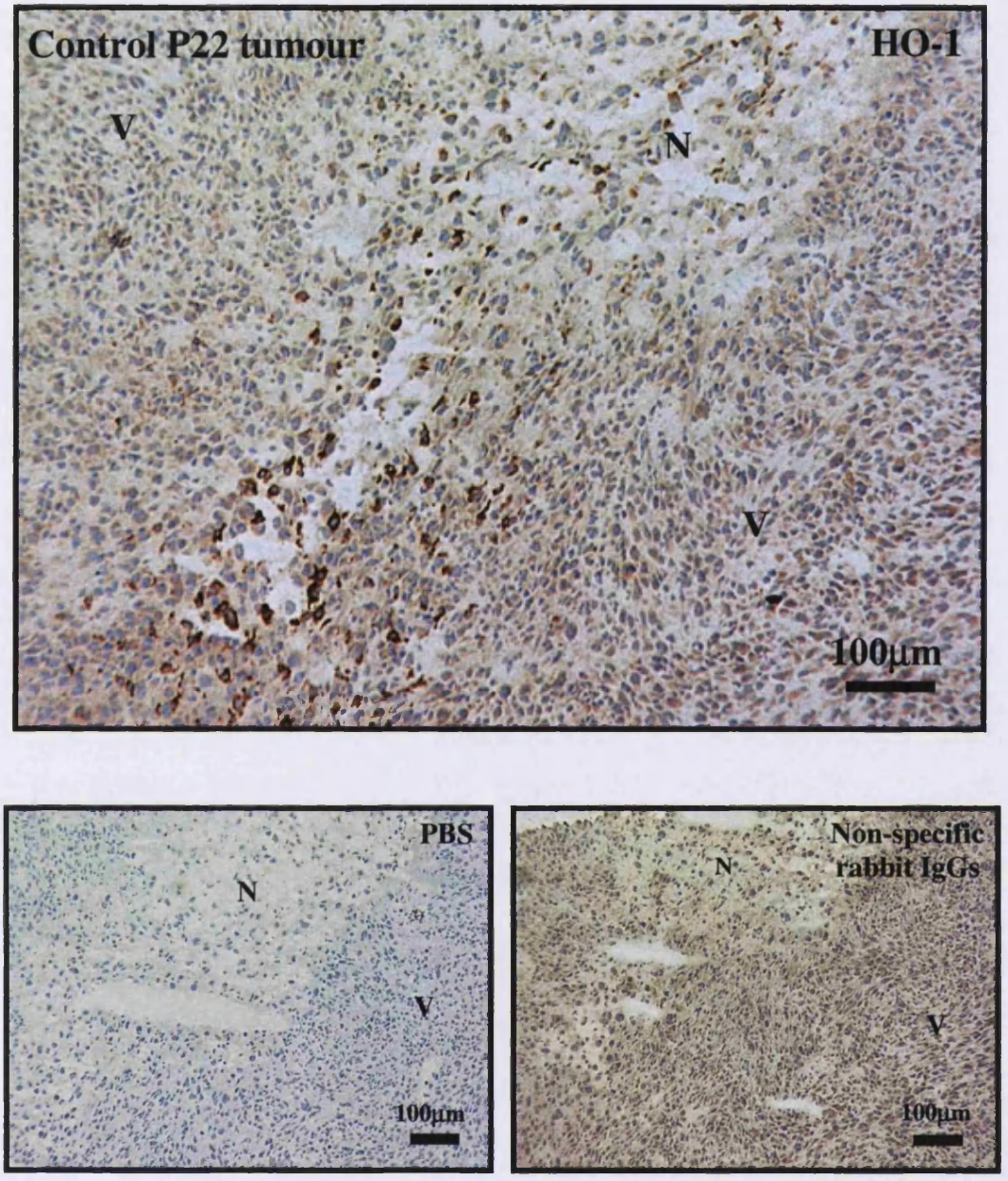

Figure 5.14 Control P22 tumour stained for HO-1. Top image shows a control P22 tumour with an area of necrosis and peri-necrotic HO-1 positive staining. Bottom images are negative controls where the primary antibody was substituted with either buffer (PBS) or non-specific rabbit immunoglobulins. N: necrosis; V: viable.

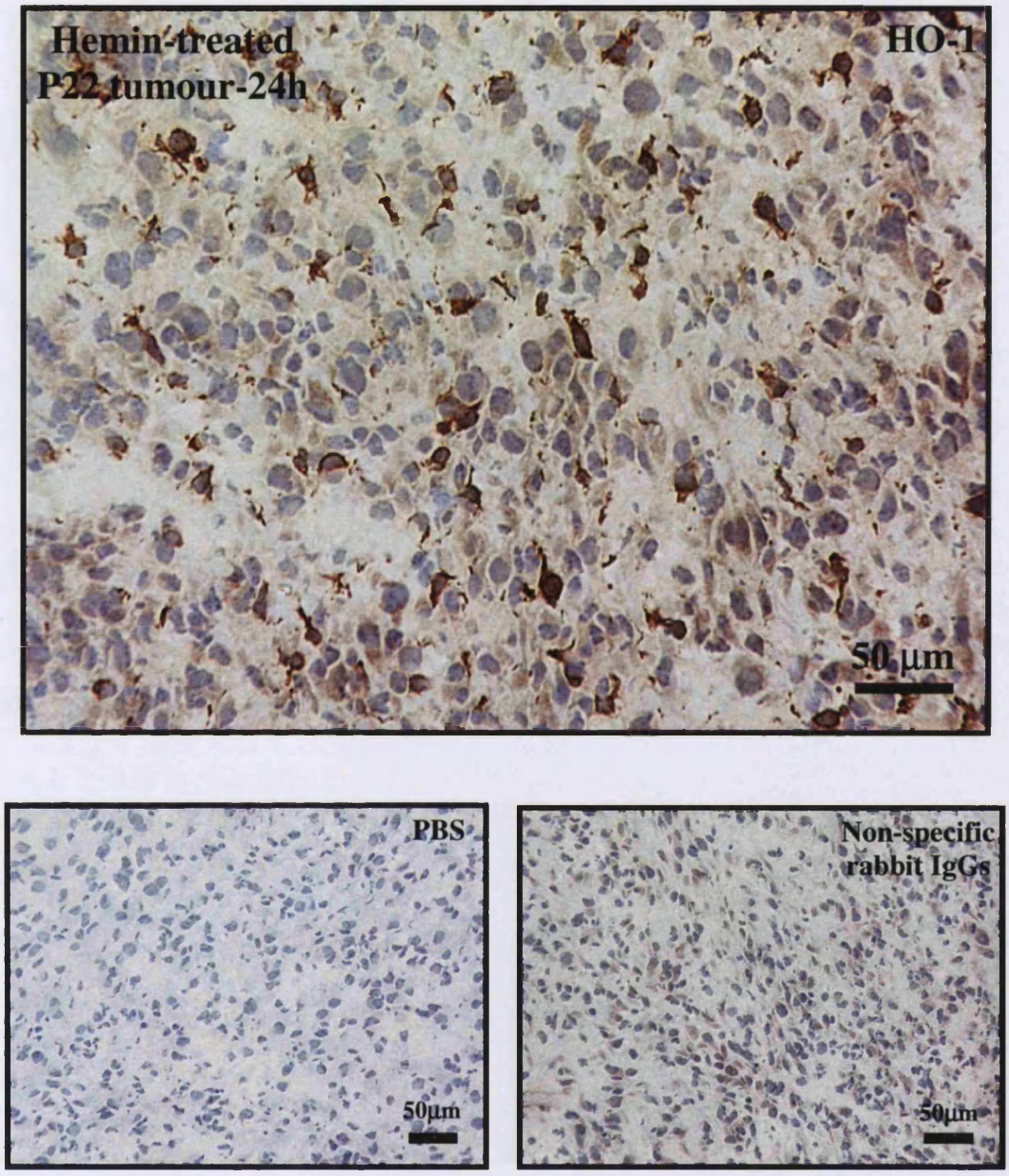

Figure 5.15 Hemin-treated P22 tumour stained for HO-1. Top image shows HO-1 positive staining in a P22 tumour excised from a hemin–treated animal (10 mg/kg ip) at 24h post-treatment. Bottom images are negative controls where the primary antibody was substituted with either buffer (PBS) or non-specific rabbit immunoglobulins.

5.3.7 Immunohistochemical Staining for Blood Vessels in P22 Tumours

Here the potential localisation of HO-1 to the vascular endothelium was investigated in P22 tumours. Prior to attempting staining the vasculature of the P22 tumour, the rat-specific endothelial cell marker, RECA-1, was tested on rat normal tissues. Figure 5.16 shows the successfully stained vasculature of rat liver. Figures 5.17 and 5.18 show the results obtained with the P22 tumour and demonstrates the presence of a high blood vessel density throughout the tissue. Larger vessels can be seen around the periphery of the tumour (Figure 5.17), whereas, smaller ones are observed elsewhere (Figure 5.18). Clearly these results confirm the well-vascularised nature of this tumour. More importantly, these findings give no indication that HO-1 could be localised to the endothelium since the protein was found to be absent from most untreated tumours (Figure 5.13).

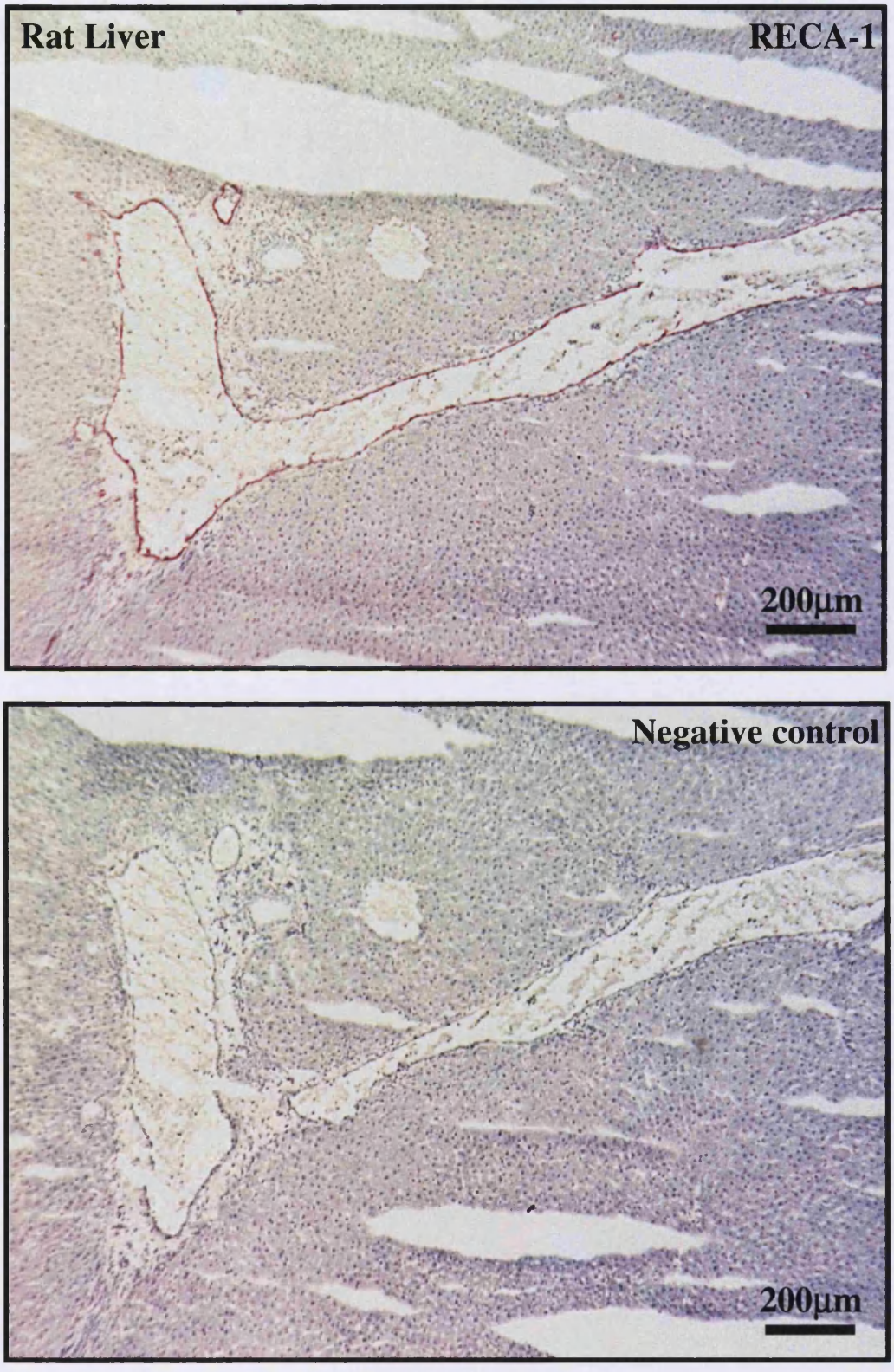

Figure 5.16 RECA-1 reactivity with endothelium in rat liver. Blood vessels are stained in red. The negative control was carried out by substituting the RECA-1 primary antibody by its isotypic control.

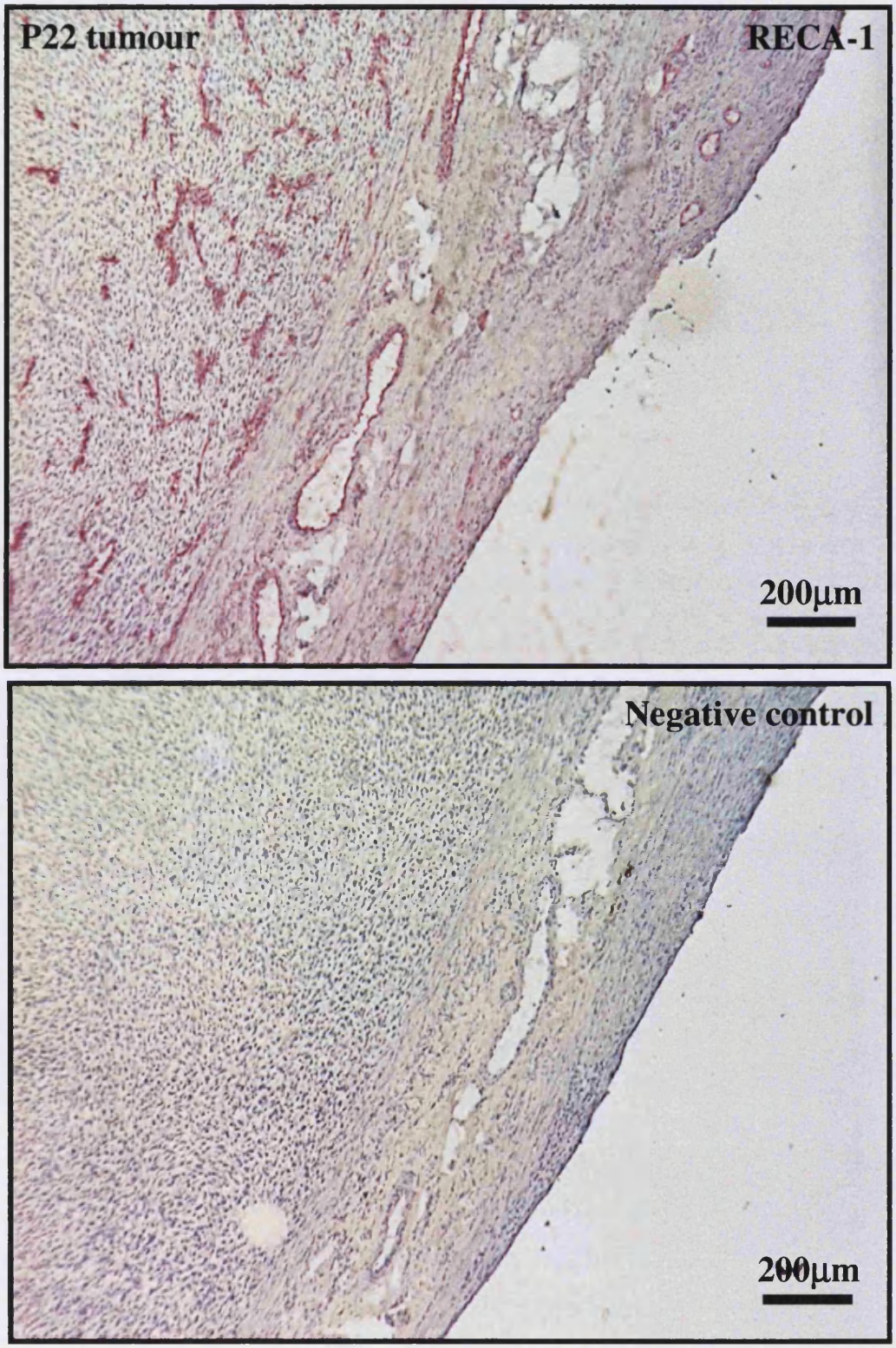

Figure 5.17 RECA-1 reactivity with endothelium in the P22 tumour. Images show the vasculature at the periphery of the tumour. The negative control was carried out by substituting the RECA-1 primary antibody by its isotypic control.

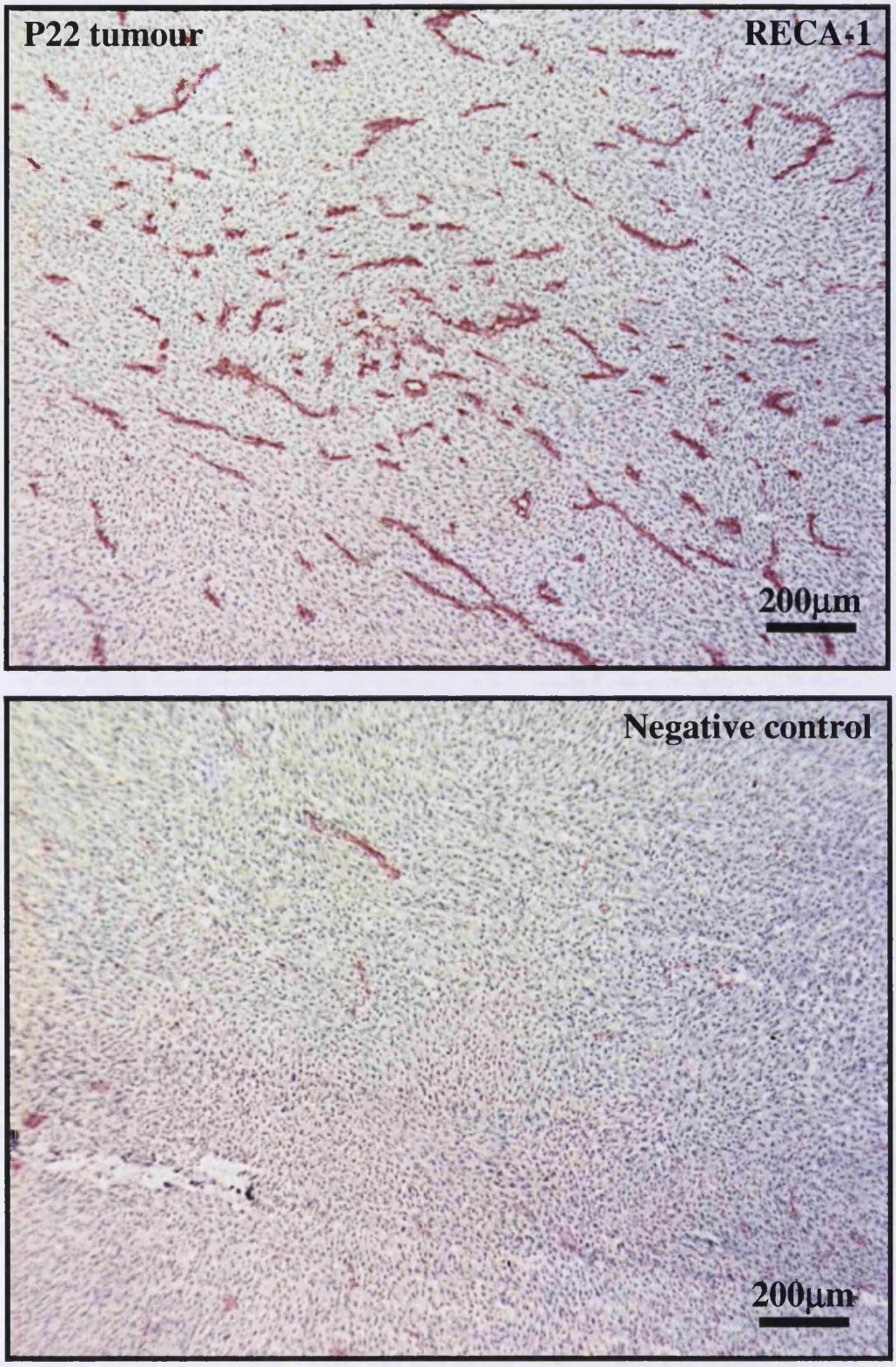

Figure 5.18 RECA-1 reactivity with endothelium in the P22 tumour. Images show the vasculature around the centre of the tumour. The negative control was carried out by substituting the RECA-1 primary antibody by its isotypic control.

5.3.8 HO-1 Immunohistochemical Analysis of CA-4-P-Treated Tumours

Tumours from animals treated with CA-4-P were analysed for HO-1 expression by immunohistochemistry using an anti-HO-1 antibody. At 24h following a 10 mg/kg dose of CA-4-P the tumours analysed were mostly negative for HO-1 staining (an example is shown in Figure 5.19). At the same dose 48h post-treatment, out of 4 tumours analysed, 2 showed significant HO-1 positive staining, which was localised to peri-necrotic areas (examples are shown in Figures 5.20/5.21 and 5.22/5.23). In the remainder 2 tumours, HO-1 staining was absent and only little necrosis was present (an example is shown in Figure 5.24). At the higher dose of CA-4-P (30 mg/kg), large areas of necrosis were observed but HO-1 positive staining was mostly absent (examples are shown in Figures 5.25 and 5.26). The results of this HO-1 immunohistochemical analysis are summarised in Table 5.1.

Group	Time Post-Treatment	n	HO-1 Staining Status and Comments
Control	-	**3**	Tumours were not necrotic and mostly HO-1 negative.
CA4P 10 mg/kg	**24h**	**3**	Only few necrotic patches present and HO-1 staining was mostly absent (Figure 5.19).
CA4P 10 mg/kg	**48h**	**4**	2/4 tumours showed important HO-1 positive staining localised in peri-necrotic areas (Figures 5.20/5.21 and 5.22/5.23). The other 2 tumours showed no HO-1 staining and also no or little necrosis (Figure 5.24).
CA4P 30 mg/kg	**24h**	**4**	Tumours were mostly necrotic and HO-1 positive staining was mostly absent (Figure 5.25).
CA4P 30 mg/kg	**48h**	**4**	Tumours had large areas of necrosis and overall HO-1 positive staining was mostly absent (Figure 5.26).

Table 5.1 Summary of the immunohistochemical analysis carried out on CA-4-P-treated tumours using the anti-HO-1 antibody.

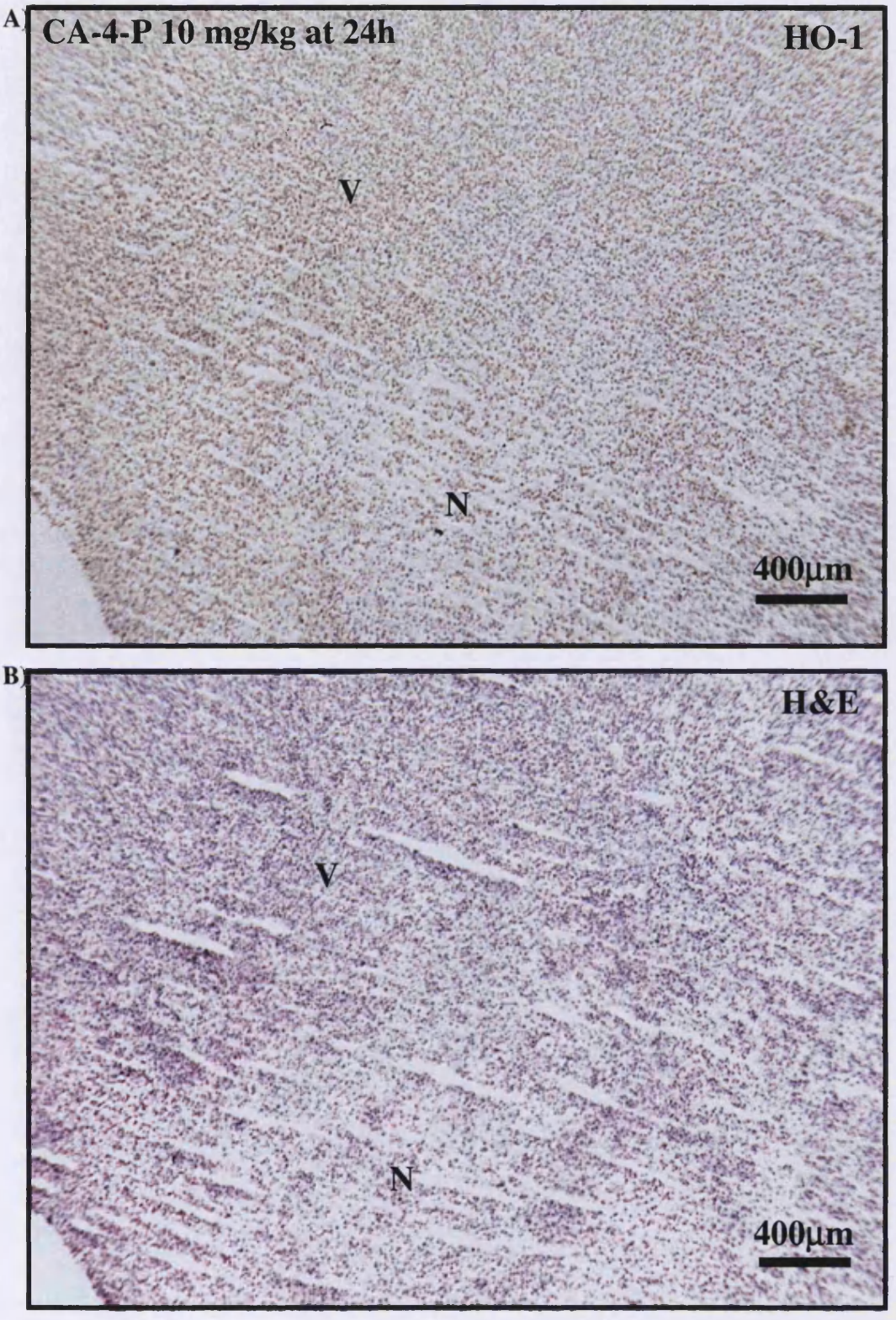

Figure 5.19 CA-4-P-treated P22 tumour stained for HO-1. **A)** HO-1 positive staining is absent in a tumour treated with CA-4-P at a dose of 10 mg/kg and excised 24h post-treatment. **B)** H&E-stained subsequent section. N: necrosis; V: viable.

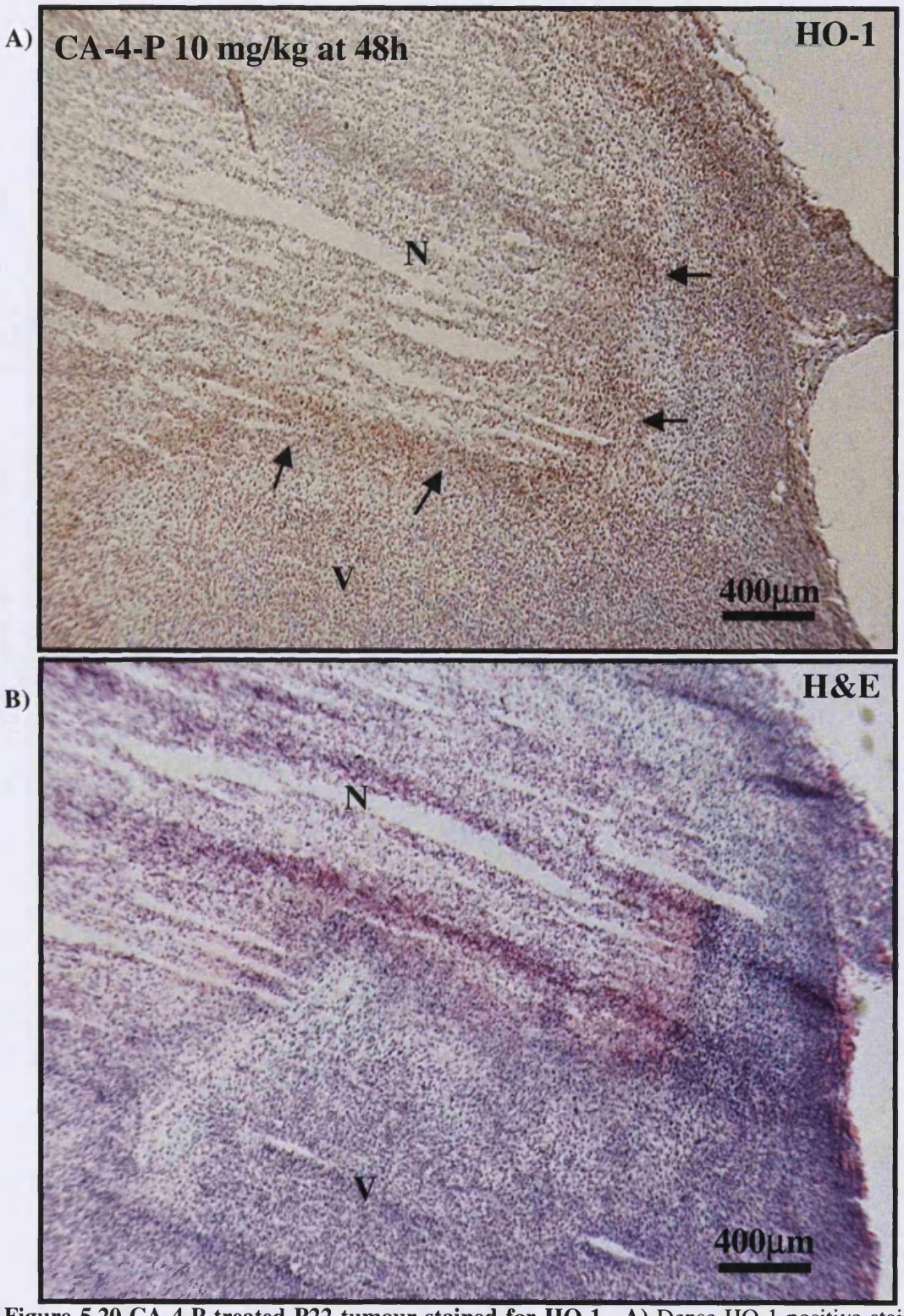

Figure 5.20 CA-4-P-treated P22 tumour stained for HO-1. **A)** Dense HO-1 positive staining (red/brown) in a single section of a tumour treated with CA-4-P at a dose of 10 mg/kg and excised 48h post-treatment. **B)** H&E-stained subsequent section demonstrating areas of necrosis. Arrows indicate areas of HO-1 positive staining. N: necrosis; V: viable.

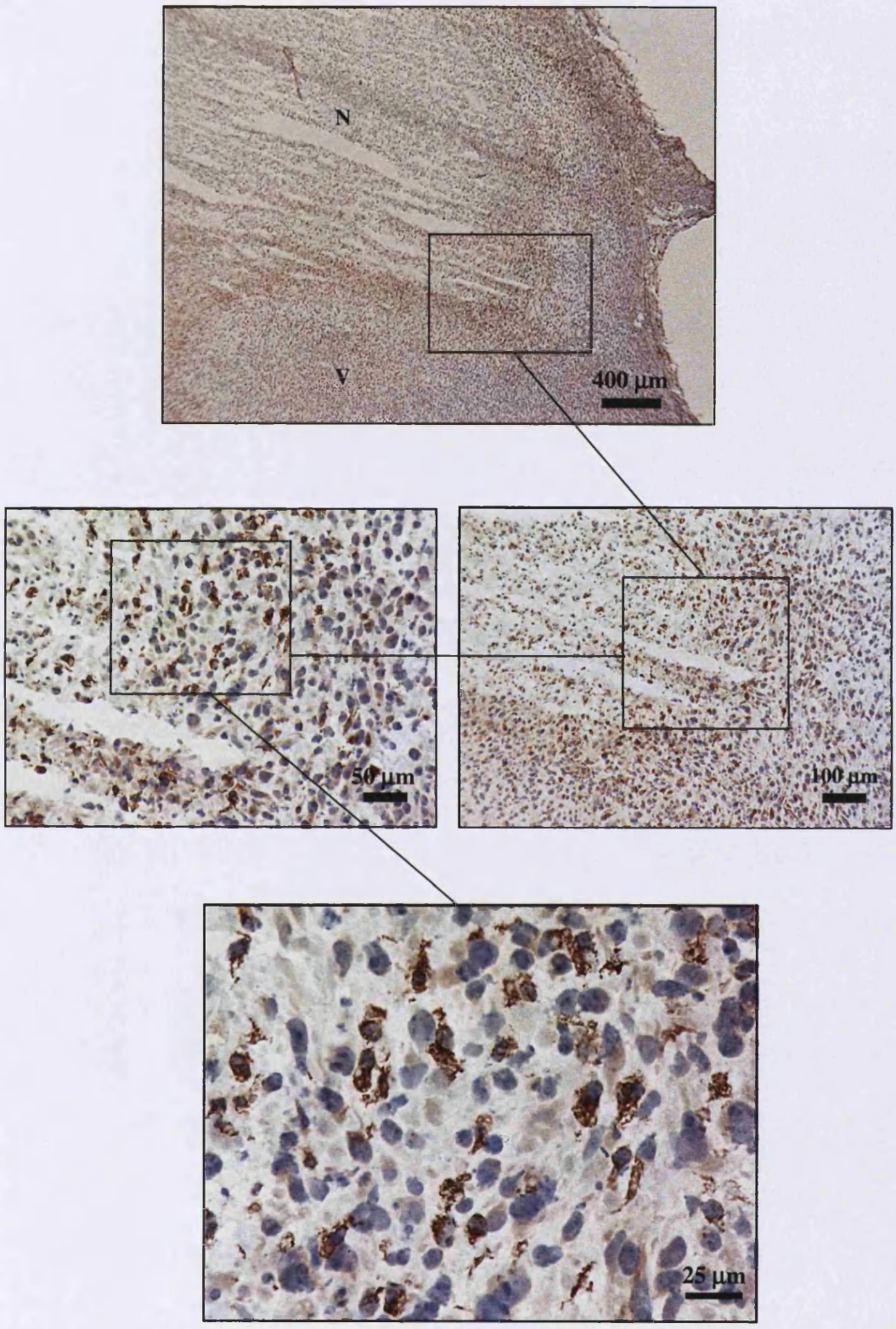

Figure 5.21 Cellular distribution of HO-1 protein in a CA-4-P-treated tumour. Higher magnification images of the same tumour section shown in Figure 5.20. N: necrosis; V: viable.

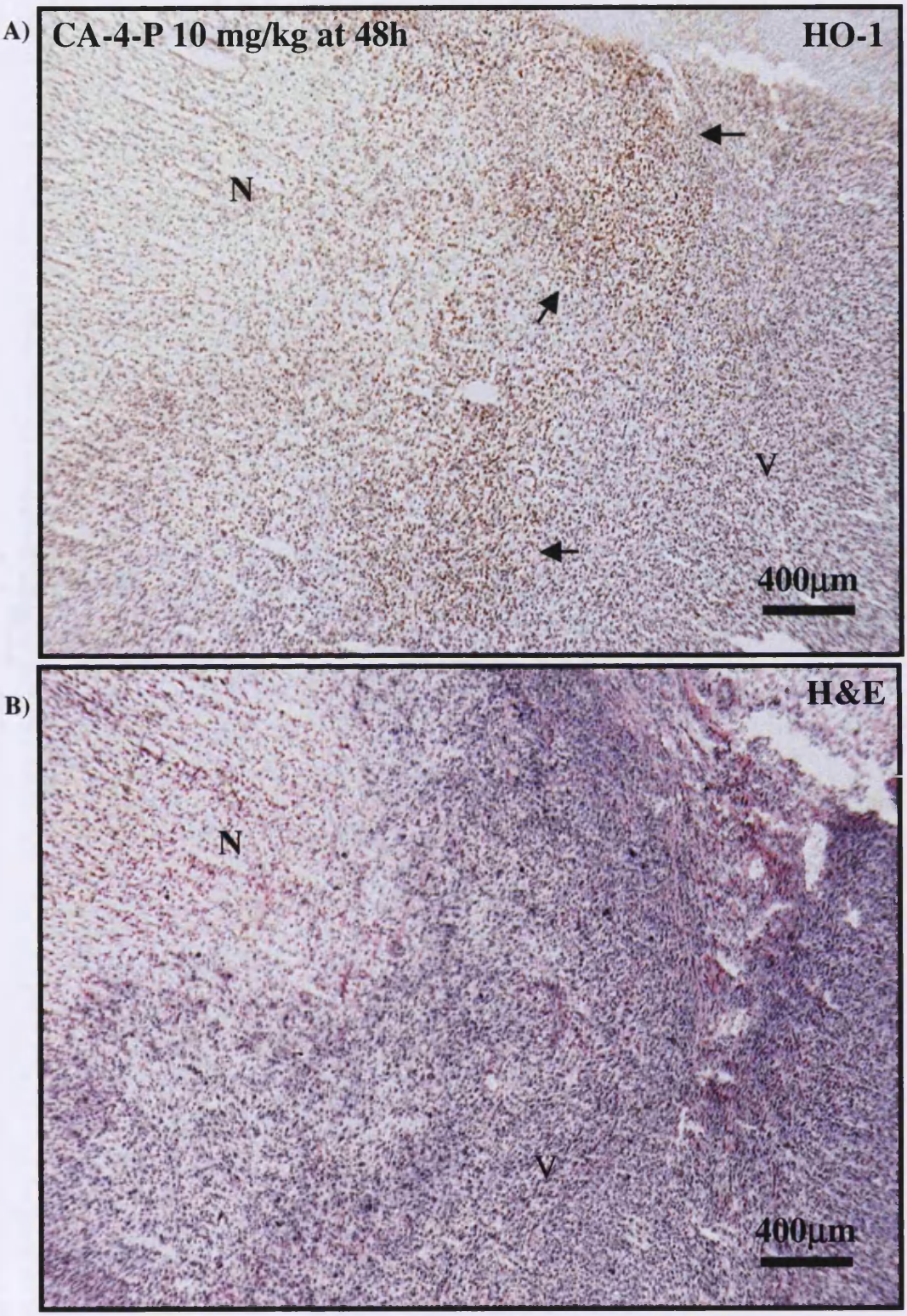

Figure 5.22 CA-4-P-treated P22 tumour stained for HO-1. **A)** Dense HO-1 positive staining (red/brown) in a section of a different CA-4-P (10 mg/kg 48h)-treated tumour as shown in Figure 5.20. **B)** H&E-stained subsequent section demonstrating areas of necrosis. Arrows indicate areas of HO-1 positive staining. N: necrosis; V: viable.

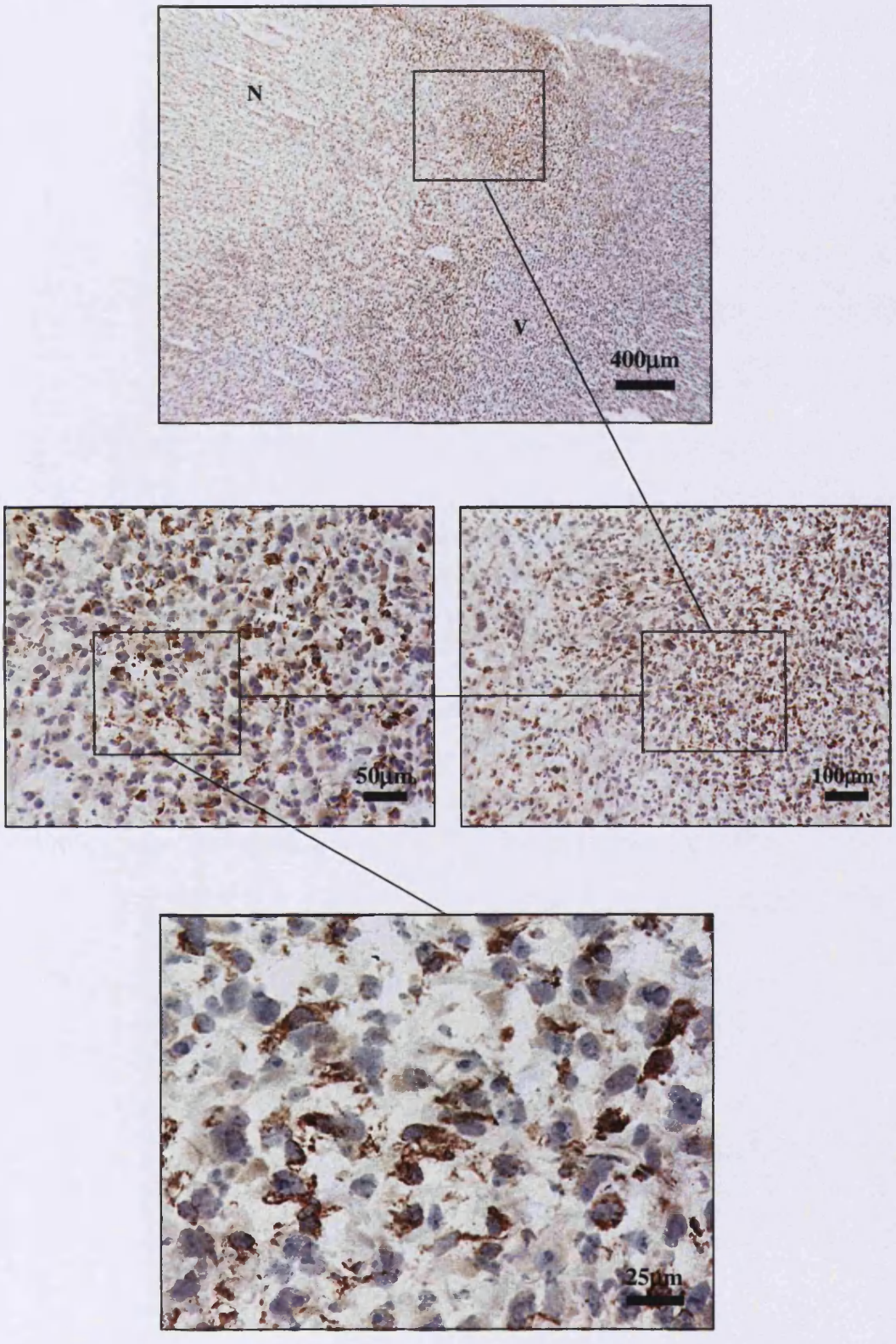

Figure 5.23 Cellular distribution of HO-1 protein in CA-4-P treated tumour. Higher magnification images of the same tumour section shown in Figure 5.22. N: necrosis; V: viable.

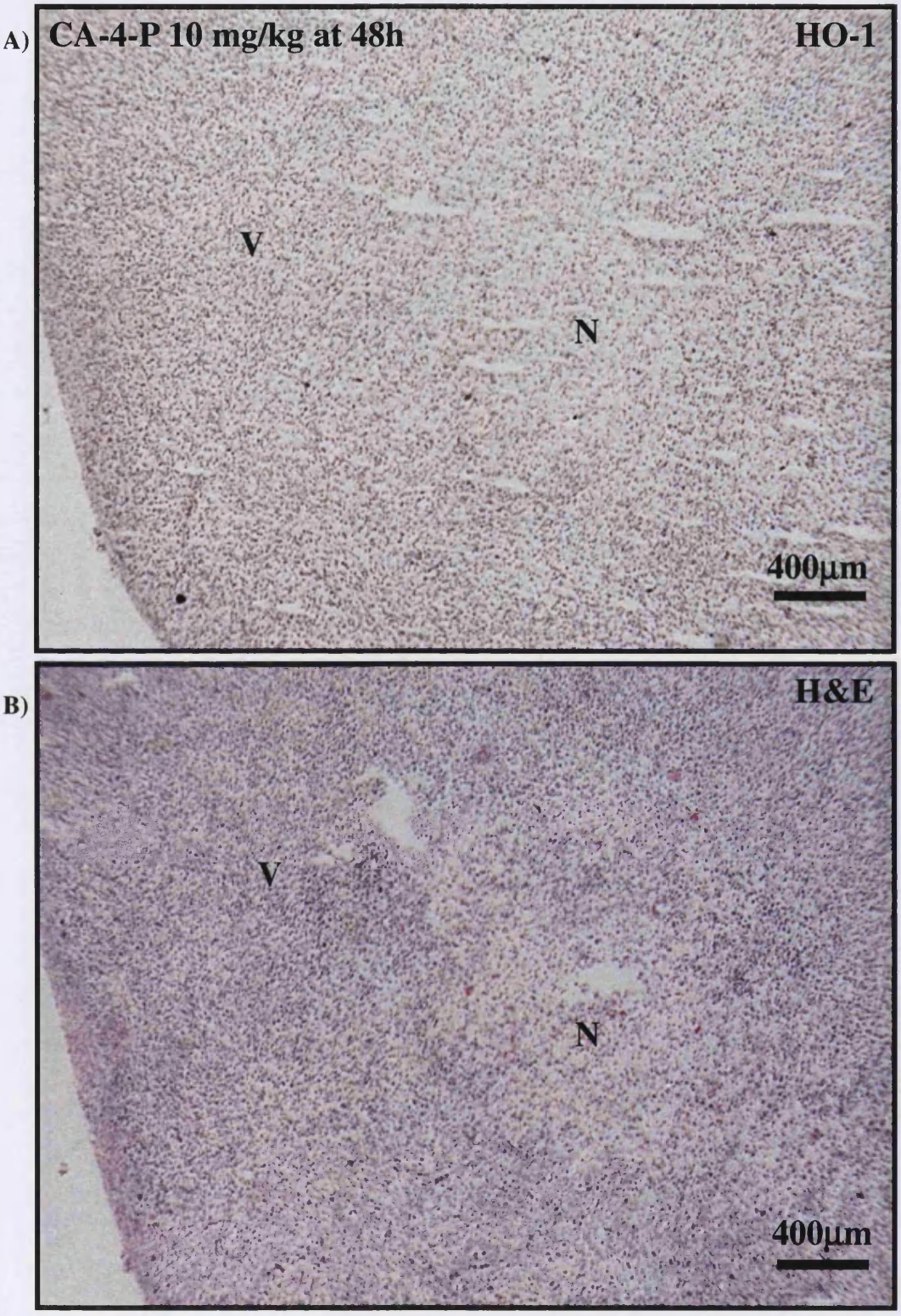

Figure 5.24 CA-4-P-treated P22 tumour stained for HO-1. A) HO-1 positive staining is absent in a tumour treated with CA-4-P at a dose of 10 mg/kg and excised 48h post-treatment. **B)** H&E-stained subsequent section. N: necrosis; V: viable.

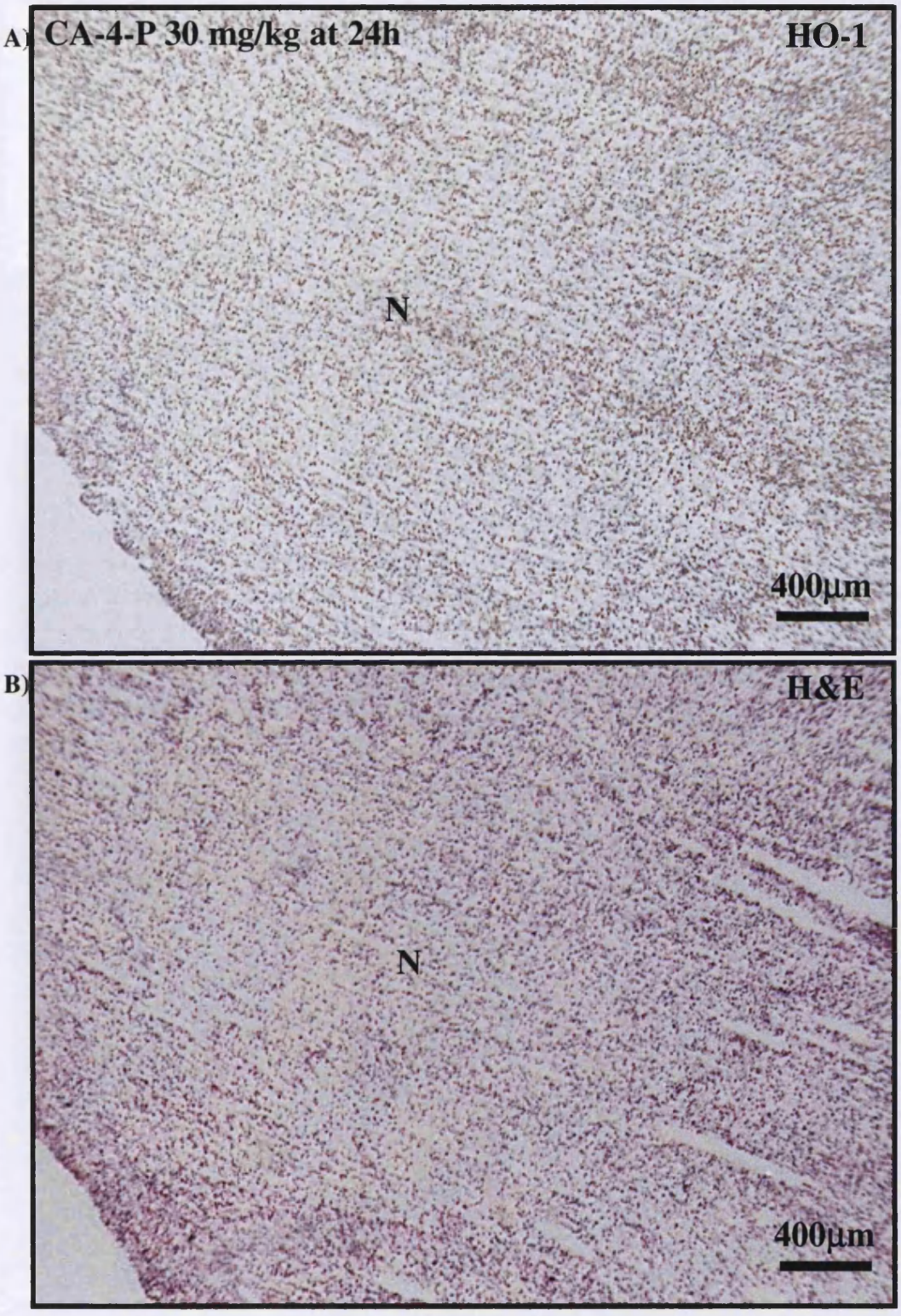

Figure 5.25 CA-4-P-treated P22 tumour stained for HO-1. A) HO-1 staining is absent in a tumour treated with CA-4-P at a dose of 30 mg/kg and excised 24h post-treatment. **B)** H&E-stained subsequent section. N: necrosis.

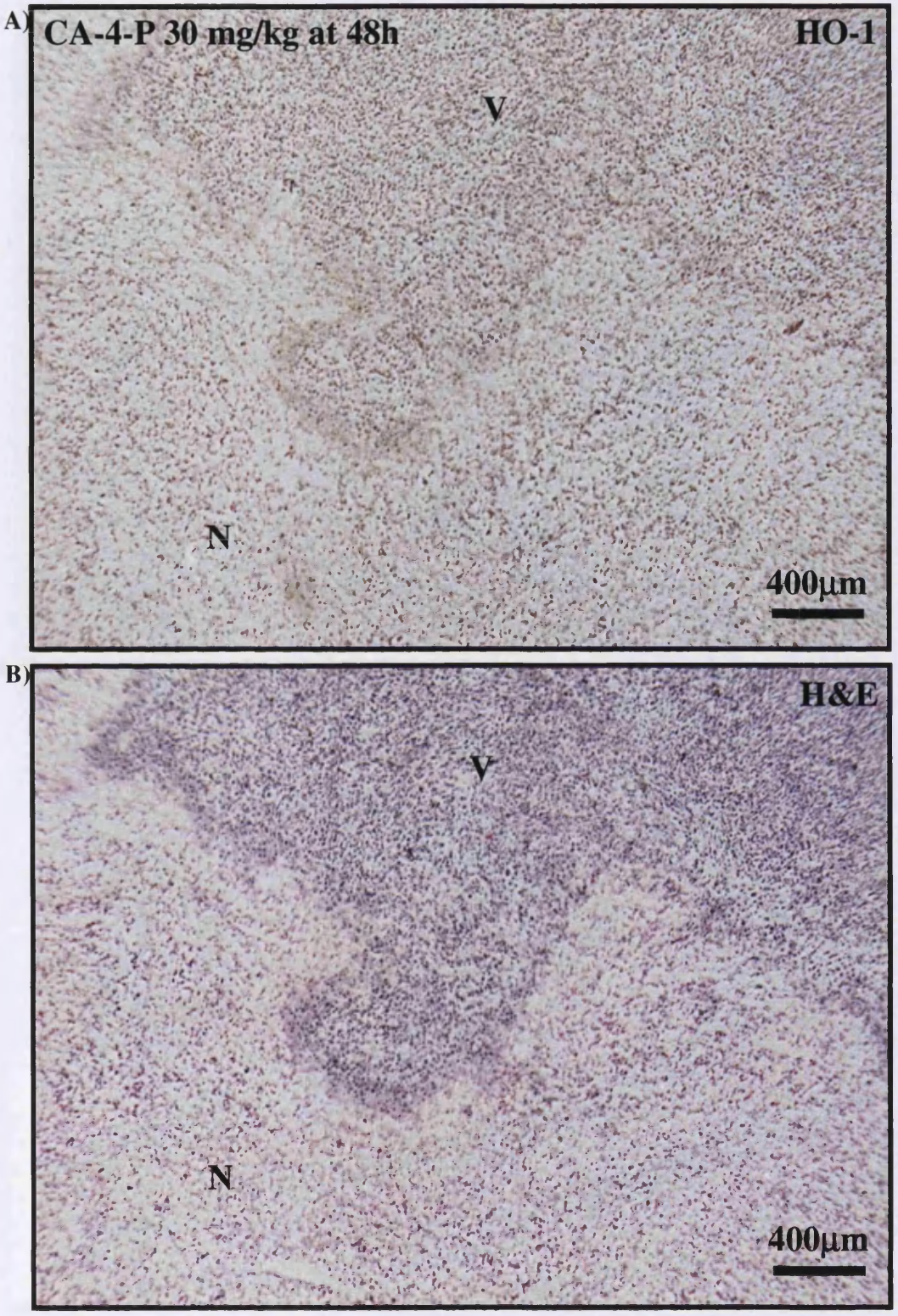

Figure 5.26 CA-4-P-treated P22 tumour stained for HO-1. A) HO-1 staining is absent in a tumour treated with CA-4-P at a dose of 30 mg/kg and excised 48h post-treatment. **B)** H&E-stained subsequent section. N: necrosis; V: viable.

5.3.9 HO-1 Expression and Macrophage Infiltration in CA-4-P-Treated Tumours

Further examination of the nature of the HO-1 expressing cells in Figures 5.20 and 5.22 revealed that there is a correlation between HO-1 expression and macrophage infiltration into the tumour tissue. Macrophage staining in control untreated tumours was mostly absent or weak (Figure 5.27). Some areas at the periphery of control tumours showed positive staining for macrophages as shown in Figure 5.27. On the other hand, the CA-4-P-treated tumours shown in Figures 5.20 and 5.22 (10 mg/kg ip-48h) showed strong macrophage positive staining that was localised to areas of HO-1 positive staining (examples are shown in Figures 5.28 and 5.29). Co-localisation of HO-1 and macrophage staining was demonstrated in the same CA-4-P-treated tumours using immunofluorescence double labelling (examples are shown in Figures 5.30 and 5.31). Figure 5.32 shows that not all the macrophages infiltrating the tumour tissue appear to express HO-1. Furthermore, in some instances HO-1 did not co-localise with macrophages. However, overall it can be concluded that macrophages were the predominant cell type expressing the protein.

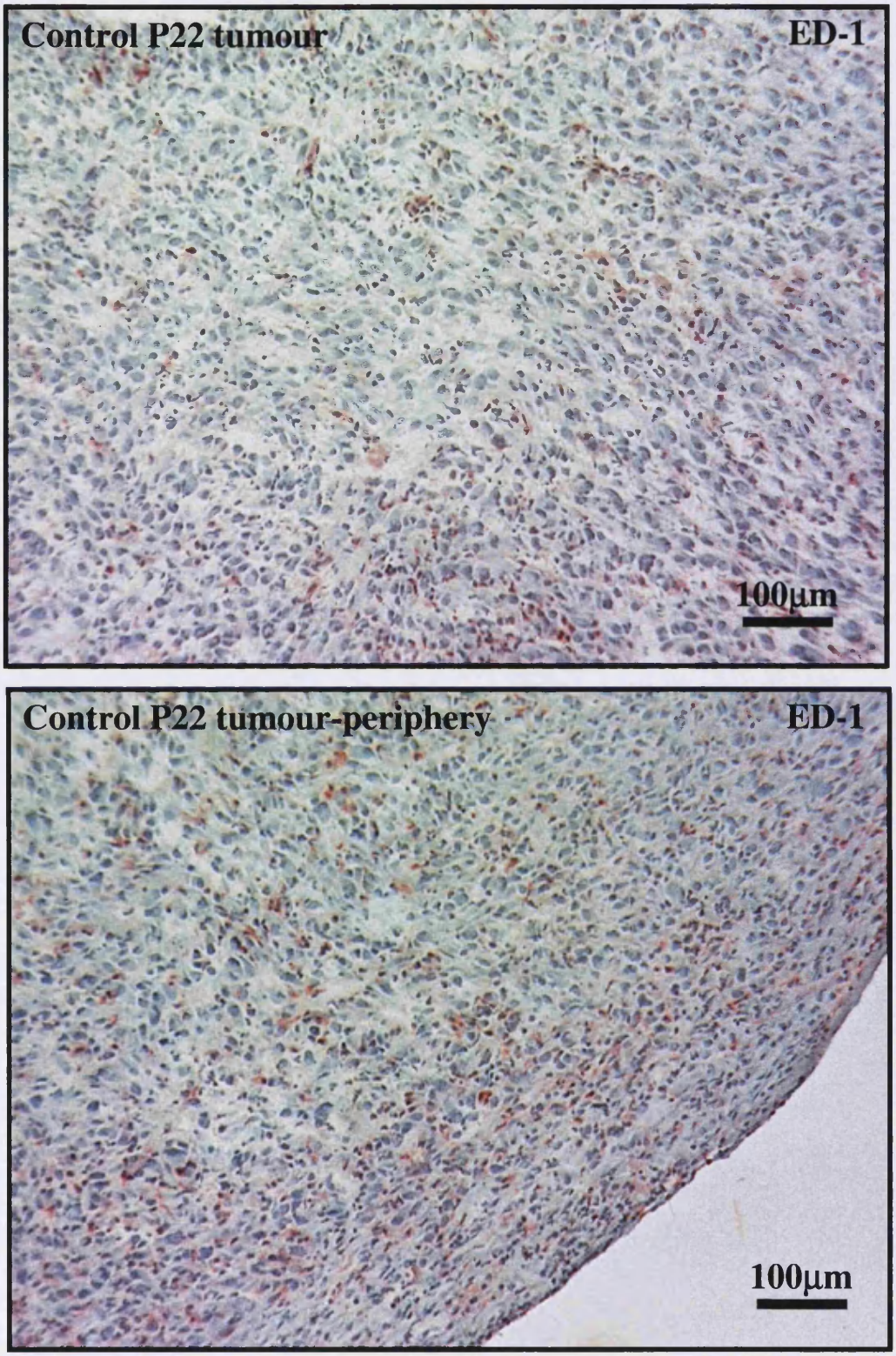

Figure 5.27 Macrophage (ED-1) staining in control P22 tumours. Macrophage positive staining is shown in red. The images were taken from 2 different control tumours and show particular areas of macrophage "hot-spots".

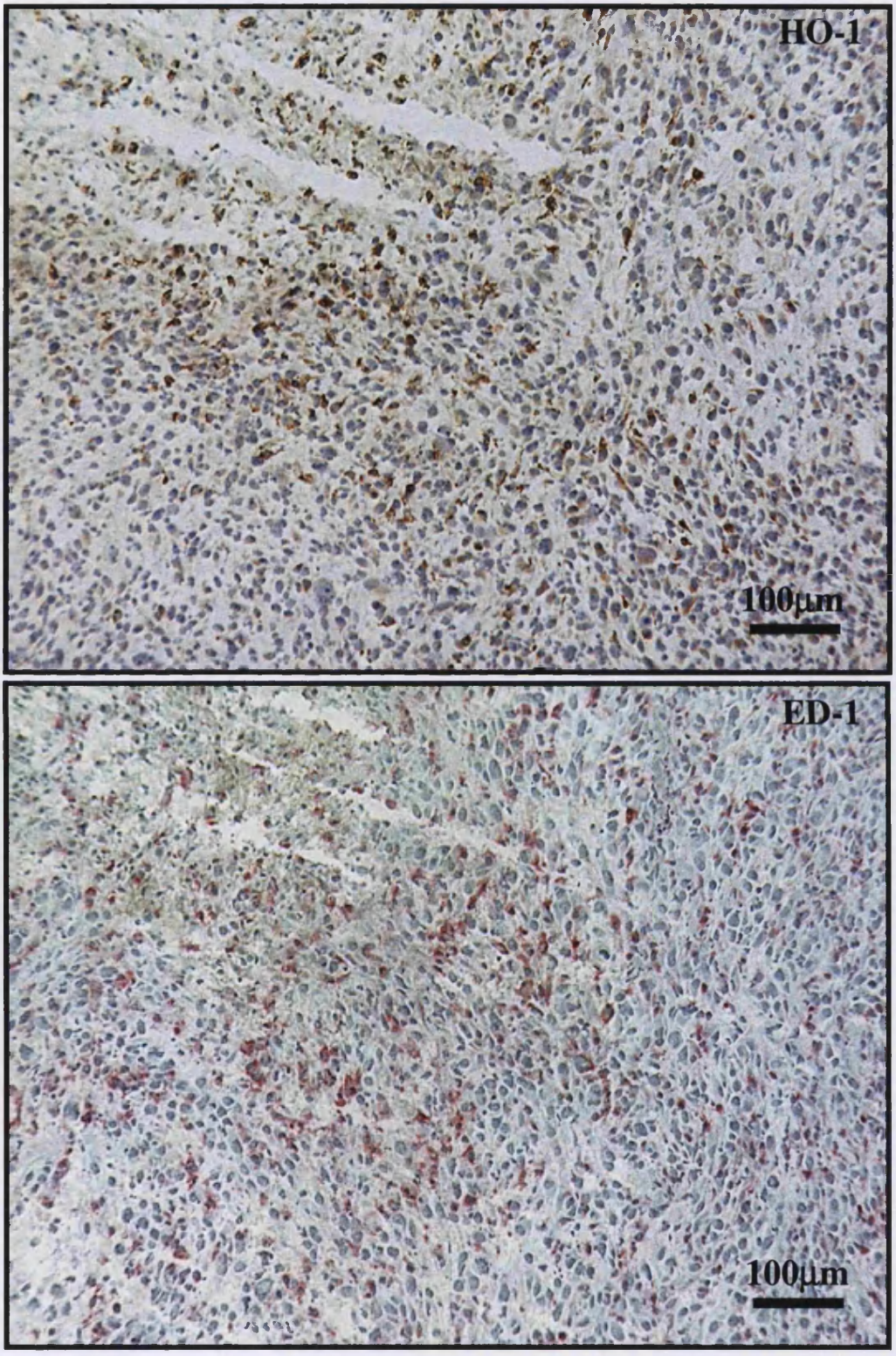

Figure 5.28 HO-1 and macrophage (ED-1) staining in a CA-4-P-treated tumour. Sections are from the same CA-4-P-treated tumour (10 mg/kg ip at 48h) as shown in Figure 5.20. Macrophage staining was carried out on consecutive sections. The images were taken from similar areas of the 2 sections and show similar localisation of HO-1 and ED-1 positive staining.

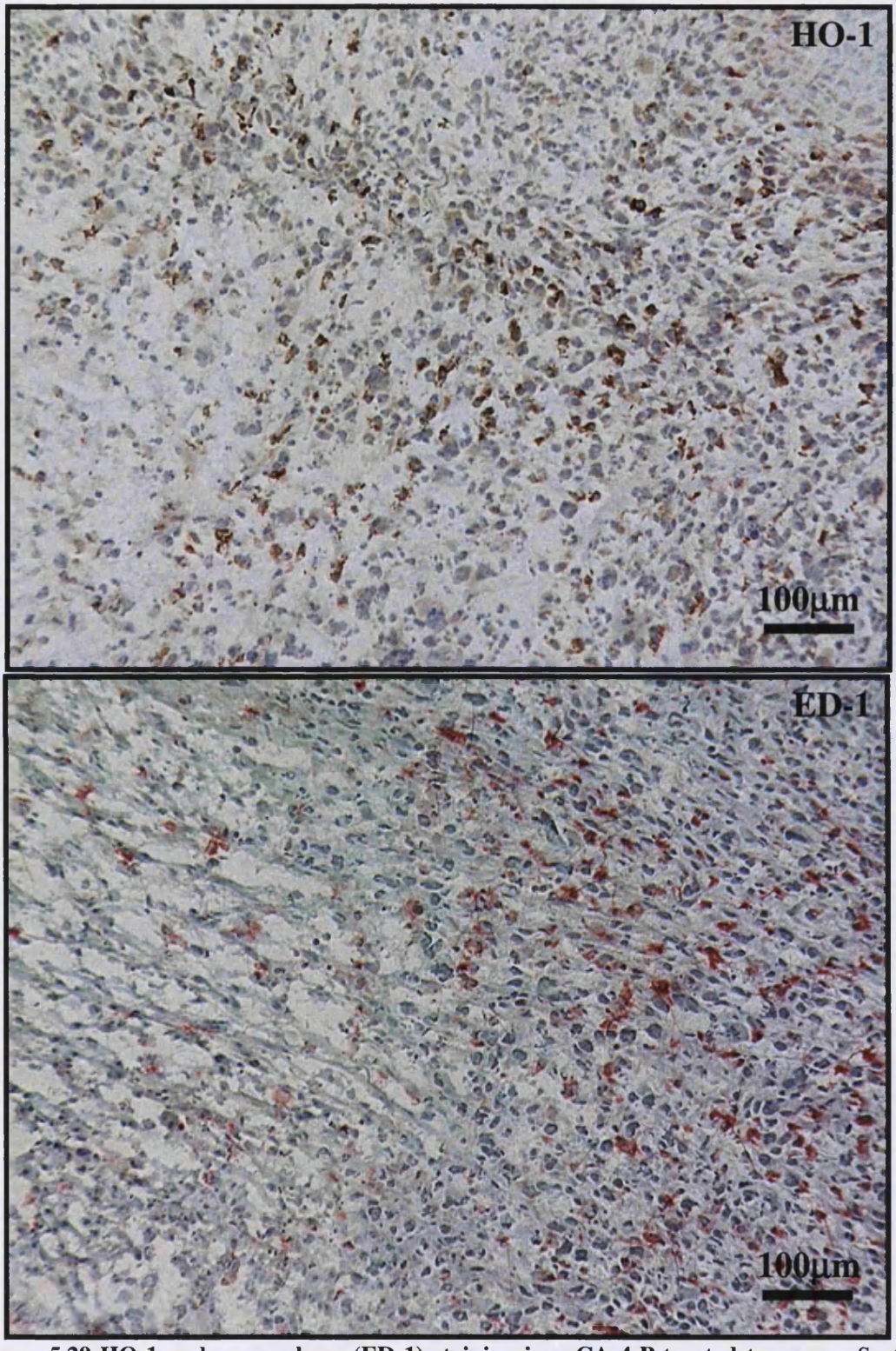

Figure 5.29 HO-1 and macrophage (ED-1) staining in a CA-4-P-treated tumour. Sections are from the same CA-4-P-treated tumour (10 mg/kg ip at 48 hours) as shown in Figure 5.22. Macrophage staining was carried out on consecutive sections. The images were taken from similar areas of the 2 sections and demonstrate similar localisation of HO-1 and ED-1 positive staining.

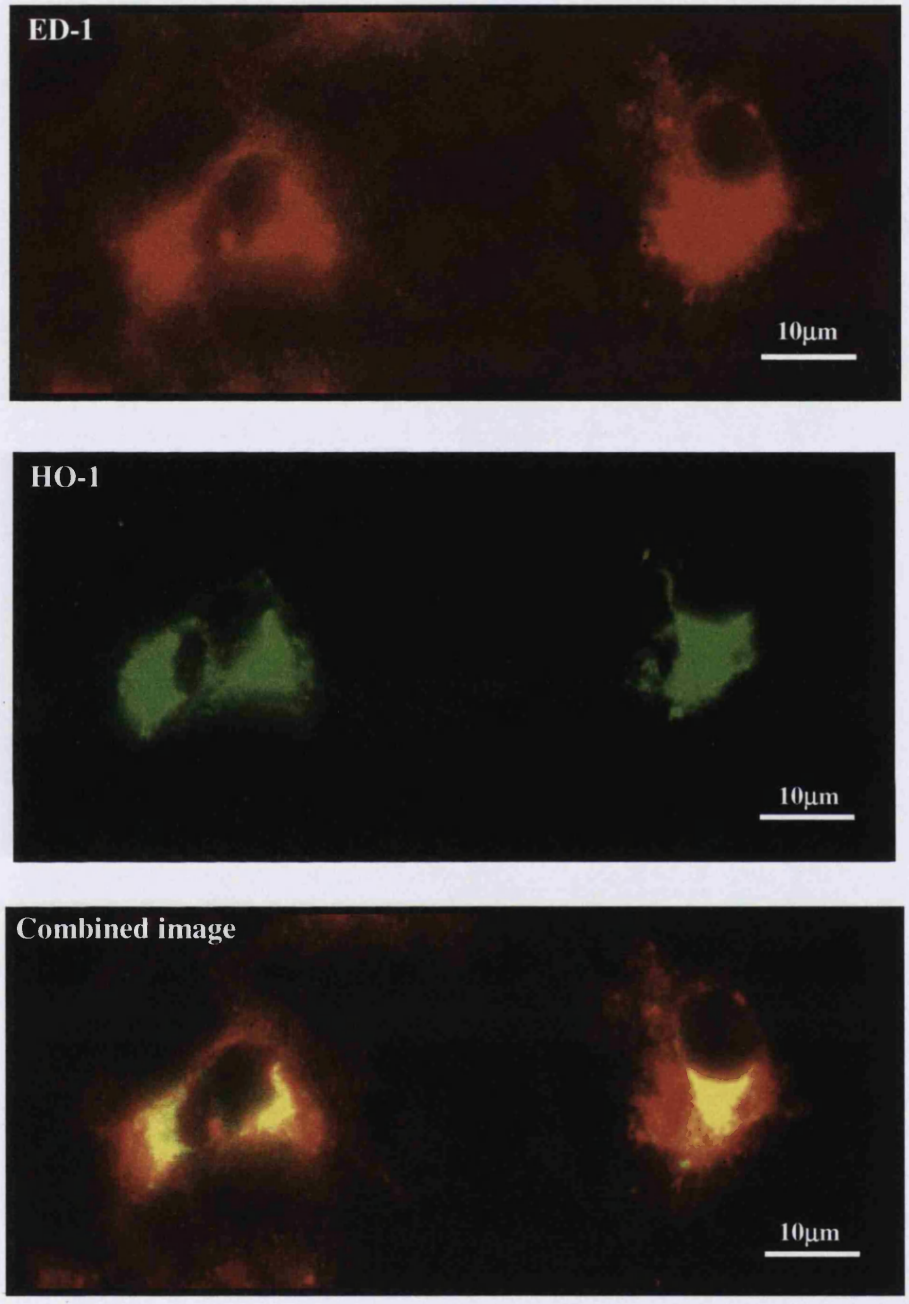

Figure 5.30 Immunofluorescence double labelling for HO-1 and the macrophage marker ED-1 in a CA-4-P-treated tumour. The double labelling was carried out on the same section from the CA-4-P-treated tumour (10 mg/kg ip at 48 hours) shown in Figure 5.22. Macrophage staining is shown in red (top) and HO-1 staining is shown in green (middle). The bottom picture is the combined image of the two top ones. Yellow in the combined image demonstrates co-localisation.

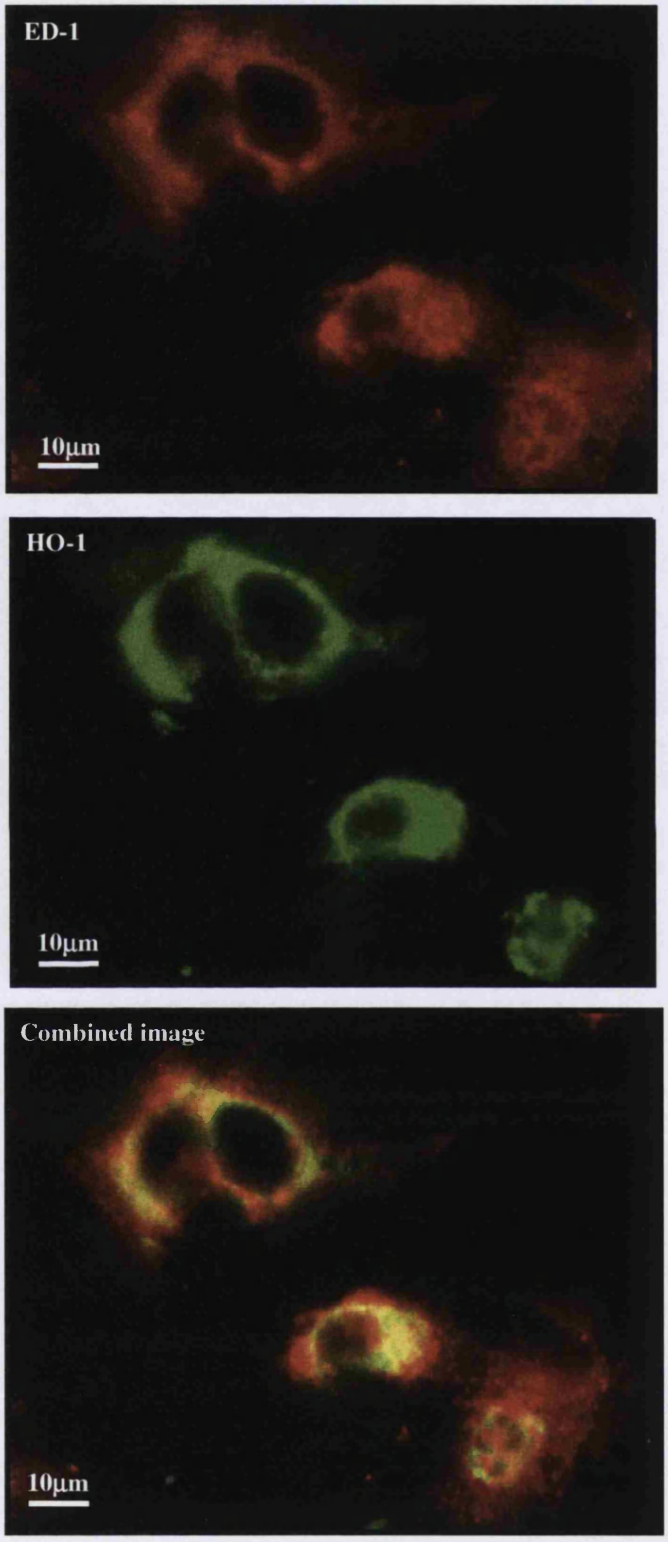

Figure 5.31 Immunofluorescence double labelling for HO-1 and the macrophage marker ED-1 in a CA-4-P-treated tumour. Images are from the same section as shown in Figure 5.30. Macrophage staining is shown in red (top) and HO-1 staining is shown in green (middle). The bottom picture is the combined image of the two top ones.

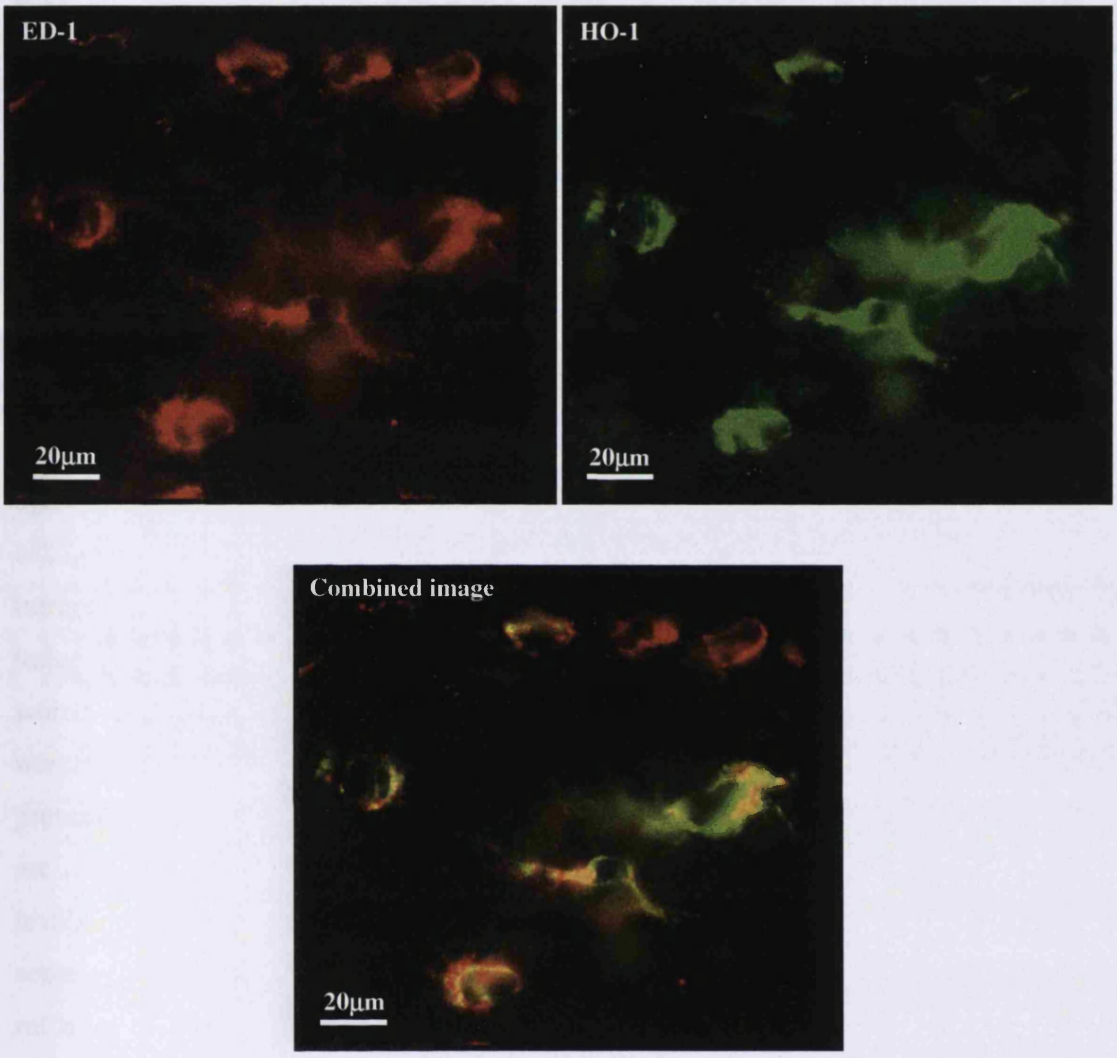

Figure 5.32 Immunofluorescence double labelling for HO-1 and the macrophage marker ED-1 in a CA-4-P-treated tumour. Images are from the same section as shown in Figures 5.30 and 5.31. Macrophage staining is shown in red (top left) and HO-1 staining is shown in green (top right). The bottom picture is the combined image of the two top ones showing that not all macrophages express HO-1.

5.4 Discussion

Effects of CA-4-P on HO in vitro

In the first part of this study the effects of the novel vascular targeting agent CA-4-P on the HO stress-induced enzyme system were investigated in tumour and endothelial cells (HUVECs) *in vitro*. The effects mediated by CA-4-P on the HO system were found to be

cell-type specific. At the early time point of 6h post-CA-4-P exposure, HO-1 protein levels were not affected in HUVECs but were decreased significantly in P22 tumour cells. A delayed increase in overall HO activity occurred in both cell types but was evident earlier and was much more pronounced in P22 tumour cells compared to HUVECs. The mechanism by which CA-4-P leads to a delayed HO-1 induction is currently unclear but could be related to a CA-4-P-induced imbalance in the redox state of cells. Indeed, NAC (the acetylated more stable form of the amino acid L-cysteine), a potent anti-oxidant, was shown to completely reverse the increase in HO-1 protein levels induced by CA-4-P treatment in P22 tumour cells. L-cysteine and NAC are the rate limiting precursors in the synthesis of glutathione, a major protector of biological structures and functions against oxidative stress. Therefore, our findings suggest that a decrease in the level of intracellular glutathione in response to CA-4-P treatment may be the stimulus for HO-1 induction in these cells. HO-1 has been shown to be induced in response to compounds which are either oxidants themselves or able to generate active intermediates or agents which are known to interfere with cellular glutathione levels (Applegate *et al.*, 1991). At present it is not clear whether the mechanisms by which CA-4-P causes HO-1 induction are related to oxidant species generation or to a direct interference of the drug with the levels of intracellular glutathione. There is evidence in the literature that stilbenes and some of their derivatives mediate HO-1 induction via glutathione depletion at least in the rat liver (Oguro *et al.*, 1996). Indeed, the authors of this study have demonstrated that stilbene oxides as well as the cis-stilbene parent compound mediate a significant decrease in glutathione content of rat liver following *in vivo* administration, with a concomitant significant increase in HO-1 mRNA. It is thought that these compounds can be conjugated with glutathione by the enzyme glutathione-*S*-transferase, with preferential conjugation towards the cis-isomer, thereby inducing prompt glutathione depletion (deSmidt *et al.*, 1987). CA-4-P is also a cis-stilbene derivative (Woods *et al.*, 1995) and at present no studies have examined whether this compound could affect intracellular glutathione content. The fact that CA-4-P mediated an increase in HO-1 protein levels and that this effect was blocked by the glutathione precursor NAC would support such a hypothesis. It would be interesting to measure intracellular glutathione content under our experimental conditions in order to test this possibility.

Despite the fact that NAC was effective at reversing the increase in HO-1 protein levels induced by CA-4-P, under these conditions, it only partially blocked the increase in overall HO enzyme activity. Therefore, CA-4-P-induced mechanisms, in addition to HO-1 protein induction, are implicated in the overall increase in HO enzyme activity observed. These mechanisms were shown to be independent from HO-2, with the protein levels remaining unchanged under the same experimental conditions. This suggests that the increase in activity is not due to changes in protein levels but may be related to direct enhancement of HO catalytic activity. Indeed, there is evidence in the literature that HO-2 activity can be directly stimulated by phosphorylation (Doré *et al*, 1999). The authors of this study demonstrated activation of HO-2 enzymatic activity by phosphorylation through the protein kinase-C pathway and concomitant neuroprotection against oxidative stress injury through bilirubin generation (Doré *et al.*, 1999). The signalling pathways which could be activated following CA-4-P treatment and which may lead to stimulation of HO enzymatic activity as well as induction in protein levels need elucidation. So far, there is evidence that CA-4-P is able to activate the stress protein kinase p38, for instance, at least in endothelial cells (Kanthou and Tozer, 2002). Furthermore, this stress activated kinase has been involved in the mechanism by which a number of compounds mediate induction of HO-1 (Elbirt *et al.*, 1998; Alam *et al.*, 2000; Chen and Maines, 2000). Investigations into this and other pathways in our systems would allow further elucidation of the complex processes, which follow CA-4-P treatment *in vitro* and perhaps also *in vivo*.

The fact that HUVECs did not significantly respond to CA-4-P exposure in terms of HO-1 induction as compared to P22 tumour cells could be related to their innate ability to cope with potential oxidant changes. Applegate and colleagues have suggested that the magnitude of the HO-1 inducible response is largely influenced by the intracellular redox state of cells (Applegate *et al.*, 1991). For instance, they found that primary epidermal keratinocytes demonstrated a lower HO-1 mRNA induction in response to sodium arsenite compared to fibroblasts isolated from the same biopsy, and this was correlated with a 2-3 fold higher glutathione levels in the former cell type compared to the latter (Applegate *et al.*, 1991). Therefore, it is possible that HUVECs are equipped with a better anti-oxidant arsenal of defence than P22 tumour cells, allowing them to deal adequately with potential oxidative changes with a minimal need for HO-1 induction, and therefore making them more resistant to CA-4-P treatment. This is an interesting hypothesis, which would

require further investigations into the levels of glutathione in HUVECs and P22 tumour cells before and following CA-4-P exposure, in order to determine whether such a correlation exists in our system. The differential effects of CA-4-P on HO-1 induction between tumour and endothelial cells could also be related to the differential effects of CA-4-P on the tubulin cytoskeleton. It was found that at 6 and 24h post-CA-4-P exposure, while P22 tumour cells still showed prominent tubulin cytoskeleton disruption, HUVECs appeared with a completely normal morphology (Figures 5.5 and 5.10). However, CA-4-P (1 μM) was previously shown to disrupt HUVECs microtubule cytoskeleton and alter their morphology when examined at early time points following a 30-minute exposure to the drug (Galbraith *et al.*, 2001; Kanthou and Tozer 2002). Therefore, it appears that CA-4-P can have more prolonged effects in tumour cells than in endothelial cells, which suggests that HUVECs may have better abilities to recover from tubulin disruption than do P22 tumour cells. There is evidence for this rapid recovery of the tubulin cytoskeleton in HUVECs following electroporation-mediated tubulin disruption (Dr Kanthou C., personal communication). These findings are also consistent with previous studies showing that recovery of HUVECs morphology following treatment with the same dose of CA-4-P as used in our studies (1 μM) occurred as early as 4h following a 30-minute exposure to the drug (Galbraith S.M. PhD thesis, 2001). The results also showed that CA-4-P significantly inhibited tumour cell proliferation, with the proliferation of HUVECs being less affected (Figures 5.4 and 5.9). These anti-proliferative effects are supported by the immunofluoresence data which show that microtubules in tumour cells do not completely reform until after 30h (Figure 5.5), whereas they are rapidly restored in HUVECs as early as 6h following the same treatment (Figure 5.10). The trypan blue assay showed that the tumour cells remain viable following exposure to CA-4-P but do not proliferate as long as the cytoskeleton is not restored, while untreated cells were able to proliferate normally when analysed at the same time points. For cell division to occur, mitotic spindles which are sensitive to tubulin binding agents, have to form appropriately so that the chromosomes can be correctly distributed into the daughter cells. If spindles fail to form then these cells will most likely not undergo a normal mitosis. Therefore, the anti-proliferative effect mediated by CA-4-P obtained here with P22 tumour cells is due to the inability of these cells to form spindles, since the cytoskeleton was affected for a long time. These results

therefore suggest a temporary cytostatic effect mediated by CA-4-P. These effects were not seen in HUVECs, which appeared with an intact cytoskeleton at the time points analysed following treatment and were shown to proliferate with no significant differences from control untreated cells. These findings further emphasise the fact that HUVECs appear to be more resistant than tumour cells to the effects of CA-4-P and this is most likely related to the differential in recovery from tubulin disruption. A recent study by Ahmed *et al.* supports the present findings showing that two human tumour cell lines, the LS174T colon carcinoma and the Hs578T breast carcinoma, were 20-30 times more sensitive to the anti-proliferative effects of CA-4-P than HUVECs (Ahmed *et al.*, 2003). However, these results are contradictory to early studies reporting the greater sensitivity of endothelial cells to CA-4-P compared to the MDA-MD-231 breast adenocarcinoma cells and fibroblasts in terms of cytotoxicity and cell proliferation (Dark *et al.*, 1997; Böhle *et al.*, 2000). These discrepancies may be due to the different cell types studied and perhaps also to the different methods used for assessment of cell viability/proliferation. With regard to the differences in sensitivity to the anti-proliferative effects of CA-4-P reported for various tumour cell lines, these may be explained on the basis of drug resistance. Indeed, there is increasing evidence supporting the concept that various alterations in microtubules may play an important role in confering tumour cells resistance to tubulin binding agents. Alterations leading to drug resistance have been associated with mutations in the β-tubulin subunit that can modify the binding of antimicrotubule drugs, changes in the expression of β-tubulin isotypes and/or microtubule associated proteins and also changes in the post-translational modifications of tubulin, which influence the stability of microtubules and their interactions with microtubule associated proteins (Drukman and Kavallaris, 2002). Despite the discrepancies outlined above, the present findings have important implications for understanding the mechanisms of action of CA-4-P and suggest that the response of tumour cells may be as important as that of endothelial cells. Further studies need to be conducted in order to clarify this issue, with particular attention paid to the response of microvascular endothelial cells, as opposed to HUVECs, and also by taking into consideration the potential effects of the tumour microenvironment.

The differential sensitivities of tumour and endothelial cells to CA-4-P described above may also account for the differences observed with regard to HO-1 induction, with the tumour cells showing a delayed recovery in the tubulin cytoskeleton and induction of HO-1, whereas the HUVECs showing more rapid recovery and no such significant HO-1 induction. It is possible that these different sensitivities translate into the activation of different signalling pathways, which may affect HO-1 induction. In P22 tumour cells, the decrease in HO activity and HO-1 protein levels at the earlier time point of 6h following exposure of P22 tumour cells to CA-4-P was found to correspond to the time when extensive damage to the tubulin cytoskeleton is also observed. At 24h, the HO enzyme activity and HO-1 protein levels normalise to control levels and this corresponds to partial recovery of the cells from the effects of the drug. This was then followed by an increase in HO-1 protein levels at 30 and 48h when complete recovery of cell morphology was seen. These findings showing delayed HO-1 induction suggest that an intact cell cytoskeleton may be required for HO-1 expression in P22 tumour cells and its disruption by CA-4-P may contribute to the impairment of the ability of these cells to produce HO-1 during the early times following the insult. Other studies support the idea that an intact cytoskeleton is critical for the expression of certain genes, for instance the induction of iNOS expression in response to inflammatory mediators (Marczin *et al.*, 1993; Marczin *et al.*, 1996). However, this is not always the case, with some studies showing that disruption of the cell cytoskeleton can lead to *induction* in the expression of some genes (Subbaramaiah *et al.*, 2000). The dependence of HO-1 production on an intact cytoskeleton could therefore explain the delayed response of the cells in terms of HO-1 induction up to 30 and 48h when cell morphology had recovered.

Although the functional significance of HO-1 protein induction following CA-4-P treatment in P22 tumour cells is lacking at present, a cytoprotective role of this enzyme is likely. This is in view of the extensive literature available on the role of HO-1 induction in cytoprotection against stress via the generation of bilirubin and CO, the products of haem degradation by HO-1 (see Chapter 1).

Effects of CA-4-P on tumour HO in vivo

In the second part of this study, we investigated the effects of CA-4-P on the HO system *in vivo* using the P22 tumour model. We found that a single dose of 30 mg/kg CA-4-P caused a decrease in overall tumour HO activity and HO-1 protein levels at 24 and 30h after treatment with recovery but no overall increase in levels thereafter. These results are difficult to interpret precisely because significant necrosis induction by this dose of CA-4-P (see Figure 6.4 in Chapter 6) would tend to mask any increased activity in the viable tumour fraction. However, there is a clear reduction in HO activity and HO-1 protein level at early times, which is consistent with the *in vitro* results. Immunohistochemical studies were carried out in an attempt to clarify the situation. Here, treatment with 30 mg/kg CA-4-P did not reveal any specific localisation of HO-1 positive staining (Table 5.1). However, we found that treatment with the clinically relevant dose of 10 mg/kg CA-4-P caused significant expression of HO-1 protein in 2 out of 4 treated tumours specifically localised to peri-necrotic areas. The fact that this effect was seen in only 2 out of 4 tumours analysed and not at all in the 30 mg/kg treatment group could relate to the relative insensitivity of the immunohistochemistry technique (see below under Methodology) and also to the great variability in the level of tissue damage and necrosis induced following CA-4-P treatment (see Figure 6.4 of Chapter 6).

Interestingly, further immunohistochemical analysis conducted to determine the nature of the HO-1 expressing cells in CA-4-P (10 mg/kg)-treated tumours revealed that macrophages infiltrating the tumours were the predominant cell type expressing the enzyme. Control untreated tumours were not necrotic and had only weak or absent macrophage staining, whereas treatment with CA-4-P led to macrophage recruitment to areas of focal necrosis, which in some areas also co-localised with HO-1 expression. It is likely that pro-inflammatory cytokines are released following vascular damage induced by CA-4-P to attract leukocytes to sites of tissue damage. Indeed, neutrophils have previously been shown to be recruited into tumours following CA-4-P treatment and to participate in the tissue damage mediated by this drug (Parkins *et al.*, 2000). Our findings that HO-1 expressing macrophages localise to peri-necrotic areas is consistent with previously reported studies showing prominent accumulation of HO-1 expressing macrophages/microglial cells in peri-necrotic areas of both experimental rat and human glioblastoma relapses (Deininger *et al.*, 2000). Nishie *et al.* have also shown that

infiltrating macrophages in human glioma samples were positively stained for HO-1, whereas tumour cells had only weak or no staining at all (Nishie *et al.*, 1999). At present, the role of these HO-1 expressing macrophages recruited following CA-4-P treatment is not clear. It is possible that they participate in tumour neovascularisation in these potentially avascular/hypoxic areas resulting from CA-4-P-induced vascular damage. In breast carcinoma samples, increased necrosis has been shown to be associated with higher levels of focal macrophage infiltration, with a high number of macrophages clustering around necrotic areas (Leek *et al.*, 1999). There is now substantial evidence implicating macrophages in angiogenesis because of their ability to secrete both pro-angiogenic cytokines and enzymes involved in the degradation of the extracellular matrix (Lewis *et al.*, 1995), and also because of a close correlation between tumour vascular density and macrophage infiltration (Leek *et al.*, 1996). Nishie *et al.* have also demonstrated a close correlation between HO-1 positive macrophages and vascular density (Nishie *et al.*, 1999). Furthermore, recent evidence points at a potential role of HO-1 in angiogenesis, with possible direct modulatory effects of HO-1 on the angiogenic process and also indirect roles via modulation of the expression of pro-angiogenic factors (see section 1.5.5.2 of Chapter 1). Since HO-1 has also been shown to have anti-apoptotic and anti-inflammatory properties (see sections 1.5.3.4 and 1.5.3.3 of Chapter 1), it is possible that expression of this enzyme by macrophages following CA-4-P may be cytoprotective and thereby contributing to recovery of the tissue. Alternatively, macrophages may be participating in tumour cell killing following CA-4-P via the generation of oxygen free radicals in a similar manner to neutrophils. In this case, their expression of HO-1 may only be a self-defence system to protect themselves against those reactive oxygen species. This possibility has been suggested by Ishii *et al.* who demonstrated induction of stress proteins, including HO-1, in macrophages following exposure to oxidative stress (Ishii *et al.*, 1999).

Effects of CA-4-P on normal tissue HO in vivo

With regard to the effects of CA4-P on normal tissues, the study examining the effects of 30 mg/kg on overall HO activity and HO-1 protein levels showed an increase in HO activity in the liver and the gut. At present the stimuli for HO-1 induction in these organs are still unknown. However for the gut, there is evidence that CA-4-P causes toxicity in this organ by inducing a type of inflammatory reaction (Tozer G.M., personal

communication). Therefore, it is possible to speculate that an increase in HO-1 could be a potential protective mechanism mounted by the cell in order to overcome the insult. For the liver, on the other hand, it is less surprising that it is the target by CA-4-P with regard to HO activation since it is the major detoxifying/metabolising organ in the body. It is very abundant in detoxifying enzymes, namely Phase 2 enzymes, which have been shown to be induced by xenobiotics and to be an effective way for protection against their possible toxic effects (Talalay, 2000). Since HO-1 has been shown to be induced by many compounds which also induce known detoxifying enzymes in the liver, it is now considered as an enzyme with important protective functions (Prestera *et al.*, 1995; Talaley, 2000). With regard to the mechanism by which CA-4-P could be inducing HO-1, there is evidence in the literature that stilbenes as well as some of their derivatives such as stilbene oxides mediate HO-1 induction in rat liver via glutathione depletion (Oguro *et al.*, 1996). As mentioned earlier, the authors of this study suggest that these compounds can be conjugated to glutathione by the enzyme glutathione-*S*-transferase thereby leading to a decrease in hepatic glutathione content. This situation would lead to an imbalance in the redox status of the cell causing the induction of HO-1 as a protective/antioxidant mechanism. Since CA-4-P is also a stilbene derivative, it is possible that similar events are occurring in the liver and the gut following *in vivo* administration of CA-4-P. This idea is supported by the *in vitro* experiments, whereby it was shown that NAC, a compound that replenishes glutathione stores, inhibits CA-4-P-mediated HO-1 induction. Although these *in vitro* experiments were carried out in P22 tumour cells, and *in vivo* these events have only been detected in the liver and gut but not in the P22 tumour, the results obtained could still explain the events occurring in the liver and the gut *in vivo*. With regard to the fact that none of the other normal tissues HO activity showed any changes following CA-4-P treatment, this could reflect possible differential sensitivities of tissues to the toxicity of the drug leading to differential induction of cytoprotective enzymes such as HO-1. Alternatively, differences in CA-4-P metabolic fate between different organs could account for this differential. The inducer of HO-1 in the liver and gut may not necessarily be the parent drug itself but possibly a metabolite of CA-4-P that is only generated in these two organs but in none of the other normal tissues. Pharmacokinetic studies have shown that the glucuronide is the major inactive metabolite detected in the plasma of human subjects following CA-4-P administration (Stratford M.R.L., unpublished data). However, lower levels of this metabolite have been measured

in the plasma of rats and mice and there is at least one other metabolite detected that remains unidentified (Stratford M.R.L., unpublished data).

Methodology

Determination of HO-1 localisation and protein levels in control P22 tumours revealed discrepancies between the results obtained with the immunohistochemical technique in this chapter and the ones obtained with the western blotting analysis reported in Chapter 3. The fact that no HO-1 positive staining was detected by immunohistochemistry in control P22 tumours, whilst western blotting revealed high levels of the HO-1 protein in these tumours (Figure 3.2 in Chapter 3) suggests the relative insensitivity of the immunohistochemistry technique. The latter could also account for the fact that HO-1 positive staining was only observed in a minority of CA-4-P-treated tumours, which presumably expressed the protein at high levels but, remained below the detection level in other tumours where the protein was expressed at lower levels. Furthermore, the inconsistency described above may also be related to the differences in sample processing for the two techniques making direct comparisons difficult. Indeed, unlike for the immunohistochemistry, sample preparation for western blotting involves protein denaturation, which may have facilitated the access and binding of the anti-HO-1 antibody to its target on the HO-1 protein, thereby giving a better signal.

5.5 Summary

The findings of this study clearly demonstrate the ability of CA-4-P to induce the expression of the stress protein HO-1 both *in vitro* and *in vivo*. HO-1 induction *in vitro* following CA-4-P treatment appears to be cell-type specific. This differential may be related to both the redox state of cells prior to CA-4-P exposure and also to the innate sensitivity of their tubulin cytoskeleton to disruption by CA-4-P, and perhaps most importantly to the ability of a particular cell type to recover from the initial drug insult. The functional significance of HO-1 induction and its potential cytoprotective effects following CA-4-P need to be further investigated. It was interesting to find that, *in vivo*, HO-1 induction was only seen in a minority of tumours and that the predominant cell type expressing the enzyme were macrophages rather than tumour cells. These results suggest the involvement of immune components in the vascular damage mediated by CA-4-P and

the potential for an anti-inflammatory role played by HO-1 induction. In addition, *in vitro* results with CA-4-P and hemin and *in vivo* results with hemin clearly showed that P22 tumour cells are capable of HO-1 induction. Therefore, it is possible that CA-4-P did induce HO-1 in P22 tumour cells *in vivo* but that the HO-1 levels remained below the detection level of the immunohistochemical assay. The relative insensitivity of the assay is demonstrated by negative staining of control tumours which had high enzyme activity and HO-1 protein levels as measured by the biochemical HO assay and western blotting, respectively. Experiments designed to test the therapeutic potential of CA-4-P-induced HO-1 induction are discussed in Chapter 6.

CHAPTER 6

EFFECTS OF MODIFYING HAEMOXYGENASE ACTIVITY ON TUMOUR GROWTH AND TREATMENT OUTCOME WITH COMBRETASTATIN A4-PHOSPHATE

6.1 Introduction

In vivo, CA-4-P has been shown to cause vascular collapse in a range of transplanted and spontaneous murine tumours as well as xenografted human tumours and vascularised metastases, at relatively non-toxic doses (Dark *et al.*, 1997; Horsman *et al.*, 1998; Chaplin *et al.*, 1999a; Tozer *et al.*, 1999; Malcontenti-Wilson *et al.*, 2001). Histological studies have shown typical induction of extensive haemorrhagic necrosis resulting from CA-4-P-mediated vascular damage with only a small rim of viable tumour remaining in the periphery (Dark *et al.*, 1997, Li *et al.*, 1998). This surviving population of cells actively participates in the re-population of the tumour, making treatment with CA-4-P a rather ineffective treatment when used as a single agent*. Therefore, several studies have examined the possibility of improving the therapeutic potential of CA-4-P by combination regimens with conventional radiotherapy and chemotherapy drugs or other novel therapeutics (see section 1.4.2 of Chapter 1).

The events that follow CA-4-P administration are likely to be complex involving several pathways, which could contribute to enhancing or diminishing the final treatment outcome (see Tozer *et al.*, 2002 for review). The stress-induced protein HO-1 has been reported to be over-expressed in human brain, prostate and renal cell carcinoma tumours as well as human gliomas and melanomas and human oesophageal squamous cell carcinomas (Hara *et al.*, 1996; Maines and Abrahamsson, 1996; Goodman *et al.*, 1997; Nishie *et al.*, 1999; Torisu-Itakura *et al.*, 2000; Yokoyama *et al.*, 2001). The results presented in Chapter 3 also show high resting levels of the HO isozymes in rodent and xenograft tumour models. The fact that administration of CA-4-P caused induction of tumour HO-1 protein levels both *in vitro* and *in vivo* suggests possible cytoprotective effects mediated by this enzyme against CA-4-P (see Chapter 5). Indeed, HO-1 has been shown to promote cell survival

* Greater efficacy of split versus single doses of CA-4-P have been recently demonstrated (Hill *et al.*, 2002).

and to act as an anti-apoptotic molecule during stress (see sections 1.5.3.4 and 1.5.4.3.3 of Chapter 1) and also to play a modulatory role during inflammation (see sections 1.5.3.3 and 1.5.4.3.2 of Chapter 1). Furthermore, there is now evidence implicating HO-1 in the process of angiogenesis (see section 1.5.5.2 of Chapter 1) suggesting the potential importance of this enzyme system in cancer.

In this chapter, the effects of the HO inhibitor SnPP on cell proliferation *in vitro* and tumour growth *in vivo* are reported. Furthermore, the potential of increasing the anti-tumour effects of CA-4-P by combination regimens with SnPP in two rodent tumour models was investigated.

6.2 Materials and Methods

6.2.1 Drug Solutions

sodium carbonate (Na_2CO_3; 50 mM) as drug vehicle

See section 5.2.1 (Chapter 5)

SnPP (1 mM stock for *in vitro* experiments)

1.87 mg SnPP (Affiniti Research Products)

5 ml Na_2CO_3

Prepare fresh before experiment and shield from light during preparation and use.

SnPP for *in vivo* experiments

Dissolved in Na_2CO_3.

Shield from light during preparation and injection into the animal.

CuPP for *in vivo* experiments

Dissolved in Na_2CO_3.

Shield from light during preparation and injection into the animal.

CA-4-P for *in vivo* experiments

Dissolved in Na_2CO_3.

6.2.2 Experimental Protocol

Initial experiments were conducted to examine the inhibitory effects of SnPP on HO enzyme activity both *in vitro* and *in vivo*. *In vitro*, SnPP was used at 1 and 10 μM final concentrations in the media. These concentrations were chosen in accordance with studies reporting that concentrations of <10 μM should be used *in vitro* to ensure reasonable selective HO inhibition without inhibition of either NOS or sGC activities (Zakhary *et al.*, 1996; Sammut *et al.*, 1998; Appleton *et al.*, 1999). *In vivo*, SnPP was administered at a dose of 45 μmol/kg ip, according to previous HO enzyme activity inhibition studies (see results in Chapter 4). This time-course of HO enzyme activity inhibition by SnPP was assessed up to 24h post-treatment. The effects of SnPP on cell proliferation *in vitro* and tumour growth *in vivo* were then examined.

Further experiments were conducted in order to investigate the effects of combining CA-4-P with the HO inhibitor, SnPP, on necrosis and tumour growth *in vivo*. The induction of haemorrhagic necrosis is a characteristic hallmark of vascular targeting agents that results from drug-induced vascular damage and collapse. It is therefore generally used as an end-point to assess the effectiveness of vascular targeting agents.

6.2.3 In Vitro and In Vivo Assessment of HO Inhibition by SnPP

In vitro, SnPP-mediated HO activity inhibition was assessed in confluent cultures of P22 tumour cells and HUVECs. Cells were collected in PBS, containing a cocktail of protease inhibitors following 24 or 48h incubations with 1 or 10 μM SnPP. Cell samples were centrifuged at 1000 rpm at 4°C for 5 minutes and the cell pellet re-suspended in PBS-$MgCl_2$. Sample preparation for HO activity analysis was carried out as described in section 5.2.2 of Chapter 5.

In vivo, a time-course experiment on SnPP-mediated HO activity inhibition was conducted in order to extend the time period previously investigated (see Figure 4.7 in Chapter 4). Rats were treated with SnPP at a dose of 45 μmol/kg ip and the tumours were excised at 1, 3, 6 or 24h post-treatment. Microsomes were prepared from tissues and analysed for HO enzyme activity as described in Chapter 2 (sections 2.4 and 2.5).

6.2.4 In Vitro Assessment of Cell Proliferation

Equal numbers of cells (2×10^4 P22 and 3×10^4 HUVECs), determined using haemocytometer counting, were plated into 60 mm tissue culture dishes. Cells were allowed to settle for 24h prior to incubation with SnPP (1 or 10 μM) for 24 or 48h. At the end of the incubation period, the medium was collected and centrifuged at 1000 rpm for 5 minutes. The remaining attached cells were treated with trypsin-EDTA and collected in warm media. An aliquot containing the floating and attached cells from each plate was then taken and the number of cells counted using a haemocytometer. Triplicate plates were used for each time point.

6.2.5 Assessment of Tumour Necrosis

The effects of HO activity inhibition by SnPP in combination with CA-4-P on necrosis induction were examined in the P22 rat tumour. SnPP (45 μmol/kg) was administered 15 minutes prior to CA-4-P (10 or 30 mg/kg). The effects of combining CuPP (45 μmol/kg) and CA-4-P (10 mg/kg) on necrosis induction were also examined following the same dosing regimen. Histological assessment of necrosis was performed on tumour sections stained with hematoxylin and eosin. Tumours were excised 24h post-treatment and immediately fixed in 10% formalin solution (Sigma) and processed for paraffin wax embedding, cutting and hematoxylin and eosin staining by the histology department (Gray Cancer Institute). Using a grid eyepiece graticule marked in 100 squares, each section from the centre of the tumour was assessed under the light microscope using the x10 objective (Hill *et al.*, 1992). Each square of the 100 was scored as viable or necrotic and this was repeated through the whole section (Hill *et al.*, 1992). Necrosis was then calculated as a percentage of the whole tumour section area.

6.2.6 In Vivo Assessment of Tumour Growth

The P22 rat carcinosarcoma and CaNT mouse mammary carcinoma tumours were implanted subcutaneously as described in Chapter 2 (sections 2.2.1 and 2.2.2). When the desired tumour size was reached (~ 6 mm for the mouse CaNT tumour; ~ 11 mm for the rat P22 tumour), the animals were treated according to the protocol shown in Table 6.1. The three orthogonal tumour diameters were measured by use of a calliper every 2 to 3 days and the animals' weights were monitored as an assessment of toxicity.

Groups	Rats Treatment Regimen on Days 0 and 3	Mice Treatment Regimen on Days 0 and 3
- Control	- no treatment	- no treatment
- SnPP alone	- 45 μmol/kg	- 90 μmol/kg
- CuPP alone	- 45 μmol/kg	- 90 μmol/kg
- CA-4-P alone	- 10 or 30 mg/kg	- 25 or 100 mg/kg
- SnPP + CA-4-P	- 45 μmol/kg SnPP + either 10 or 30 mg/kg CA-4-P	- 90 μmol/kg SnPP + either 25 or 100 mg/kg CA-4-P
- CuPP + CA-4-P	- 45 μmol/kg CuPP + either 10 or 30 mg/kg CA-4-P	- 90 μmol/kg CuPP + either 25 or 100 mg/kg CA-4-P

Note: All drugs were administered ip and SnPP or CuPP were injected 15 minutes prior to CA-4-P administration.

Table 6.1 Experimental protocol for tumour growth delay experiments in P22 rat carcinosarcoma and mouse CaNT mammary carcinoma tumours.

6.2.7 Data Analysis

In vivo tumour growth curves were plotted using tumour volumes. Tumour volume was calculated by use of the formula:

$$V=(\pi \times d_1 \times d_2 \times d_3)/6$$

V: volume

d_1,d_2 and d_3: are the measured three orthogonal diameters of the tumour.

The tumour volumes for each animal were normalised to the mean volume on treatment day 0 using the following formula:

$$Vn=(\overline{V_0}/mV_0) \times mV_{0,1,2,3,....}$$

Vn: normalised volume

$\overline{V_0}$: mean volume on day 0 across the treatment groups

mV_0: measured volume on day 0 for individual animals

$mV_{0,1,2,3,....}$: measured volume for individual animals from day 0 onwards

6.2.8 Statistics

Statistical analysis was applied as described in Chapter 2 (section 2.12). For non-parametric data, significance tests were carried out on the data groups using the Kruskal-Wallis one-way ANOVA test followed by a comparison between the specific groups using the Wilcoxon test. Values of $p<0.05$ were considered significant.

6.3 Results

6.3.1 Effects of HO Inhibition on Tumour Growth

6.3.1.1 Effects of HO Inhibitors on Cell Proliferation In Vitro

Continuous incubation of cells with the HO inhibitor SnPP at 1 and 10 μM concentrations showed no effects on proliferation of P22 tumour cells (Figure 6.1A). This is in contrast to HUVECs, where SnPP mediated a modest but significant dose-dependent decrease in proliferation with a 16 and 23% decrease in cell number compared to control on day 2 with 1 and 10 μM SnPP, respectively (Figure 6.1B). Under these conditions SnPP inhibited HO enzyme activity in both cell types as shown in Table 6.2, with some indication that on day 2 SnPP was more effective at inhibiting HO activity in P22 tumour cells than in HUVECs.

Cell Type	% HO Activity Inhibition on Day 1		% HO Activity Inhibition on Day 2	
	SnPP 1μM	SnPP 10μM	SnPP 1μM	SnPP 10μM
P22 Tumour Cells	94.50±2.37	99.94±0.06	100	100
HUVECs	81.86±18.14	100	98.23±1.76	69.53±14.11

Table 6.2 SnPP-mediated HO activity inhibition *in vitro*. Confluent cultures of P22 tumour cells or HUVECs were exposed continuously to SnPP 1 or 10 μM. HO enzyme activity was determined on day 1 or 2 of treatment. Triplicate plates were used for each treatment and time point. Values are means of the triplicates ± 1 standard error of the mean and expressed as % enzyme activity inhibition relative to the respective control levels.

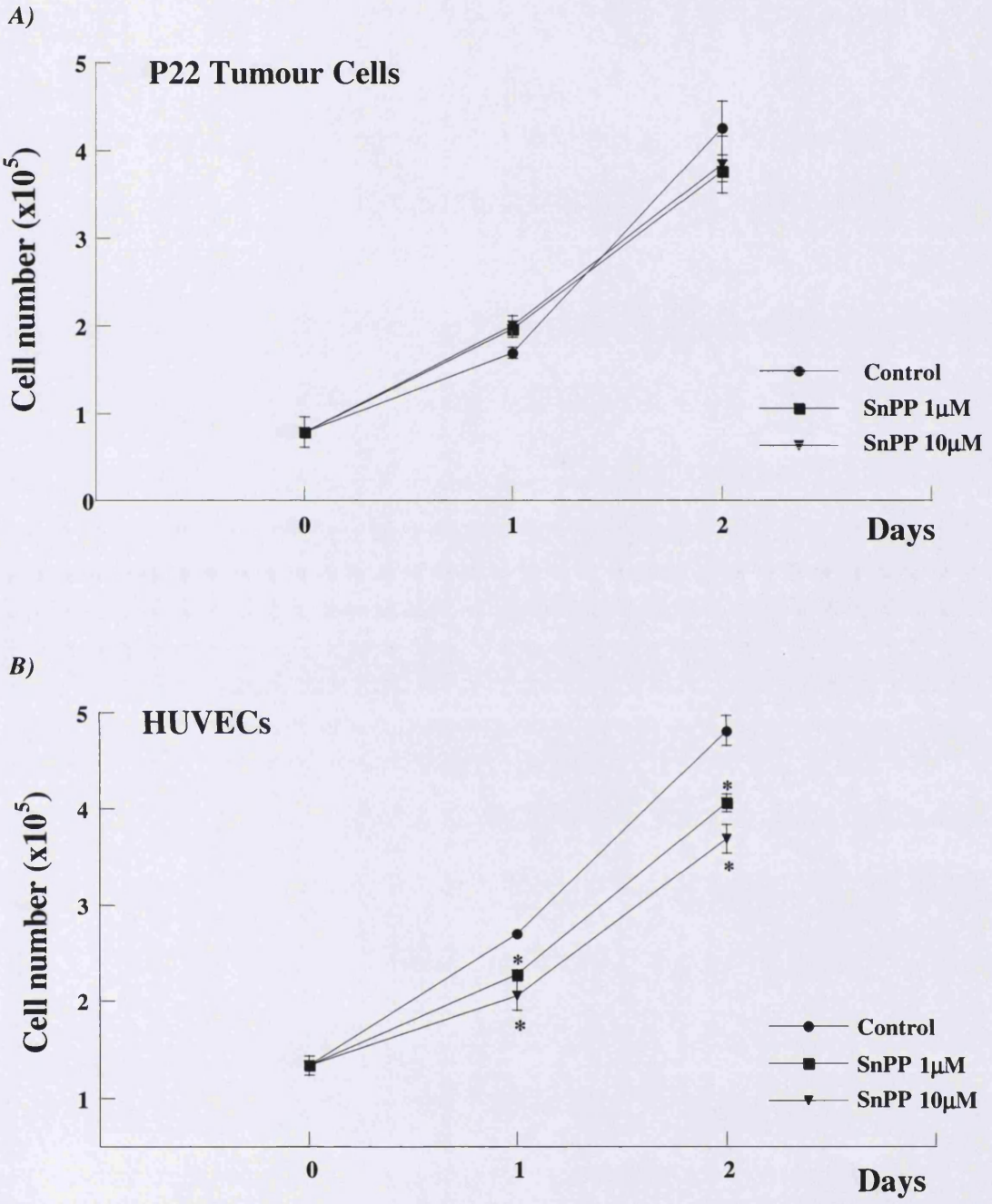

Figure 6.1 Effects of SnPP-mediated HO inhibition on cell proliferation *in vitro*. P22 tumour cells (A) or HUVECs (B) were exposed continuously to SnPP 1 or 10 μM. Cell number was determined by haemocytometer counting at 0, 1 and 2 days of cell harvest. Triplicate plates were used for each treatment and time point. The data are means of the triplicate values and error bars are ± 1 standard error of the mean. * represents a significant difference from control ($p<0.05$).

6.3.1.2 Effects of SnPP on Tumour HO Enzyme Activity and Growth In Vivo

As shown in Table 6.3 a single injection of SnPP at a dose of 45 μmol/kg caused prolonged HO enzyme activity inhibition for up to 24h post-treatment with the enzyme activity still inhibited by 96.47% at this time point.

Examining the effects of SnPP on tumour growth revealed that administration of SnPP (45 μmol/kg) on days 0 and 3 of treatment caused a small delay in tumour growth of ~ 1.5 days when comparing the treated tumour on day 6 with the untreated control of the same size (Figure 6.2). Administration of an equivalent dose CuPP, which was shown in Chapter 4 not to inhibit HO enzyme activity (see Figure 4.7), caused a similar delay in tumour growth as SnPP (Figure 6.2). On the other hand, the drug vehicle had no significant effect on tumour growth (Figure 6.2). Both SnPP and CuPP had very little effects on the animals' weights. CuPP caused a maximum weight loss of ~ 1.67% following the second dose on day 4, while, SnPP induced ~ 0.70% weight loss on day 1 (Figure 6.3). The drug vehicle on its own induced ~ 0.57% weight loss on day 1 (Figure 6.3).

Time Post-Treatment (h)	**1**	**3**	**6**	**24**
% HO Activity Inhibition	99.90±0.09	99.06±0.41	99.58±0.11	96.47±0.60

Table 6.3 SnPP-mediated HO activity inhibition *in vivo*. Animals were administered SnPP at a dose of 45 μmol/kg ip. Tumours were excised at 1, 3, 6 or 24h post-treatment for HO activity determination. The % HO activity inhibition was calculated from the respective controls at each time point. The values are the means 3 animals per group ± 1 standard error of the mean.

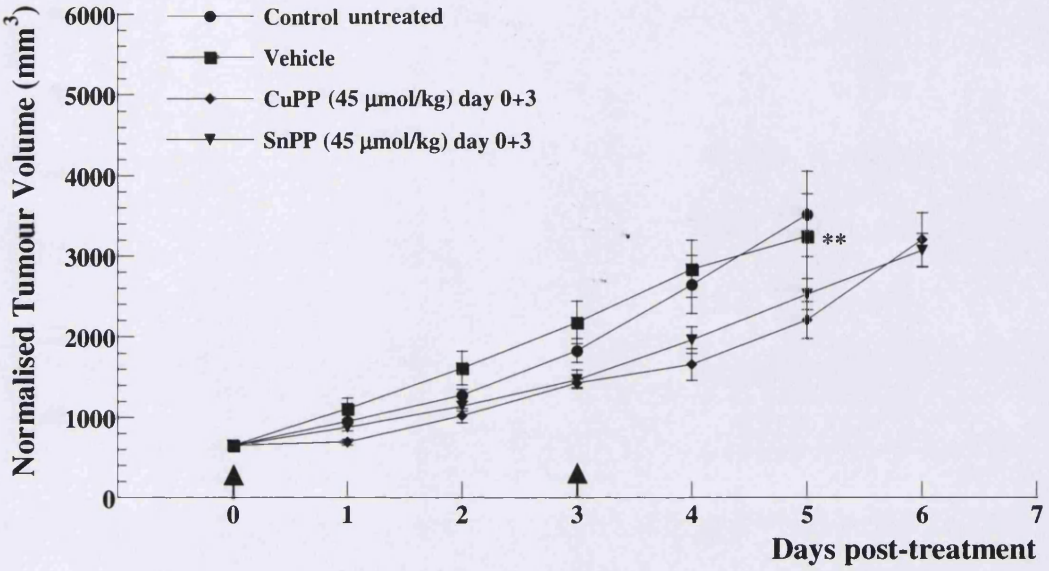

Figure 6.2 Effects of SnPP and CuPP on P22 tumour growth. SnPP (45 µmol/kg ip) or CuPP (45 µmol/kg ip) were administered on days 0 and 3. Arrows indicate treatment days. The data are means of 5-7 animals per group. Error bars are ± 1 standard error of the mean. ** 4 animals instead of 6. Early loss of animals was due to ulceration of tumours.

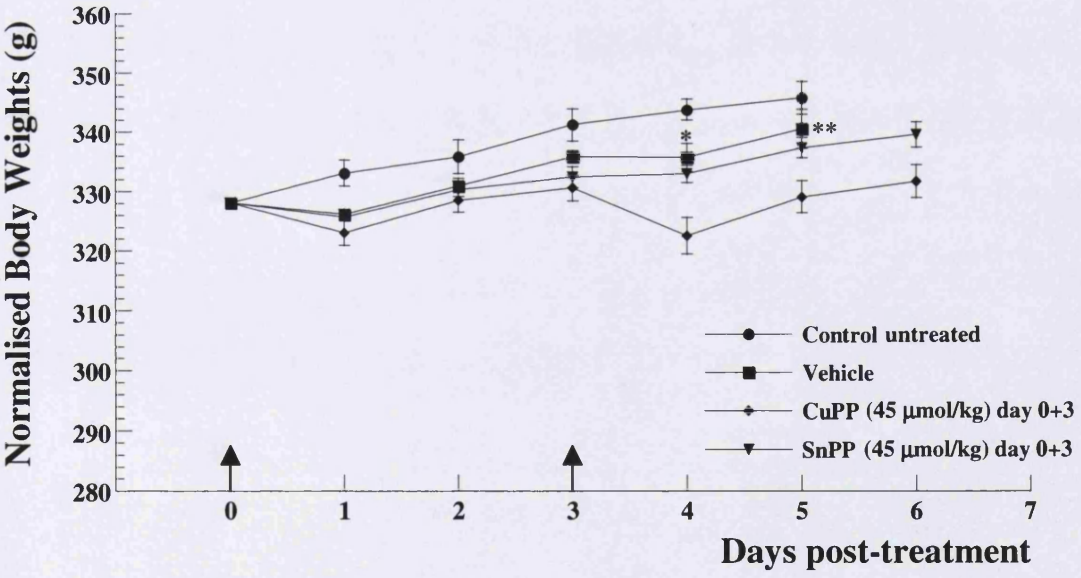

Figure 6.3 Effects of SnPP and CuPP on animals' weights. SnPP (45 µmol/kg ip) or CuPP (45 µmol/kg ip) were administered on days 0 and 3. The data are means of the same group of animals shown in Figure 6.2. Error bars are ± 1 standard error of the mean. * 5 animals instead of 6. ** 4 animals instead of 6. Arrows indicate treatment days. Loss of animals was due to either ulceration of the tumours or increased tumour burden.

6.3.2 Effects of HO Inhibition on CA-4-P-Mediated Necrosis

Figure 6.4 shows that no necrosis was present in either untreated control P22 tumours, SnPP or CuPP treated tumours. On the other hand, treatment with CA-4-P (10 mg/kg) showed a great variability in the level of necrosis induced ranging from 0 to 26.4% (Figure 6.4). This variability did not improve with the higher dose of CA-4-P (30 mg/kg) with the level of necrosis induced ranging from 0 to 73.4% (Figure 6.4). Combinations of SnPP with 10 and 30 mg/kg CA-4-P showed no improvement in the variability as compared to CA-4-P treatment alone, clearly indicative that the numbers of animals were insufficient to draw any definitive conclusions. However, combination of CuPP with CA-4-P 10 mg/kg did give an indication of enhancement of necrosis level compared to CA-4-P treatment alone, which was statistically significant with the Wilcoxon test for non-parametric data ($p<0.02$) (Figure 6.4).

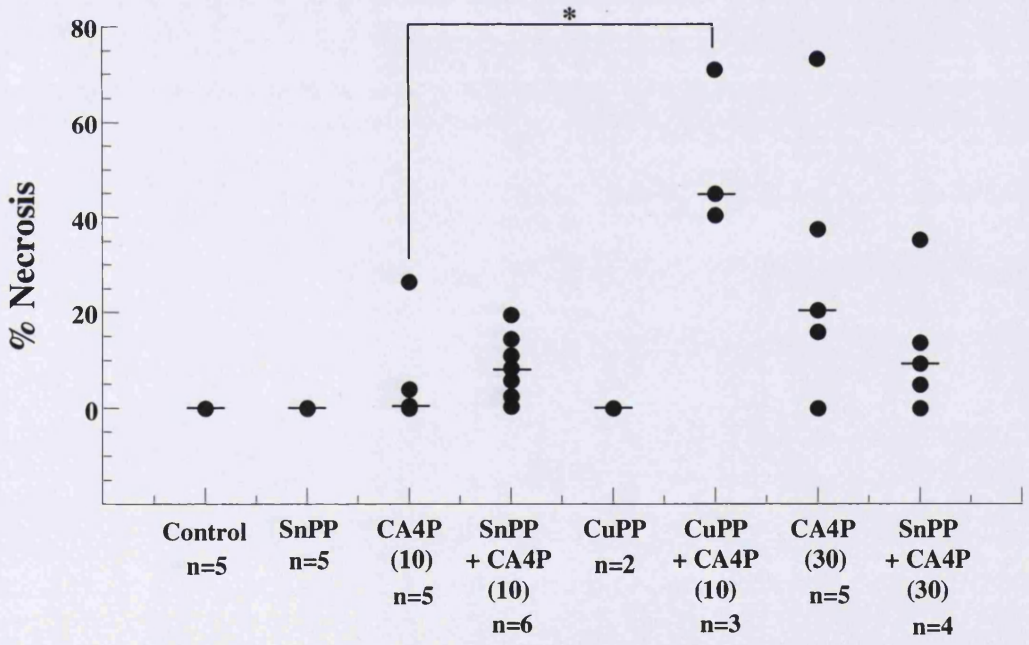

Figure 6.4 Effects of SnPP and CuPP alone or in combination with CA-4-P on tumour necrosis. SnPP or CuPP were injected at a dose of 45 µmol/kg 15 minutes prior to CA-4-P administration (10 or 30 mg/kg). Tumours were excised at 24h post-treatment. The graph shows the % necrosis scored for 1 section per tumour. Each point represents an individual tumour. * is statistically significant with the Wilcoxon test for non-parametric data ($p<0.02$). ⊸ median.

6.3.3 Effects of Combination Therapy with HO Inhibitors and Combretastatin A4-Phosphate on Tumour Growth

6.3.3.1 In the Rat P22 Carcinosarcoma Model

In this study, only untreated animals were used as control since the drug vehicle was shown in the previous study to have no significant effects on tumour growth (Figure 6.2). Similarly to the results presented in Figure 6.2, administration of SnPP at a dose of 45 μmol/kg ip on days 0 and 3 induced a small growth delay of ~ 1.5 days when comparing the treated tumour on day 8 with the untreated control of the same size (Figure 6.5A).

Treatment with CA-4-P at a dose of 10 mg/kg ip also given on days 0 and 3 caused a greater retardation in tumour growth of ~ 2.5 days when comparing the treated tumour on day 8 with the untreated control of the same size (Figure 6.5A). Combining SnPP and CA-4-P treatments did not enhance the effects on P22 tumour growth of either compounds alone (Figure 6.5A). SnPP administration did not significantly affect the animals' ability to gain weight as compared to controls (Figure 6.6A). On the other hand, CA-4-P (10 mg/kg) caused a maximum weight loss of 5.56% on day 4 as compared to day 0, with recovery following on subsequent days (Figure 6.6A). The combination SnPP and CA-4-P did not worsen the effects of CA-4-P on the animals' weights, inducing a maximum weight loss of 4.3% on day 5 as compared to day 0 (Figure 6.6A). The animals recovered on subsequent days (Figure 6.6A).

The higher dose of CA-4-P, 30 mg/kg given on days 0 and 3, was more effective than 2x10 mg/kg inducing around 6 days tumour growth delay when comparing the treated tumour on day 14 with the untreated control of the same size (Figure 6.5B). The maximum weight loss at this dose of CA-4-P was ~ 12.84% on day 4 as compared to day 0 (Figure 6.6B). The combination with SnPP further retarded tumour growth by ~ 2 days as compared to CA-4-P alone without any increased toxicity (maximum weight loss of 10.71% on day 4) (Figure 6.6B). Animals' weights in both the CA-4-P and SnPP+CA-4-P groups started to recover from day 5 returning to their initial weight on day 14 (Figure 6.6B).

The effects of CA-4-P in combination with CuPP on tumour growth in the P22 tumour are shown in Figure 6.7. Similarly to the results presented in Figure 6.2, administration of

CuPP at a dose of 45 μmol/kg ip on days 0 and 3 induced a small growth delay of ~1.5 day when comparing the untreated tumour on day 8 with the untreated control of the same size (Figure 6.7A). Combination with CA-4-P 2x10 mg/kg or 2x30 mg/kg did not enhance the anti-tumour effects mediated by CA-4-P alone (Figure 6.7A, B). CuPP, unlike SnPP, caused a minor retardation of rat weight gain (comparison of Figures 6.8A and 6.6A). However, combination of CuPP with CA-4-P at 2x10 mg/kg or 2x30 mg/kg did not increase the weight loss obtained with CA-4-P alone (Figures 6.8A, B). For the higher CA-4-P dose, the combination appeared less toxic (Figure 6.8B).

Note: Results for SnPP and CuPP are separated in Figures 6.5 to 6.8 for clarity. However, data shown in Panel A of Figure 6.5 to 6.8 form a single experiment, those in Panel B form a separate experiment. Therefore, data for Control and CA-4-P alone in Figures 6.5 and 6.6 are repeated in Figures 6.7 and 6.8.

A)

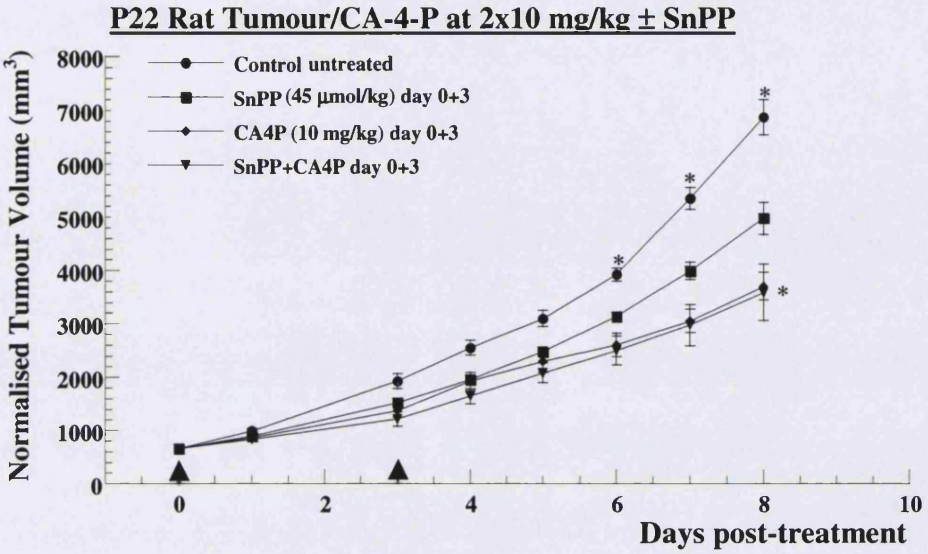

B)

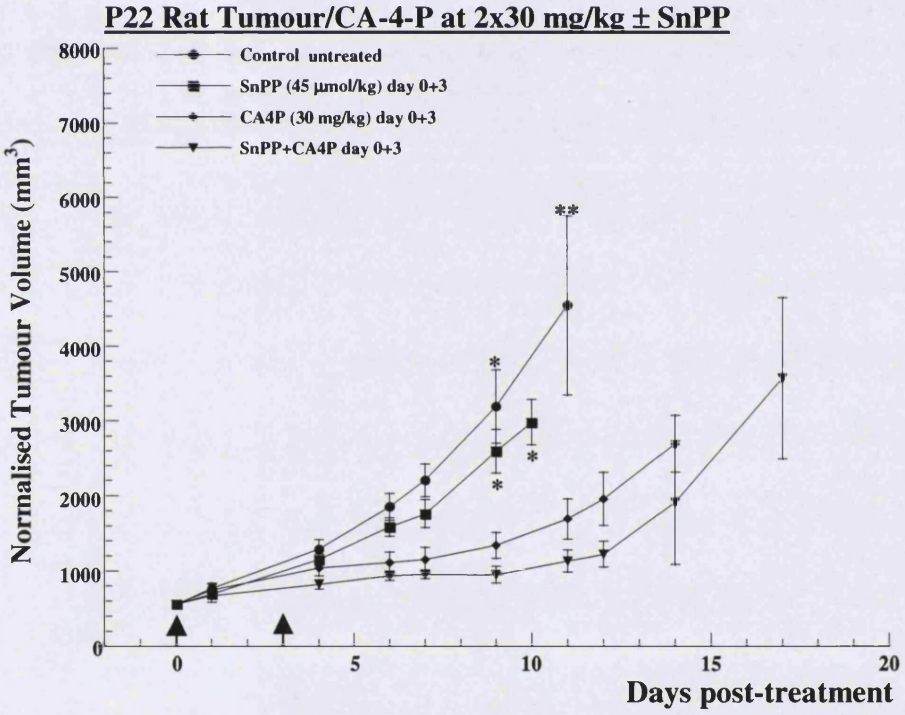

Figure 6.5 Effects of combination therapy with SnPP and CA-4-P on P22 tumour growth. ***A)*** SnPP (45 µmol/kg ip) was administered 15 minutes prior to CA-4-P 10 mg/kg ip. The data are means of 6 animals per group (* 5 animals). ***B)*** SnPP (45 µmol/kg ip) was administered 15 minutes prior to CA-4-P 30 mg/kg ip. The data are means of 5 animals per group (* 4 animals; ** 3 animals). Error bars are ± 1 standard error of the mean. ***A*** and ***B*** are independent experiments. Arrows indicate treatment days. Early loss of animals was due to ulceration of the tumours.

A)

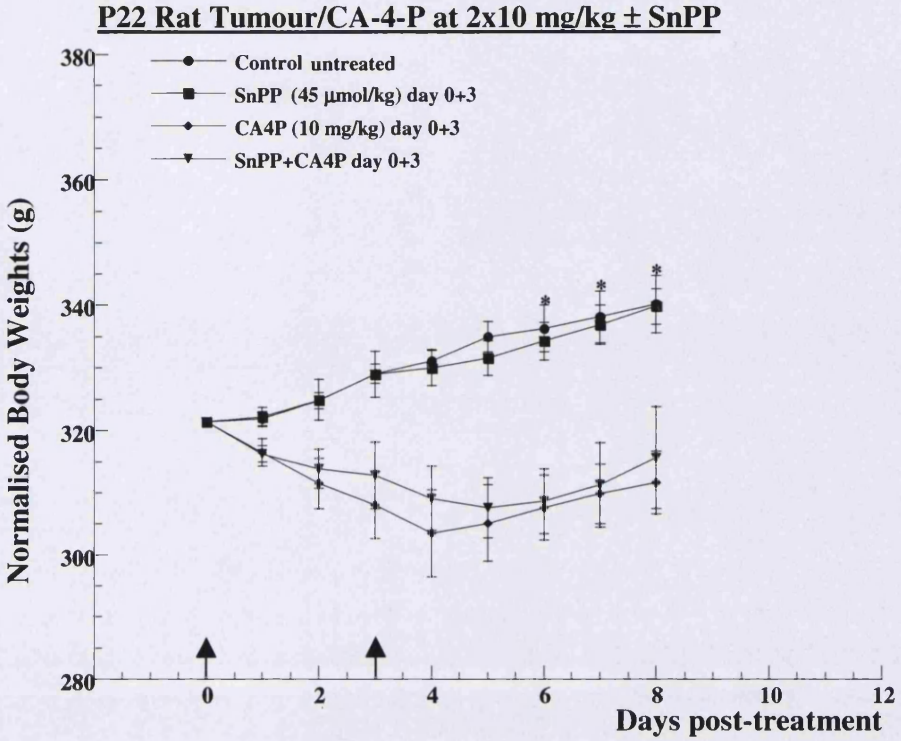

B)

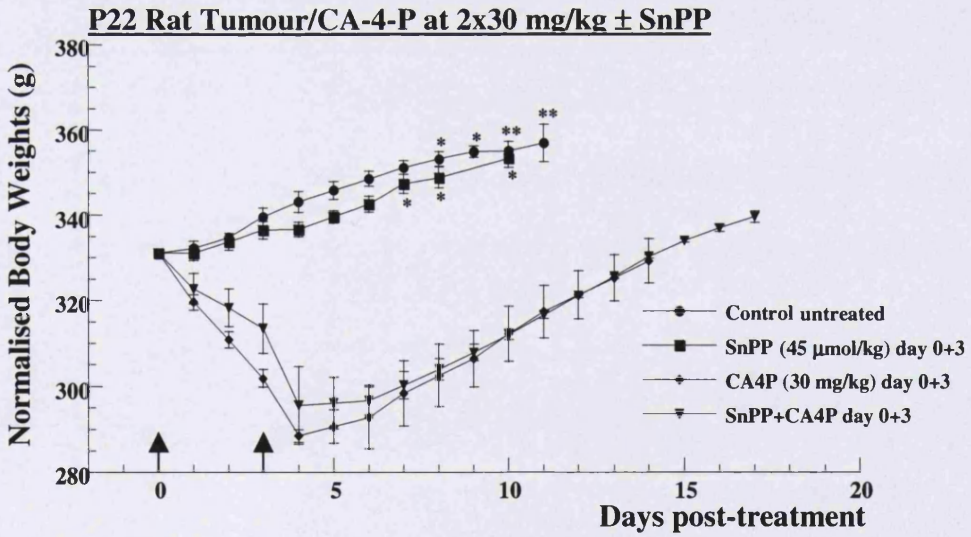

Figure 6.6 Effects of combination therapy with SnPP and CA-4-P on animals' weights. ***A)*** SnPP (45 µmol/kg ip) was administered 15 minutes prior to CA-4-P 10 mg/kg ip. The data are means of the same group of 6 animals as shown in Figure 6.5A (* 5 animals). ***B)*** SnPP (45 µmol/kg ip) was administered 15 minutes prior to CA-4-P 30 mg/kg ip. The data are means of the same group of 5 animals as shown on Figure 6.5B (* 4 animals; ** 3 animals). Error bars are ± 1 standard error of the mean. ***A*** and ***B*** are independent experiments. Arrows indicate treatment days.

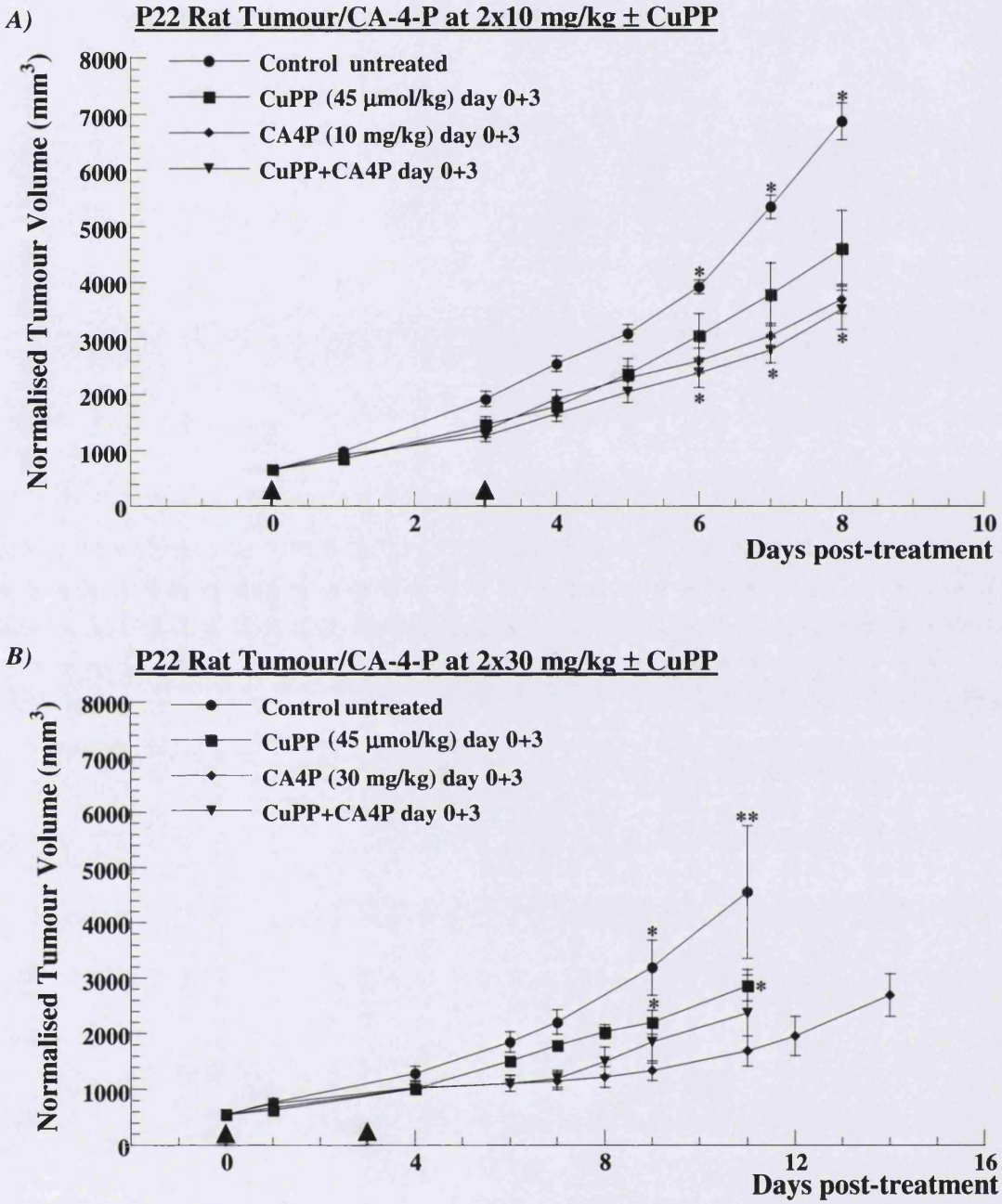

Figure 6.7 Effects of combination therapy with CuPP and CA-4-P on P22 tumour growth. ***A)*** CuPP (45 µmol/kg ip) was administered 15 minutes prior to CA-4-P 10 mg/kg ip. The data are means of 6 animals per group (* 5 animals instead of 6). ***B)*** CuPP (45 µmol/kg ip) was administered 15 minutes prior to CA-4-P 30 mg/kg ip. The data are means of 5 animals per group (* 4 animals instead of 5; ** 3 animals instead of 5). Error bars are ± 1 standard error of the mean. ***A*** and ***B*** are independent experiments. Arrows indicate treatment days. Early loss of animals was due to ulceration of tumours.

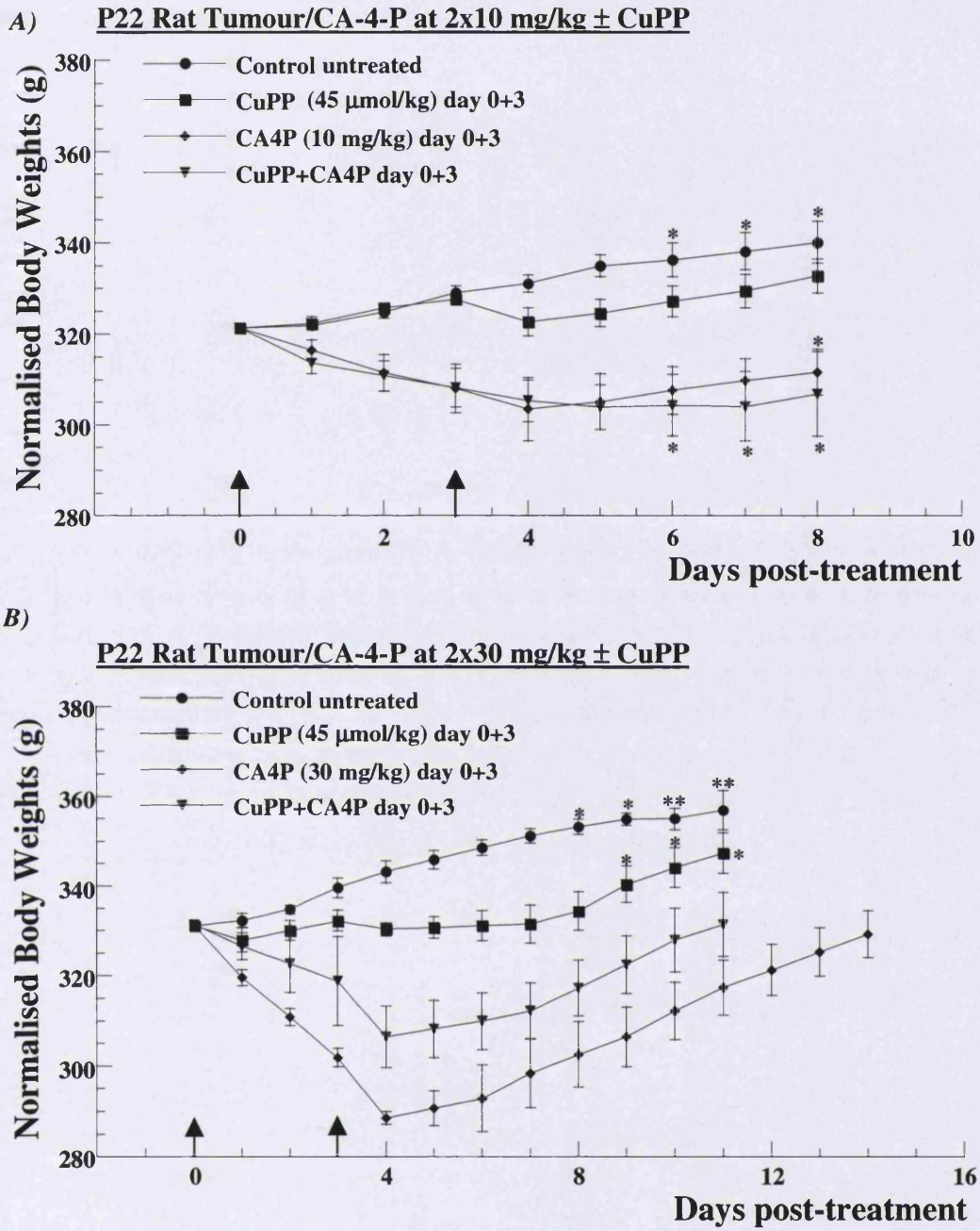

Figure 6.8 Effects of combination therapy with CuPP and CA-4-P on animal's weights. ***A)*** CuPP (45 µmol/kg ip) was administered 15 minutes prior to CA-4-P 10 mg/kg ip. The data are means of the same group of animals as shown in Figure 6.7A (* 5 animals instead of 6). ***B)*** CuPP (45 µmol/kg ip) was administered 15 minutes prior to CA-4-P 30 mg/kg ip. The data are means of the same group of animal as shown in Figure 6.7B (* 4 animals instead of 5; ** 3 animals instead of 5). Error bars are ± 1 standard error of the mean. ***A*** and ***B*** are independent experiments. Arrows indicate treatment days.

6.3.3.2 In the Mouse CaNT Mammary Carcinoma Model

The same experimental protocol and dosing regimen used in the P22 tumour growth delay experiments were carried out using the CaNT mouse mammary carcinoma tumour model. A roughly equivalent dose of SnPP in the mouse of 90 μmol/kg given on days 0 and 3 did not affect tumour growth, which is in contrast to the results obtained in the rat where SnPP caused a small growth delay (Figures 6.5 and 6.9). Similarly to the rat, administration of CA-4-P at 2x25 mg/kg mediated a significant tumour growth delay of ~ 2 days (Figure 6.9A). An enhancement in the anti-tumour effects of CA-4-P were only seen when SnPP was combined with the higher dose of CA-4-P (2x100 mg/kg) where a further 2 days retardation in tumour growth was observed (Figure 6.9B). Figures 6.10A and 6.10B show that in contrast to the rat there are no significant changes in the mice weights throughout the treatment period.

In contrast to SnPP, CuPP administered at a dose of 90 μmol/kg on days 0 and 3 induced ~ 2 days tumour growth delay similar to CA-4-P 2x25 mg/kg (Figure 6.11A). Furthermore, enhancement in the anti-tumour effects of CA-4-P was seen when combining CuPP with both the low and high doses of CA-4-P (2x25 and 2x100 mg/kg) (Figure 6.11A, B). No significant effects on the animals' weights were observed throughout the treatment (Figure 6.12). Weights of control animals are not shown here but are known to be stable in control untreated mature mice (Hill S.A., personal communication).

Note: Data shown in Figures 6.9 to 6.12 form a single experiment.

A)

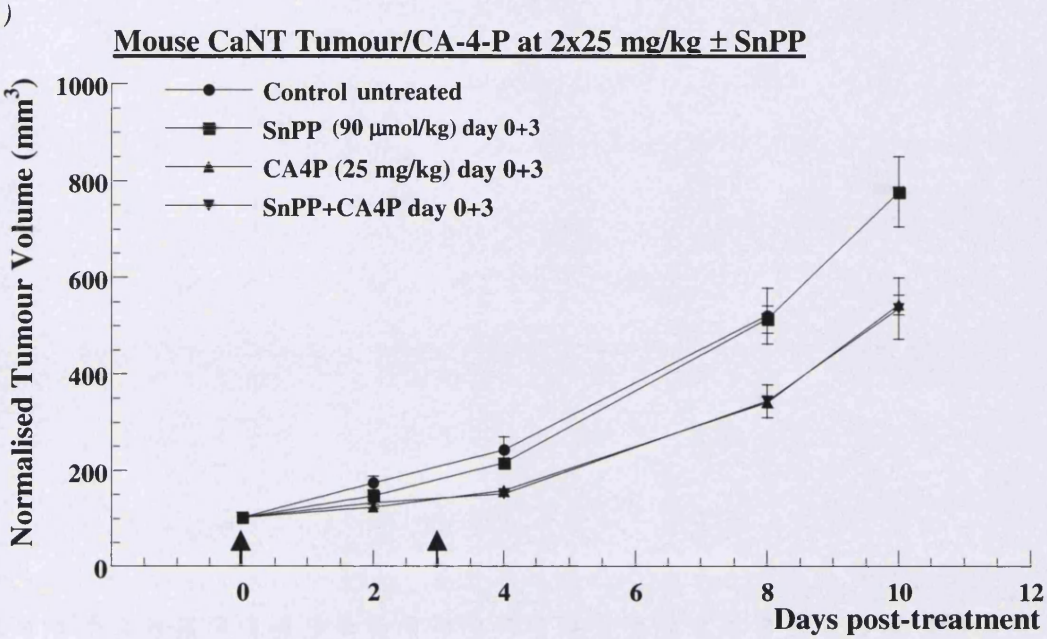

B)

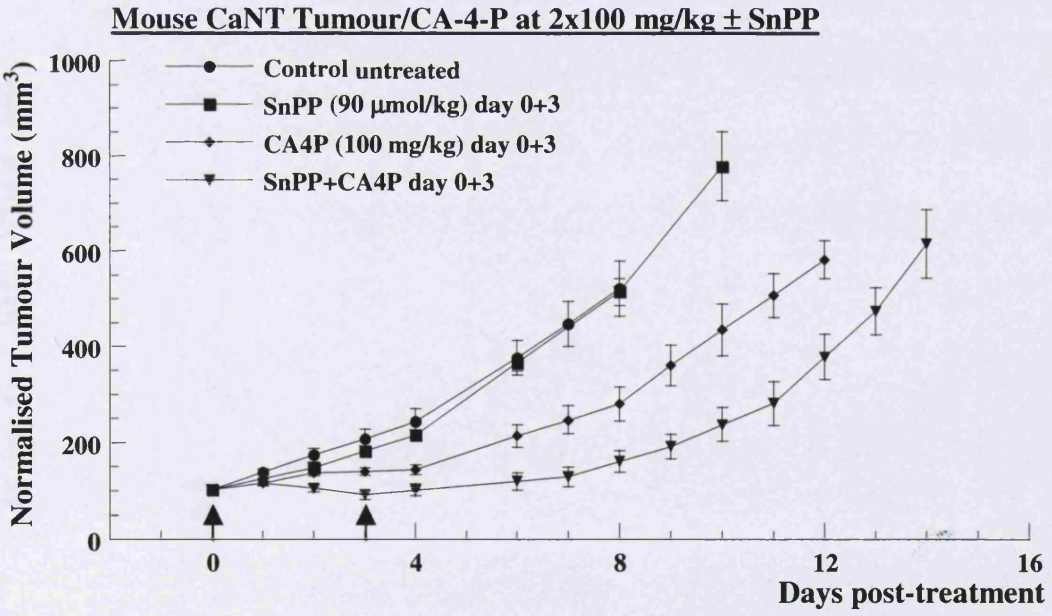

Figure 6.9 Effects of combination therapy with SnPP and CA-4-P on CaNT tumour growth. ***A)*** SnPP (90 µmol/kg ip) was administered 15 minutes prior to CA-4-P 25 mg/kg ip. ***B)*** SnPP (90 µmol/kg ip) was administered 15 minutes prior to CA-4-P 100 mg/kg ip. In ***A)*** and ***B)*** the data are means of 5 animals per group. Error bars are ± 1 standard error of the mean. Arrows indicate treatment days.

A)

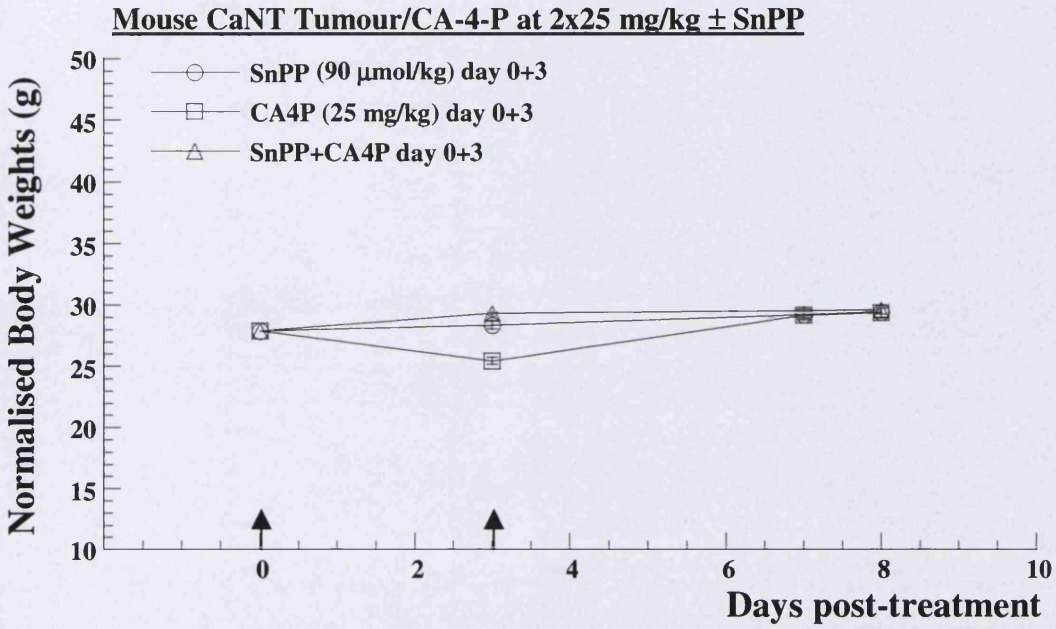

B)

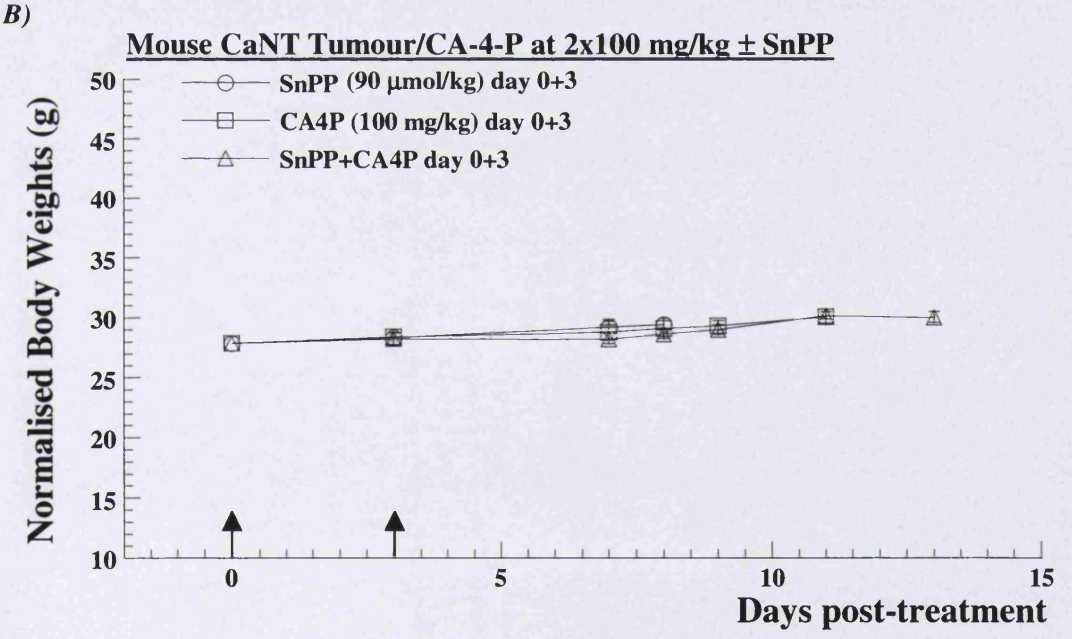

Figure 6.10 Effects of combination therapy with SnPP and CA-4-P on animals' weights. ***A)*** SnPP (90 µmol/kg ip) was administered 15 minutes prior to CA-4-P 25 mg/kg ip. ***B)*** SnPP (90 µmol/kg ip) was administered 15 minutes prior to CA-4-P 100 mg/kg ip. In ***A)*** and ***B)*** the data are means of the same group of animals as shown in Figure 6.9A, B. Error bars are ± 1 standard error of the mean. Arrows indicate treatment days.

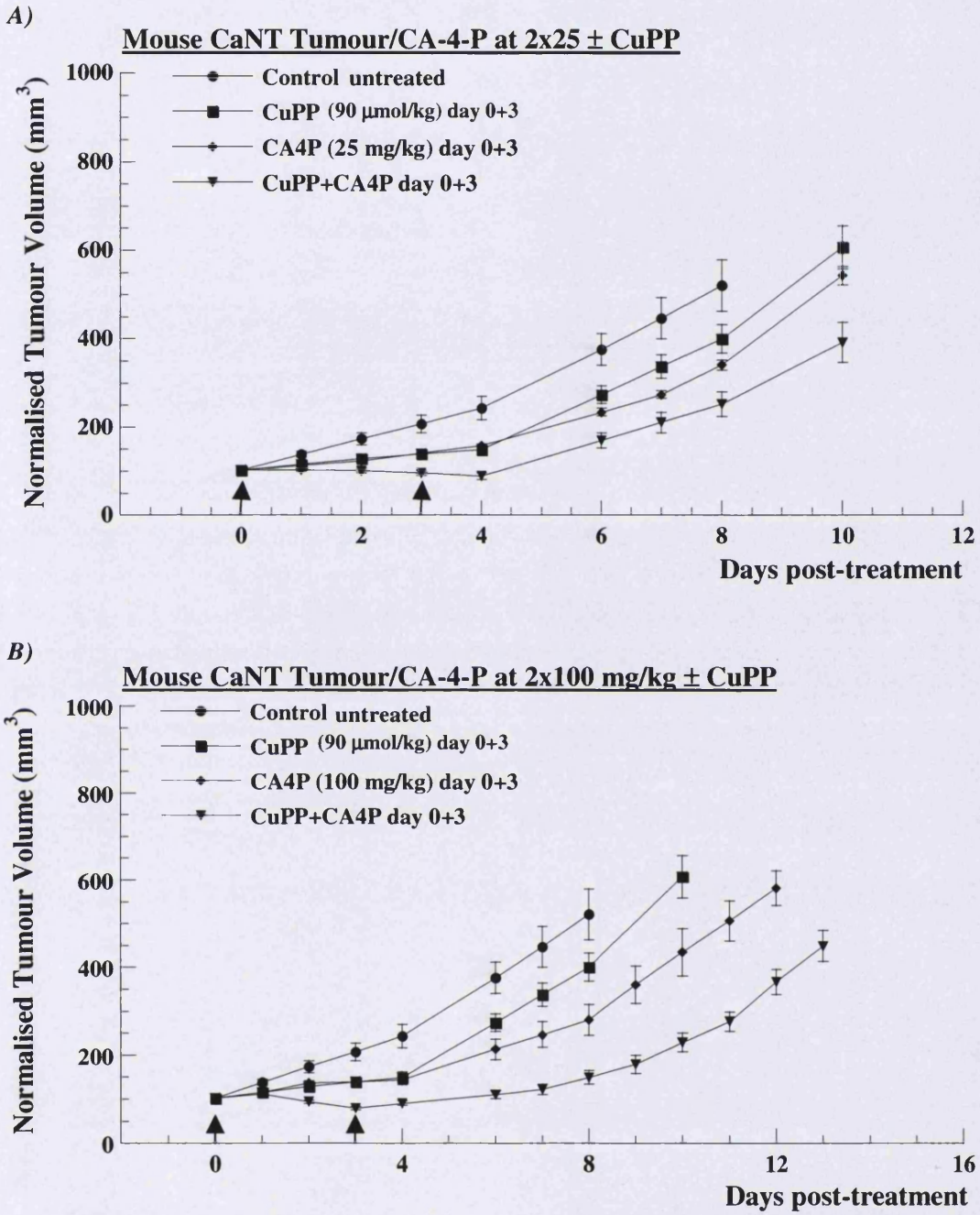

Figure 6.11 Effects of combination therapy with CuPP and CA-4-P on CaNT tumour growth. ***A)*** CuPP (90 µmol/kg ip) was administered 15 minutes prior to CA-4-P 25 mg/kg ip. ***B)*** CuPP (90 µmol/kg ip) was administered 15 minutes prior to CA-4-P 100 mg/kg ip. In ***A)*** and ***B)*** the data are means of 5 animals per group. Error bars are ± 1 standard error of the mean. Arrows indicate treatment days.

A)

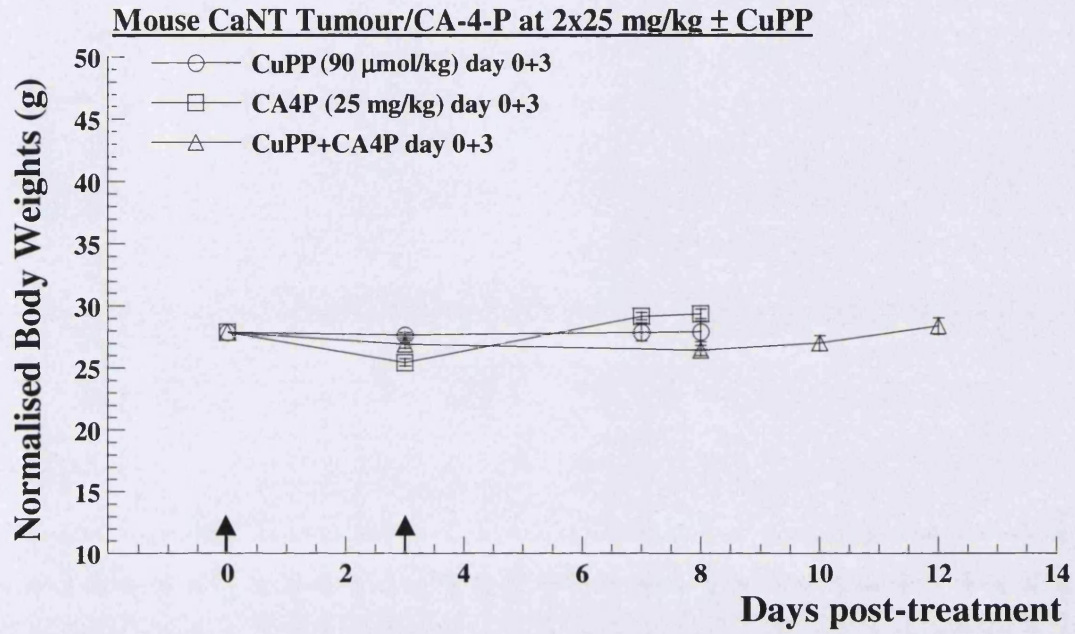

B)

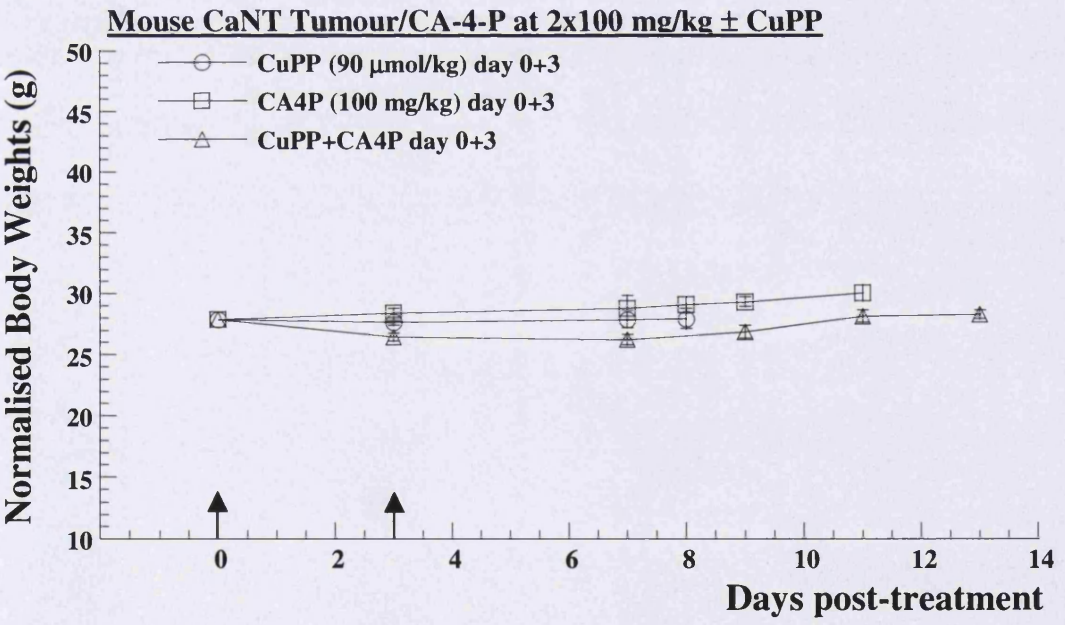

Figure 6.12 Effects of combination therapy with CuPP and CA-4-P on animals' weights. *A)* CuPP (90 µmol/kg ip) was administered 15 minutes prior to CA-4-P 25 mg/kg ip. *B)* CuPP (90 µmol/kg ip) was administered 15 minutes prior to CA-4-P 100 mg/kg ip. In *A)* and *B)* the data are means of the same group of animals as shown in Figure 6.11A, B. Error bars are ± 1 standard error of the mean. Arrows indicate treatment days.

6.4 Discussion

In the first part of this study we investigated the role of endogenous HO enzyme activity in tumour and endothelial cell proliferation *in vitro* and tumour growth *in vivo*. *In vitro*, HO enzyme activity inhibition by SnPP was found to decrease the proliferation of endothelial cells but did not affect P22 tumour cells. The role of HO-1 in cell growth and proliferation has been investigated in various cell types, although there are no reported studies examining tumour cells. Studies using over-expression of HO-1 have shown it to inhibit proliferation of smooth muscle cells, renal and pulmonary epithelial cells by causing cell cycle arrest (see section 1.5.3.5 of Chapter 1). There is now substantial evidence implicating CO in this anti-proliferative role mediated by HO-1 (see section 1.5.4.3.4 of Chapter 1). However, these findings contrast with our results in endothelial cells (Figure 6.1B) and those obtained in another study, whereby HO-1 over-expression was shown to increase the proliferation rate of endothelial cells (Deramaudt *et al.*, 1998). It is likely that these effects of HO-1 on cell proliferation are cell-type and condition specific and dependent on the level of HO-1 expression/activity inhibition achieved. However, the results certainly suggest a potential role for this enzyme system in angiogenesis and hence tumour growth and invasion (see section 1.5.5.2 of Chapter 1).

In vivo, ip administration of SnPP and CuPP to tumour-bearing animals resulted in a small delay in the growth of P22 tumours in rats (Figure 6.2). SnPP was shown to mediate a near to complete HO enzyme activity inhibition for up to 24h following a single dose (Table 6.3). In contrast, CuPP was shown not to mediate any inhibitory effects on the enzyme activity for up to 1h following a single dose (see Figure 4.7 in Chapter 4) and therefore it can be assumed that no inhibition occurs at later time points. Previous studies with SnPP in the rat have also shown prolonged inhibitory effects with this compound on spleen, liver and kidney HO enzyme activity for up to 7 days following a single subcutaneous dose of the agent at 20 μmol/kg (Anderson *et al.*, 1983). As explained in Chapter 4, care must be taken with extrapolation of *ex-vivo* measurements of enzyme activity to the *in vivo* situation. However, the effects of CuPP and SnPP are clearly different, in this regard, suggesting that the mechanisms producing the tumour growth delay are also different for the two compounds. The results suggest that the growth delay mediated by SnPP is associated with HO enzyme activity inhibition, whereas those mediated by CuPP are not. A single dose of CuPP caused a 45% decrease in tumour

blood flow rate (see Figure 4.9 in Chapter 4) and it is likely that its effect on tumour growth is associated with this effect. On the other hand, the effects mediated by SnPP on tumour growth may be related to an anti-angiogenic effect, as described above. Certainly, no direct anti-proliferative effect was observed in P22 tumour cells *in vitro* (Figure 6.1) that could explain the SnPP-induced growth delay *in vivo*.

In contrast to the P22 tumour, administration of a roughly equivalent dose of SnPP to tumour-bearing mice had no effect on growth of the CaNT tumour (Figure 6.9), whereas CuPP mediated a small retardation in the growth of this tumour (Figure 6.11). Again, these results suggest distinct mechanisms of action for these two compounds, although the effects on HO enzyme activity were not investigated in this tumour.

Doi and colleagues have reported impressive growth inhibitory effects mediated by the HO inhibitor ZnPP in an experimental solid tumour model in rats (AH136B rat hepatoma) (Doi *et al.*, 1999). In this study, ZnPP was administered intra-arterially to the tumour via the feeding artery and was shown to significantly inhibit HO enzyme activity 24h after a single injection. Suppression of HO enzyme activity was sustained for up to 7 days following a single injection, although only a single tumour was assessed at that time point (Doi *et al.*, 1999). Differences in the extent of the growth modulatory effects of HO inhibitors *in vivo* may be attributed to several factors including different tumour models used and also different routes of administration of the compounds. The dependence of tumour cells on HO activity for proliferation may also differ between tumour types. In the current study, proliferation of P22 tumour cells was independent of HO, whereas the tumour used by Doi and colleagues was heavily dependent on HO activity. Finally, the possibility of non-specific effects mediated by these metalloporphyrins, with regard to inhibition of other haem containing enzymes such as NOS and sGC (see discussion of Chapter 4), should be stressed in terms of their possible effects on tumour growth. Indeed, chronic NOS inhibition has been shown to significantly slow tumour growth (Orucevic and Lala, 1996).

In this study we also investigated the potential for improving the anti-tumour effects of CA-4-P by combination therapy with the HO inhibitor SnPP. The histological studies on P22 tumours examining necrosis induction following CA-4-P alone or in combination with SnPP were inconclusive. This was due to the large variability between tumours in

the extent of necrosis induction by CA-4-P alone (Figure 6.4). With regard to the effects of the combination on the growth of P22 tumours, a minor enhancement in the growth delay induced by CA-4-P alone was only observed for the higher CA-4-P dose (2x30 mg/kg). There is some inconsistency between the tumour growth obtained in the current study and the immunohistochemical data described in Chapter 5, where CA-4-P-mediated HO-1 induction was only observed for 10 mg/kg and not 30 mg/kg CA-4-P. However, as discussed in Chapter 5, this is most likely due to the insensitivity of the immunohistochemical assay and the heterogeneity of tumour response. It should be noted that CA-4-P alone, in this repeated dose schedule, produced a profound growth delay in both the P22 and CaNT tumours. This is consistent with previous data showing greatly increased efficacy of split versus single doses of CA-4-P in the CaNT and a spontaneous mouse mammary tumour model (T138) (Hill *et al.*, 2002). Taken together these findings would indicate that HO inhibition using SnPP is only useful in combination with relatively effective doses of CA-4-P (in this case 2x30 mg/kg rather than 2x10 mg/kg). Furthermore, particular attention needs to be focussed on those tumours that significantly show induction of HO-1 following CA-4-P and specifically examine, in this population, the potential for increasing the anti-tumour effects of CA-4-P when combined with SnPP. Finally, it is possible that the dosing regimen chosen for these studies was not optimal and therefore further experiments with different drug scheduling need to be carried out. For instance, pre-conditioning tumours by administration of SnPP a few days prior to SnPP+CA-4-P might render tumours more susceptible to subsequent CA-4-P dosing.

In the mouse CaNT tumours, a significant improvement in the anti-tumour effects of CA-4-P (2x100 mg/kg) was shown in combination with SnPP. As for the rat, this effect was only seen with the higher dose of CA-4-P, suggesting that there could be a threshold of tissue damage that needs to be induced by CA-4-P in order for HO activity inhibition by SnPP to cause a further delay in tumour growth. Since SnPP by itself did not have any effect on tumour growth, it is likely that the enhancement in CA-4-P's anti-tumour effects by SnPP are related to the cytoprotective and potential anti-inflammatory roles of HO-1 (see section 1.5.3 of Chapter 1). The vascular effects of CA-4-P *in vivo* have been shown to closely resemble that of an acute inflammatory-type of reaction (Tozer *et al.*, 2001) and to be accompanied by a significant recruitment of neutrophils (Parkins *et al.*, 2000) and macrophages (Chapter 5) into tumours. The expression of HO-1 has been shown to play

an important modulatory role in inflammation and to mediate tissue protection in these conditions. Therefore, inhibition of HO activity by SnPP could be playing an important role in sustaining a pro-inflammatory state initially induced by CA-4-P. This situation would lead to prolonged tissue damage, delaying recovery, which would translate into a further retardation in tumour growth. The time-course of this tissue recovery could initially be examined histologically. Furthermore, both HO-1 and CO have been reported to play an important role in modulating the expression of inflammatory mediators such as IL-10 and TNF-α (Otterbein *et al.*, 2000; Lee and Chau, 2002). Therefore, it would be of interest to investigate the level of expression of these inflammatory mediators following both CA-4-P treatments alone and in combination with SnPP. Finally, as mentioned earlier, tumour pre-conditioning by repeated SnPP administration several days prior to the start of CA-4-P treatment may further sensitise the tumour to CA-4-P-induced tissue damage.

The fact that the SnPP+CA-4-P treatment regimen was more effective in the CaNT tumour than the P22 is not related to differences in the level of HO since overall HO enzyme activity and HO-1 protein levels were found to be very similar in both tumours (Chapter 3). Therefore, it is important to determine the other factors involved in making a particular tumour type more or less sensitive to this combination regimen. Alternatively, the differences observed could be related to the different doses of CA-4-P used in the mouse and the rat. Because a dose of 30 mg/kg of CA-4-P in the rat is roughly equivalent to 60 mg/kg in the mouse, it is possible that the 2x100 mg/kg used for these studies in the mouse was more effective than the 2x30 mg/kg used in the rat. Hence, the greater effectiveness of the combination therapy in the mouse than in the rat (Figures 6.5 and 6.9). Unlike in mice, administration of higher doses of CA-4-P to rats is limited by toxicity. Indeed, while administration of CA-4-P at 2x10 and 2x30 mg/kg to rats induced weight loss and diarrhoea (Figure 6.6), mice tolerated doses of 2x25 and 2x100 mg/kg CA-4-P very well with no significant effects on their weight (Figure 6.10). At present, it is not clear which animal model is likely to best reflect the human situation.

The effects of combining CA-4-P treatment with CuPP were also investigated in both the P22 and CaNT tumour models. In the P22 tumour, the combination regimen did not enhance the anti-tumour effects mediated by either the low or high doses of CA-4-P

(Figure 6.7). This is despite the fact that CuPP by itself mediated a small delay in tumour growth and that, in combination with CA-4-P (2x10 mg/kg), seemed to increase the level of necrosis induced by CA-4-P alone, although only a few animals were used for this study (Figure 6.4). On the other hand, in the CaNT tumour, CuPP administration enhanced the anti-tumour effects mediated by both the low (2x25 mg/kg) and high doses of CA-4-P (2x100 mg/kg). At present it is not clear what could be the mechanism behind these effects, but as shown for the P22 tumour it could be related to the blood flow modifying properties of CuPP. The fact that SnPP and CuPP mediated different effects on tumour growth when administered on their own also suggests different mechanisms of action. Further investigations into the effects of the two compounds on HO enzyme activity in the CaNT tumour need to be conducted in order to confirm the HO inhibitory effects of SnPP in this tumour model.

In conclusion, this study has clearly demonstrated the potential promise of combining CA-4-P treatment with the HO inhibitor SnPP. At present the mechanism involved in these effects is unclear but seems to be unrelated to potential tumour growth modulatory effects of HO-1. Rather, these effects are more likely linked to the pro-angiogenic and also anti-inflammatory/cytoprotective roles of HO-1. These findings could have important clinical applications since SnPP has already been used safely in humans, including newborn infants, to suppress serum bilirubin levels (Berglund *et al.*, 1988; Kappas *et al.*, 1988). These studies have also demonstrated the potential promise of using CuPP in combination with CA-4-P.

6.5 Summary

The major findings of this study consist in that HO inhibition by SnPP has only minor effects on tumour growth *in vivo*. However, combination therapy with the anti-vascular agent CA-4-P has shown potential promise. Further investigations into the mechanism of this enhancement in the anti-tumour effects of CA-4-P would allow further understanding and potential improvement and optimisation in the dosing regimen. The fact that SnPP has previously been used safely in human subjects suggests the potential for clinical applications of this new anti-cancer strategy. However, the potential limitation is that the combination seems most promising at most effective doses of CA-4-P. The dosing

regimen chosen for the studies with the lower doses of CA-4-P may not have been adequate and therefore, further experiments are needed in order to optimise this strategy.

CHAPTER 7

CONCLUDING DISCUSSION AND FUTURE WORK

• The major finding of this work consists in the potential therapeutic promise for using the metalloporphyrins SnPP and CuPP to improve the anti-tumour effects mediated by the vascular targeting agent CA-4-P. Indeed, combination treatments of CA-4-P with either SnPP or CuPP were shown to further delay the growth of mouse CaNT mammary carcinoma and rat P22 carcinosarcoma tumours compared to treatment with CA-4-P alone. Clinical applications of this new strategy may be envisaged since SnPP was previously used safely in human subjects, including newborn infants, in order to decrease excessive serum bilirubin levels (Berglund *et al.*, 1988; Kappas *et al.*, 1988). However, limitations of this strategy may be in the fact that the metalloporphyrins enhanced the anti-tumour effects of only high doses of CA-4-P. Therefore, further experiments varying the scheduling regimen are required in order to optimise this strategy. Currently, the mechanism behind the enhancement in the anti-tumour effects of CA-4-P by SnPP/CuPP is not clear. As suggested in the previous chapter, in the case of the combination with SnPP the enhancement in the growth delay mediated by CA-4-P alone may be due to an SnPP-mediated sustained pro-inflammatory state initially induced by CA-4-P. It would be therefore interesting to examine the intra-tumour levels of pro- and anti-inflammatory mediators such as TNF-α and IL-10, for instance, before and following treatment with CA-4-P and the combination regimen. This would allow further understanding of the potential role of the immune system in the prolonged growth delay effects of CA-4-P. In the case of the combination with CuPP, the blood flow modifying properties of this metalloporphyrin may be playing an important role in enhancing the anti-tumour effects of CA-4-P, at least in the mouse CaNT tumour. Finally, the potential usefulness of this strategy needs to be further evaluated in other tumour models.

• High levels of the HO-1/HO-2 isozymes and high overall HO enzyme activity levels in a range of rodent and xenografted human tumours were reported in the present studies. These findings further highlight potential important roles for this enzyme system in cancer progression and possibly therapy. The high levels of HO-1 may be due to local factors released from the tumour cells themselves or tumour-associated immune cells such as

macrophages and neutrophils. Moreover, the specific tumour microenvironment characterised by hypoxia and oxidative stress may also be at the origin of the high HO-1 levels observed in several tumour types, these conditions being two well-known inducers of HO-1 (see discussion in Chapter 3). Other factors such as NO levels may also play a role since studies have demonstrated the ability of NO donors to induce HO-1 (see discussion in Chapter 3). Further experiments need to be conducted on tumour cells under conditions that mimic the *in vivo* tumour microenvironment in order to confirm the factors mentioned above as potential stimuli for HO-1 in tumours *in vivo*.

• Currently, the biological significance of this relationship between malignant behaviour and HO-1 over-expression is still unclear. Recently, HO-1 over-expression has been shown to be able to directly modulate the angiogenic process and to affect the production of key angiogenic factors (Deramaudt *et al.*, 1998; Dulak *et al.*, 2002). In this thesis, the HO inhibitor, SnPP, was shown to decrease the proliferation of HUVECs but not tumour cells *in vitro* and to cause a small delay in the growth of the P22 rat tumour but not the CaNT mouse tumour *in vivo*. These effects observed in the P22 tumour may be related to the anti-angiogenic effects of SnPP and could be tumour-type or species specific. Further studies examining the role of HO-1 in tumour angiogenesis are required. Another HO inhibitor, ZnPP, was also shown to impressively suppress tumour growth in rats (Doi *et al.*, 1999). The differences in the extent of the effects mediated by the two metalloporphyrins on tumour growth may be due to several factors including different tumour models, routes of administration of the compounds and possibly different mechanisms of action knowing the non-selectivity of some metalloporphyrins at inhibiting HO. Comparison studies between different metalloporphyrins, their HO inhibitory capabilities and their effects on tumour growth would be of interest in order to clarify further the potential relationship between endogenous HO activity and tumour growth. Furthermore, because of the potential problems outlined in Chapters 4 and 6 with regard to the possibility of overestimation of the extent and length of HO enzyme activity inhibition, a more appropriate method than the biochemical assay used in these studies for measuring HO activity inhibition would be extremely valuable to assess precisely the extent of HO inhibition *in vivo*. Measurement of bilirubin levels directly in tumour samples by HPLC analysis, for instance, would give a better estimation of the level of HO

activity inhibition *in vivo* in response to metalloporphyrins. Such a method might also allow for better scheduling and perhaps improved therapeutic effects.

• Understanding the factors and pathways that play a role in the maintenance and regulation of tumour blood flow has obvious therapeutic implications. Improving blood flow to tumours may be important for the delivery of anticancer drugs, whereas shut down of tumour blood flow can lead to secondary tumour cell death and tumour growth delay. The studies presented here have demonstrated, using the HO inhibitor SnPP, a minor role played by the HO/CO system in the maintenance and regulation of tumour blood flow in the P22 rat tumour model. It was previously shown that inhibition of NOS caused a large reduction in blood flow to the P22 tumour and this pathway may therefore represent the major contributor to blood flow regulation and maintenance in this model (Tozer *et al.*, 1997). However, it would be interesting to examine both the effects of exposure to low concentrations of CO and the effects of administration of the novel CO releasing molecules (Motterlini *et al.*, 2002) on tumour blood flow rate in this model and also others. Because under resting conditions blood vessels in many tumours are near to maximally dilated, these studies may be best performed under conditions where tumour blood vessels are pre-constricted in order to clarify whether CO is capable of playing a vasodilatory role in the tumour vasculature.

• The findings presented also highlight the important blood flow modifying effects mediated by CuPP. Elucidation of its mechanism of action would certainly allow further understanding of the pathways responsible for the regulation and maintenance of blood flow in tumours.

• Investigations on the role of the cytoprotective enzyme HO-1 in the effects mediated by the novel vascular targeting agent CA-4-P *in vitro* have demonstrated differential effects between P22 tumour cells and HUVECs. Recovery from tubulin depolymerisation following CA-4-P exposure was much slower in tumour cells than in HUVECs and a greater anti-proliferative effect was also seen in the tumour cells. The latter is an interesting finding since it contrasts the reported studies showing a greater sensitivity of endothelial cells compared to MDA-MD-231 beast adenocarcinoma cells and fibroblasts in terms of cytotoxicity and cell proliferation (Dark *et al.*, 1997; Böhle *et al.*, 2000).

Similar studies using other tumour and endothelial cell types are required to clarify this issue, which has important implications for understanding the mechanisms of the prolonged effects of CA-4-P. With regard to HO-1 induction following CA-4-P exposure, the effects appeared earlier and were much more pronounced in tumour cells than HUVECs. This differential may be related to the innate ability of different cell types to cope with oxidant changes. Appelegate and colleagues have suggested that the magnitude of the HO-1 inducible response is largely influenced by the intracellular redox state of cells (Applegate *et al.*, 1991). It would be therefore interesting to determine the levels of intracellular glutathione and relate these findings to the magnitude of HO-1 induction, the time-course of recovery and also the extent of the anti-proliferative effects mediated by CA-4-P. Testing of this hypothesis could be extended to other tumour cell types and using other tubulin binding agents such as colchicine, the vinca alkaloids and taxol for comparison. *In vivo* experiments could also be conducted to test whether glutathione depletors such as buthionine sulphoximine could render the tumour more sensitive to the effects of CA-4-P leading to a greater anti-tumour effect of the combination. The fact that the anti-oxidant and glutathione precursor NAC completely abolished HO-1 induction in response to CA-4-P in P22 tumour cells suggests that the drug may be causing an imbalance in the redox state of cells possibly via glutathione depletion. Measurement of cellular glutathione content following CA-4-P exposure would clarify this issue and also whether glutathione depletion is the actual stimulus for HO-1 induction in this system. The biological significance of HO-1 induction upon exposure to CA-4-P is unclear at present. Further experiments examining the potential cytoprotective effects of HO-1 induction against the effects mediated by CA-4-P are required. Of particular interest would be to investigate the role of HO-1 during the recovery phase and also in the anti-proliferative effects caused by CA-4-P. These studies could be taken further by examining whether the cytoprotective effects of HO-1 could be substituted by biliverdin/bilirubin, the biologically active products of haem degradation by HO.

• Trying to extrapolate the *in vitro* data obtained in P22 tumour cells to the *in vivo* situation is rather difficult considering the complexity of the events that occur following systemic administration of CA-4-P. *In vivo*, the induction of HO-1 following treatment with the clinically relevant dose of 10 mg/kg CA-4-P as detected by immunohistochemistry did not seem to have any major biological significance since no

enhancement in the anti-tumour effects of CA-4-P was observed when combined with the HO inhibitor SnPP. However, a minor enhancement was observed when the combination was used with the higher dose of CA-4-P (2x30 mg/kg), although the immunohistochemical analysis did not show induction in HO-1 with this dose of CA-4-P. It is possible that the scheduling regimen with the low dose CA-4-P was not appropriate and therefore further studies modifying and optimising the scheduling of the combination are required in order to elucidate completely the potential role of HO-1 in CA-4-P-mediated damage. For instance, pre-conditioning tumours by repeated administration of SnPP days prior to dosing with the combination may render tumours more susceptible to subsequent CA-4-P treatment. It was also very interesting to find that the major cell-type expressing HO-1 following CA-4-P treatment (10 mg/kg) was the infiltrating macrophages and not the tumour cells. *In vitro* studies need to be carried out to investigate the effects of CA-4-P on the HO system in macrophages. It would also be valuable to establish a co-culture system composed of tumour cells and macrophages in order to determine the effects of treatment of tumour cells with CA-4-P on the HO system and behaviour (migration) of macrophages. This may help determine whether CA-4-P treatment induces the release of factors from the tumour cells that may affect the HO system in macrophages.

• Finally, the above discussion illustrates the need for further work on the role of the HO system in cancer and its treatment with anti-vascular therapies. Determination of the role of HO-1 in tumour growth and angiogenesis and studies to optimise combination strategies with HO inhibitors and vascular targeting drugs and understanding the mechanisms involved are required. The findings and ideas generated from this work have stimulated further studies within the Tumour Microcirculation Group at the Gray Cancer Institute.

REFERENCES

Ahmed, B., L. I. Van Eijk, et al. (2003). "Vascular targeting effect of combretastatin A-4 phosphate dominates the inherent angiogenesis inhibitory activity." Int J Cancer **105**: 20-25.

Aizawa, T., N. Ishizaka, et al. (1999). "Balloon injury does not induce heme oxygenase-1 expression, but administration of hemin inhibits neointimal formation in balloon-injured rat carotid artery." Biochem Biophys Res Commun **261**(2): 302-7.

Alam, J. and Z. Den (1992). "Distal AP-1 binding sites mediate basal level enhancement and TPA induction of the mouse heme oxygenase-1 gene." J Biol Chem **267**(30): 21894-900.

Alam, J., D. Stewart, et al. (1999). "Nrf2, a Cap'n'Collar transcription factor, regulates induction of the heme oxygenase-1 gene." J Biol Chem **274**(37): 26071-8.

Alam, J., C. Wicks, et al. (2000). "Mechanism of heme oxygenase-1 gene activation by cadmium in MCF-7 mammary epithelial cells. Role of p38 kinase and Nrf2 transcription factor." J Biol Chem **275**(36): 27694-702.

Alberts, B., Bray, D., Lewis, J., Raff, M., Roberts, K., Watson, J. D. (1989). Chapter 11 The Cytoskeleton. Molecular Biology of the Cell, Second Ed. Garland Publishing Inc. New York.

Anderson, K. E., Simionatto, C.S., Drummond, G.S., Kappas, A. (1983). "Tissue distribution and disposition of tin-protoporphyrin, a potent competitive inhibitor of heme oxygenase." J Pharmacol Exp Ther **228**(2): 327-33.

Applegate, L. A., P. Luscher, et al. (1991). "Induction of heme oxygenase: a general response to oxidant stress in cultured mammalian cells." Cancer Res **51**(3): 974-8.

Appleton, S. D., M. L. Chretien, et al. (1999). "Selective inhibition of heme oxygenase, without inhibition of nitric oxide synthase or soluble guanylyl cyclase, by metalloporphyrins at low concentrations." Drug Metab Dispos **27**(10): 1214-9.

Arap, W., M. G. Kolonin, et al. (2002). "Steps toward mapping the human vasculature by phage display." Nat Med **8**(2): 121-27.

Asahara, T., C. Bauters, et al. (1995). "Synergistic effect of vascular endothelial growth factor and basic fibroblast growth factor on angiogenesis in vivo." Circulation **92**(9 Suppl): II365-71.

Baguley, B. C., K. M. Holdaway, et al. (1991). "Inhibition of growth of colon 38 adenocarcinoma by vinblastine and colchicine: evidence for a vascular mechanism." Eur J Cancer **27**(4): 482-7.

Baguley, B. C. (2001). "Small-molecule cytokine inducers causing tumor necrosis." Curr Opin Investig Drugs **2**(7): 967-75.

Balla, G., H. S. Jacob, et al. (1992). "Ferritin: a cytoprotective antioxidant stratagem of endothelium." J Biol Chem **267**(25): 18148-53.

Balla, J., H. S. Jacob, et al. (1993). "Endothelial-cell heme uptake from heme proteins: induction of sensitization and desensitization to oxidant damage." Proc Natl Acad Sci U S A **90**(20): 9285-9.

Baranano, D. E. and S. H. Snyder (2001). "Neural roles for heme oxygenase: contrasts to nitric oxide synthase." Proc Natl Acad Sci U S A **98**(20): 10996-1002.

Benjamin, L. E. and E. Keshet (1997). "Conditional switching of vascular endothelial growth factor (VEGF) expression in tumors: induction of endothelial cell shedding and regression of hemangioblastoma-like vessels by VEGF withdrawal." Proc Natl Acad Sci U S A **94**(16): 8761-6.

Benjamin, L. E., D. Golijanin, et al. (1999). "Selective ablation of immature blood vessels in established human tumors follows vascular endothelial growth factor withdrawal." J Clin Invest **103**(2): 159-65.

Berglund, L., B. Angelin, et al. (1988). "Sn-protoporphyrin lowers serum bilirubin levels, decreases biliary bilirubin output, enhances biliary heme excretion and potently inhibits hepatic heme oxygenase activity in normal human subjects." Hepatology **8**(3): 625-31.

Bibby, M. C., J. A. Double, et al. (1989). "Reduction of tumor blood flow by flavone acetic acid: a possible component of therapy." J Natl Cancer Inst **81**(3): 216-20.

Bingle, L., N. J. Brown, et al. (2002). "The role of tumour-associated macrophages in tumour progression: implications for new anticancer therapies." J Pathol **196**(3): 254-65.

Bohle, A. S., I. Leuschner, et al. (2000). "Combretastatin A-4 prodrug: a potent inhibitor of malignant hemangioendothelioma cell proliferation." Int J Cancer **87**(6): 838-43.

Boehle, A. S., B. Sipos, et al. (2001). "Combretastatin A-4 prodrug inhibits growth of human non-small cell lung cancer in a murine xenotransplant model." Ann Thorac Surg **71**(5): 1657-65.

Boehm, T., J. Folkman, et al. (1997). "Antiangiogenic therapy of experimental cancer does not induce acquired drug resistance." Nature **390**(6658): 404-7.

Boldt, D. H. (1999). "New perspectives on iron: an introduction." Am J Med Sci **318**(4): 207-12.

Boucher, Y., L. T. Baxter, et al. (1990). "Interstitial pressure gradients in tissue-isolated and subcutaneous tumors: implications for therapy." Cancer Res **50**(15): 4478-84.

Bowie, A. and L. A. O'Neill (2000). "Oxidative stress and nuclear factor-kappaB activation: a reassessment of the evidence in the light of recent discoveries." Biochem Pharmacol **59**(1): 13-23.

Braggins, P. E., G. M. Trakshel, et al. (1986). "Characterization of two heme oxygenase isoforms in rat spleen: comparison with the hematin-induced and constitutive isoforms of the liver." Biochem Biophys Res Commun **141**(2): 528-33.

Brooks, P. C., A. M. Montgomery, et al. (1994). "Integrin alpha v beta 3 antagonists promote tumor regression by inducing apoptosis of angiogenic blood vessels." Cell **79**(7): 1157-64.

Brouard, S., L. E. Otterbein, et al. (2000). "Carbon monoxide generated by heme oxygenase 1 suppresses endothelial cell apoptosis." J Exp Med **192**(7): 1015-26.

Brown, L. F., M. Detmar, et al. (1997). "Vascular permeability factor/vascular endothelial growth factor: a multifunctional angiogenic cytokine." Exs **79**: 233-69.

Brouard, S., P. O. Berberat, et al. (2002). "Heme oxygenase-1-derived carbon monoxide requires the activation of transcription factor NF-kappa B to protect endothelial cells from tumor necrosis factor-alpha-mediated apoptosis." J Biol Chem **277**(20): 17950-61.

Brune, B. and V. Ullrich (1987). "Inhibition of platelet aggregation by carbon monoxide is mediated by activation of guanylate cyclase." Mol Pharmacol **32**(4): 497-504.

Cao, Y., R. W. Ji, et al. (1996). "Kringle domains of human angiostatin. Characterization of the anti-proliferative activity on endothelial cells." J Biol Chem **271**(46): 29461-7.

Cao, Y. (1999). "Therapeutic potentials of angiostatin in the treatment of cancer." Haematologica **84**(7): 643-50.

Carmeliet, P. (2000). "Mechanisms of angiogenesis and arteriogenesis." Nat Med **6**(4): 389-95.

Carmeliet, P. and R. K. Jain (2000). "Angiogenesis in cancer and other diseases." Nature **407**(6801): 249-57.

Carswell, E. A., L. J. Old, et al. (1975). "An endotoxin-induced serum factor that causes necrosis of tumors." Proc Natl Acad Sci U S A **72**(9): 3666-70.

Caudill, T. K., T. C. Resta, et al. (1998). "Role of endothelial carbon monoxide in attenuated vasoreactivity following chronic hypoxia." Am J Physiol **275**(4 Pt 2): R1025-30.

Cavallo, T., R. Sade, et al. (1972). "Tumor angiogenesis. Rapid induction of endothelial mitoses demonstrated by autoradiography." J Cell Biol **54**(2): 408-20.

Cavallo, T., R. Sade, et al. (1973). "Ultrastructural autoradiographic studies of the early vasoproliferative response in tumor angiogenesis." Am J Pathol **70**(3): 345-62.

Chang, Y. S., E. di Tomaso, et al. (2000). "Mosaic blood vessels in tumors: frequency of cancer cells in contact with flowing blood." Proc Natl Acad Sci U S A **97**(26): 14608-13.

Chaplin, D. J., S. A. Hill, et al. (1998). "Modification of tumor blood flow: current status and future directions." Semin Radiat Oncol **8**(3): 151-63.

Chaplin, D. J. and G. J. Dougherty (1999). "Tumour vasculature as a target for cancer therapy." Br J Cancer **80 Suppl 1**: 57-64.

Chaplin, D. J., G. R. Pettit, et al. (1999a). "Anti-vascular approaches to solid tumour therapy: evaluation of combretastatin A4 phosphate." Anticancer Res **19**(1A): 189-95.

Chen, K. and M. D. Maines (2000). "Nitric oxide induces heme oxygenase-1 via mitogen-

activated protein kinases ERK and p38." Cell Mol Biol (Noisy-le-grand) **46**(3): 609-17.

Ching, L. M., W. R. Joseph, et al. (1994). "Induction of tumor necrosis factor-alpha messenger RNA in human and murine cells by the flavone acetic acid analogue 5,6-dimethylxanthenone-4-acetic acid (NSC 640488)." Cancer Res **54**(4): 870-2.

Ching, L. M., Z. Cao, et al. (2002). "Induction of endothelial cell apoptosis by the antivascular agent 5,6-Dimethylxanthenone-4-acetic acid." Br J Cancer **86**(12): 1937-42.

Clark, J. E., R. Foresti, et al. (2000a). "Dynamics of haem oxygenase-1 expression and bilirubin production in cellular protection against oxidative stress." Biochem J **348 Pt 3**: 615-9.

Clark, J. E., R. Foresti, et al. (2000b). "Heme oxygenase-1-derived bilirubin ameliorates postischemic myocardial dysfunction." Am J Physiol Heart Circ Physiol **278**(2): H643-51.

Coceani, F. (2000). "Carbon monoxide in vasoregulation: the promise and the challenge." Circ Res **86**(12): 1184-6.

Cruse, I. and M. D. Maines (1988). "Evidence suggesting that the two forms of heme oxygenase are products of different genes." J Biol Chem **263**(7): 3348-53.

Cuzzocrea, S., D. P. Riley, et al. (2001). "Antioxidant therapy: a new pharmacological approach in shock, inflammation, and ischemia/reperfusion injury." Pharmacol Rev **53**(1): 135-59.

Dahllof, B., A. Billstrom, et al. (1993). "Estramustine depolymerizes microtubules by binding to tubulin." Cancer Res **53**(19): 4573-81.

Dameron, K. M., O. V. Volpert, et al. (1994). "Control of angiogenesis in fibroblasts by p53 regulation of thrombospondin-1." Science **265**(5178): 1582-4.

Dark, G. G., S. A. Hill, et al. (1997). "Combretastatin A-4, an agent that displays potent and selective toxicity toward tumor vasculature." Cancer Res **57**(10): 1829-34.

Das, K. C. and C. W. White (1997). "Activation of NF-kappaB by antineoplastic agents. Role of protein kinase C." J Biol Chem **272**(23): 14914-20.

Dawson, T. M. and S. H. Snyder (1994). "Gases as biological messengers: nitric oxide and carbon monoxide in the brain." J Neurosci **14**(9): 5147-59.

Deininger, M. H., R. Meyermann, et al. (2000). "Heme oxygenase (HO)-1 expressing macrophages/microglial cells accumulate during oligodendroglioma progression." Brain Res **882**(1-2): 1-8.

Denekamp, J., S. A. Hill, et al. (1983). "Vascular occlusion and tumour cell death." Eur J Cancer Clin Oncol **19**(2): 271-5.

Denekamp, J. (1990). "Vascular attack as a therapeutic strategy for cancer." Cancer Metastasis Rev **9**(3): 267-82.

Deramaudt, B. M., S. Braunstein, et al. (1998). "Gene transfer of human heme oxygenase into coronary endothelial cells potentially promotes angiogenesis." J Cell Biochem **68**(1): 121-7.

Deramaudt, B. M., P. Remy, et al. (1999). "Upregulation of human heme oxygenase gene expression by Ets-family proteins." J Cell Biochem **72**(3): 311-21.

Deroanne, C. F., A. Hajitou, et al. (1997). "Angiogenesis by fibroblast growth factor 4 is mediated through an autocrine up-regulation of vascular endothelial growth factor expression." Cancer Res **57**(24): 5590-7.

deSmidt, P. C., M. A. McCarrick, et al. (1987). "Stereoselectivity and enantioselectivity of glutathione S-transferase toward stilbene oxide substrates." Biochem Int **14**(3): 401-8.

Doi, K., T. Akaike, et al. (1999). "Induction of haem oxygenase-1 nitric oxide and ischaemia in experimental solid tumours and implications for tumour growth." Br J Cancer **80**(12): 1945-54.

Doré, S., M. Takahashi, et al. (1999). "Bilirubin, formed by activation of heme oxygenase-2, protects neurons against oxidative stress injury." Proc Natl Acad Sci U S A **96**(5): 2445-50.

Downing, K. H. (2000). "Structural basis for the interaction of tubulin with proteins and drugs that affect microtubule dynamics." Annu Rev Cell Dev Biol **16**: 89-111.

Drummond, G. S. and A. Kappas (1981). "Prevention of neonatal hyperbilirubinemia by tin protoporphyrin IX, a potent competitive inhibitor of heme oxidation." Proc Natl Acad Sci U S A

78(10): 6466-70.

Duckers, H. J., M. Boehm, et al. (2001). "Heme oxygenase-1 protects against vascular constriction and proliferation." Nat Med **7**(6): 693-8.

Duijvestijn, A. M., H. van Goor, et al. (1992). "Antibodies defining rat endothelial cells: RECA-1, a pan-endothelial cell-specific monoclonal antibody." Lab Invest **66**(4): 459-66.

Dulak, J., A. Jozkowicz, et al. (2002). "Heme oxygenase activity modulates vascular endothelial growth factor synthesis in vascular smooth muscle cells." Antioxid Redox Signal **4**(2): 229-40.

Durante, W. and A. I. Schafer (1998). "Carbon monoxide and vascular cell function (Review)." Int J Mol Med **2**(3): 255-262.

Dvorak, H. F. and I. Gresser (1989). "Microvascular injury in pathogenesis of interferon-induced necrosis of subcutaneous tumors in mice." J Natl Cancer Inst **81**(7): 497-502.

Eberhard, A., S. Kahlert, et al. (2000). "Heterogeneity of angiogenesis and blood vessel maturation in human tumors: implications for antiangiogenic tumor therapies." Cancer Res **60**(5): 1388-93.

Eddy, H. A. (1980). "Alterations in tumor microvasculature during hyperthermia." Radiology **137**(2): 515-21.

Eder, J. P., Jr., J. G. Supko, et al. (2002). "Phase I clinical trial of recombinant human endostatin administered as a short intravenous infusion repeated daily." J Clin Oncol **20**(18): 3772-84.

Eikesdal, H. P., R. Bjerkvig, et al. (2001). "Combretastatin A-4 and hyperthermia: potent combination for the treatment of solid tumors." Radiother Oncol **60**(2): 147-54.

Elbirt, K. K., A. J. Whitmarsh, et al. (1998). "Mechanism of sodium arsenite-mediated induction of heme oxygenase-1 in hepatoma cells. Role of mitogen-activated protein kinases." J Biol Chem **273**(15): 8922-31.

Eliceiri, B. P. and D. A. Cheresh (1999). "The role of alphav integrins during angiogenesis:

insights into potential mechanisms of action and clinical development." J Clin Invest **103**(9): 1227-30.

Erickson, H. P. (1975). "Negatively stained vinblastine aggregates." Ann N Y Acad Sci **253**: 51-2.

Fahy, J. (2001). "Modifications in the "upper" velbenamine part of the Vinca alkaloids have major implications for tubulin interacting activities." Curr Pharm Des **7**(13): 1181-97.

Fajardo, L. F., A. B. Schreiber, et al. (1985). "Thermal sensitivity of endothelial cells." Radiat Res **103**(2): 276-85.

Fan, T. P., R. Jaggar, et al. (1995). "Controlling the vasculature: angiogenesis, anti-angiogenesis and vascular targeting of gene therapy." Trends Pharmacol Sci **16**(2): 57-66.

Folkman, J. (1971). "Tumor angiogenesis: therapeutic implications." N Engl J Med **285**(21): 1182-6.

Folkman, J. (1990). "What is the evidence that tumors are angiogenesis dependent?" J Natl Cancer Inst **82**(1): 4-6.

Folkman, J. (1995). "Angiogenesis in cancer, vascular, rheumatoid and other disease." Nat Med **1**(1): 27-31.

Fong, T. A., L. K. Shawver, et al. (1999). "SU5416 is a potent and selective inhibitor of the vascular endothelial growth factor receptor (Flk-1/KDR) that inhibits tyrosine kinase catalysis, tumor vascularization, and growth of multiple tumor types." Cancer Res **59**(1): 99-106.

Foresti, R. & Motterlini, R. (1999). The heme oxygenase pathway and its interaction with nitric oxide in the control of cellular homeostasis. *Free Radic Res*, **31,** 459-75.

Foresti, R., P. Sarathchandra, et al. (1999). "Peroxynitrite induces haem oxygenase-1 in vascular endothelial cells: a link to apoptosis." Biochem J **339 (Pt 3)**: 729-36.

Friebe, A., G. Schultz, et al. (1996). "Sensitizing soluble guanylyl cyclase to become a highly CO-sensitive enzyme." Embo J **15**(24): 6863-8.

Galbraith, S. M., D. J. Chaplin, et al. (2001). "Effects of combretastatin A4 phosphate on endothelial cell morphology in vitro and relationship to tumour vascular targeting activity in vivo." Anticancer Res **21**(1A): 93-102.

Gille, J., R. A. Swerlick, et al. (1997). "Transforming growth factor-alpha-induced transcriptional activation of the vascular permeability factor (VPF/VEGF) gene requires AP-2-dependent DNA binding and transactivation." Embo J **16**(4): 750-9.

Gomez, D. E., D. F. Alonso, et al. (1997). "Tissue inhibitors of metalloproteinases: structure, regulation and biological functions." Eur J Cell Biol **74**(2): 111-22.

Gonzales, S., M. A. Erario, et al. (2002). "Heme Oxygenase-1 Induction and Dependent Increase in Ferritin. a protective antioxidant stratagem in hemin-treated rat brain." Dev Neurosci **24**(2-3): 161-8.

Goodman, A. I., M. Choudhury, et al. (1997). "Overexpression of the heme oxygenase gene in renal cell carcinoma." Proc Soc Exp Biol Med **214**(1): 54-61.

Goto, F., K. Goto, et al. (1993). "Synergistic effects of vascular endothelial growth factor and basic fibroblast growth factor on the proliferation and cord formation of bovine capillary endothelial cells within collagen gels." Lab Invest **69**(5): 508-17.

Gourley, G. R. (1997). "Bilirubin metabolism and kernicterus." Adv Pediatr **44**: 173-229.

Graser, T., Y. P. Vedernikov, et al. (1990). "Study on the mechanism of carbon monoxide induced endothelium-independent relaxation in porcine coronary artery and vein." Biomed Biochim Acta **49**(4): 293-6.

Gray, L. H., Cinger, A.D., Ebert, M., Hornsey, S., Scott, O.C. (1953). "Concentration of oxygen dissolved in tissues at the time of irradiation as a factor in radiotherapy." Br J Radiol **26**: 638.

Griendling, K. K., D. Sorescu, et al. (2000). "Modulation of protein kinase activity and gene expression by reactive oxygen species and their role in vascular physiology and pathophysiology." Arterioscler Thromb Vasc Biol **20**(10): 2175-83.

Grosios, K., P. M. Loadman, et al. (2000). "Combination chemotherapy with combretastatin A-4 phosphate and 5-fluorouracil in an experimental murine colon adenocarcinoma." Anticancer Res **20**(1A): 229-33.

Grossfeld, G. D., D. A. Ginsberg, et al. (1997). "Thrombospondin-1 expression in bladder cancer: association with p53 alterations, tumor angiogenesis, and tumor progression." J Natl Cancer Inst **89**(3): 219-27.

Grundemar, L. and L. Ny (1997). "Pitfalls using metalloporphyrins in carbon monoxide research." Trends Pharmacol Sci **18**(6): 193-5.

Gundersen, G. G. and T. A. Cook (1999). "Microtubules and signal transduction." Curr Opin Cell Biol **11**(1): 81-94.

Hanahan, D. and R. A. Weinberg (2000). "The hallmarks of cancer." Cell **100**(1): 57-70.

Hara, E., K. Takahashi, et al. (1996). "Expression of heme oxygenase and inducible nitric oxide synthase mRNA in human brain tumors." Biochem Biophys Res Commun **224**(1): 153-8.

Hashizume, H., P. Baluk, et al. (2000). "Openings between defective endothelial cells explain tumor vessel leakiness." Am J Pathol **156**(4): 1363-80.

Hayashi, S., R. Takamiya, et al. (1999). "Induction of heme oxygenase-1 suppresses venular leukocyte adhesion elicited by oxidative stress: role of bilirubin generated by the enzyme." Circ Res **85**(8): 663-71.

Hill, S., K. B. Williams, et al. (1989). "Vascular collapse after flavone acetic acid: a possible mechanism of its anti-tumour action." Eur J Cancer Clin Oncol **25**(10): 1419-24.

Hill, S. A., K. B. Williams, et al. (1992). "A comparison of vascular-mediated tumor cell death by the necrotizing agents GR63178 and flavone acetic acid." Int J Radiat Oncol Biol Phys **22**(3): 437-41.

Hill, S. A., S. J. Lonergan, et al. (1993). "Vinca alkaloids: anti-vascular effects in a murine

tumour." Eur J Cancer **29A**(9): 1320-4.

Hill, S. A., D. J. Chaplin, et al. (2002). "Schedule dependence of combretastatin A4 phosphate in transplanted and spontaneous tumour models." Int J Cancer **102**(1): 70-4.

Hill-Kapturczak, N., V. Thamilselvan, et al. (2001). "Mechanism of heme oxygenase-1 gene induction by curcumin in human renal proximal tubule cells." Am J Physiol Renal Physiol **281**(5): F851-9.

Hintz, S. R., C. B. Kim, et al. (1988). "Lack of inhibition of intestinal heme oxygenase by antibiotics and tin-protoporphyrin." Pediatr Res **23**(1): 50-3.

Holmgren, L., M. S. O'Reilly, et al. (1995). "Dormancy of micrometastases: balanced proliferation and apoptosis in the presence of angiogenesis suppression." Nat Med **1**(2): 149-53.

Holmund, J. T., W. C. Kopp, et al. (1995). "A phase I clinical trial of flavone-8-acetic acid in combination with interleukin 2." J Natl Cancer Inst **87**(2): 134-6.

Horsman, M. R., E. Ehrnrooth, et al. (1998). "The effect of combretastatin A-4 disodium phosphate in a C3H mouse mammary carcinoma and a variety of murine spontaneous tumors." Int J Radiat Oncol Biol Phys **42**(4): 895-8.

Horsman, M. R., R. Murata, et al. (2000). "Combretastatins novel vascular targeting drugs for improving anti-cancer therapy. Combretastatins and conventional therapy." Adv Exp Med Biol **476**: 311-23.

Huang, X., G. Molema, et al. (1997). "Tumor infarction in mice by antibody-directed targeting of tissue factor to tumor vasculature." Science **275**(5299): 547-50.

Immenschuh, S., T. Kietzmann, et al. (1998). "The rat heme oxygenase-1 gene is transcriptionally induced via the protein kinase A signaling pathway in rat hepatocyte cultures." Mol Pharmacol **53**(3): 483-91.

Inguaggiato, P., L. Gonzalez-Michaca, et al. (2001). "Cellular overexpression of heme oxygenase-1 up-regulates p21 and confers resistance to apoptosis." Kidney Int **60**(6): 2181-91.

Irigoyen, J. P., D. Besser, et al. (1997). "Cytoskeleton reorganization induces the urokinase-type plasminogen activator gene via the Ras/extracellular signal-regulated kinase (ERK) signaling pathway." J Biol Chem **272**(3): 1904-9.

Ishii, T., K. Itoh, et al. (1999). "Oxidative stress-inducible proteins in macrophages." Free Radic Res **31**(4): 351-5.

Iyer, S., D. J. Chaplin, et al. (1998). "Induction of apoptosis in proliferating human endothelial cells by the tumor-specific antiangiogenesis agent combretastatin A-4." Cancer Res **58**(20): 4510-4.

Jordan, M. A., R. L. Margolis, et al. (1986). "Identification of a distinct class of vinblastine binding sites on microtubules." J Mol Biol **187**(1): 61-73.

Jordan, M. A., R. J. Toso, et al. (1993). "Mechanism of mitotic block and inhibition of cell proliferation by taxol at low concentrations." Proc Natl Acad Sci U S A **90**(20): 9552-6.

Jordan, M. A. and L. Wilson (1998). "Microtubules and actin filaments: dynamic targets for cancer chemotherapy." Curr Opin Cell Biol **10**(1): 123-30.

Jordan, M. A. (2002). "Mechanism of action of antitumor drugs that interact with microtubules and tubulin." Curr Med Chem-Anti-Cancer Agents **2**: 1-17.

Kaide, J. I., F. Zhang, et al. (2001). "Carbon monoxide of vascular origin attenuates the sensitivity of renal arterial vessels to vasoconstrictors." J Clin Invest **107**(9): 1163-71.

Kakolyris, S., A. Giatromanolaki, et al. (1999). "Assessment of vascular maturation in non-small cell lung cancer using a novel basement membrane component, LH39: correlation with p53 and angiogenic factor expression." Cancer Res **59**(21): 5602-7.

Kallinowski, F., K. H. Schlenger, et al. (1989). "Tumor blood flow: the principal modulator of oxidative and glycolytic metabolism, and of the metabolic micromilieu of human tumor xenografts in vivo." Int J Cancer **44**(2): 266-72.

Kanthou, C. and G. M. Tozer (2002). "The tumor vascular targeting agent combretastatin A-4-phosphate induces reorganization of the actin cytoskeleton and early membrane blebbing in human endothelial cells." Blood **99**(6): 2060-9.

Kappas, A. and G. S. Drummond (1986). "Control of heme metabolism with synthetic metalloporphyrins." J Clin Invest **77**(2): 335-9.

Kappas, A., G. S. Drummond, et al. (1988). "Sn-protoporphyrin use in the management of hyperbilirubinemia in term newborns with direct Coombs-positive ABO incompatibility." Pediatrics **81**(4): 485-97.

Kerr, D. J., T. Maughan, et al. (1989). "Phase II trials of flavone acetic acid in advanced malignant melanoma and colorectal carcinoma." Br J Cancer **60**(1): 104-6.

Kety, S. S. (1960a). "Blood tissue exchange methods. Theory of blood-tissue exchange and its application to measurement of blood flow." Methods in Medical Research **8**: 223-227.

Kety, S. S. (1960b). "Measurement of local blood flow by the exchange of an inert, diffusible substance." Methods in Medical Research **8**: 228-235.

Kharitonov, V. G., V. S. Sharma, et al. (1995). "Basis of guanylate cyclase activation by carbon monoxide." Proc Natl Acad Sci U S A **92**(7): 2568-71.

Kim, K. J., B. Li, et al. (1993). "Inhibition of vascular endothelial growth factor-induced angiogenesis suppresses tumour growth in vivo." Nature **362**(6423): 841-4.

Konerding, M. A., C. Van Ackern, et al. (1998). Morphological aspects of tumour angiogenesis and microcirculation. Blood perfusion and microenvironment of human tumors-Implications for clinical radiooncology. M. Molls and P. Vaupel, Springer.

Kozma, F., R. A. Johnson, et al. (1999). "Contribution of endogenous carbon monoxide to regulation of diameter in resistance vessels." Am J Physiol **276**(4 Pt 2): R1087-94.

Krammer, B. (2001). "Vascular effects of photodynamic therapy." Anticancer Res **21**(6B): 4271-7.

Lamb, N. J., G. J. Quinlan, et al. (1999). "Haem oxygenase shows pro-oxidant activity in microsomal and cellular systems: implications for the release of low-molecular-mass iron." Biochem J **344 Pt 1**: 153-8.

Landuyt, W., B. Ahmed, et al. (2001). "In vivo antitumor effect of vascular targeting combined with either ionizing radiation or anti-angiogenesis treatment." Int J Radiat Oncol Biol Phys **49**(2): 443-50.

Lavrovsky, Y., M. L. Schwartzman, et al. (1994). "Identification of binding sites for transcription factors NF-kappa B and AP-2 in the promoter region of the human heme oxygenase 1 gene." Proc Natl Acad Sci U S A **91**(13): 5987-91.

Lee, J. C., D. C. Kim, et al. (2002a). "Interleukin-12 inhibits angiogenesis and growth of transplanted but not in situ mouse mammary tumor virus-induced mammary carcinomas." Cancer Res **62**(3): 747-55.

Lee, P. J., J. Alam, et al. (1996). "Overexpression of heme oxygenase-1 in human pulmonary epithelial cells results in cell growth arrest and increased resistance to hyperoxia." Proc Natl Acad Sci U S A **93**(19): 10393-8.

Lee, P. J., B. H. Jiang, et al. (1997). "Hypoxia-inducible factor-1 mediates transcriptional activation of the heme oxygenase-1 gene in response to hypoxia." J Biol Chem **272**(9): 5375-81.

Lee, P. J., S. L. Camhi, et al. (2000). "AP-1 and STAT mediate hyperoxia-induced gene transcription of heme oxygenase-1." Am J Physiol Lung Cell Mol Physiol **279**(1): L175-82.

Lee, T. S. and L. Y. Chau (2002). "Heme oxygenase-1 mediates the anti-inflammatory effect of interleukin-10 in mice." Nat Med **8**(3): 240-6.

Leek, R. D., R. J. Landers, et al. (1999). "Necrosis correlates with high vascular density and focal macrophage infiltration in invasive carcinoma of the breast." Br J Cancer **79**(5-6): 991-5.

Leek, R. D., C. E. Lewis, et al. (1996). "Association of macrophage infiltration with angiogenesis and prognosis in invasive breast carcinoma." Cancer Res **56**(20): 4625-9.

Lejeune, F. J., C. Ruegg, et al. (1998). "Clinical applications of TNF-alpha in cancer." Curr Opin Immunol **10**(5): 573-80.

Lejeune, F. J. (2002). "Clinical use of TNF revisited: improving penetration of anti-cancer agents by increasing vascular permeability." J Clin Invest **110**(4): 433-5.

Lewis, C. E., R. Leek, et al. (1995). "Cytokine regulation of angiogenesis in breast cancer: the role of tumor-associated macrophages." J Leukoc Biol **57**(5): 747-51.

Li, L., A. Rojiani, et al. (1998). "Targeting the tumor vasculature with combretastatin A-4 disodium phosphate: effects on radiation therapy." Int J Radiat Oncol Biol Phys **42**(4): 899-903.

Liekens, S., E. De Clercq, et al. (2001). "Angiogenesis: regulators and clinical applications." Biochem Pharmacol **61**(3): 253-70.

Lin, H. and J. J. McGrath (1988). "Vasodilating effects of carbon monoxide." Drug Chem Toxicol **11**(4): 371-85.

Lin, P., P. Polverini, et al. (1997). "Inhibition of tumor angiogenesis using a soluble receptor establishes a role for Tie2 in pathologic vascular growth." J Clin Invest **100**(8): 2072-8.

Liotta, L. A., J. Kleinerman, et al. (1974). "Quantitative relationships of intravascular tumor cells, tumor vessels, and pulmonary metastases following tumor implantation." Cancer Res **34**(5): 997-1004.

Liu, N., X. Wang, et al. (2000). "Developmentally regulated expression of two transcripts for heme oxygenase-2 with a first exon unique to rat testis: control by corticosterone of the oxygenase protein expression." Gene **241**(1): 175-83.

Long, B. H. and C. R. Fairchild (1994). "Paclitaxel inhibits progression of mitotic cells to G1 phase by interference with spindle formation without affecting other microtubule functions during anaphase and telephase." Cancer Res **54**(16): 4355-61.

Luca, M., S. Huang, et al. (1997). "Expression of interleukin-8 by human melanoma cells up-regulates MMP-2 activity and increases tumor growth and metastasis." Am J Pathol **151**(4): 1105-13.

Lyden, D., K. Hattori et al. (2001). "Impaired recruitment of bone-marrow-derived endothelial and hematopoietic precursor cells blocks tumor angiogenesis and growth." Nat Med **7**(11): 1194-

1201.

Mahadevan, V., S. T. Malik, et al. (1990). "Role of tumor necrosis factor in flavone acetic acid-induced tumor vasculature shutdown." Cancer Res **50**(17): 5537-42.

Maines, M. D., G. M. Trakshel, et al. (1986). "Characterization of two constitutive forms of rat liver microsomal heme oxygenase. Only one molecular species of the enzyme is inducible." J Biol Chem **261**(1): 411-9.

Maines, M. D. (1988). "Heme oxygenase: function, multiplicity, regulatory mechanisms, and clinical applications." Faseb J **2**(10): 2557-68.

Maines, M. D. (1990). Heme oxygenase: Clinical applications and functions, Boca Raton, CRC Press.

Maines, M. D. and G. M. Trakshel (1992). "Differential regulation of heme oxygenase isozymes by Sn- and Zn-protoporphyrins: possible relevance to suppression of hyperbilirubinemia." Biochim Biophys Acta **1131**(2): 166-74.

Maines, M. D., R. D. Mayer, et al. (1993). "Induction of kidney heme oxygenase-1 (HSP32) mRNA and protein by ischemia/reperfusion: possible role of heme as both promotor of tissue damage and regulator of HSP32." J Pharmacol Exp Ther **264**(1): 457-62.

Maines, M. D. and P. A. Abrahamsson (1996). "Expression of heme oxygenase-1 (HSP32) in human prostate: normal, hyperplastic, and tumor tissue distribution." Urology **47**(5): 727-33.

Maines, M. D. (1997). "The heme oxygenase system: a regulator of second messenger gases." Annu Rev Pharmacol Toxicol **37**: 517-54.

Maines, M. D. (2000). "The heme oxygenase system and its functions in the brain." Cell Mol Biol **46**(3): 573-85.

Makimoto, H., K. Koizumi, et al. (1999). "Tumor vascular targeting using a tumor-tissue endothelium-specific monoclonal antibody as an effective strategy for cancer chemotherapy." Biochem Biophys Res Commun **260**(2): 346-50.

Malcontenti-Wilson, C., V. Muralidharan, et al. (2001). "Combretastatin A4 prodrug study of effect on the growth and the microvasculature of colorectal liver metastases in a murine model." Clin Cancer Res 7(4): 1052-60.

Mandriota, S. J. and M. S. Pepper (1997). "Vascular endothelial growth factor-induced in vitro angiogenesis and plasminogen activator expression are dependent on endogenous basic fibroblast growth factor." J Cell Sci **110 (Pt 18)**: 2293-302.

Marczin, N., A. Papapetropoulos, et al. (1993). "Prevention of nitric oxide synthase induction in vascular smooth muscle cells by microtubule depolymerizing agents." Br J Pharmacol **109**(3): 603-5.

Marczin, N., T. Jilling, et al. (1996). "Cytoskeleton-dependent activation of the inducible nitric oxide synthase in cultured aortic smooth muscle cells." Br J Pharmacol **118**(5): 1085-94.

Margolis, R. L. and L. Wilson (1977). "Addition of colchicine--tubulin complex to microtubule ends: the mechanism of substoichiometric colchicine poisoning." Proc Natl Acad Sci U S A **74**(8): 3466-70.

Marks, G. S., B. E. McLaughlin, et al. (1997). "Heme oxygenase activity and immunohistochemical localization in bovine pulmonary artery and vein." J Cardiovasc Pharmacol **30**(1): 1-6.

Masuya, Y., K. Hioki, et al. (1998). "Involvement of the tyrosine phosphorylation pathway in induction of human heme oxygenase-1 by hemin, sodium arsenite, and cadmium chloride." J Biochem (Tokyo) **124**(3): 628-33.

Matsuno, F., Y. Haruta, et al. (1999). "Induction of lasting complete regression of preformed distinct solid tumors by targeting the tumor vasculature using two new anti-endoglin monoclonal antibodies." Clin Cancer Res **5**(2): 371-82.

Maulik, N., H. S. Sharma, et al. (1996). "Induction of the haem oxygenase gene expression during the reperfusion of ischemic rat myocardium." J Mol Cell Cardiol **28**(6): 1261-70.

McCoubrey, W. K., Jr. and M. D. Maines (1994). "The structure, organization and differential

expression of the gene encoding rat heme oxygenase-2." Gene **139**(2): 155-61.

McCoubrey, W. K., Jr., B. Eke, et al. (1995). "Multiple transcripts encoding heme oxygenase-2 in rat testis: developmental and cell-specific regulation of transcripts and protein." Biol Reprod **53**(6): 1330-8.

McCoubrey, W. K., Jr., T. J. Huang, et al. (1997). "Isolation and characterization of a cDNA from the rat brain that encodes hemoprotein heme oxygenase-3." Eur J Biochem **247**(2): 725-32.

Molls, M. and P. Vaupel (1998). The impact of the tumor microenvironment on experimental and clinical radiation oncology and other therapeutic modalities. Blood perfusion and microenvironment of human tumors-Implications for clinical radiooncology. M. Molls and P. Vaupel, Springer.

Morita, T. and S. Kourembanas (1995). "Endothelial cell expression of vasoconstrictors and growth factors is regulated by smooth muscle cell-derived carbon monoxide." J Clin Invest **96**(6): 2676-82.

Morse, D. and A. M. Choi (2002). "Heme oxygenase-1: the "emerging molecule" has arrived." Am J Respir Cell Mol Biol **27**(1): 8-16.

Motterlini, R., R. Foresti, et al. (1996). "NO-mediated activation of heme oxygenase: endogenous cytoprotection against oxidative stress to endothelium." Am J Physiol **270**(1 Pt 2): H107-14.

Motterlini, R., R. Foresti, et al. (2000). "Endothelial heme oxygenase-1 induction by hypoxia. Modulation by inducible nitric-oxide synthase and S-nitrosothiols." J Biol Chem **275**(18): 13613-20.

Motterlini, R., J. E., Clark, et al. (2002). "Carbon monoxide-releasing molecules: characterization of biochemical and vascular activities." Circ Res **90**(2): E17-24.

Murata, R., D. W. Siemann, et al. (2001a). "Interaction between combretastatin A-4 disodium phosphate and radiation in murine tumors." Radiother Oncol **60**(2): 155-61.

Murata, R., J. Overgaard, et al. (2001b). "Combretastatin A-4 disodium phosphate: a vascular targeting agent that improves that improves the anti-tumor effects of hyperthermia, radiation, and

mild thermoradiotherapy." Int J Radiat Oncol Biol Phys **51**(4): 1018-24.

Murphy, B. J., K. R. Laderoute, et al. (1993). "Enhancement of heme oxygenase expression and activity in A431 squamous carcinoma multicellular tumor spheroids." Cancer Res **53**(12): 2700-3.

Na, G. C. and S. N. Timasheff (1982). "In vitro vinblastine-induced tubulin paracrystals." J Biol Chem **257**(17): 10387-91.

Nabha, S. M., N. R. Wall, et al. (2000). "Effects of combretastatin A-4 prodrug against a panel of malignant human B-lymphoid cell lines." Anticancer Drugs **11**(5): 385-92.

Naik, J. S. and B. R. Walker (2001). "Homogeneous segmental profile of carbon monoxide-mediated pulmonary vasodilation in rats." Am J Physiol Lung Cell Mol Physiol **281**(6): L1436-43.

Nelkin, B. D. and D. W. Ball (2001). "Combretastatin A-4 and doxorubicin combination treatment is effective in a preclinical model of human medullary thyroid carcinoma." Oncol Rep **8**(1): 157-60.

Nishie, A., M. Ono, et al. (1999). "Macrophage infiltration and heme oxygenase-1 expression correlate with angiogenesis in human gliomas." Clin Cancer Res **5**(5): 1107-13.

Nogales, E., S. G. Wolf, et al. (1995). "Structure of tubulin at 6.5 A and location of the taxol-binding site." Nature **375**(6530): 424-7.

Ny, L., K. E. Andersson, et al. (1995). "Inhibition by zinc protoporphyrin-IX of receptor-mediated relaxation of the rat aorta in a manner distinct from inhibition of haem oxygenase." Br J Pharmacol **115**(1): 186-90.

Oguro, T., M. Hayashi, et al. (1996). "Heme oxygenase-1 gene expression by a glutathione depletor, phorone, mediated through AP-1 activation in rats." Biochem Biophys Res Commun **221**(2): 259-65.

O'Reilly, M. S., L. Holmgren, et al. (1994). "Angiostatin: a novel angiogenesis inhibitor that mediates the suppression of metastases by a Lewis lung carcinoma." Cell **79**(2): 315-28.

O'Reilly, M. S., T. Boehm, et al. (1997). "Endostatin: an endogenous inhibitor of angiogenesis and

tumor growth." Cell **88**(2): 277-85.

Orucevic, A. and P. K. Lala (1996). "NG-nitro-L-arginine methyl ester, an inhibitor of nitric oxide synthesis, ameliorates interleukin 2-induced capillary leakage and reduces tumour growth in adenocarcinoma-bearing mice." Br J Cancer **73**(2): 189-96.

Oshika, Y., K. Masuda, et al. (1998). "Thrombospondin 2 gene expression is correlated with decreased vascularity in non-small cell lung cancer." Clin Cancer Res **4**(7): 1785-8.

Otterbein, L. E., J. K. Kolls, et al. (1999). "Exogenous administration of heme oxygenase-1 by gene transfer provides protection against hyperoxia-induced lung injury." J Clin Invest **103**(7): 1047-54.

Otterbein, L. E., F. H. Bach, et al. (2000). "Carbon monoxide has anti-inflammatory effects involving the mitogen-activated protein kinase pathway.PG - 422-8." Nat Med **6**(4).

Otterbein, L. E. and A. M. Choi (2000). "Heme oxygenase: colors of defense against cellular stress." Am J Physiol Lung Cell Mol Physiol **279**(6): L1029-37.

Ozawa, S., H. Shinohara, et al. (2001). "Suppression of angiogenesis and therapy of human colon cancer liver metastasis by systemic administration of interferon-alpha." Neoplasia **3**(2): 154-64.

Panchenko, M. V., H. W. Farber, et al. (2000). "Induction of heme oxygenase-1 by hypoxia and free radicals in human dermal fibroblasts." Am J Physiol Cell Physiol **278**(1): C92-C101.

Papetti, M. and I. M. Herman (2002). "Mechanisms of normal and tumor-derived angiogenesis." Am J Physiol Cell Physiol **282**(5): C947-70.

Parkins, C. S., A. L. Holder, et al. (2000). "Determinants of anti-vascular action by combretastatin A-4 phosphate: role of nitric oxide." Br J Cancer **83**(6): 811-6.

Pedley, R. B., S. A. Hill, et al. (2001). "Eradication of colorectal xenografts by combined radioimmunotherapy and combretastatin a-4 3-O-phosphate." Cancer Res **61**(12): 4716-22.

Peterson, H. I. (1991). "Modification of tumour blood flow--a review." Int J Radiat Biol **60**(1-2): 201-10.

Petrache, I., L. E. Otterbein, et al. (2000). "Heme oxygenase-1 inhibits TNF-alpha-induced apoptosis in cultured fibroblasts." Am J Physiol Lung Cell Mol Physiol **278**(2): L312-9.

Pettit, G. R., S. B. Singh, et al. (1987). "Isolation, structure, and synthesis of combretastatins A-1 and B-1, potent new inhibitors of microtubule assembly, derived from Combretum caffrum." J Nat Prod **50**(1): 119-31.

Pettit, G. R., S. B. Singh, et al. (1989). "Isolation and structure of the strong cell growth and tubulin inhibitor combretastatin A-4." Experientia **45**(2): 209-11.

Peyton, K. J., S. V. Reyna, et al. (2002). "Heme oxygenase-1-derived carbon monoxide is an autocrine inhibitor of vascular smooth muscle cell growth." Blood **99**(12): 4443-8.

Plowman, J., V. L. Narayanan, et al. (1986). "Flavone acetic acid: a novel agent with preclinical antitumor activity against colon adenocarcinoma 38 in mice." Cancer Treat Rep **70**(5): 631-5.

Polte, T., A. Abate, et al. (2000). "Heme oxygenase-1 is a cGMP-inducible endothelial protein and mediates the cytoprotective action of nitric oxide." Arterioscler Thromb Vasc Biol **20**(5): 1209-15.

Poss, K. D. and S. Tonegawa (1997a). "Heme oxygenase 1 is required for mammalian iron reutilization." Proc Natl Acad Sci U S A **94**(20): 10919-24.

Poss, K. D. and S. Tonegawa (1997b). "Reduced stress defense in heme oxygenase 1-deficient cells." Proc Natl Acad Sci U S A **94**(20): 10925-30.

Prestera, T., P. Talalay, et al. (1995). "Parallel induction of heme oxygenase-1 and chemoprotective phase 2 enzymes by electrophiles and antioxidants: regulation by upstream antioxidant-responsive elements (ARE)." Mol Med **1**(7): 827-37.

Prise, V. E., D. J. Honess, et al. (2002). "The vascular response of tumor and normal tissues in the rat to the vascular targeting agent, combretastatin A-4-phosphate, at clinically relevant doses." Int J Oncol **21**(4): 717-26.

Proietti, E., F. Belardelli, et al. (1988). "Tumor necrosis factor alpha induces early morphologic and metabolic alterations in Friend leukemia cell tumors and fibrosarcomas in mice." Int J Cancer **42**(4): 582-91.

Puri, R. K. and J. P. Siegel (1993). "Interleukin-4 and cancer therapy." Cancer Invest **11**(4): 473-86.

Raju, V. S., W. K. McCoubrey, Jr., et al. (1997). "Regulation of heme oxygenase-2 by glucocorticoids in neonatal rat brain: characterization of a functional glucocorticoid response element." Biochim Biophys Acta **1351**(1-2): 89-104.

Ramos, K. S., H. Lin, et al. (1989). "Modulation of cyclic guanosine monophosphate levels in cultured aortic smooth muscle cells by carbon monoxide." Biochem Pharmacol **38**(8): 1368-70.

Ran, S., B. Gao, et al. (1998). "Infarction of solid Hodgkin's tumors in mice by antibody-directed targeting of tissue factor to tumor vasculature." Cancer Res **58**(20): 4646-53.

Reinhold, H. S. and B. Endrich (1986). "Tumour microcirculation as a target for hyperthermia." Int J Hyperthermia **2**(2): 111-37.

Ribatti, D., A. Vacca, et al. (2001). "The role of mast cells in tumour angiogenesis." Br J Haematol **115**(3): 514-21.

Risau, W. (1997). "Mechanisms of angiogenesis." Nature **386**(6626): 671-4.

Robaye, B., R. Mosselmans, et al. (1991). "Tumor necrosis factor induces apoptosis (programmed cell death) in normal endothelial cells in vitro." Am J Pathol **138**(2): 447-53.

Rosette, C. and M. Karin (1995). "Cytoskeletal control of gene expression: depolymerization of microtubules activates NF-kappa B." J Cell Biol **128**(6): 1111-9.

Rotenberg, M. O. and M. D. Maines (1990). "Isolation, characterization, and expression in Escherichia coli of a cDNA encoding rat heme oxygenase-2." J Biol Chem **265**(13): 7501-6.

Rotenberg, M. O. and M. D. Maines (1991). "Characterization of a cDNA-encoding rabbit brain heme oxygenase-2 and identification of a conserved domain among mammalian heme oxygenase isozymes: possible heme-binding site?" Arch Biochem Biophys **290**(2): 336-44.

Ruegg, C., A. Yilmaz, et al. (1998). "Evidence for the involvement of endothelial cell integrin alphaVbeta3 in the disruption of the tumor vasculature induced by TNF and IFN-gamma." Nat

Med **4**(4): 408-14.

Ruoslahti, E. (2000). "Targeting tumor vasculature with homing peptides from phage display." Semin Cancer Biol **10**(6): 435-42.

Ryter, S. W., Tyrrell, R.M. (2000). "The heme synthesis and degradation pathways: role in oxidant sensitivity-Heme oxygenase has both pro- and antioxidant properties." Free Radic Biol Med **28** (2): 289-309.

Saaristo, A., T. Karpanen, et al. (2000). "Mechanisms of angiogenesis and their use in the inhibition of tumor growth and metastasis." Oncogene **19**(53): 6122-9.

Sackett, D. L. (1995). "Vinca site agents induce structural changes in tubulin different from and antagonistic to changes induced by colchicine site agents." Biochemistry **34**(21): 7010-9.

Sackett, D. and T. Fojo (1997). "Taxanes." Cancer Chemother Biol Response Modif **17**: 59-79.

Sammut, I. A., R. Foresti, et al. (1998). "Carbon monoxide is a major contributor to the regulation of vascular tone in aortas expressing high levels of heme oxygenase-1." Br J Pharmacol **125**(7): 1437-44.

Sato, Y. (2001). "Role of ETS family transcription factors in vascular development and angiogenesis." Cell Struct Funct **26**(1): 19-24.

Schaeffer, H. J. and M. J. Weber (1999). "Mitogen-activated protein kinases: specific messages from ubiquitous messengers." Mol Cell Biol **19**(4): 2435-44.

Schwartz, S. M. (2001). "A protective player in the vascular response to injury." Nat Med **7**(6): 656-7.

Sethi, J. M., L. E. Otterbein, et al. (2002). "Differential modulation by exogenous carbon monoxide of TNF-alpha stimulated mitogen-activated protein kinases in rat pulmonary artery endothelial cells." Antioxid Redox Signal **4**(2): 241-8.

Shaheen, R. M., D. W. Davis, et al. (1999). "Antiangiogenic therapy targeting the tyrosine kinase receptor for vascular endothelial growth factor receptor inhibits the growth of colon cancer liver

metastasis and induces tumor and endothelial cell apoptosis." Cancer Res **59**(21): 5412-6.

Shibahara, S., M. Yoshizawa, et al. (1993). "Functional analysis of cDNAs for two types of human heme oxygenase and evidence for their separate regulation." J Biochem (Tokyo) **113**(2): 214-8.

Shimomura, K., T. Manda, et al. (1988). "Recombinant human tumor necrosis factor-alpha: thrombus formation is a cause of anti-tumor activity." Int J Cancer **41**(2): 243-7.

Shiraishi, F., L. M. Curtis, et al. (2000). "Heme oxygenase-1 gene ablation or expression modulates cisplatin-induced renal tubular apoptosis." Am J Physiol Renal Physiol **278**(5): F726-36.

Soares, M. P., Y. Lin, et al. (1998). "Expression of heme oxygenase-1 can determine cardiac xenograft survival." Nat Med **4**(9): 1073-7.

Soares, M. P., A. Usheva, et al. (2002). "Modulation of endothelial cell apoptosis by heme oxygenase-1-derived carbon monoxide." Antioxid Redox Signal **4**(2): 321-9.

Stearns, M. E. and K. D. Tew (1988). "Estramustine binds MAP-2 to inhibit microtubule assembly in vitro." J Cell Sci **89 (Pt 3)**: 331-42.

Stevenson, D. K., H. J. Vreman, et al. (2000). "Carbon monoxide detection and biological investigations." Trans Am Clin Climatol Assoc **111**: 61-75.

Stocker, R., Y. Yamamoto, et al. (1987a). "Bilirubin is an antioxidant of possible physiological importance." Science **235**(4792): 1043-6.

Stocker, R., A. N. Glazer, et al. (1987b). "Antioxidant activity of albumin-bound bilirubin." Proc Natl Acad Sci U S A **84**(16): 5918-22.

Stocker, R. (1990). "Induction of haem oxygenase as a defence against oxidative stress." Free Radic Res Commun **9**(2): 101-12.

Streit, M., P. Velasco, et al. (1999a). "Overexpression of thrombospondin-1 decreases angiogenesis and inhibits the growth of human cutaneous squamous cell carcinomas." Am J Pathol

155(2): 441-52.

Streit, M., L. Riccardi, et al. (1999b). "Thrombospondin-2: a potent endogenous inhibitor of tumor growth and angiogenesis." Proc Natl Acad Sci U S A **96**(26): 14888-93.

Subbaramaiah, K., J. C. Hart, et al. (2000). "Microtubule-interfering agents stimulate the transcription of cyclooxygenase-2. Evidence for involvement of ERK1/2 AND p38 mitogen-activated protein kinase pathways." J Biol Chem **275**(20): 14838-45.

Suematsu, M., S. Kashiwagi, et al. (1994). "Carbon monoxide as an endogenous modulator of hepatic vascular perfusion." Biochem Biophys Res Commun **205**(2): 1333-7.

Suematsu, M., N. Goda, et al. (1995). "Carbon monoxide: an endogenous modulator of sinusoidal tone in the perfused rat liver." J Clin Invest **96**(5): 2431-7.

Suttner, D. M. and P. A. Dennery (1999). "Reversal of HO-1 related cytoprotection with increased expression is due to reactive iron." Faseb J **13**(13): 1800-9.

Takamiya, R., M. Murakami, et al. (2002). "Stabilization of mast cells by heme oxygenase-1: an anti-inflammatory role." Am J Physiol Heart Circ Physiol **283**(3): H861-70.

Talalay, P. (2000). "Chemoprotection against cancer by induction of phase 2 enzymes." Biofactors **12**(1-4): 5-11.

Tenhunen, R., H. S. Marver, et al. (1968). "The enzymatic conversion of heme to bilirubin by microsomal heme oxygenase." Proc Natl Acad Sci U S A **61**(2): 748-55.

Tenhunen, R., H. S. Marver, et al. (1970). "The enzymatic catabolism of hemoglobin: stimulation of microsomal heme oxygenase by hemin." J Lab Clin Med **75**(3): 410-21.

Terry, C. M., J. A. Clikeman, et al. (1998). "Effect of tumor necrosis factor-alpha and interleukin-1 alpha on heme oxygenase-1 expression in human endothelial cells." Am J Physiol **274**(3 Pt 2): H883-91.

Terry, C. M., J. A. Clikeman, et al. (1999). "TNF-alpha and IL-1alpha induce heme oxygenase-1 via protein kinase C, Ca^{2+}, and phospholipase A2 in endothelial cells." Am J Physiol **276**(5 Pt 2):

H1493-501.

Tew, K. D., J. P. Glusker, et al. (1992). "Preclinical and clinical perspectives on the use of estramustine as an antimitotic drug." Pharmacol Ther **56**(3): 323-39.

Thorpe, P. E. and F. J. Burrows (1995). "Antibody-directed targeting of the vasculature of solid tumors." Breast Cancer Res Treat **36**(2): 237-51.

Thorpe, P. E. and S. Ran (2000). "Tumor infarction by targeting tissue factor to tumor vasculature." Cancer J **6 Suppl 3**: S237-44.

Tischer, E., R. Mitchell, et al. (1991). "The human gene for vascular endothelial growth factor. Multiple protein forms are encoded through alternative exon splicing." J Biol Chem **266**(18): 11947-54.

Togane, Y., T. Morita, et al. (2000). "Protective roles of endogenous carbon monoxide in neointimal development elicited by arterial injury." Am J Physiol Heart Circ Physiol **278**(2): H623-32.

Toi, M., Matsumoto, T., et al. (2001). "Vascular endothelial growth factor: its prognostic, predictive, and therapeutic implications." Lancet Oncol **2**(11): 667-73.

Torisu, H., M. Ono, et al. (2000). "Macrophage infiltration correlates with tumor stage and angiogenesis in human malignant melanoma: possible involvement of TNFalpha and IL-1alpha." Int J Cancer **85**(2): 182-8.

Torisu-Itakura, H., M. Furue, et al. (2000). "Co-expression of thymidine phosphorylase and heme oxygenase-1 in macrophages in human malignant vertical growth melanomas." Jpn J Cancer Res **91**(9): 906-10.

Tozer, G. M., S. Lewis, et al. (1990). "The relationship between regional variations in blood flow and histology in a transplanted rat fibrosarcoma." Br J Cancer **61**(2): 250-7.

Tozer, G. M. and C. C. Morris (1990). "Blood flow and blood volume in a transplanted rat fibrosarcoma: comparison with various normal tissues." Radiother Oncol **17**(2): 153-65.

Tozer, G. M. and K. M. Shaffi (1993). "Modification of tumour blood flow using the hypertensive agent, angiotensin II." Br J Cancer **67**(5): 981-8.

Tozer, G. M., K. M. Shaffi, et al. (1994). "Characterisation of tumour blood flow using a 'tissue-isolated' preparation." Br J Cancer **70**(6): 1040-6.

Tozer, G. M. and S. A. Everett (1997). "Nitric oxide in tumour biology and cancer therapy. Part 1: Physiological aspects." Clin Oncol (R Coll Radiol) **9**(5): 282-93.

Tozer, G. M., V. E. Prise, et al. (1997). "Inhibition of nitric oxide synthase induces a selective reduction in tumor blood flow that is reversible with L-arginine." Cancer Res **57**(5): 948-55.

Tozer, G. M., V. E. Prise, et al. (1998). "The comparative effects of the NOS inhibitor, Nomega-nitro-L-arginine, and the haemoxygenase inhibitor, zinc protoporphyrin IX, on tumour blood flow." Int J Radiat Oncol Biol Phys **42**(4): 849-53.

Tozer, G. M., V. E. Prise, et al. (1999). "Combretastatin A-4 phosphate as a tumor vascular-targeting agent: early effects in tumors and normal tissues." Cancer Res **59**(7): 1626-34.

Tozer, G. M., V. E. Prise, et al. (2001). "Mechanisms associated with tumor vascular shut-down induced by combretastatin A-4 phosphate: intravital microscopy and measurement of vascular permeability." Cancer Res **61**(17): 6413-22.

Tozer, G. M., C. Kanthou, et al. (2002). "The biology of the combretastatins as tumour vascular targeting agents." Int J Exp Pathol **83**(1): 21-38.

Trakshel, G. M., R. K. Kutty, et al. (1986). "Purification and characterization of the major constitutive form of testicular heme oxygenase. The noninducible isoform." J Biol Chem **261**(24): 11131-7.

Tsunoda, S., I. Ohizumi, et al. (1999). "Specific binding of TES-23 antibody to tumour vascular endothelium in mice, rats and human cancer tissue: a novel drug carrier for cancer targeting therapy." Br J Cancer **81**(7): 1155-61.

Ueda, S., H. Masutani, et al. (2002). "Redox control of cell death." Antioxid Redox Signal **4**(3): 405-14.

Vachharajani, T. J., J. Work, et al. (2000). "Heme oxygenase modulates selectin expression in different regional vascular beds." Am J Physiol Heart Circ Physiol **278**(5): H1613-7.

Vaupel, P., K. Schlenger, et al. (1992). "Blood flow and tissue oxygenation of human tumors: an update." Adv Exp Med Biol **317**: 139-51.

Vedernikov, Y. P., T. Graser, et al. (1989). "Similar endothelium-independent arterial relaxation by carbon monoxide and nitric oxide." Biomed Biochim Acta **8**: 601-603.

Vihinen, P. and V. M. Kähäri (2002). "Matrix metalloproteinases in cancer: prognostic markers and therapeutic targets." Int J Cancer **99**(2): 157-66.

Vlodavsky, I., G. Korner, et al. (1990). "Extracellular matrix-resident growth factors and enzymes: possible involvement in tumor metastasis and angiogenesis." Cancer Metastasis Rev **9**(3): 203-26.

Volpert, O. V., T. Fong, et al. (1998). "Inhibition of angiogenesis by interleukin 4." J Exp Med **188**(6): 1039-46.

Verma, A., D. J. Hirsch, et al. (1993). "Carbon monoxide: a putative neural messenger." Science **259**(5093): 381-4.

Wakabayashi, Y., R. Takamiya, et al. (1999). "Carbon monoxide overproduced by heme oxygenase-1 causes a reduction of vascular resistance in perfused rat liver." Am J Physiol **277**(5 Pt 1): G1088-96.

Walker, P. R. and J. F. Whitfield (1985). "Cytoplasmic microtubules are essential for the formation of membrane-bound polyribosomes." J Biol Chem **260**(2): 765-70.

Wang, R., Z. Wang, et al. (1997a). "Carbon monoxide-induced vasorelaxation and the underlying mechanisms." Br J Pharmacol **121**(5): 927-34.

Wang, R. and L. Wu (1997b). "The chemical modification of KCa channels by carbon monoxide in vascular smooth muscle cells." J Biol Chem **272**(13): 8222-6.

Watanabe, N., Y. Niitsu, et al. (1988). "Toxic effect of tumor necrosis factor on tumor vasculature in mice." Cancer Res **48**(8): 2179-83.

Willis, D., A. R. Moore, et al. (1996). "Heme oxygenase: a novel target for the modulation of the inflammatory response." Nat Med **2**(1): 87-90.

Willoughby, D. A., A. R. Moore, et al. (2000). "Resolution of inflammation." Int J Immunopharmacol **22**(12): 1131-5.

Woods, J. A., J. A. Hadfield, et al. (1995). "The interaction with tubulin of a series of stilbenes based on combretastatin A-4." Br J Cancer **71**(4): 705-11.

Yachie, A., Y. Niida, et al. (1999). "Oxidative stress causes enhanced endothelial cell injury in human heme oxygenase-1 deficiency." J Clin Inv **103**(1): 129-35.

Yancopoulos, G. D., S. Davis, et al. (2000). "Vascular-specific growth factors and blood vessel formation." Nature **407**(6801): 242-8.

Yao, L., S. E. Pike, et al. (2000). "Effective targeting of tumor vasculature by the angiogenesis inhibitors vasostatin and interleukin-12." Blood **96**(5): 1900-5.

Yokoyama, S., S. Mita, et al. (2001). "Prediction of radiosensitivity in human esophageal squamous cell carcinomas with heme oxygenase-1: a clinicopathological and immunohistochemical study." Oncol Rep **8**(2): 355-8.

Yoshida, T., S. Takahashi, et al. (1974). "Partial purification and reconstitution of the heme oxygenase system from pig spleen microsomes." J Biochem (Tokyo) **75**(5): 1187-91.

Yuan, A., P. C. Yang, et al. (2000). "Interleukin-8 messenger ribonucleic acid expression correlates with tumor progression, tumor angiogenesis, patient survival, and timing of relapse in non-small-cell lung cancer." Am J Respir Crit Care Med **162**(5): 1957-63.

Zagzag, D., A. Hooper, et al. (1999). "In situ expression of angiopoietins in astrocytomas identifies angiopoietin-2 as an early marker of tumor angiogenesis." Exp Neurol **159**(2): 391-400.

Zakhary, R., S. P. Gaine, et al. (1996). "Heme oxygenase 2: endothelial and neuronal localization and role in endothelium-dependent relaxation." Proc Natl Acad Sci U S A **93**(2): 795-8.

Zhang, F., J. I. Kaide, et al. (2001). "Vasoregulatory function of the heme-heme oxygenase-carbon monoxide system." Am J Hypertens **14**(6 Pt 2): 62S-67S.

Zhang, M., B. H. Zhang, et al. (2002). "Overexpression of heme oxygenase-1 protects smooth muscle cells against oxidative injury and inhibits cell proliferation." Cell Res **12**(2): 123-32.

Ziche, M. and L. Morbidelli (2000). "Nitric oxide and angiogenesis." J Neurooncol **50**(1-2): 139-48.

Zwi, L. J., B. C. Baguley, et al. (1989). "Blood flow failure as a major determinant in the antitumor action of flavone acetic acid." J Natl Cancer Inst **81**(13): 1005-13.

PUBLICATIONS

Khelifi A.F., Prise V.E., Foresti R., Clark J.E., Kanthou C., Motterlini R., Tozer G.M. (2002). Heme oxygenase and the novel tumour-specific anti-vascular compound combretastatin A4-phosphate. In: Heme Oxygenase in Biology and Medicine. Abraham NG, Alam J, Nath KA, Ed. Kluwer Academic/Plenum Publishers, p303 (Book chapter).

Khelifi A.F., Prise V.E., Tozer G.M. (2003). Effects of tin-protoporphyrin IX on blood flow in a rat tumor model. Exp Biol Med (Maywood). 228(5): 481-5.